Coordination Chemistry Reviews 253 (2009) 2698–2741

Contents lists available at ScienceDirect

Coordination Chemistry Reviews

journal homepage: www.elsevier.com/locate/ccr

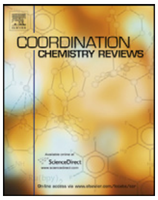

Review

Polynuclear transition metal complexes of metal$\cdots$metal-bridging compartmental pyrazolate ligands

Julia Klingele[a,b,*], Sebastian Dechert[a], Franc Meyer[a,**]

[a] *Institut für Anorganische Chemie, Georg-August-Universität, Tammanstraße 4, D-37077 Göttingen, Germany*
[b] *Institut für Anorganische und Analytische Chemie, Albert-Ludwigs-Universität, Albertstraße 21, D-79104 Freiburg, Germany*

Contents

Abbreviations: py, pyridine; 4-Phpy, 4-phenyl pyridine; 3-Brpy, 3-bromo pyridine; 3-Clpy, 3-chloro-pyridine; 3-Mepy, 3-methyl pyridine; 4-Mepy, 3-methyl pyridine; 4-NMe$_2$py, 4-dimethylamine pyridine; bpy, 4,4′-bipyridine; nta, nitrilotriacetate; acac$^-$, acetyl acetonate; picen, *N*,*N*′-bis-(2-pyridylmethyl)ethylenediamine; hfac, hexafluoromethylacetylacetonate; trpy, 2,2′:6′,2″-terpyridine; BzOH, benzoic acid; 4,4′-dpdo, 4,4′-dipyridyl-*N*,*N*′-dioxide; COD, 1,5-cyclooctadiene; edda^{2-}, ethylenediamine-*N*,*N*′-diacetate; trdda^{2-}, trimethylethylenediamine-*N*,*N*′-diacetate; eddp^{2-}, ethylenediamine-*N*,*N*′-dipropionate; cdda^{2-}, 1,2-cyclohexanediamine-*N*,*N*′-diacetate; bpy, 2,2′-bipyridine; Him, imidazolium cation; Me$_2$en, *N*,*N*′-dimethylethylenediamine; TFB, tetrafluorobenzo[5,6]bicycle[2.2.2]octa-2,5,7-triene; dme, 1,2-dimethoxyethane; *p*-tol, *para*-toluyl; Ph, phenyl; Bu, *n*-butyl; MAO, metyl aluminoxane; PPN, Bis(triphenylphosphoranylidene)ammonium; cy, cyclohexyl; oaa, 2-oxazetidinylacetate; 3,5-DTBC, 3,5-di-*tert*-butylcatechol; 3,5-DTBQ, 3,5-di-*tert*-butylquinone; TCCH$_2$, tetrachloro-*o*-catechol; TCQ, tetrachloro-*o*-quinone; NaBNPP, sodium bis-(4-nitrophenyl)phosphate; DMP, dimethyl phosphate; NPP, 4-nitrophenyl phosphate; pyr, pyrrolidine; cnge, 2-cyanoguanidine = dicyandiamide; Im, 1-methyl-imidazole; Ada, adamantyl; NPPP, (4-nitrophenyl)phenylphosphonate; TMPNP, thymidine 5′-monophosphate 4-nitrophenylester; DMA, dimethyl acetamide; HPNP, 2-hydroxypropyl-*p*-nitrophenyl phosphate.

* Corresponding author at: Institut für Anorganische und Analytische Chemie, Albert-Ludwigs-Universität, Albertstrasse 21, D-79104 Freiburg, Germany,
Fax: +49 0761 2036001.

** Corresponding author at: Institut für Anorganische Chemie , Georg-August-Universität, Tammanstraße 4, D-37077 Göttingen, Germany, Tel.: +49 0551 393012;
fax: +49 0551 3993063.

E-mail addresses: julia.klingele@ac.uni-freiburg.de (J. Klingele), franc.meyer@chemie.uni-goettingen.de (F. Meyer).

doi:10.1016/j.ccr.2009.03.026

ARTICLE INFO

Article history:
Received 1 August 2008
Accepted 31 March 2009
Available online 8 April 2009

Keywords:
Pyrazole
N-ligands
Bridging ligands
Reactivity
Bimetallic complexes
Oligonuclear complexes

ABSTRACT

The present article reviews the structures and properties of di-, oligo- and polynuclear transition metal complexes of substituted pyrazolate (pz) ligands with ligating side arms (D_n) in which the N_2-unit of the pyrazole ring acts as a bridge between two metal centres. Extensive literature surveys covering the literature until the beginning of 2008 of symmetrical 3,5-disubstituted ligands of the type D-pz-D-, D_2-pz-D_2- and D_3-pz-D_3 with uni-, bi- and terdentate side arms, respectively, as well as of unsymmetrical 3,5-disubstituted ligands of the type $D^1{}_n$-pz-$D^2{}_m$, are presented together with a comprehensive survey of the structurally characterised complexes thereof. Catalytic and/or stoichiometric reactions of the dinuclear systems are discussed where appropriate.

1. Introduction

The interest in dinuclear transition metal complexes stems from the expectation that two metal centres in close proximity should be able to interact magnetically and/or electronically, thus giving rise to novel properties and reactivities. Through cooperative electronic and/or steric effects between the two metal centres, distinct reactivity patterns may arise, which are not available to their mononuclear analogues. For instance, the oxidising and reducing power of dinuclear systems is expected to be greater, simply because of the fact that both metal centres could contribute to the redox processes [1]. Another driving force for research in this area is the fact that dinuclear transition metal complexes often allow the recognition and binding and/or activation of substrate molecules, which may lead to distinct stoichiometric or catalytic reactions. Appropriately constructed dinuclear transition metal complexes can therefore be used to mimic metalloproteins featuring dinuclear active sites [2]. Among the ligands that are capable of positioning two metal centres in close proximity, heterocyclic bridging ligands with two adjacent nitrogen donor atoms appear to be particular suitable candidates for realising that demand. Certain aspects of the coordination chemistry of such nitrogen-heterocyclic bridging ligands [3], for example pyridazines [4,5], 1,2,4,5-tetrazines [6], 1,2,4-triazoles [7–9], 1,3,4-thiadiazazoles [8,10] or 1,3,4-oxadiazoles [8] have been dealt with in previous reviews. The use of the pyrazolate moiety as the bridging unit of ligand systems has gained considerable attention and various reviews dealing with the general coordination chemistry of pyrazole and its simplest derivatives [2,11–16] or with poly(1-pyrazolyl)borate [17,18] or poly(1-pyrazolyl)alkanes [12,19] have been published to date.

A common strategy to gain some control of the coordination behaviour of bridging ligands is to introduce substituents carrying additional donor atoms thus creating polydentate binding sites, which enhance the stability of the resulting complexes due to the chelating effect. A very effective implementation of this strategy is the use of 3,5-disubstituted pyrazolate ligands. This field of research has been rapidly growing for the past few years and it is likely to continue so for some time. Despite the wealth of information available on this topic so far only a few aspects of this field have been briefly covered in some specialist reviews [2,15,16,20]. A comprehensive overview of this topic, which the present review is aimed at giving, seems appropriate and timely.

The pyrazolate anion is known to exhibit three coordination modes on binding metal centres (Scheme 1). It can act as an anionic monodentate (a), an anionic *endo*-bidentate (b) or an anionic *exo*-bidentate (c) ligand. This review covers in detail *exo*-bridged pyrazolato complexes carrying two metal-coordinating ligand side arms (d).

The aim of this review article is to give a perspicuous overview of this diverse topic. Owing to the variety of structural features found in the ligands, abbreviations indicating the nature of the ligands are preferred over numbers or characters. These abbreviations are constructed in such a way as to highlight the donor functions or to imply the ligand structures, where appropriate. In symmetrical 3,5-substituted pyrazole ligands the substituent token is simply put in front of the core (pz). Thus 3,5-di-(2-pyridyl)pyrazole is abbreviated as H**py_2-pz**. Unsymmetrical ligands get two different tokens on each side of the pz unit. Substituents in the 4-position of the pyrazole are written in parentheses, so that the ligand 4-chloro-3-phenyl-5-(6-methyl-2-pyridyl)pyrazole is abbreviated as H^{6Me}**py-pz(Cl)-Ph**. In order to cope with the different types of donor functionalities simple amine groups are abbreviated as "**N**", amide groups as "**N^{CO}**", imine groups as "**N=C**" and so on. Pyrazole ligands bearing macrocyclic side arms are indicated by an italic "***c***" for cyclic, as in H**(*c*N_3)$_2$-pz**. Macrocyclic ligands are denoted using the subscript "**2m**" while cryptate ligands bear the subscript "**3m**". We are well aware that the ligand abbreviations used herein are not easy to cope with but we feel that in combination with the graphical sketches they are unambiguous and more meaningful than simple numbers or characters.

2. Symmetrical pyrazolate ligands with unidentate side arms: bis-bidentate pyrazolate ligands

2.1. 3,5-Di-(2-pyridyl)pyrazole (Hpy_2-pz)

The first symmetrical compartmental pyrazolate ligand to be used as a ligand in coordination chemistry was 3,5-di-(2-pyridyl)pyrazole (H**py_2-pz**) (Scheme 2). Without the use of chelating co-ligands and a stoichiometry of metal to ligand of 1:1, by far the most common coordination mode is the 2:2-type coordination, although a few examples of 1:1 coordination compounds are known (Scheme 2) [21,22].

2.1.1. 2:2-Type complexes of Hpy_2-pz

As early as 1969, Ball and Blake reported the first 2:2-type complexes of **py_2-pz$^-$** and nickel(II), which they

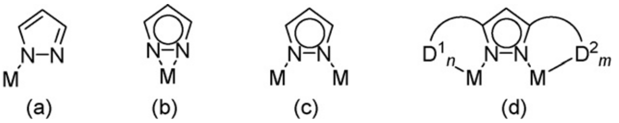

Scheme 1. Coordination modes of the pyrazolate anion: (a) anionic monodentate; (b) anionic *endo*-bidentate; (c) anionic *exo*-bidentate; (d) coordination mode covered in detail by this review.

Table 1
Survey of crystallographically characterised complexes.

Complex	M:L	Bridge	Coord.-sphere[a]	M···pz···M [Å][b]	CCDC code[c]	Refs.
$[Ni^{II}_2(\mathbf{py_2\text{-}pz})_2(MeOH)_4]Cl_2\cdot 2H_2O$ (**1**)	2:2	$(\mu\text{-}pz)_2$	N_4O_2 oct.	–/–	KAPWIH	[24]
$\{$*cis*-$[Cu^{II}_2(\mathbf{py_2\text{-}pz})_2(H_2O)_2](NO_3)_2\cdot 2H_2O\}_2$ (**2**)	2:2 (4:4)	$(\mu\text{-}pz)_2$	N_4O sq.-py.	4.044	PAKKIV	[26]
cis-$[Cu^{II}_2(\mathbf{py_2\text{-}pz})_2(H_2O)_2](ClO_4)_2$ (**3**)	2:2	$(\mu\text{-}pz)_2$	N_4O sq.-py.	4.038(4)	FESQUQ	[27]
$\{$*trans*-$[Cu_2(\mathbf{py_2\text{-}pz})_2(ClO_4)_2]\cdot H_2O\}_2$ (**4**)	2:2 (4:4)	$(\mu\text{-}pz)_2$	N_4O sq.-py.	4.05	ZOGJOU	[28]
trans-$[Fe^{II}_2(\mathbf{py_2\text{-}pz})_2(NCBH_3)_2(py)_2]$ (**5**)	2:2	$(\mu\text{-}pz)_2$	N_6 oct.	4.24 (hs); 4.07 (ls)	AWICEO; AWICEO01	[30]
trans-$[Fe^{II}_2(\mathbf{py_2\text{-}pz})_2(NCBH_3)_2(4\text{-}Phpy)_2]$ (**6**)	2:2	$(\mu\text{-}pz)_2$	N_6 oct.	4.2147(8) (hs, 296 K); 4.2000(8) (hs, 200 K); 4.0605(8) (ls, 200 K); 4.0434(6) (ls, 100 K)	DAKPAH; DAKPAH01; DAKPAH02	[31]
$[Fe^{II}_2(\mathbf{py_2\text{-}pz})_2(NCS)_2(py)_2]$ (**7**)	2:2	$(\mu\text{-}pz)_2$	N_6 oct.	4.229(3)	617521	[33]
trans-$[Co^{II}_2(\mathbf{py_2\text{-}pz})_2(NCS)_2(4\text{-}Phpy)_2]$ (**8**)	2:2	$(\mu\text{-}pz)_2$	N_6 oct.	–/–	RAZHIK	[34]
(*trans*-$[Fe^{II}_2(\mathbf{py_2\text{-}pz})_2(NCS)_2(bpy)])_\infty$ (**9**)	2:2	$(\mu\text{-}pz)_2$	N_6 oct.	4.217(1) (hs, 200 K); 4.047(1) (ls, 150 K)	YECNAW; YECNAW01	[35]
$[(nta)Cr^{III}(\mathbf{py_2\text{-}pz})Fe^{II}(picen)](BF_4)$ (**10**)	2:1	$\mu\text{-}pz$	Cr: N_3O_3 oct.; Fe: N_6 oct.	4.472(1)	YITFIQ	[36]
$[(acac)_2Cr^{III}(\mathbf{py_2\text{-}pz})Ce^{III}(hfac)_3]$ (**11**)	2:1	$\mu\text{-}pz$	Cr: N_2O_4 oct.; Ce: N_2O_6 bi.-tr. pr.	4.33	UMEVIR; UMEVIR01	[38,173]
$[(acac)_2Cr^{III}(\mathbf{py_2\text{-}pz})Nd^{III}(hfac)_3]$ (**12**)	2:1	$\mu\text{-}pz$	Cr: N_2O_4 oct.; Nd: N_2O_6 bi.-tr. pr.	–/–	CENNAL	[173]
$[(acac)_2Cr^{III}(\mathbf{py_2\text{-}pz})Sm^{III}(hfac)_3]$ (**13**)	2:1	$\mu\text{-}pz$	Cr: N_2O_4 oct.; Sm: N_2O_6 bi.-tr. pr.	–/–	CENNEP	[173]
$[(acac)_2Cr^{III}(\mathbf{py_2\text{-}pz})Gd^{III}(hfac)_3]$ (**14**)	2:1	$\mu\text{-}pz$	Cr: N_2O_4 oct.; Gd: N_2O_6 bi.-tr. pr.	–/–	CENMUE	[173]
$[(acac)_2Cr^{III}(\mathbf{py_2\text{-}pz})Dy^{III}(hfac)_3]$ (**15**)	2:1	$\mu\text{-}pz$	Cr: N_2O_4 oct.; Dy: N_2O_6 bi.-tr. pr.	–/–	CENMOY	[173]
$[(acac)_2Cr^{III}(\mathbf{py_2\text{-}pz})Er^{III}(hfac)_3]$ (**16**)	2:1	$\mu\text{-}pz$	Cr: N_2O_4 oct.; Er: N_2O_6 bi.-tr. pr.	–/–	UMEVOX; UMEVOX01	[38,173]
$[(acac)_2Cr^{III}(\mathbf{py_2\text{-}pz})Yb^{III}(hfac)_3]$ (**17**)	2:1	$\mu\text{-}pz$	Cr: N_2O_4 oct.; Yb: N_2O_6 bi.-tr. pr.	4.65	UMEVEN; UMEVEN01	[38,173]
$[Ru^{II}_2(\mathbf{py_2\text{-}pz})(trpy)_2(\mu\text{-}Cl)](PF_6)_2$ (**18**)	2:1	$(\mu\text{-}pz)(\mu\text{-}Cl)$	N_5Cl oct.	–/–	IBALIH	[39]
$[Ru^{II}_2(\mathbf{py_2\text{-}pz})(trpy)_2(\mu\text{-}OAc)](PF_6)_2$ (**19**)	2:1	$(\mu\text{-}pz)(\mu\text{-}OAc)$	N_5O oct.	–/–	IBALON	[39]
$[\{Fe^{II}(\mathbf{py_2\text{-}pz})_3\}_2Fe^{II}_3(\mu_3\text{-}O)](NCS)_2\cdot 10H_2O$ (**20**)	6:5	$(\mu\text{-}pz)$; $(\mu_3\text{-}O)$	N_6 oct.; N_4O trig.-bipy.	–/–	LENXUY	[40]
$[Cu^{II}_4(\mathbf{^{6Me}py\text{-}pz\text{-}py})_4(\mu\text{-}NO_3)(NO_3)_2](NO_3)$ (**21**)	4:4	$(\mu\text{-}pz)$; $(\mu\text{-}NO_3)$	N_4O sq.-py.	4.162(6)–4.196(7)	IJASOB	[42]
$[Cu^{II}_2(\mathbf{^{6Me}py\text{-}pz(Cl)\text{-}Ph})_2Cl_2(DMF)_2]$ (**22**)	2:2	$(\mu\text{-}pz)_2$	N_3ClO sq.-py.	3.917(3)	166472	[43]
$[Ru^{II}_2(\mathbf{^{6Me}py_2\text{-}pz})(\eta^6\text{-}p\text{-}cymene)_2Cl_2](PF_6)$ (**23**)	2:1	$\mu\text{-}pz$	$N_2Cl(\eta^6\text{-}cymene)$ oct.	4.445	WITBEG	[44]
$[Ru^{II}_2(\mathbf{^{6Me}py_2\text{-}pz})(\eta^6\text{-}p\text{-}cymene)_2(NO_3)_2](PF_6)$ (**24**)	2:1	$\mu\text{-}pz$	$N_2O(\eta^6\text{-}cymene)$ oct.	4.420	WITBIK	[44]
$[Ru^{II}_2(\mathbf{^{6Me}py_2\text{-}pz})(\eta^6\text{-}p\text{-}cymene)_2(NO_2)_2](PF_6)$ (**25**)	2:1	$\mu\text{-}pz$	$N_3(\eta^6\text{-}cymene)$ oct.	4.468	WITBUW	[44]
$[Ru^{II}_2(\mathbf{^{6Me}py_2\text{-}pz})(\eta^6\text{-}p\text{-}cymene)_2(H_2O)_2](BF_4)_3$ (**26**)	2:1	$\mu\text{-}pz$	$N_2O(\eta^6\text{-}cymene)$ oct.	4.456	WITBOQ	[44]
$[Ru^{II}_2(\mathbf{^{6Me}py_2\text{-}pz})(\eta^6\text{-}p\text{-}cymene)_2(MeCN)_2](BF_4)_3$ (**27**)	2:1	$\mu\text{-}pz$	$N_3(\eta^6\text{-}cymene)$ oct.	4.482	WITCAD	[44]
$[Ru^{II}_2(\mathbf{^{6Me}py_2\text{-}pz(NO_2)})(\eta^6\text{-}p\text{-}cymene)_2Cl_2](PF_6)$ (**28**)	2:1	$\mu\text{-}pz$	$N_2Cl(\eta^6\text{-}cymene)$ oct.	4.418	121434	[44]
$[Ru^{II}_2(\mathbf{^{6Me}py_2\text{-}pz})(trpy)_2CH_2(O)CMe](PF_6)_2\cdot 0.5OCMe_2$ (**29**$\cdot 0.5OCMe_2$)	2:1	$(\mu\text{-}pz)(\mu\text{-}CH_2(O)CR)$	N_5C oct.; N_5O oct.	4.314(3)	WUQFAP	[45]
$[Ru^{II}_2(\mathbf{^{6Me}py_2\text{-}pz})(trpy)_2Cl](BF_4)_2$ (**30**)	2:1	$(\mu\text{-}pz)(\mu\text{-}Cl)$	N_5Cl oct.	3.8610(8)	WUQDOB	[45]
$[Ru^{II}_2(\mathbf{^{4Me}py_2\text{-}pz})(trpy)_2Cl](PF_6)_2\cdot 0.5MeOH$ (**31**)	2:1	$(\mu\text{-}pz)(\mu\text{-}Cl)$	N_5Cl oct.	3.891(1)	WUQDUH	[45]
$[Co^{II}_5(\mathbf{^{6Me}py_2\text{-}pz})_2(OAc)_8(H_2O)_2]$ (**32**)	5:2	$(\mu\text{-}pz)(\mu\text{-}OAc)$; $(\mu\text{-}OAc)_3$	N_2O_3 oct.; O_6 oct.	4.280(4)	MIJQIF	[46]
$(NBu_4)_2[Pd^{II}_2(\mathbf{(O_2C)_2\text{-}pz})_2]$ (**33**)	2:2	$(\mu\text{-}pz)_2$	N_2O_2 sq.-pl.	3.888(1)	JIRXUD	[47]
$(NBu_4)_2[Cu^{II}_2\mathbf{(O_2C)_2\text{-}pz)}_2]$ (**34**)	2:2	$(\mu\text{-}pz)_2$	N_2O_2 sq.-pl.	3.978(1)	JIRYAK	[47]
cis-$(Et_3NH)_2[Cu^{II}_2(\mathbf{(O_2C)_2\text{-}pz})_2(H_2O)_2]$ (**35**)	2:2	$(\mu\text{-}pz)_2$	N_2O_3 sq.-py.	3.962	AVUQEN	[48]
$(Me_2NH_2)_2[Cu^{II}_2(\mathbf{(O_2C)_2\text{-}pz})_2(H_2O)_2]$ (**36**)	2:2	$(\mu\text{-}pz)_2$	N_2O_3 sq.-py.	–/–	GAWRUS	[49]
$[Zn^{II}_2(\mathbf{(O_2C)_2\text{-}pz})_2(H_2O)_4](Him)_2$ (**37**)	2:2	$(\mu\text{-}pz)_2$	N_4O_2 oct.	–/–	SAZQOQ	[50]
$(Bu_4N)_2[(V^{IV}O)_2(\mathbf{(O_2C)_2\text{-}pz})_2]$ (**38**)	2:2	$(\mu\text{-}pz)_2$	N_2O_3 sq.-py.	4.206	PAGZEC	[51]
$[Cu^{II}_2(H\mathbf{(O_2C)_2pz})_2]\cdot 4,4'\text{-}dpdo$ (**39**)	2:2	$(\mu\text{-}pz)_2$	N_2O_3 sq.-py.	3.439	OKEHOB	[53]
$[\{Na_2(\mu\text{-}H_2O)_2\}\{Cu^{II}_2(\mathbf{(O_2C)_2\text{-}pz})\}_2]_\infty$ (**40**)	2:2 (polymeric)	$(\mu\text{-}pz)_2$	N_2O_2 sq.-pl.	–/–	AVUQIR	[48]
$[\{Ni^{II}(H_2O)_4\}\{Ni^{II}_2(\mathbf{(O_2C)_2\text{-}pz})_2(H_2O)_4\}]_\infty$ (**41**)	2:2 (polymeric)	$(\mu\text{-}pz)_2$	N_2O_4 oct.	–/–	AVUQOX	[48]
$(Bu_4N)[Rh^{II}_2\mathbf{(O_2C)_2\text{-}pz}(CO)_4]$ (**42**)	2:1	$\mu\text{-}pz$	NOC_2 sq.-pl.	4.53	KOSWEU	[54]
$Na[Cr^{III}_2\mathbf{(O_2C)_2\text{-}pz}(edda)_2]\cdot 5H_2O$ (**43**)	2:1	$\mu\text{-}pz$	N_3O_3 oct.	4.473(3)	ZOTPIH	[56]
$Na[Cr^{III}_2\mathbf{(O_2C)_2\text{-}pz}(trdda)_2]\cdot 3H_2O$ (**44**)	2:1	$\mu\text{-}pz$	N_3O_3 oct.	4.560(4)	ZOTPON	[56]
$Na[Cr^{III}_2(\mathbf{(O_2C)_2\text{-}pz})(eddp)_2]\cdot 6H_2O$ (**45**)	2:1	$\mu\text{-}pz$	N_3O_3 oct.	4.574(4)	GUFHOE	[57]

Table 1 (*Continued*)

Complex	M:L	Bridge	Coord.-sphere[a]	M···pz···M [Å][b]	CCDC code[c]	Refs.
[Ru$^{\mathrm{II}}_{2}$**(O$_2$C)$_2$-pz**(bpy)$_2$](ClO$_4$)·H$_2$O (**46**)	2:1	μ-pz	N$_4$O$_2$ oct.	4.685(3)	HUHPOP	[58]
[Ru$^{\mathrm{II}}$Os$^{\mathrm{II}}$**(O$_2$C)$_2$-pz**(bpy)$_2$](ClO$_4$)·H$_2$O (**47**)	2:1	μ-pz	N$_4$O$_2$ oct.	4.690(3)	HUHPUV	[58]
[Os$^{\mathrm{II}}_{2}$**(O$_2$C)$_2$-pz**(bpy)$_2$](ClO$_4$)·H$_2$O (**48**)	2:1	μ-pz	N$_4$O$_2$ oct.	4.662(2)	ERUXIY	[59]
[(Bz$_2$Sn$^{\mathrm{IV}}$)$_6$(**(O$_2$C)$_2$-pz**)$_4$(μ-OH)$_2$(Bz$_2$Sn$^{\mathrm{IV}}$Cl)$_2$]$_\infty$ (**49**)	2:1	(μ-pz)(μ-O); (μ-pz)(μ-OH)	NO$_3$C$_2$; N$_2$O$_3$C$_2$	–/–	JETPII	[61]
[{(Bz$_2$Sn$^{\mathrm{IV}}$)$_6$(**(O$_2$C)$_2$-pz**)$_4$(μ-OH)$_2$(py)$_2$}{(Bz$_2$Sn$^{\mathrm{IV}}$)$_2$(μ_3-O)(μ-OH)}$_2$]$_\infty$ (**50**)	2:1	(μ-pz)(μ-O); (μ-pz)(μ-OH)	NO$_3$C$_2$; N$_2$O$_3$C$_2$	–/–	JETPOD	[61]
[Cu$^{\mathrm{II}}_{3}$**(O$_2$C)$_2$-pz**(Me$_2$en)$_2$(H$_2$O)$_2$]·8H$_2$O (**51**)	3:2	μ-pz	N$_3$O$_2$ sq.-py., N$_2$O$_2$ sq.-pl.	4.3992(12)	TAJKEV	[62]
[Cu$^{\mathrm{II}}_{3}$**(O$_2$C)$_2$-pz**(MeOH)$_6$(H$_2$O)$_4$] (**52**)	3:2	μ-pz	NO$_5$ sq.-py., N$_2$O$_4$ oct.	4.4518(11)	TAJKAR	[62]
[Cu$^{\mathrm{II}}_{3}$(**(O$_2$C)$_2$-pz**)$_2$ (H$_2$O)$_4$]$_\infty$ (**53**)	3:2 (polymeric)	μ-pz	NO$_5$ sq.-py., N$_2$O$_4$ oct.	4.356(1)	UHUNEQ	[63]
trans-[Cu$^{\mathrm{II}}_{2}$(**N$_2$-pz**)$_2$Br$_2$] (**54**)	2:2	(μ-pz)$_2$	N$_2$O$_2$Br sq.-py.	3.947(4)	KOPSAJ	[64]
[Ag$^{\mathrm{I}}$(**INO$_2$-pz**)]$_\infty$ (**55**)	1:1 (polymeric)	μ-pz	N$_2$(+N$_2$) lin. (tetracoord.)[d]	–/–	EWEHET	[66]
meso($\Lambda\Delta$)-[Ru$^{\mathrm{II}}_{2}$**Bim$_2$-pz**(bpy)$_4$](ClO$_4$)$_3$·5H$_2$O (**56**)	2:1	μ-pz	N$_6$ oct.	4.717(3)	LOCROK	[67]
[Ru$^{\mathrm{II}}_{2}$**Bth$_2$-pz**(bpy)$_4$](ClO$_4$)$_3$·H$_2$O (**57**)	2:1	μ-pz	N$_6$ oct.	4.723(3)	JUQVIA	[68]
[Pd$^{\mathrm{II}}_{2}$(**(^{i}Pr$_2$N=C)$_2$-pz**)Cl$_3$] (**58**)	2:1	(μ-pz)(μ-Cl)	N$_2$Cl$_2$ sq.-pl.	3.740(1)	JELLES	[71]
[Pd$^{\mathrm{II}}_{2}$(**(^{i}Pr$_2$N=C)$_2$-pz(Me)**)Cl$_3$] (**59**)	2:1	(μ-pz)(μ-Cl)	N$_2$Cl$_2$ sq.-pl.	3.764(1)	JELLAO	[71]
[Ni$^{\mathrm{II}}_{6}$(**(^{i}Pr$_2$PhN=C)$_2$-pz**)$_3$(μ-Cl)$_8$(μ_6-Cl)] (**60**)	6:3	(μ-pz)(μ-Cl)	N$_2$Cl$_4$ oct.	4.167(2)–4.216(2)	ICEZUL	[70]
[Ni$^{\mathrm{II}}_{2}$(**(^{i}Pr$_2$N=C)$_2$-pz**)Br$_3$]$_3$ (**61**)	6:3	(μ-pz)(μ-Br)	N$_2$Br$_4$ oct.	4.191(1)–4.238(1)	JELLIW	[71]
[Ni$^{\mathrm{II}}_{4}$(**(^{i}Pr$_2$PhN=C)$_2$-pz**)$_2$(μ-Cl)$_2$(μ_3-Cl)$_2$Cl$_2$(EtOH)$_2$] (**62**)	4:2	(μ-pz)(μ-Cl)	N$_2$Ocl$_3$ oct.	3.670(1)	ICIBAX	[70]
trans-[Ni$^{\mathrm{II}}_{2}$(H**(Me$_2$PhN)$_2$-pz**)$_2$Cl$_2$] (**63**)	2:2	(μ-pz)$_2$	N$_4$Cl sq.-py.	3.960	BERQIZ	[72]
[Ni$^{\mathrm{II}}_{2}$(**(Me$_2$PhN)$_2$-pz**)$_2$]Cl$_2$ (**64**)	2:2	(μ-pz)$_2$	N$_4$ sq.-pl.	3.830(8)	BERQOF	[72]
[Ni$^{\mathrm{II}}_{2}$(**(Me$_2$PhN)$_2$-pz**)$_2$](ClO$_4$)$_2$ (**65**)	2:2	(μ-pz)$_2$	N$_4$ sq.-pl.	3.841	BERQUL	[72]
[Pd$^{\mathrm{II}}_{2}$(**(Me$_2$PhN)$_2$-pz**)$_2$](ClO$_4$)$_2$ (BF$_4$)$_2$ (**66**)	2:2	(μ-pz)$_2$	N$_4$ sq.-pl.	3.954	BERRAS	[72]
[Ni$^{\mathrm{II}}_{2}$(**(^{i}Pr$_2$PhN)$_2$-pz**)$_2$](ClO$_4$)$_2$ (**67**)	2:2	(μ-pz)$_2$	N$_4$ sq.-pl.	3.842	BERREW	[72]
[Pd$^{\mathrm{II}}_{2}$(**(^{i}Pr$_2$PhN)$_2$-pz**)$_2$](BF$_4$)$_2$ (**68**)	2:2	(μ-pz)$_2$	N$_4$ sq.-pl.	3.997	BERRIA	[72]
[Ni$^{\mathrm{II}}_{2}$(**(^{i}PrPhN)$_2$-pz**)$_2$](ClO$_4$)$_2$ (**69**)	2:2	(μ-pz)$_2$	N$_4$ sq.-pl.	3.853(2)	BERRUM	[72]
[Ni$^{\mathrm{II}}_{2}$**(Me$_2$PhN)$_2$-pz**)(**^{i}Pr$_2$PhN)$_2$-pz**)](ClO$_4$)$_2$ (**70**)	2:2	(μ-pz)$_2$	N$_4$ sq.-pl.	3.848	BERROG	[72]
[Pt$^{\mathrm{II}}_{2}$**(XN)$_2$-pz**I$_3$] (X = CH$_2$-CH$_2$-OMe) (**71**)	2:1	(μ-pz)(μ-I)	N$_2$I$_2$ sq.-pl-	3.867	QEWFAA	[73]
[(CO)Rh$^{\mathrm{II}}$**P$_2$-pz**(μ-Ph$_2$P)Rh$^{\mathrm{I}}$(CO)(CH$_3$)I]·Et$_2$O(**72**)	2:1	(μ-pz)(μ-Ph$_2$P)	NP$_2$C sq.-pl.; NP$_2$C$_2$I oct.	3.766	DEFZUJ	[75]
[Rh$^{\mathrm{I}}_{4}$(**P$_2$-pz**)$_2$(CO)$_4$(μ_4-H)](BPh$_4$) (**73**)	4:2	(μ-pz)(μ-H)	NPCH sq.-pl.	3.4730(8); 3.4153(6)	VOGDEA; VOGDEA01	[76,78]
[Rh$^{\mathrm{I}}_{4}$(**P$_2$-pz**)$_2$(CO)$_4$(μ_4-*p*-tol-C$\equiv$C)](BPh$_4$) (**74**)	4:2	(μ-pz)(μ-η^1:η^2-C$\equiv$CR)	NPC$_2$Rh$_2$; NPC$_3$Rh; NPC$_2$Rh$_2$; NPC$_2$Rh	3.6767(4); 3.7592(6)	ARIYAB	[77]
[Rh$^{\mathrm{I}}_{4}$(**P$_2$-pz**)$_2$(CO)$_4$(μ_4-C$\equiv$C)] (**75**)	4:2	(μ-pz)(μ-η^1:η^2-C$\equiv$C)	NPC$_2$ sq.-pl.; NPC$_2$Rh	3.815(1); 3.849(1)	ARIYEF	[77]
[Rh$^{\mathrm{I}}_{2}$(**P$_2$-pz**)(CO)$_2$(C$\equiv$CH)] (**76**)·1.4C$_6$H$_6$	2:1	(μ-pz)(μ-η^1:η^2-C$\equiv$CR)	NPC$_2$ sq.-pl; NPC$_3$ sq.-pl.	3.7718(2)	FENNIW	[78]
[Rh$^{\mathrm{I}}_{2}$(**P$_2$-pz**)(CO)$_2$(C$\equiv$CSiMe$_3$)] (**77**)·H$_2$O	2:1	(μ-pz)(μ-η^1:η^2-C$\equiv$CR)	NPC$_2$ sq.-pl; NPC$_3$ sq.-pl.	3.7939(9)	FENNOC	[78]
[Rh$^{\mathrm{I}}_{2}$(**P$_2$-pz**)(CO)$_2$(C$\equiv$CBu)] (**78**)	2:1	(μ-pz)(μ-η^1:η^2-C$\equiv$CR)	NPC$_2$ sq.-pl; NPC$_3$ sq.-pl.	3.6588(9)	FENNUI	[78]
[Rh$^{\mathrm{I}}_{2}$(**P$_2$-pz**)(CO)$_2$(C$\equiv$CPh)] (**79**)	2:1	(μ-pz)(μ-η^1:η^2-C$\equiv$CR)	NPC$_2$ sq.-pl; NPC$_3$ sq.-pl.	3.6882(5)	FENPAQ	[78]
[Rh$^{\mathrm{I}}_{2}$(**P$_2$-pz**)(CO)$_2$(*p*-tol-C$\equiv$C)] (**80**)	2:1	(μ-pz)(μ-η^1:η^2-C$\equiv$CR)	NPC$_2$ sq.-pl; NPC$_3$ sq.-pl.	3.6169(4)	FENPEU	[78]
[Rh$_2$**P$_2$-pz**(CO)$_2$(μ-Co(CO)$_4$)] (**81**)	2 + 1:1	(μ-pz)(μ-Co)	NPC$_2$Co; C$_4$Rh$_2$	3.8131(6)	FENPIY	[78]
[Rh$_2$**P$_2$-pz**(CO)$_2$(μ-Mn(CO)$_5$)] (**82**)	2 + 1:1	(μ-pz)(μ-Mn)	NPC$_2$Mn; C$_4$Rh$_2$	3.8846(5)	FENPOE	[78]
[Rh$^{\mathrm{I}}_{4}$(**P$_2$-pz**)$_2$(CO)$_4$(μ_4-O)] (**83**)	4:2	(μ-pz)(μ-O)	NPCO sq.-pl.	3.644(1); 3.651(2)	FENPUK	[78]
[Rh$^{\mathrm{I}}$Ir$^{\mathrm{I}}$(**P$_2$-pz)**(CO)$_2$(*p*-tol-C$\equiv$C)] (**84**)	2:1	(μ-pz)(μ-η^1:η^2-C$\equiv$CR)	NPC$_2$ sq.-pl; NPC$_3$ sq.-pl.	3.656(1)	–/–	[80]
[Ag$^{\mathrm{I}}_{4}$(**(NHC$^{\mathrm{Me}}$)$_2$-pz**)$_2$](PF$_6$)$_2$·0.5Et$_2$O (**85**).	4:2	μ-pz	CN (+Ag$_2$) lin.	3.295(2)	–/–	[81]

$\mathrm{Ag^{I}{}_{4}}(\mathbf{(NHC^{Benz})_{2}\text{-}pz})_{2}](\mathrm{PF_{6}})_{2}\cdot 4\mathrm{MeCN}$ (**86**)	4:2	μ-pz	CN (+Ag) lin.	−/−	656556	[82]
$[\mathrm{Ag^{I}{}_{4}}(\mathbf{(NHC^{Mes})_{2}\text{-}pz})_{2}](\mathrm{BF_{4}})_{2}\cdot 4\mathrm{MeCN}$ (**87**)	4:2	μ-pz	CN (+Ag) lin.	−/−	656557	[82]
$[\mathrm{Au^{I}{}_{4}}(\mathbf{(NHC^{Me})_{2}\text{-}pz})_{2}](\mathrm{PF_{6}})_{2}$ (**88**)	4:2	μ-pz	CN (+Ag) lin.	3.276(1)	−/−	[81]
$[\mathrm{Ag^{I}{}_{4}}(\mathbf{(NHC)_{2}\text{-}pz_{m}})_{2}](\mathrm{BF_{4}})_{2}\cdot 4\mathrm{MeOH}$ (**89**)	4:2	μ-pz	CN (+Ag) lin.	3.223(1)	656558	[82]
$[\mathrm{Ag^{I}{}_{8}}(\mathbf{(NHC^{Ph\mathit{i}Pr2})_{2}\text{-}pz})_{4}](\mathrm{PF_{6}})_{4}$ (**90**)	8:4	μ-pz	N_2 lin.	3.6996(5); 3.6754(5)	−/−	[83]
$[\mathrm{Pd^{II}{}_{2}}(\mathbf{(NHC^{Me})_{2}\text{-}pz})(\mathrm{allyl})_{2}](\mathrm{PF_{6}})$ (**91**)	2:1	μ-pz	CNC_3 sq.-pl.	−/−	667628	[84]
$[\mathrm{Pd^{II}{}_{2}}(\mathbf{(NHC^{PhMe2})_{2}\text{-}pz})(\mathrm{allyl})_{2}](\mathrm{PF_{6}})$ (**92**)	2:1	μ-pz	CNC_3 sq.-pl	3.9711(5)	667630	[84]
$[\mathrm{Pd^{II}{}_{2}}(\mathbf{(NHC^{Ph\mathit{i}Pr2})_{2}\text{-}pz})(\mathrm{allyl})_{2}](\mathrm{PF_{6}})$ (**93**);	2:1	μ-pz	CNC_3 sq.-pl	−/−	667629	[84]
$[\mathrm{Pd^{II}{}_{2}}(\mathbf{(NHC^{PhMe2})_{2}\text{-}pz})(\mathrm{methallyl})](\mathrm{PF_{6}})$ (**94**)	2:1	μ-pz	CNC_3 sq.-pl	3.9929(4)	667631	[84]
$[\mathrm{Rh^{I}{}_{2}}(\mathbf{(NHC^{Ph\mathit{i}Pr2})_{2}\text{-}pz})(\mathrm{COD})_{2}](\mathrm{PF_{6}})$ (**95**)	2:1	μ-pz	CNC_6 sq.-pl.	4.213	−/−	[85]
$[\mathrm{Ni^{II}{}_{2}}(\mathbf{(NHC^{Ph\mathit{i}Pr2})_{2}\text{-}pz})_{2}](\mathrm{PF_{6}})_{2}$ (**96**)	2:1	μ-pz	CNC_6 sq.-pl.	3.712	−/−	[85]
trans-$[\mathrm{Cu^{II}{}_{2}}(\mathbf{(N^{OH}{=}C)_{2}\text{-}pz(Me)})_{2}\mathrm{Cl_{2}}]\cdot 2\mathrm{H_{2}O}$ (**97a**)	2:2	$(\mu\text{-pz})_2$	N_3OCl sq.-py.	3.832(1)	WAPMEF	[86]
trans-$[\mathrm{Cu^{II}{}_{2}}(\mathbf{(N^{OH}{=}C)_{2}\text{-}pz(Me)})_{2}\mathrm{Cl_{2}}]\cdot 2\mathrm{H_{2}O}$ (**97b**)	2:2	$(\mu\text{-pz})_2$	N_3OCl sq.-py.	3.815(1)	WAPMEF01	[86]
trans-$[\mathrm{Cu^{II}{}_{2}}(\mathbf{(EtO_{2}C)_{2}\text{-}pz})_{2}(\mathrm{NO_{3}})(\mathrm{H_{2}O})](\mathrm{NO_{3}})$ (**98**)	2:2	$(\mu\text{-pz})_2$	N_2O_3 sq.-py.	3.968	−/−	[87]
$[\mathrm{Cu^{II}{}_{2}}(\mathbf{S_{2}\text{-}pz})_{2}(\mathrm{OCMe_{2}})(\mathrm{BF_{4}})(\mu\text{-}\mathrm{BF_{4}})]$ (**99**)	2:2	$(\mu\text{-pz})_2$	N_2S_2OF oct.; $N_2S_2F_2$ oct.	3.828	ROJDAV	[88]
trans-$[\mathrm{Cu^{II}{}_{2}}(\mathbf{MeS_{2}\text{-}pz})_{2}(\mathrm{ONO_{2}})_{2}]$ (**100**)	2:2	$(\mu\text{-pz})_2$	N_2S_2O sq.-py.	3.8147(4)	XAWQOC	[89]
trans-$[\mathrm{Cu^{II}{}_{2}}(\mathbf{MeS_{2}\text{-}pz})_{2}(\mathrm{ClO_{4}})_{2}(\mathrm{MeOH})_{2}]$ (**101**)	2:2	$(\mu\text{-pz})_2$	N_2S_2O2 oct.	3.8185(6)	XAWQUI	[89]
$\mathrm{K}[\mathrm{Mn^{I}{}_{2}}(\mathbf{Cp_{2}\text{-}pz})(\mathrm{CO})_{4}]$ (**102**)	2:1	μ-pz	$NCpC_2$ tetr.	−/−	162374	[90,91]
$[\mathrm{Li_{2}}(\mathbf{Flu_{2}\text{-}pz})(\mathrm{thf})_{4}][\mathrm{Li(thf)_{4}}]$ (**103**)	2:1	μ-pz	$CNFluO_2$	−/−	EDIXUK	[92]
$[\mathrm{Cu^{II}{}_{4}}(\mathrm{H}\mathbf{(pyN^{CO})_{2}\text{-}pz})_{4}]\cdot 8\mathrm{H_{2}O}$ (**104**)	4:4	μ-pz	N_4O sq.-py.	4.0768(4)	636108	[94]
$[\mathrm{Ni^{II}{}_{4}}(\mathrm{H}\mathbf{(pyN^{CO})_{2}\text{-}pz})_{4}]\cdot 8\mathrm{H_{2}O}$ (**105**)	4:4	μ-pz	N_4 sq.-pl.	3.9134(5)	636109	[94]
$[\mathrm{Cu^{II}{}_{2}Ni^{II}{}_{2}}(\mathrm{H}\mathbf{(pyN^{CO})_{2}\text{-}pz})_{4}]\cdot 8\mathrm{H_{2}O}$ (**106**)	4:4	μ-pz	Cu^{II}- and Ni^{II}-ions are not distinguished	−/−	636110	[94]
trans-$[\mathrm{Cu^{II}{}_{2}}(\mathbf{(NC_{2}NH)_{2}\text{-}pz})_{2}](\mathrm{BPh_{4}})_{2}$ (**107**)	2:2	$(\mu\text{-pz})_2$	N_5 sq.-py.	3.903(2)	KEJSOH	[95]
$[\mathrm{Mn^{II}{}_{2}}(\mathbf{(pyN)_{2}\text{-}pz})_{2}](\mathrm{BPh_{4}})_{2}\cdot 2\mathrm{tol}$ (**108**)	2:2	$(\mu\text{-pz})_2$	N_6 oct.	4.181(2)	TILQOU	[96]
$[\mathrm{Zn^{II}{}_{2}}\mathbf{(N^{Me}N^{Me})_{2}\text{-}pz}(\mathrm{H_{2}O})(\mathrm{oaa})]_{2}(\mathrm{ClO_{4}})$ (**109**)	2:1	$(\mu\text{-pz})(\mu\text{-}O_2C)$	N_3O_2 sq.-py.	4.1359(6)	DATVUQ	[108]
$[\mathrm{Co^{II}{}_{2}}\mathbf{(N^{Me}C_{3}N^{Me})_{2}\text{-}pz}(\mu\text{-}\mathrm{Cl})\mathrm{Cl_{2}}]$ (**110**)	2:1	$(\mu\text{-pz})(\mu\text{-Cl})$	N_5 trig.-bipy.	3.913	ROJCEY	[97]
cis-$[\mathrm{Ni^{II}{}_{2}}(\mathbf{(N^{Me}C_{3}N^{Me})_{2}\text{-}pz})(\mu\text{-}\mathrm{OH})(\mathrm{MeCN})_{2}](\mathrm{ClO_{4}})_{2}$ (**111**)	2:1	$(\mu\text{-pz})(\mu\text{-OH})$	N_5[e]	3.493	VACHIQ	[98]
trans-$[\mathrm{Cu^{II}{}_{2}}\mathbf{(N^{Me}C_{3}N^{Me})_{2}\text{-}pz}(\mu\text{-}\mathrm{OH})(\mathrm{EtOH})_{2}]$ (**112**)	2:1	$(\mu\text{-pz})(\mu\text{-OH})$	N_5 sq.-py.	3.540(1)	ADILOO	[104]
trans-$[\mathrm{Cu^{II}{}_{2}}\mathbf{(N^{Me}N^{Me})_{2}\text{-}pz}(\mu\text{-}\mathrm{O_{2}COMe})(\mathrm{MeOH})_{2}](\mathrm{ClO_{4}})_{2}$ (**113**)	2:1	$(\mu\text{-pz})(\mu\text{-}O_2COMe)$	N_5 sq.-py.	4.088(1)	ADILEE	[104]
$[\mathrm{Cu^{II}{}_{4}}(\mathbf{(N^{Me}N^{Me})_{2}\text{-}pz})_{2}(\mu_{3}\text{-}\mathrm{CO_{3}})(\mathrm{H_{2}O})_{2}(\mu\text{-}\mathrm{ClO_{4}})](\mathrm{ClO_{4}})$ (**114**)	4:2	μ-pz; $(\mu\text{-pz})(\mu\text{-}O_2CO)(\mu\text{-}O_2ClO_2)$	N_3O_2 sq.-py.	4.001(1); 4.279(1)	FEGTAN	[107]
$[\mathrm{Cu^{II}{}_{6}}(\mathbf{(N^{Me}N^{Me})_{2}\text{-}pz})_{2}(\mu\text{-}\mathrm{OH})_{6}](\mathrm{BF_{4}})_{4}$ (**115**)	6:2	$(\mu\text{-pz})(\mu\text{-OH})$	N_3O_2 sq.-py.; NO_4 sq.-py.; N_2O_3 sq.-py.	3.327(2)	FEGTER	[107]
$[\mathrm{Cu^{II}{}_{2}}\mathbf{(N^{Me}C_{3}N^{Me})_{2}\text{-}pz}(\mu\text{-}\mathrm{Cl})\mathrm{Cl_{2}}]$ (**116**)	2:1	$(\mu\text{-pz})(\mu\text{-Cl})$	N_3Cl_2 sq.-py.	3.918	NOCDEO	[99]
$[\mathrm{Cu^{II}{}_{4}}(\mathbf{(N^{Me}N^{Me})_{2}\text{-}pz})_{2}(\mu\text{-}\mathrm{Cl})_{4}(\mathrm{Cl})_{2}]$ (**117**)	4:2	$(\mu\text{-pz})(\mu\text{-Cl})_4$	N_3Cl_2 sq.-py.	3.924	NOCDIS	[99]
$[\mathrm{Cu^{II}{}_{2}}\mathbf{(N^{Me}N^{Me})_{2}\text{-}pz}(\mu\text{-}\mathrm{Cl})_{3}]$ (**118**)	2:1, polymer	$(\mu\text{-pz})(\mu\text{-Cl})$	N_3Cl_2 sq.-py.	4.028	−/−	[99]
$[\mathrm{Cu^{II}{}_{2}}(\mathrm{H}\mathbf{N^{Me}N^{Me})_{2}\text{-}pz}(\mathrm{TCC})(\mathrm{H_{2}O})_{2}(\mathrm{ClO_{4}})](\mathrm{ClO_{4}})$ (**119**)	2:1	$(\mu\text{-pz})$	N_3O_2 sq.-py.; N_2O_3 sq.-py.	4.202(1)	ADILUU	[104]
$[\mathrm{Cu^{II}{}_{2}}\mathbf{(N^{Me}N^{Me})_{2}\text{-}pz}(\mathrm{TCC})(\mathrm{EtCN})(\mathrm{H_{2}O})](\mathrm{PF_{6}})$ (**120**)	2:1	$(\mu\text{-pz})$	N_4O sq.-py.; N_3O_2 sq.-py.	4.288(1)	ADIMEF	[104]
$[\mathrm{Ni^{II}{}_{4}}(\mathbf{(N^{Me}N^{Me})_{2}\text{-}pz})_{2}(\mathrm{OC(NH_{2})_{2}})_{2}(\mu_{3}\text{-}\mathrm{OC(NH_{2})(NH)})_{2}](\mathrm{ClO_{4}})_{4}$ (**121**)	4:2	$(\mu\text{-pz})(\mu\text{-urea})$	N_4O_2 oct.; N_4 sq.-pl.	4.232	DAVREX	[100]
$[\mathrm{Ni^{II}{}_{2}}\mathbf{(N^{Me}N^{Me})_{2}\text{-}pz}(\mu\text{-}\mathrm{OAc})(\mathrm{OC(NHMe)_{2}})_{2}(\mathrm{MeOH})_{2}](\mathrm{ClO_{4}})_{2}$ (**122**)	2:1	$(\mu\text{-pz})(\mu\text{-OAc})$	N_3O_3 oct.	4.316	CIQMEU	[101]
$[\mathrm{Ni^{II}{}_{2}}\mathbf{(N^{Me}N^{Me})_{2}\text{-}pz}(\mu\text{-}\mathrm{OAc})(\mathrm{OAc})_{2}\mathrm{Na(H_{2}O)(OCMe_{2})}](\mathrm{BPh_{4}})$ (**123**)	2 + 1:1	$(\mu\text{-pz})(\mu\text{-OAc})$	N_3O_3 oct.	4.291	CIQMIY	[101]
$[\mathrm{Cu^{II}{}_{4}}(\mathbf{(N^{Me}N^{Me})_{2}\text{-}pz})_{2}(\mu_{4}\text{-}\mathrm{O_{2}})(\mu\text{-}\mathrm{OH})_{2}](\mathrm{PF_{6}})_{2}$ (**124**)	4:2	$(\mu\text{-pz})(\mu\text{-}O_2)$	N_3O_2 sq.-py.	3.902	GOSQUA	[102]
$[\mathrm{Cu^{II}{}_{4}}(\mathbf{(N^{Me}N^{Me})_{2}\text{-}pz})_{2}(\mu\text{-}\mathrm{OH})_{4}](\mathrm{PF_{6}})_{2}$ (**125**)	4:2	$(\mu\text{-pz})$	N_3O_2 sq.-py.	4.348	GOSBAS	[102]
$[\mathrm{Zn^{II}{}_{2}}\mathbf{(N^{Me}N^{Me})_{2}\text{-}pz}(\mu\text{-}\mathrm{NO_{3}})(\mathrm{NO_{3}})_{2}]$ (**126**)	2:1	$(\mu\text{-pz})(\mu\text{-}NO_3)$	N_3O_3 oct.	3.918	AQEQOC	[105]
$[\mathrm{Zn^{II}{}_{4}}(\mathbf{(N^{Me}N^{Me})_{2}\text{-}pz})_{2}(\mu_{4}\text{-}\mathrm{CO_{3}})(\mu\text{-}\mathrm{OH})_{2}](\mathrm{BPh_{4}})_{2}$ (**127**)	4:2	$(\mu\text{-pz})(\mu\text{-}O_2CO)$	N_3O_2 trig.-bipy.	4.113; 4.156	AQEQUI	[105]
$[\mathrm{Zn^{II}{}_{4}}(\mathbf{(N^{Me}N^{Me})_{2}\text{-}pz})_{2}(\mu_{3}\text{-}\mathrm{NPP})(\mu\text{-}\mathrm{OH})_{2}](\mathrm{ClO_{4}})_{2}$ (**128**)	4:2	$(\mu\text{-pz})(\mu\text{-NPP})$	N_3O_2 trig.-bipy.	4.257(2)	SABHAF	[106]
$[\mathrm{Zn^{II}{}_{2}}\mathbf{(N^{Me}N^{Me})_{2}\text{-}pz}(\mu\text{-}\mathrm{DMP})(\mathrm{NO_{3}})_{2}]$ (**129**)	2:1	$(\mu\text{-pz})(\mu\text{-}O_2P(OMe)_2)$	N_3O_3 oct.	4.307	SABGUY	[106]
$[\mathrm{Ni^{II}{}_{2}}\mathbf{(N^{Me}N^{Me})_{2}\text{-}pz}(\mu\text{-}1,3\text{-}\mathrm{N_{3}})_{3}]_{\infty}$ (**130**)	2:1, polymer	$(\mu\text{-pz})(\mu\text{-}1,3\text{-}N_3)$	N_6 oct.	4.469	QOYXIL	[103]
$[\mathrm{Ni^{II}{}_{4}}(\mathbf{(N^{Me}C_{3}N^{Me})_{2}\text{-}pz)}_{2}(\mu\text{-}1,1\text{-}\mathrm{N_{3}})_{2}(\mu_{3}\text{-}1,1,3\text{-}\mathrm{N_{3}})_{2}(\mathrm{N_{3}})_{2}]$ (**131**)	4:2	$(\mu\text{-pz})(\mu\text{-}1,1\text{-}N_3)_2$	N_6 oct.	3.350(3)	YABNIZ	[109]
$[\mathrm{Ni^{II}{}_{2}}(\mathbf{(N^{Me}C_{3}N^{Me})_{2}\text{-}pz})(\mu\text{-}1,1\text{-}\mathrm{N_{3}})(\mathrm{O_{2}NO})_{2}]\cdot\mathrm{C_{4}H_{10}O}$ (**132**)	2:1	$(\mu\text{-pz})(\mu\text{-}1,1\text{-}N_3)$	N_4O_2 oct.	3.6575(2)	KENBEL	[110]
$[\mathrm{Ni^{II}{}_{4}}(\mathbf{(N^{Me}C_{3}N^{Me})_{2}\text{-}pz})_{2}(\mu\text{-}1,1\text{-}\mathrm{N_{3}})_{2}(\mu\text{-}1,3\text{-}\mathrm{N_{3}})_{2}](\mathrm{ClO_{4}})_{2}\cdot 2\mathrm{CH_{4}O}\cdot 0.5\mathrm{H_{2}O}$ (**133**)	4:2	$(\mu\text{-pz})(\mu\text{-}1,1\text{-}N_3)$	N_5 sq.-py.	3.620(1)	KENBIP	[110]
$[\mathrm{Ni^{II}{}_{4}}(\mathbf{(N^{Me}C_{3}N^{Me})_{2}\text{-}pz})_{2}(\mu\text{-}1,1\text{-}\mathrm{N_{3}})_{2}(\mu\text{-}1,3\text{-}\mathrm{N_{3}})_{2}](\mathrm{ClO_{4}})_{2}\cdot\mathrm{C_{3}H_{6}O}\cdot\mathrm{C_{5}H_{12}}$ (**134**)	4:2	$(\mu\text{-pz})(\mu\text{-}1,1\text{-}N_3)$	N_5 sq.-py.	3.614(1)	KERYIQ	[110]
$[\mathrm{Ni^{II}{}_{4}}(\mathbf{(N^{Me}C_{3}N^{Me})_{2}\text{-}pz})_{2}(\mu\text{-}1,1\text{-}\mathrm{N_{3}})_{2}(\mu\text{-}1,3\text{-}\mathrm{N_{3}})_{2}](\mathrm{BPh_{4}})_{2}\cdot\mathrm{C_{3}H_{6}O}$ (**135**)	4:2	$(\mu\text{-pz})(\mu\text{-}1,1\text{-}N_3)$	N_5 sq.-py.	3.645(1)	KENBOV	[110]

Table 1 (*Continued*)

Complex	M:L	Bridge	Coord.-sphere[a]	M···pz···M [Å][b]	CCDC code[c]	Refs.
[Zn$^{II}_2$H**(Opyr)$_2$-pz**(μ-Cl)Cl$_3$]·0.5OCMe$_2$ (**136**)	2:1	(μ-pz)(μ-Cl)	N_2OCl_2 trig.-bipy.	3.701(1); 3.696(1)	QUTFEQ	[111]
trans-[Cu$^{II}_2$**(pyC$_2$N^{Me})$_2$-pz**F(MeOH)$_2$(BF$_4$)](BF$_4$) (**137**)	2:1	μ-pz	N_3F_2 sq.-py.; N_3O_2 sq.-py	4.2903(8)	BICDAT	[112]
trans-[Cu$^{II}_2$**(pyC$_2$N^{Me})$_2$-pz**F(H$_2$O)$_2$(MeOH)](BF$_4$)$_2$ (**138**)	2:1	μ-pz	N_3FO sq.-py.; N_3O_2 sq.-py	4.287(1)	BICDEX	[112]
[Cu$^{II}_2$(**(pyC$_2$N^{Me})$_2$-pz**)(MeOH)$_2$(NO$_3$)$_2$] (**139**)	2:1	μ-pz	N_3O_2 sq.-py.	4.357(1)	617183	[113]
[Ni$^{II}_2$(**(pyC$_2$N^{Me})$_2$-pz**)(μ-Cl)Cl$_2$(H$_2$O)$_2$]$_2$·2H$_2$O (**140**)	4:2	(μ-pz)(μ-Cl)	N_3OCl_2 oct.	4.1119(5)	KICREU	[114]
[Cu$^{II}_2$(**(pyC$_2$N=C)$_2$-pz**)(H$_2$O)$_2$(OAc)$_3$] (**141**)	2:1	μ-pz	N_3O_2 trig.-bipy.; N_3O_3 oct.	4.4005(5)	YETBAB	[115]
[Cu$^{II}_2$(**(pyC$_2$N=C)$_2$-pz**)(NCS)$_2$(DMF)]BF$_4$ (**142**)	2:1	μ-pz	N_4 sq.-pl.; N_4O sq.-py.	4.5063	YESZOM	[115]
[Cu$^{II}_2$(H**(py=NN^{CO})$_2$-pz**)(μ-OH)(NO$_3$)(H$_2$O)](NO$_3$)·2H$_2$O (**143**)	2:1	(μ-pz)(μ-OH)	N_3O_2 sq.-py.	3.282	–/–	[116]
[Cu$^{II}_2$(H**(py=NN^{CO})$_2$-pz**)(μ-OH)(H$_2$O)$_2$](ClO$_4$)·H$_2$O (**144**)	2:1	(μ-pz)(μ-OH)	N_3O_2 sq.-py.	3.308	–/–	[116]
[Cu$^{II}_2$(H**(pim=NN^{CO})$_2$-pz**)(μ-OH)(H$_2$O)][Cu$^{II}_2$(H**(pim=NN^{CO})$_2$-pz**)(μ-OH)(ClO$_4$)](ClO$_4$)$_3$·4H$_2$O (**145**)	4:2	(μ-pz)(μ-OH)	N_3O_2 sq.-py.; N_3O sq.-pl.	3.244; 3.254	–/–	[116]
[Mn$^{III}_4$(**(Obz=N)$_2$-pz**)$_2$(μ-OMe)$_4$(MeOH)$_4$](ClO$_4$)$_2$ (**146**)	4:2	(μ-pz)(μ-OMe)	N_2O_4 oct.	3.485(3)	–/–	[117]
cis-[Cu$^{II}_2$**(pyS)$_2$-pz**(μ-N$_3$)(N$_3$)$_2$]·^{i}PrOH (**147**)	2:1	(μ-pz)(μ-N$_3$)	N_4S sq.-py.	3.486(2)	GUGJUN; GUGJUN01	[120,121]
cis-[Cu$^{II}_2$**(pyS)$_2$-pz**(μ-Br)Br(H$_2$O)]Br·2H$_2$O (**148**)	2:1	(μ-pz)(μ-Br)	N_2SOBr sq.-py.; N_2SBr_2 sq.-py.	3.706(2)	GUGKAU; GUGKAU01	[120,121]
cis-[Cu$^{II}_2$**(pyS)$_2$-pz**(μ-Cl)Cl(H$_2$O)]Cl·2H$_2$O (**149**)	2:1	(μ-pz)(μ-Br)	N_2SOCl sq.-py.; N_2SCl_2 sq.-py.	3.6356(8)	QIVQIV	[121]
[Ni$^{II}_4$(**(SN)$_2$-pz**)$_2$(μ_4-1,1,3,3-N$_3$)(μ-1,1-N$_3$)$_2$(μ-OAc)$_2$](ClO$_4$) (**150**)	4:2	(μ-pz)(μ-1,3-N$_3$)	N_4SO oct.	4.525(1); 4.477(1)	YAHLAV	[122]
[Ni$^{II}_4$(**(SN)$_2$-pz**)$_2$(μ_4-1,1,3,3-N$_3$)(μ-1,1-N$_3$)$_2$(μ-O$_2$CPh)$_2$](ClO$_4$) (**151**)	4:2	(μ-pz)(μ-1,3-N$_3$)	N_4SO oct.	4.452(1); 4.459(1)	YAHLEZ	[122]
trans-[Co$^{II}_2$**(N$^{Et}_2$N)$_2$-pz**(μ-Cl)Cl$_2$] (**152**)	2:1	(μ-pz)(μ-Cl)	N_3Cl_2 trig.-py.	3.818	ROJCAU	[97]
cis-[Co$^{II}_2$**(N$^{Me}_2$C$_3$N)$_2$-pz**(μ-Cl)Cl$_2$] (**153**)	2:1	(μ-pz)(μ-Cl)	N_3Cl_2 trig.-py.	3.942	ROJBOH	[97]
[Ni$^{II}_2$**(N$^{Et}_2$N)$_2$-pz**(μ-Cl)Cl$_2$] (**154**)	2:1	(μ-pz)(μ-Cl)	N_3Cl_2 sq.-py.	3.829	DEQWOL	[132]
[Ni$^{II}_2$**(N$^{Me}_2$C$_3$N)$_2$-pz**(μ-Cl)Cl$_2$] (**155**)	2:1	(μ-pz)(μ-Cl)	N_3Cl_2 sq.-py.	3.917	DEQWUR	[132]
[Co$^{II}_2$**(N$^{Et}_2$N)$_2$-pz**(μ-Cl)](BPh$_4$)$_2$ (**156**)	2:1	(μ-pz)(μ-Cl)	N_4Cl trig.-py.	3.833	ROJBIB	[97]
[Co$^{II}_2$**(N$^{Me}_2$C$_3$N)$_2$-pz**(μ-Cl)](BPh$_4$)$_2$ (**157**)	2:1	(μ-pz)(μ-Cl)	N_4Cl trig.-py.	3.909	ROJBUN	[97]
[Co$^{II}_2$**(N$^{Me}_2$C$_3$N)$_2$-pz**(μ-F)](BPh$_4$)$_2$ (**158**)	2:1	(μ-pz)(μ-F)	N_4F trig.-bipy.	3.577	NIDBAD	[126]
[Co$^{II}_2$**(N$^{Et}_2$N)$_2$-pz**(H$_2$O)F](BPh$_4$)$_2$ (**159**)	2:1	(μ-pz)(HOH···F)	N_4O trig.-bipy.; N_4F trig.-bipy.	4.282	NIDBEH	[126]
[Co$^{II}_2$**(N$^{Et}_2$N)$_2$-pz**(μ-Br)](BPh$_4$)$_2$ (**160**)	2:1	(μ-pz)(μ-Br)	N_4Br trig.-bipy.	3.935	NIDBIL	[126]
[Co$^{II}_2$**(N$^{Et}_2$N)$_2$-pz**(μ-1,3-N$_3$)](BPh$_4$)$_2$ (**161**)	2:1	(μ-pz)(μ-1,3-N$_3$)	N_5 trig.-bipy.	4.415	NIDBUX	[126]
[Zn$^{II}_2$**(N$^{Me}_2$C$_3$N)$_2$-pz**(μ-OH)](BPh$_4$)$_2$ (**162**)	2:1	(μ-pz)(μ-OH)	N_4O trig.-bipy.	3.613	NUHHUT	[124]
[Zn$^{II}_2$**(N$^{Et}_2$N)$_2$-pz**(μ-O$_2$H$_3$)](BPh$_4$)$_2$ (**163**)	2:1	(μ-pz)(μ-O$_2$H$_3$)	N_4O trig.-bipy.	4.374	NUHHON	[124]
[Zn$^{II}_2$**(N$^{Et}_2$N)$_2$-pz**(μ-O$_2$COH)](BPh$_4$)$_2$ (**164**)	2:1	(μ-pz)(μ-O$_2$COH)	N_4O trig.-bipy.	4.180	NUHJAB	[124]
[Zn$^{II}_2$**(N$^{Et}_2$N)$_2$-pz**(μ-oaa)](ClO$_4$)$_2$ (**165**)	2:1	(μ-pz)(μ-O$_2$C)	N_4O sq.-py.	4.1842(5)	DATVIE	[108]
[Zn$^{II}_2$**(N$^{Me}_2$C$_3$N)$_2$-pz**(oaa)$_2$](H$_3$O)(ClO$_4$)$_2$ (**166**)	2:1	(μ-pz)	$N_3O(O)$	4.328(1)	DATVOK	[108]
[Zn$^{II}_2$**(N$^{Et}_2$N)$_2$-pz**(μ-C$_3$H$_4$NO)](ClO$_4$)$_2$·MeOH (**167**)	2:1	(μ-pz)(μ-NOC)	N_5 trig.-bipy.; N_4O trig.-bipy.	4.277(1)	MARGAO	[133]
[Zn$^{II}_2$**(N$^{Et}_2$N)$_2$-pz**(μ-OAc)](ClO$_4$)$_2$·MeOH (**168**)	2:1	(μ-pz)(μ-OAc)	N_4O trig.-bipy.	4.2200(5)	644427	[135]
[Ni$^{II}_2$**(N$^{Me}_2$C$_3$N)$_2$-pz**(μ-OH)](BPh$_4$)$_2$ (**169**)	2:1	(μ-pz)(μ-OH)	N_4O trig.-bipy.	3.643	HOCJEO	[127]
[Ni$^{II}_2$**(N$^{Et}_2$N)$_2$-pz**(μ-O$_2$H$_3$)](BPh$_4$)$_2$ (**170**)	2:1	(μ-pz)(μ-O$_2$H$_3$)	N_4O sq.-py.	4.452	HOCKEP	[127]
[Ni$^{II}_2$**(N$^{Et}_2$N)$_2$-pz**(μ-O$_2$H$_3$)](ClO$_4$)$_2$ (**171**)	2:1	(μ-pz)(μ-O$_2$H$_3$)	N_4O sq.-py.	4.380(1)	ICASOU	[130]
[Cu$^{II}_2$**(N$^{Et}_2$N)$_2$-pz**(μ-O$_2$H$_3$)](BPh$_4$)$_2$ (**172**)	2:1	(μ-pz)(μ-O$_2$H$_3$)	N_4O sq.-py.	4.418(2)	ICASUA	[130]
[Ni$^{II}_2$**(N$^{Et}_2$N)$_2$-pz**(μ-NHCONH$_2$)](ClO$_4$)$_2$ (**173**)	2:1	(μ-pz)(μ-NHCOR)	$N_{4.5}O_{0.5}$[f] sq.-py.	4.357(2)	PIKQOP	[125]
[Ni$^{II}_2$**(N$^{Et}_2$N)$_2$-pz**(μ-O$_2$CNH$_2$)](ClO$_4$)$_2$ (**174**)	2:1	(μ-pz)(μ-O$_2$CR)	N_4O sq.-py.	4.229(1)	PIKQUV	[125]
[Ni$^{II}_2$**(N$^{Et}_2$N)$_2$-pz**(MeOH···OMe)](ClO$_4$)$_2$ (**175**)	2:1	μ-pz	N_4O sq.-py.	4.552	HAFMAD	[131]
[Ni$^{II}_2$**(N$^{Et}_2$N)$_2$-pz**(μ-NHOCPh)](ClO$_4$)$_2$ (**176**)	2:1	(μ-pz)(μ-NHCOPh)	N_5[e]; N_4O[e]	4.285	HOCJUE	[127]
[Ni$^{II}_2$(**N$^{Et}_2$N)$_2$-pz**(μ-1,3-NCO)](ClO$_4$)$_2$ (**177**)	2:1	(μ-pz)(μ-1,3-NCO)	N_5 trig.-bipy.; N_4O trig.-bipy.	4.383	HOCHUC	[127]
trans-[Ni$^{II}_2$**(N$^{Et}_2$N)$_2$-pz**(μ-O$_2$CC$_3$H$_6$OH)](ClO$_4$)$_2$ (**178**)	2:1	(μ-pz)(μ-O$_2$CR)	N_4O sq.-pl.	4.303	HOCJIS	[127]
[Ni$^{II}_2$**(N$^{Et}_2$N)$_2$-pz**(μ-OAc)(OAc)](BPh$_4$) (**179**)	2:1	(μ-pz)(μ-O$_2$CR)	N_4O trig.-bipy.; N_3O_2 oct.	4.189	HOCJAK	[127]
[Ni$^{II}_2$**(N$^{Et}_2$N)$_2$-pz**(μ-NHC≡N)](ClO$_4$)$_2$ (**180**)	2:1	(μ-pz)(μ-NHC≡N)	N_5 trig.-bipy.	4.458	MALTUO	[128]

$[\mathrm{Ni^{II}_2}\mathbf{(N^{Et}{}_2N)_2\text{-}pz}(\mu\text{-cnge})](\mathrm{ClO_4})_2$ (**181**)	2:1	$(\mu\text{-pz})(\mu\text{-}\mathrm{N{\equiv}CN{=}CNH(NH_2)})$	$\mathrm{N_5}$[e]; $\mathrm{N_4(NC)}$ sq.-py.[g]	3.985	MALVEA	[128]
$[\mathrm{Ni^{II}_2}\mathbf{(N^{Et}{}_2N)_2\text{-}pz}(\mathrm{cnge})_2](\mathrm{ClO_4})_3$ (**182**)	2:1	$\mu\text{-pz}$	$\mathrm{N_5}$ trig.-bipy.	4.586	MALVOK	[128]
$[\mathrm{Ni^{II}_2}\mathbf{(N^{Et}{}_2N)_2\text{-}pz}(\mu\text{-}o\text{-}\mathrm{O(N{\equiv}C)Ph})](\mathrm{ClO_4})_2$ (**183**)	2:1	$(\mu\text{-pz})(\mu\text{-}o\text{-}\mathrm{HO(N{\equiv}C)Ph})$	$\mathrm{N_5}$ sq.-py.	4.587	MALVIE	[128]
$[\mathrm{Ni^{II}_2}\mathbf{(N^{Et}{}_2N)_2\text{-}pz}(\mu\text{-}1,3\text{-}\mathrm{N_3})](\mathrm{ClO_4})_2$ (**184**)	2:1	$(\mu\text{-pz})(\mu\text{-}1,3\text{-}\mathrm{N_3})$	$\mathrm{N_5}$ trig.-bipy.	4.421(2)	YABNAR	[109]
$[\mathrm{Ni^{II}_2}\mathbf{(N^{Me}{}_2C_3N)_2\text{-}pz}(\mu\text{-}1,1\text{-}\mathrm{N_3})(\mathrm{NO_3})_2]$ (**185**)	2:1	$(\mu\text{-pz})(\mu\text{-}1,1\text{-}\mathrm{N_3})$	$\mathrm{N_4O_2}$ oct.	3.660(2)	YABMUK	[109]
$[\mathrm{Ni^{II}_4}(\mathbf{(N^{Me}{}_2C_3N)_2\text{-}pz})_2(\mu\text{-}1,1\text{-}\mathrm{N_3})_2(\mu\text{-}1,3\text{-}\mathrm{N_3})_2](\mathrm{BPh_4})_2$ (**186**)	4:2	$(\mu\text{-pz})(\mu\text{-}1,1\text{-}\mathrm{N_3})$	$\mathrm{N_5}$ sq.-py.	3.639(2)	YABNEV	[109]
$[\mathrm{Ni^{II}_2H}\mathbf{(N^{Me}{}_2C_3N)_2\text{-}pz}(\mu\text{-OH})(\mathrm{MeCN})_2](\mathrm{ClO_4})_3$ (**187**)	2:1	$(\mu\text{-pz})(\mu\text{-OH})$	$\mathrm{N_4O}$ trig.-bipy.	3.476	VACLEQ	[98]
$[\mathrm{Ni^{II}_2H}\mathbf{(N^{Me}{}_2C_3N)_2\text{-}pz}(\mu\text{-OH})(\mathrm{DMF})_2](\mathrm{ClO_4})_3$ (**188**)	2:1	$(\mu\text{-pz})(\mu\text{-OH})$	$\mathrm{N_3O_2}$ sq.-py.	3.501	VACLIU	[98]
$[\mathrm{Ni^{II}_2H}\mathbf{(N^{Me}{}_2C_3N)_2\text{-}pz}(\mu\text{-OH})(\mathrm{NCS})_2](\mathrm{ClO_4})$ (**189**)	2:1	$(\mu\text{-pz})(\mu\text{-OH})$	$\mathrm{N_4O}$ sq.-py.	3.638	VACPAQ	[98]
$[\mathrm{Ni^{II}_2}\mathbf{(N^{Et}{}_2N)_2\text{-}pz}(\mu\text{-CN})(\mathrm{MeCN})](\mathrm{ClO_4})_2$ (**190**)	2:1	$(\mu\text{-pz})(\mu\text{-CN})$	$\mathrm{N_6}$ oct.; $\mathrm{N_3C}$ sq.-pl.	4.002	NEPDUH	[129]
$\{[\mathrm{Ni^{II}_2}\mathbf{(N^{Et}{}_2N)_2\text{-}pz}(\mu\text{-CN})]_4[\mathrm{Ni^{II}}(\mu\text{-CN})_4]\}(\mathrm{ClO_4})_6$ (**191**)	9:4	$(\mu\text{-pz})(\mu\text{-CN})$	$\mathrm{N_6}$ oct.; $\mathrm{N_3C}$ sq.-pl.	4.022; 3.994; 4.024; 4.033	NEPFAP	[129]
cis-$[\mathrm{Cu^{II}_2H_2}\mathbf{(N^{Me}{}_2C_3N)_2\text{-}pz}(\mu\text{-OH})(\mathrm{BF_4})_2]$ (**192**)	2:1	$(\mu\text{-pz})(\mu\text{-OH})$	$\mathrm{N_3OF}$ sq.-py.	3.447(2)	ADILAA	[104]
trans-$[\mathrm{Cu^{II}_2}\mathbf{(N^{Et}{}_2N)_2\text{-}pz}(\mathrm{MeOH{\cdots}OMe})](\mathrm{ClO_4})_2$ (**193**)	2:1	$\mu\text{-pz}$	$\mathrm{N_4O}$[e]	4.553(1)	ADILII	[104]
trans-$[\mathrm{Cu^{II}_2H}\mathbf{(N^{Et}{}_2N)_2\text{-}pz}(\mathrm{TCC})(\mathrm{H_2O})](\mathrm{ClO_4})_2$ (**194**)	2:1	$\mu\text{-pz}$	$\mathrm{N_3O_2}$ sq.-py.; $\mathrm{N_4O}$ sq.-py.	4.202(1)	ADIMAB	[104]
$[\mathrm{Zn^{II}_2}\mathbf{(N^{Et}{}_2N)_2\text{-}pz}(\mathrm{HO{\cdots}HOMe})](\mathrm{ClO_4})_2$ (**195**)	2:1	$\mu\text{-pz}$	$\mathrm{N_4O}$ trig.-bipy.	4.406(1)	SABGEI	[106]
$[\mathrm{Zn^{II}_2}\mathbf{(N^{Et}{}_2N)_2\text{-}pz}(\mu\text{-DMP})](\mathrm{ClO_4})_2$ (**196**)	2:1	$(\mu\text{-pz})(\mu\text{-DMP})$	$\mathrm{N_4O}$ trig.-bipy.	4.406(1)	SABGOS	[106]
$[\mathrm{Ni^{II}_2H_4}\mathbf{[(FN)_2C_3N]_2\text{-}pz}(\mu\text{-Cl})\mathrm{Cl_2}]$ (**197**)	2:1	$(\mu\text{-pz})(\mu\text{-Cl})$	$\mathrm{N_3Cl_2}$ sq.-py.; $\mathrm{N_4Cl_2}$ oct.	3.991	DEQXEC	[132]
$[\mathrm{Co^{II}_2H_4}\mathbf{[(FN)_2C_3N]_2\text{-}pz}(\mu\text{-Cl})\mathrm{Cl_2}]$ (**198**)	2:1	$(\mu\text{-pz})(\mu\text{-Cl})$	$\mathrm{N_3Cl_2}$ sq.-py.; $\mathrm{N_4Cl_2}$ oct.	3.992	DEQXIG	[132]
$[\mathrm{Co^{II}_2H_5}\mathbf{[(FN)_2C_3N]_2\text{-}pz}\mathrm{Cl_4}]$ (**199**)	2:1	$(\mu\text{-pz})(\mu\text{-Cl})$	$\mathrm{NCl_3}$ tetr.; $\mathrm{N_4Cl_2}$ oct.	3.751	DEQXAY	[132]
$[n\mathrm{Pr_4N}]_2[\mathrm{Co^{II}_2H_4}\mathbf{({}^tBu\text{-}urea_2N)_2\text{-}pz}(\mu\text{-Cl})]\cdot\mathrm{DMA}$ (**200**)	2:1	$(\mu\text{-pz})(\mu\text{-Cl})$	$\mathrm{N_4Cl}$ trig.-bipy.	4.1132(3)	CEHXUJ	[136]
$[n\mathrm{Pr_4N}]_2[\mathrm{Co^{II}_2H_4}\mathbf{({}^iPr\text{-}urea_2N)_2\text{-}pz}(\mu\text{-Cl})]\cdot0.5\mathrm{DMA}$ (**201**)	2:1	$(\mu\text{-pz})(\mu\text{-Cl})$	$\mathrm{N_4Cl}$ trig.-bipy.	–/–	CEHXOD	[136]
$[n\mathrm{Pr_4N}]_2[\mathrm{Co^{II}_2H_4}\mathbf{({}^iPr\text{-}urea_2N)_2\text{-}pz}(\mu\text{-OH})]$ (**202**)	2:1	$(\mu\text{-pz})(\mu\text{-OH})$	$\mathrm{N_4O}$ trig.-bipy.	3.5857(5)	–/–	[137]
$[n\mathrm{Pr_4N}]_2[\mathrm{Co^{II}_2H_4}\mathbf{({}^iPr\text{-}urea_2N)_2\text{-}pz}(\mu\text{-}1,3\text{-}\mathrm{OC(NH)Me})]\cdot\mathrm{DMA}$ (**203**)	2:1	$(\mu\text{-pz})(\mu\text{-ONHC})$	$\mathrm{N_5}$ trig.-bipy.; $\mathrm{N_4O}$ trig.-bipy.	4.482(1)	–/–	[137]
$[n\mathrm{Pr_4N}]_2[\mathrm{Co^{II}_2H_4}\mathbf{({}^tBu\text{-}urea_2N)_2\text{-}pz}(\mu\text{-}1,3\text{-}\mathrm{OC(NH)Me})]\cdot\mathrm{DMA}$ (**204**)	2:1	$(\mu\text{-pz})(\mu\text{-ONHC})$	$\mathrm{N_5}$ trig.-bipy.; $\mathrm{N_4O}$ trig.-bipy.	4.6697(5)	–/–	[137]
$[n\mathrm{Pr_4N}]_2[\mathrm{Co^{II}_2H_4}\mathbf{({}^iPr\text{-}urea_2N)_2\text{-}pz}(\mu\text{-}1,3\text{-OAc})]\cdot\mathrm{DMA}$ (**205**)	2:1	$(\mu\text{-pz})(\mu\text{-}1,3\text{-OAc})$	$\mathrm{N_4O}$ trig.-bipy.	4.311(1)	–/–	[137]
$[n\mathrm{Pr_4N}]_2[\mathrm{Co^{II}_2H_4}\mathbf{({}^tBu\text{-}urea_2N)_2\text{-}pz}(\mu\text{-}1,3\text{-OAc})]\cdot\mathrm{DMA}$ (**206**)	2:1	$(\mu\text{-pz})(\mu\text{-}1,3\text{-OAc})$	$\mathrm{N_4O}$ trig.-bipy.	4.6507(5)	–/–	[137]
$[\mathrm{Cu^{II}_2}\mathbf{(py_2N)_2\text{-}pz}(\mathrm{MeOH})\mathrm{F}](\mathrm{BF_4})_2$ (**207**)	2:1	$\mu\text{-pz}$	$\mathrm{N_4F}$ trig.-bipy.; $\mathrm{N_4O}$ trig.-bipy.	4.291(1)	BICCOG	[112]
$[\mathrm{Cu^{II}_2}\mathbf{[(pyC_2)_2N]_2\text{-}pz}(\mathrm{MeOH})\mathrm{F}](\mathrm{BF_4})_2$ (**208**)	2:1	$\mu\text{-pz}$	$\mathrm{N_4F}$ sq.-py.; $\mathrm{N_4O}$ sq.-py.	4.430(1)	BICCUM	[112]
$[\mathrm{Cu^{II}_2}\mathbf{[(pyC_2)_2N]_2\text{-}py}(\mathrm{OH})](\mathrm{ClO_4})_2$ (**209**)	2:1	$(\mu\text{-pz})(\mu\text{-OH})$	$\mathrm{N_4O}$ sq.-py.	–/–	617184	[113]
$[\mathrm{Cu^{II}_2}\mathbf{[(pyC_2)_2N]_2\text{-}py}(\mathrm{OH})](\mathrm{CF3SO_3})_2$ (**210**)	2:1	$(\mu\text{-pz})(\mu\text{-OH})$	$\mathrm{N_4O}$ sq.-py.	3.518(5)	617185	[113]
$[\mathrm{Ni^{II}_2}\mathbf{[(pyC_2)_2N]_2\text{-}pz}(\mu\text{-Cl})\mathrm{Cl_2}]\cdot2\mathrm{MeOH}$ (**211**)	2:1	$(\mu\text{-pz})(\mu\text{-Cl})$	$\mathrm{N_4Cl_2}$ oct.	4.0917(6)	KICQUJ	[114]
$[\mathrm{Ni^{II}_2}\mathbf{[(pyC_2)_2N]_2\text{-}pz}(\mu\text{-Cl})\mathrm{MeOH}](\mathrm{ClO_4})_2$ (**212**)	2:1	$(\mu\text{-pz})(\mu\text{-Cl})$	$\mathrm{N_4ClO}$ oct.; $\mathrm{N_4Cl}$ sq.-py.	4.0038(8)	KICRAQ	[114]
$[\mathrm{Ni^{II}_2}\mathbf{(py_2N)_2\text{-}pz}(\mu\text{-Cl})\mathrm{Cl}(\mathrm{MeOH})_2]\mathrm{Cl}\cdot2\mathrm{MeOH}$ (**213**)	2:1	$\mu\text{-pz}$	$\mathrm{N_4ClO}$ oct.	4.6007(7)	KICRIY	[114]
$[\mathrm{Zn^{II}_2}\mathbf{(py_2N)_2\text{-}pz}(\mu\text{-OAc})](\mathrm{ClO_4})_2\cdot\mathrm{OCMe_2}$ (**214**)	2:1	$(\mu\text{-pz})(\mu\text{-OAc})$	$\mathrm{N_4O}$ trig.-bipy.	3.9794(8)	644426	[135]
$[\mathrm{Zn^{II}_2}\mathbf{[(pyC_2)_2N]_2\text{-}pz}(\mu\text{-OH})](\mathrm{ClO_4})_2$ (**215**)	2:1	$(\mu\text{-pz})(\mu\text{-OH})$	$\mathrm{N_4O}$[e]	3.479(1)	KARXIL	[138]
$[\mathrm{Zn^{II}_2}\mathbf{(py_2N)_2\text{-}pz}(\mathrm{OH})(\mathrm{MeOH})](\mathrm{ClO_4})_2$ (**216**)	2:1	$\mu\text{-pz}$	$\mathrm{N_4O}$ trig.-bipy.	4.1518(6)	KARXOR	[138]
$[\mathrm{Zn^{II}_2}\mathbf{[(pyC_2)_2N]_2\text{-}pz}(\mathrm{O_2P(OMe)_2})](\mathrm{ClO_4})_2$ (**217**)	2:1	$(\mu\text{-pz})(\mu\text{-}\mathrm{O_2P(OMe)_2})$	$\mathrm{N_4O}$ trig.-bipy.	4.402(1)	KARXUX	[138]
$[\mathrm{Zn^{II}_2}\mathbf{(py_2N)_2\text{-}pz}(\mathrm{O_2P(OMe)_2})](\mathrm{ClO_4})_2$ (**218**)	2:1	$(\mu\text{-pz})(\mu\text{-}\mathrm{O_2P(OMe)_2})$	$\mathrm{N_4O}$ trig.-bipy.	4.212(1)	KARYAE	[138]
$[\mathrm{Zn^{II}_2}\mathbf{(py_2N)_2\text{-}pz}(\mu\text{-}\mathrm{C_3H_4NO})](\mathrm{ClO_4})_2\cdot\mathrm{OCMe_2}$ (**219**)	2:1	$(\mu\text{-pz})(\mu\text{-NOC})$	$\mathrm{N_5}$ trig.-bipy.; $\mathrm{N_4O}$ trig.-bipy.	4.015(1)	MARGES	[133]
$[\mathrm{Zn^{II}_2}\mathbf{(Im_2N)_2\text{-}pz}(\mu\text{-OAc})](\mathrm{ClO_4})_2\cdot2\mathrm{OCMe_2}$ (**220**)	2:1	$(\mu\text{-pz})(\mu\text{-OAc})$	$\mathrm{N_4O}$ trig.-bipy.	3.9216(6)	644424	[135]
$[\mathrm{Zn^{II}_2}\mathbf{(Im_2N)_2\text{-}pz}(\mu\text{-OAc})](\mathrm{ClO_4})_2\cdot2\mathrm{MeCN}$ (**221**)	2:1	$(\mu\text{-pz})(\mu\text{-OAc})$	$\mathrm{N_4O}$ trig.-bipy.	3.863(1)	644425	[135]
$[\mathrm{Zn^{II}_2}\mathbf{(ImpyN)_2\text{-}pz}(\mu\text{-OAc})](\mathrm{ClO_4})_2\cdot0.5\mathrm{OCMe_2}$ (**222**)	2:1	$(\mu\text{-pz})(\mu\text{-OAc})$	$\mathrm{N_4O}$ trig.-bipy.	4.0151(6)	644428	[135]
$[\mathrm{Zn^{II}_2}\mathbf{(ImN^{Et}N)_2\text{-}pz}(\mu\text{-OAc})](\mathrm{ClO_4})_2\cdot\mathrm{OCMe_2}$ (**223**)	2:1	$(\mu\text{-pz})(\mu\text{-OAc})$	$\mathrm{N_4O}$ trig.-bipy.	4.003(1)	644429	[135]
$[\mathrm{Cu^{II}_2}\mathbf{(Im_2N)_2\text{-}pz}(\mathrm{OMe})(\mathrm{MeOH})](\mathrm{ClO_4})_2\cdot\mathrm{MeCN}$ (**224**)	2:1	$\mu\text{-pz}$	$\mathrm{N_4O}$ sq.-py.	4.3405(6)	–/–	[139]
$[\mathrm{Cu^{II}_2}\mathbf{(Im_2N)_2\text{-}pz}(\mathrm{OMe})(\mathrm{MeOH})](\mathrm{NO_3})_2\cdot5\mathrm{H_2O}$ (**225**)	2:1	$\mu\text{-pz}$	$\mathrm{N_4O}$ sq.-py.	–/–	–/–	[139]
$[\mathrm{Cu^{II}_2}\mathbf{(Im_2N)_2\text{-}pz}(\mathrm{NO_3})(\mathrm{H_2O})]_2(\mathrm{NO_3})_4\cdot5\mathrm{H_2O}$ (**226**)	4:2	$(\mu\text{-pz})_2$	$\mathrm{N_5}$ trig.-bipy.; $\mathrm{N_3O_2}$ sq.-py.	3.8674(6)	–/–	[139]
$[\mathrm{Ni^{II}_2}\mathbf{(S_2N)_2\text{-}pz}(\mu\text{-Cl})\mathrm{Cl_2}](\mathrm{ClO_4})_2$ (**227**)	2:1	$(\mu\text{-pz})(\mu\text{-Cl})$	$\mathrm{N_2S_2Cl_2}$ oct.	3.823	NICVUQ	[141]
$[\mathrm{Ni^{II}_2}\mathbf{(S_2N)_2\text{-}pz}(\mu\text{-OAc})(\mathrm{OCMe_2})_2]$ (**228**)	2:1	$(\mu\text{-pz})(\mu\text{-OAc})$	$\mathrm{N_2S_2O_2}$ oct.	4.162	CIQLOD	[101]
$[\mathrm{Ni^{II}_2}\mathbf{(S_2N)_2\text{-}pz}(\mu\text{-OAc})(\mathrm{benzylurea})_2)](\mathrm{ClO_4})_2$ (**229**)	2:1	$(\mu\text{-pz})(\mu\text{-OAc})$	$\mathrm{N_2S_2O_2}$ oct.	4.196	CIQLUJ	[101]
$[\mathrm{Ni^{II}_4}(\mathbf{(S_2N)_2\text{-}pz})_2(\mu\text{-}1,1,3\text{-}\mathrm{N_3})_2(\mu\text{-}1,3\text{-}\mathrm{N_3})(\mu\text{-OAc})](\mathrm{ClO_4})_2$ (**230**)	4:2	$(\mu\text{-pz})(\mu\text{-}1,3\text{-}\mathrm{N_3})$	$\mathrm{N_4SO}$ oct.; $\mathrm{N_4S_2}$ oct.	4.479; 4.461	HUXPUL; HUXPUL01	[142,143]
$[\mathrm{Ni^{II}_4}(\mathbf{(S_2N)_2\text{-}pz})_2(\mu\text{-}1,1,3,3\text{-}\mathrm{N_3})(\mu\text{-}1,1\text{-}\mathrm{N_3})_2(\mu\text{-OAc})_2)](\mathrm{ClO_4})$ (**231**)[h]	4:2	$(\mu\text{-pz})(\mu\text{-}1,3\text{-}\mathrm{N_3})$	$\mathrm{N_4SO}$ oct.	–/–	–/–	[142]
$[\mathrm{Ni^{II}_4}(\mathbf{(S_2N)_2\text{-}pz})_2(\mu\text{-}1,1,3,3\text{-}\mathrm{N_3})(\mu\text{-}\mathrm{O_2C\text{-}Ada})_4)](\mathrm{ClO_4})$ (**232**)	4:2	$(\mu\text{-pz})(\mu\text{-}1,3\text{-}\mathrm{N_3})$	$\mathrm{N_3SO_2}$ oct.	4.521(1); 4.508(1)	HUXQAS; HUXQAS01	[122,142]

Table 1 (*Continued*)

Complex	M:L	Bridge	Coord.-sphere[a]	M···pz···M [Å][b]	CCDC code[c]	Refs.
$[Ni^{II}_4(\mathbf{(S_2N)_2\text{-}pz})_2(\mu\text{-}1,1,3,3\text{-}N_3)(\mu\text{-}1,1\text{-}N_3)_2(\mu\text{-}O_2CPh)_2)](ClO_4)$ (**233**)	4:2	$(\mu\text{-}pz)(\mu\text{-}1,3\text{-}N_3)$	N_4SO oct.	4.452(1)	–/–	[122]
$[Ni^{II}_4(\mathbf{(^{\mathit{i}}PrS_2N)_2\text{-}pz})_2(\mu\text{-}1,1,3,3\text{-}N_3)(\mu\text{-}1,1\text{-}N_3)_2(\mu\text{-}OAc)_2)](ClO_4)$ (**234**)[h]	4:2	$(\mu\text{-}pz)(\mu\text{-}1,3\text{-}N_3)$	N_4SO oct.	–/–	–/–	[122]
$[Ni^{II}_4(\mathbf{(^{\mathit{i}}PrS_2N)_2\text{-}pz})_2(\mu\text{-}1,1,3,3\text{-}N_3)(\mu\text{-}1,1\text{-}N_3)_2(\mu\text{-}O_2C\text{-}Ada)_2)](ClO_4)$ (**235**)	4:2	$(\mu\text{-}pz)(\mu\text{-}1,3\text{-}N_3)$	N_4SO oct.	4.502(1)	YAHLID	[122]
$[Ni^{II}_4(\mathbf{(MeS_2N)_2\text{-}pz})_2(\mu\text{-}1,1,3,3\text{-}N_3)(\mu\text{-}O_2C\text{-}Ada)_4)](ClO_4)$ (**236**)[h]	4:2	$(\mu\text{-}pz)(\mu\text{-}1,3\text{-}N_3)$	N_4SO oct.	–/–	–/–	[122]
$[Ni^{II}_4(\mathbf{(S_2N)_2\text{-}pz})_2(\mu\text{-}1,1,3\text{-}N_3)_2(\mu\text{-}1,3\text{-}N_3)(\mu\text{-}O_2CPh)](ClO_4)_2$ (**237**)	4:2	$(\mu\text{-}pz)(\mu\text{-}1,3\text{-}N_3)$	N_4SO oct.; N_4S_2 oct.	4.466(1)	FODSIB	[143]
$[Ni^{II}_4(\mathbf{(^{\mathit{i}}PrS_2N)_2\text{-}pz})_2(\mu\text{-}1,1,3\text{-}N_3)_2(\mu\text{-}1,3\text{-}N_3)(\mu\text{-}O_2CPh)](ClO_4)_2$ (**238**)	4:2	$(\mu\text{-}pz)(\mu\text{-}1,3\text{-}N_3)$	N_4SO oct.; N_4S_2 oct.	4.449(2)	FODSUN	[143]
$[Ni^{II}_2\mathbf{(S_2N)_2\text{-}pz}(\mu\text{-}1,3\text{-}N_3)(OCMe_2)](ClO_4)_2$ (**239**)	2:1	$(\mu\text{-}pz)(\mu\text{-}1,3\text{-}N_3)$	N_3S_2O oct.	4.441(4)	611376	[144]
$[Ni^{II}_2\mathbf{(S_2N)_2\text{-}pz}(\mu\text{-}1,3\text{-}N_3)(OCMe_2)](BPh_4)_2$ (**240**)	2:1	$(\mu\text{-}pz)(\mu\text{-}1,3\text{-}N_3)$	N_3S_2O oct.	4.383(5)	611377	[144]
$[Ni^{II}_4(\mathbf{(S_2N)_2\text{-}pz})_2(\mu\text{-}1,1,3\text{-}N_3)_2(MeOH)_2](ClO_4)_4$ (**241**)	4:2	$(\mu\text{-}pz)(\mu\text{-}1,3\text{-}N_3)$	N_3S_2O oct.; N_4S_2 oct.	4.383(1)	611378	[144]
$[Ni^{II}_2\mathbf{(S_2N)_2\text{-}pz}(\mu\text{-}1,3\text{-}N_3)_2]_n(ClO_4)_n\cdot 2nCH_2Cl_2$ (**242**) (space group $P2_1/c$)	2:1, polymer	$(\mu\text{-}pz)(\mu\text{-}1,3\text{-}N_3)$	N_4S_2 oct.	–/–	611379	[144]
$[Ni^{II}_2\mathbf{(S_2N)_2\text{-}pz}(\mu\text{-}1,3\text{-}N_3)_2]_n(ClO_4)_n\cdot 2nCH_2Cl_2$ (**243**) (space group $P2_1/n$)	2:1, polymer	$(\mu\text{-}pz)(\mu\text{-}1,3\text{-}N_3)$	N_4S_2 oct.	–/–	611380	[144]
$[Ni^{II}_2\mathbf{(S_2N)_2\text{-}pz}(\mu\text{-}1,3\text{-}N_3)_2]_n(BPh_4)_n\cdot 0.58nOCMe_2$ (**244**)	2:1, polymer	$(\mu\text{-}pz)(\mu\text{-}1,3\text{-}N_3)$	N_4S_2 oct.	–/–	611381	[144]
$[Ni^{II}_2\mathbf{(S_2N)_2\text{-}pz}(\mu\text{-}1,3\text{-}N_3)(N_3)_2]$ (**245**)	2:1	$(\mu\text{-}pz)(\mu\text{-}1,3\text{-}N_3)$	N_4S_2 oct.	4.5538(8) (133 K); 4.5201(8) (253 K)	TAYLEL; TAYLEL01; TAYLEL02; TAYLEL03	[145]
$[Ni^{II}_2(\mathbf{S_2N\text{-}pz\text{-}N_3})(\mu\text{-}Cl)Cl_2]$ (**246**)	2:1	$(\mu\text{-}pz)(\mu\text{-}Cl)$	N_2S_2Cl oct.; N_3Cl_2 sq.-py	3.823	NICWAX	[141]
$[Ni^{II}_2(\mathbf{S_2N\text{-}pz\text{-}N_3})(\mu\text{-}Cl)Cl](BPh_4)$ (**247**)	2:1	$(\mu\text{-}pz)(\mu\text{-}Cl)$	N_2S_2Cl oct.; N_4Cl sq.-py	3.903	NICWEB	[141]
$([Ni^{II}_2(\mathbf{S_2N\text{-}pz\text{-}N_3})(\mu\text{-}OAc)(urea))](ClO_4)_2$ (**248**)	2:1	$(\mu\text{-}pz)(\mu\text{-}OAc)$	$N_2S_2O_2$ oct.; N_4O trig.-bipy.	4.221	CIQMAQ	[101]
cis-$[Cu^{II}_2\mathbf{(\mathit{c}N_3)_2\text{-}pz}(\mu\text{-}1,3\text{-}N_3)](PF_6)_2$ (**249**)	2:1	$(\mu\text{-}pz)(\mu\text{-}1,3\text{-}N_3)$	N_5 sq.-py.	4.15	ZADTIH	[146]
trans-$[Ni^{II}_2\mathbf{(\mathit{c}N_3)_2\text{-}pz}(\mu\text{-}1,3\text{-}N_3)(H_2O)_2](ClO_4)_2$ (**250**)	2:1	$(\mu\text{-}pz)(\mu\text{-}1,3\text{-}N_3)$	N_5O oct.	4.45	SAQMUS	[147]
$[Cu^{II}_2\mathbf{(\mathit{c}N_2S)_2\text{-}pz}(\mu\text{-}O_2SO_2)(H_2O)](PF_6)$ (**251**)	2:1	$(\mu\text{-}pz)(\mu\text{-}O_2SO_2)$	N_3SO trig.-bipy.; N_3SO_2 oct.	4.16	SAQNED	[147]
$[Cu^{II}_2\mathbf{(\mathit{c}NS_2)_2\text{-}pz}(\mu\text{-}Cl)](ClO_4)_2$ (**252**)	2:1	$(\mu\text{-}pz)(\mu\text{-}Cl)$	N_2S_2Cl trig.-bipy.	3.70	SAQMOM	[147]
$[Cu^{II}_2\mathbf{(\mathit{c}NS_2)_2\text{-}pz}(\mu\text{-}Br)](ClO_4)_2$ (**253**)	2:1	$(\mu\text{-}pz)(\mu\text{-}Br)$	N_2S_2Br trig.-bipy.	3.76	SAQNAZ	[147]
$[Cu^{II}_2\mathbf{(\mathit{c}N_3)_2\text{-}pz}(\mu\text{-}O_2PPh_2)](ClO_4)_2$ (**254**)	2:1	$(\mu\text{-}pz)(\mu\text{-}O_2PPh_2)$	N_4O sq.-py.	4.210	WABSIC	[149]
$[Cu^{II}_4(\mathbf{(\mathit{c}N_3)_2\text{-}pz})_2(\mu_4\text{-}O_4P)](ClO_4)_3$ (**255**)	4:2	$(\mu\text{-}pz)(\mu\text{-}O_4P)$	N_4O sq.-py.	4.03; 4.10	WABSOI	[149]
trans-$[Zn^{II}_2\mathbf{(\mathit{c}^{\mathit{i}}PrN_3)_2\text{-}pz}(\mu\text{-}OH)](ClO_4)_2$ (**256**)	2:1	$(\mu\text{-}pz)(\mu\text{-}OH)$	N_4O sq.-py.	3.460	SABGIM	[106]
$[Ni^{II}_2\mathbf{(\mathit{c}^{\mathit{i}}PrN_3)_2\text{-}pz}(\mu\text{-}O_2H_3)](ClO_4)_2$ (**257**)	2:1	$(\mu\text{-}pz)(\mu\text{-}O_2H_3)$	N_4O[e]	4.475	OHATOG	[152]
$[Cu^{II}_2\mathbf{(\mathit{c}^{\mathit{i}}PrN_3)_2\text{-}pz}(\mu\text{-}O_2H_3)](ClO_4)_2$ (**258**)	2:1	$(\mu\text{-}pz)(\mu\text{-}O_2H_3)$	N_4O[e]	4.41	617186	[113]
$[Ni^{II}_2\mathbf{(\mathit{c}N_3)\text{-}pz\text{-}(C_2\mathit{c}N_3)}(\mu\text{-}OH)](BPh_4)_2$ (**259**)	2:1	$(\mu\text{-}pz)(\mu\text{-}OH)$	N_4O sq.-py.	3.500	OHATUM	[152]
$[Ni^{II}_2\mathbf{(\mathit{c}^{\mathit{i}}PrN_3)_2\text{-}pz}(\mu\text{-}OAc)](BPh_4)_2$ (**260**)	2:1	$(\mu\text{-}pz)(\mu\text{-}OAc)$	N_4O trig.-bipy.	4.269	OHAVAU	[152]
$[Ni^{II}_2\mathbf{(\mathit{c}N_3)\text{-}pz\text{-}(C_2\mathit{c}N_3)}(\mu\text{-}NHCONH_2)](ClO_4)_2$ (**261**)	2:1	$(\mu\text{-}pz)(\mu\text{-}NHCONHR)$	N_5 sq.-py.; N_4O[e]	4.282	OHAVEY	[152]
$[Ni^{II}_2\mathbf{(\mathit{c}N_3)\text{-}pz\text{-}(C_2\mathit{c}N_3)}(\mu\text{-}NHCONHPh)](ClO_4)_2$ (**262**)	2:1	$(\mu\text{-}pz)(\mu\text{-}NHCONHR)$	N_5 sq.-py.; N_4O[e]	4.255	OHAVIC	[152]
$[Ni^{II}_2\mathbf{(\mathit{c}N_3)\text{-}pz\text{-}(C_2\mathit{c}N_3)}(\mu\text{-}NHCONHCH_2Ph)](ClO_4)_2$ (**263**)	2:1	$(\mu\text{-}pz)(\mu\text{-}NHCONHR)$	N_5 sq.-py.; N_4O[e]	4.265	OHAVOI	[152]
$[Ni^{II}_2\mathbf{(\mathit{c}_{\mathit{i}}PrN_3)_2\text{-}pz}(\mu\text{-}O_2CNH_2)](ClO_4)_2$ (**264**)	2:1	$(\mu\text{-}pz)(\mu\text{-}O_2CR)$	N_4O sq.-py	4.262	OHAVUO	[152]
$[Ni^{II}_2\mathbf{(\mathit{c}_{\mathit{i}}PrN_3)_2\text{-}pz}(\mu\text{-}OCN)(NCO)](ClO_4)$ (**265**)	2:1	$(\mu\text{-}pz)(\mu\text{-}OCN)$	N_5O oct.; N_5 sq.-py.	4.661	OHAWAV	[152]
$[Ni^{II}_2\mathbf{(\mathit{c}^{\mathit{i}}PrN_3)_2\text{-}pz}(\mu\text{-}NHCOOMe)](ClO_4)$ (**266**)	2:1	$(\mu\text{-}pz)(\mu\text{-}OCNHR)$	N_5 sq.-py.; N_4O sq.-py.	4.281	OHAWEZ	[152]
$[Cu^{II}_2H_6\mathbf{(NN_2\text{-}pz)_{2m}}](ClO_4)_2$ (**267**)	2:2[i]	$(\mu\text{-}pz)_2$	N_5 sq.-py.	3.924(3)	POKVAM	[156]
$[Zn^{II}_2H_6\mathbf{(NN_2\text{-}pz)_{2m}}](ClO_4)_2$ (**268**)	2:2[i]	$(\mu\text{-}pz)_2$	N_5 sq.-py.	3.99	FEBFAU	[162]
$[Cu^{II}_2H_6\mathbf{[N(NC_3)_2\text{-}pz]_{2m}}](ClO_4)_2$ (**269**)	2:2[i]	$(\mu\text{-}pz)_2$	N_5 sq.-py.	3.96	FEBFEY	[162]
$[Zn^{II}_2H_6\mathbf{[N(NC_3)_2\text{-}pz]_{2m}}](ClO_4)_2$ (**270**)	2:2[i]	$(\mu\text{-}pz)_2$	N_5 sq.-py.	3.96	FEBFIC	[162]
$[Cu^{II}_4(H_4\mathbf{(N_2\text{-}pz)_{2m}})_2(H_2O)_2(ClO_4)_2](ClO_4)_2$ (**271**)	4:4[i]	$(\mu\text{-}pz)_2$	N_4O sq.-py.	3.967	XITTUP	[158]
$[Cu^{II}_2\mathbf{[(N{=}C)_2\text{-}pz]_{2m}}(OAc)_2]$ (**272**)	2:2[i]	$(\mu\text{-}pz)_2$	N_4O sq.-py.	4.0160(8)	YETBEF	[115]

[Cu$^{II}_2$**[(N=C)$_2$-pz]$_{2m}$**(NCS)$_2$] (**273**)	2:2[i]	(μ-pz)$_2$	N$_5$ sq.-py.	4.004(2)	YESZUS	[115]
[Cu$^{II}_2$H$_8$**N$_2$(N$_2$-pz)$_{3m}$**](ClO$_4$)$_3$·2H$_2$O (**274**)	2:2[i]	(μ-pz)$_2$	N$_4$O sq.-py.	3.960(3); 3.960(3)	EBAREE; EBAREE01[j]	[160,161]
[Ni$^{II}_4$(**P-pz-N$_2$**)$_2$(μ-Cl)$_4$Cl$_2$] (**275**)	4:2	(μ-pz)(μ-Cl)	NPCl$_2$ sq.-pl.; N$_3$Cl$_3$ oct.	3.780(6)	QUPPEW	[164]
[Ni$^{II}_2$**P-pz-NS$_2$**(μ-Cl)Cl$_2$] (**276**)	2:1	(μ-pz)(μ-Cl)	NPCl$_2$ sq.-pl.; N$_2$S$_2$Cl$_2$ oct.	3.697(5)	QUPNUK	[164]
[Pd^{II}Ni^{II}**P-pz-NS$_2$**(μ-Cl)Cl$_2$] (**277a**)	2:1	(μ-pz)(μ-Cl)	Pd: NPCl$_2$ sq.-pl.; Ni: N$_2$S$_2$Cl$_2$ oct.	3.808(2)	QUPNOE	[164]
[Pd^{II}Ni^{II}**P-pz-NS$_2$**(μ-Cl)Cl$_2$]·2CH$_2$Cl$_2$ (**277b**)	2:1	(μ-pz)(μ-Cl)	Pd: NPCl$_2$ sq.-pl.; Ni: N$_2$S$_2$Cl$_2$ oct.	3.806(4)	QUPPAS	[164]
[Pd$^{II}_2$(**P-pz-py**)(η^3-allyl)$_2$](BF$_4$) (**278**)	2:1	μ-pz	NP(allyl); N$_2$(allyl)	4.566(1)	OCOXIO	[79]
[Ir^{I}**P-pz-py**(COD)] (**279**)	1:1	–/–	NP(COD)	–/–	–/–	[79]
[Pd^{II}(η^3-allyl)**P-pz-py**Ir^{I}(COD)](BF$_4$) (**280**)	2:1	μ-pz	Pd: NP(allyl); Ir: N$_2$(COD)	4.639(1)	DAJROW; DAJROW01	[79,165]
[Ir^{I}(COD)**P-pz-py**Pd^{II}(η^3-allyl)](BF$_4$) (**281**)	2:1	μ-pz	Ir: NP(COD); Pd: N$_2$(allyl)	4.300(2); 4.292(2)	DAJRUC; DAJRUC01	[79,165]
[Ir^{I}(COD)**P-pz-py**Rh^{I}(η^4-COD)](BF$_4$) (**282**)	2:1	μ-pz	Ir: NP(COD); Rh: N$_2$(COD)	4.444(1)	OCOXOU	[79]
[Rh$^{I}_2$**P-pz-py**(CO)$_4$](BF$_4$) (**283**)	2:1	μ-pz	NPC$_2$ sq.-pl.; N$_2$C$_2$ sq.-pl.	4.253(1)	–/–	[80]
[Rh$^{I}_2$**PO-pz-py**(CO)$_4$](BF$_4$) (**284**)	2:1	μ-pz	NOC$_2$ sq.-pl.; N$_2$C$_2$ sq.-pl.	4.166(2)	–/–	[80]
[Pd^{II}(η^3-allyl)**P-pz-py**Ir^{I}(CO)$_2$](BF$_4$) (**285**)	2:1	μ-pz	Pd: NP(allyl); Ir: N$_2$C$_2$ sq.-pl.	4.336(1)	–/–	[80]
[Rh$^{I}_2$(CO)**P-pz-py**Rh^{I}(μ-Me$_3$Si-C≡C)(CO)] (**286**)	2:1	(μ-pz)(μ-η^1:η^2-C≡CR)	NPC$_3$ sq.-pl; NPC$_2$ sq.-pl.	3.877(2)	–/–	[80]
[Ni$^{II}_4$(H$_2$**(N^{CO}-pz-py)$_2$**)$_2$(DMSO)$_6$(NO$_3$)(H$_2$O)](NO$_3$)$_3$·H$_2$O·3DMSO·OCMe$_2$ (**287**)	4:4[i]	(μ-pz)$_2$	N$_4$O$_2$ oct.; N$_2$O$_4$ oct.	4.022(1)	171625	[166]
[Cu$^{II}_4$(H$_2$**(N^{CO}-pz-py)$_2$**)$_2$(DMSO)$_2$(EtOH)$_2$](picrate)$_4$ (**288**)	4:4[i]	(μ-pz)$_2$	N$_3$O$_2$ sq.-py.	3.9340(3)	XIPJUB	[166]
[Cu$^{II}_4$(H$_2$**(N^{CO}-pz-py)$_2$**)$_2$(H$_2$O)$_4$](NO$_3$)$_4$·5.5H$_2$O (**289**)	4:4[i]	(μ-pz)$_2$	N$_3$O$_2$ sq.-py.	3.9556(8)	XIPKAI	[166]
[Cu$^{II}_2$Pd**(N^{CO}-pz-py)$_2$** (μ-OH)(μ-OAc)] (**290**)[h]	3:2[i]	μ-pz	Pd: N$_4$ sq.-pl.; Cu: N$_2$O$_2$ sq.-pl.	–/–	–/–	[167]
[Mn^{I}(CO)$_2$**Cp-pz-Npy$_2$**Zn^{II}(Cl)] (**291**)	2:1	μ-pz	Mn^{I}: NCpC$_2$ tetr.; Zn^{II}: N$_4$Cl trig.-bipy.	4.152	MIRSUB	[168]
[Mn^{I}(CO)$_2$**Cp-pz-N(C$_2$py)$_2$**Zn^{II}(OAc)]·DMF·H$_2$O (**292**)	2:1	μ-pz	Mn^{I}: NCpC$_2$ tetr.; Zn^{II}: N$_4$O trig.-bipy.	4.1423(9)	MANCEK	[169]
[Mn^{I}(CO)$_2$**Cp-pz-Npy$_2$**Ni^{II}(NO$_3$)]·DMF (**293**)	2:1	μ-pz	Mn^{I}: NCpC$_2$ tetr.; Ni^{II}: N$_4$O$_2$ oct.	4.247(1)	638867	[172]
[Mn^{I}(CO)$_2$**Cp-pz-Npy$_2$**Co^{II}(NO$_3$)]·Et$_2$O (**294**)	2:1	μ-pz	Mn^{I}: NCpC$_2$ tetr.; Co^{II}: N$_4$O(+O).	4.1357(5)	631167	[171]
[Mn^{I}(CO)$_2$**Cp-pz-Npy$_2$**Mn^{II}(Cl)] (**295**)	2:1	μ-pz	Mn^{I}: NCpC$_2$ tetr.; Mn^{II}: N$_4$Cl trig.-bipy.	4.2175(4)	JAQQOI	[170]
[Mn^{I}(CO)$_2$**Cp-pz-Npy$_2$**Mn^{II}(Br)(DMF)] (**296**)	2:1	μ-pz	Mn^{I}: NCpC$_2$ tetr.; Mn^{II}: N$_4$OBr oct.	4.3813(5)	JAQQUO	[170]
[Mn^{I}(CO)$_2$**Cp-pz-Npy$_2$**Mn^{II}(OAc)] (**297**)	2:1	μ-pz	Mn^{I}: NCpC$_2$ tetr.; Mn^{II}: N$_4$O$_2$ oct.	4.257(1)	JAQRAV	[170]
[Mn^{I}(CO)$_2$**Cp-pz-Npy$_2$**Mn^{II}(DMF)$_2$](ClO$_4$) (**298**)	2:1	μ-pz	Mn^{I}: NCpC$_2$ tetr.; Mn^{II}: N$_4$O$_2$ oct.	4.2550(5)	JAQREZ	[170]
[Mn^{I}(CO)$_2$**Cp-pz-N(C$_2$py)$_2$**Zn^{II}(OAc)] (**299**)	2:1	μ-pz	Mn^{I}: NCpC$_2$ tetr.; Zn^{II}: N$_4$O$_2$ oct.	4.3915(6)	MANCIO	[169]
[Mn^{I}(CO)$_2$**Cp-pz-N(C$_2$py)$_2$**Zn^{II}](ClO$_4$) (**300**)	2:1	μ-pz	Mn^{I}: NCpC$_2$ tetr.; Zn^{II}: N$_4$ tetr.	4.0601(5)	MANCOU	[169]
[Mn^{I}(CO)$_2$**Cp-pz-N(C$_2$py)$_2$**Co^{II}(NO$_3$)]·0.5Et$_2$O (**301**)	2:1	μ-pz	Mn^{I}: NCpC$_2$ tetr.; Co^{II}: N$_4$O$_2$ oct.	4.4153(5)	631168	[171]
[Mn^{I}(CO)$_2$**Cp-pz-N(C$_2$py)$_2$**Co^{II}(OAc)]·0.5Et$_2$O (**302**)	2:1	μ-pz	Mn^{I}: NCpC$_2$ tetr.; Co^{II}: N$_4$O$_2$ oct.	4.494(2)	631169	[171]
[Mn^{I}(CO)$_2$**Cp-pz-N(C$_2$py)$_2$**Ni^{II}(NO$_3$)] (**303**)	2:1	μ-pz	Mn^{I}: NCpC$_2$ tetr.; Ni^{II}: N$_4$O$_2$ oct.	4.247(1)	638868	[172]
[Mn^{I}(CO)$_2$**Cp-pz-N(C$_2$py)$_2$**Ni^{II}(OAc)] (**304**)	2:1	μ-pz	Mn^{I}: NCpC$_2$ tetr.; Ni^{II}: N$_4$O$_2$ oct.	4.507(1)	638869	[172]

---

[a] Oct. = distorted octahedral; sq.-py. = distorted square-pyramidal (if not described in the literature the differentiation between distorted square-pyramidal and distorted trigonal-bipyramidal is estimated only); bi.-tr.-pr. = distorted bicapped trigonal-prismatic; tetr. = distorted tetrahedral; sq.-pl. = distorted square-planar; trig.-bipy = distorted trigonal-bipyramidal (if not described in the literature the differentiation between distorted square-pyramidal and distorted trigonal-bipyramidal is estimated only).

[b] Even with two or more independent molecules in the crystallographic unit the metal···metal distances of one molecule only are given.

[c] The CCDC deposition number is given where the CCDC code was not available.

[d] N$_2$(+N$_2$) lin. (tetracoord.) = basic linear coordination with two more distal donor atoms, leading to a tetracoordinate geometry.

[e] In the literature described as intermediate coordination between distorted trigonal-bipyramidal and distorted square-pyramidal.

[f] N and O atoms of the bridging deprotonated urea co-ligand are disordered over two sites.

[g] Fourfold N-coordination with an additional side-on C≡N-coordination.

[h] The poor quality of the structural data precludes a more detailed analysis.

[i] The ratio metal ion-to-pyrazolate moiety is given and does not correspondent to the metal ion-to-ligand-ratio.

[j] The molecular structure has been published twice; both CCDC codes and references are given.

Table 2
Survey of magnetically analysed complexes[a].

Complex	Magnetic coupling constant J/cm^{-1} or observed SCO phenomenon	Refs.
$[Co^{II}_2(\mathbf{py_2\text{-}pz})_2(NO_3)]\cdot 2H_2O$	–/–	[25]
$[Co^{II}_2(\mathbf{py_2\text{-}pz})_2(NCS)]\cdot H_2O$	–/–	[25]
$[Ni^{II}_2(\mathbf{py_2\text{-}pz})_2(NO_3)]\cdot H_2O$	–/–	[25]
$[Ni^{II}_2(\mathbf{py_2\text{-}pz})_2(NCS)]\cdot H_2O$	–/–	[25]
$\{\textit{cis}\text{-}[Cu^{II}_2(\mathbf{py_2\text{-}pz})_2(H_2O)_2](NO_3)_2\cdot 2H_2O\}_2$ (**2**)	−180	[26]
$\textit{cis}\text{-}[Cu^{II}_2(\mathbf{py_2\text{-}pz})_2(H_2O)_2](ClO_4)_2$ (**3**)	−368.3	[27]
$\{\textit{trans}\text{-}[Cu_2(\mathbf{py_2\text{-}pz})_2(ClO_4)_2]\cdot H_2O\}_2$ (**4**)	–/–	[28]
$\textit{trans}\text{-}[Fe^{II}_2(\mathbf{py_2\text{-}pz})_2(NCS)_2(3\text{-}Brpy)_2]$	SCO	[29]
$\textit{trans}\text{-}[Fe^{II}_2(\mathbf{py_2\text{-}pz})_2(NCBH_3)_2(py)_2]$ (**5**)	SCO	[30]
$\textit{trans}\text{-}[Fe^{II}_2(\mathbf{py_2\text{-}pz})_2(NCBH_3)_2(4\text{-}Phpy)_2]$ (**6**)	SCO	[31]
$\textit{trans}\text{-}[Fe^{II}_2(\mathbf{py_2\text{-}pz})_2(NCSe)_2(py)_2]$	SCO	[33]
$\textit{trans}\text{-}[Fe^{II}_2(\mathbf{py_2\text{-}pz})_2(NCS)_2(py)_2]$ (**7**)	SCO as powder	[29,33]
$\textit{trans}\text{-}[Co^{II}_2(\mathbf{py_2\text{-}pz})_2(NCS)_2(4\text{-}Phpy)_2]$ (**8**)	−8.78	[34]
$[Fe^{II}_2(\mathbf{py_2\text{-}pz})_2(NCBH_3)_2(4\text{-}Phpy)_2]$	SCO	[34]
$(\textit{trans}\text{-}[Fe^{II}_2(\mathbf{py_2\text{-}pz})_2(NCS)_2(bpy)])_\infty$ (**9**)	SCO	[35]
$[(nta)Cr^{III}(\mathbf{py_2\text{-}pz})Fe^{II}(picen)](BF_4)$ (**10**)	–/–	[36]
$[(nta)Cr^{III}(\mathbf{py_2\text{-}pz})Fe^{II}(dpea)](BF_4)$	–/–	[37]
$[\{Fe^{II}(\mathbf{py_2\text{-}pz})_3\}_2Fe^{II}_3(\mu_3\text{-}O)](NCS)_2\cdot 10H_2O$ (**20**)	−29.0	[40]
$[Co^{II}_2(\mathbf{^{6Me}py_2\text{-}pz})(NO_3)(OH)]\cdot H_2O$	–/–	[25]
$[Ni^{II}_2(\mathbf{^{6Me}py_2\text{-}pz})(NO_3)(OH)]\cdot H_2O$	–/–	[25]
$[Cu^{II}_2(\mathbf{^{6Me}py_2\text{-}pz})Cl_3]$	−204.0	[41]
$[Co^{II}_2(\mathbf{^{6Me}py\text{-}pz\text{-}py})_2(NO_3)]\cdot H_2O$	–/–	[25]
$[Ni^{II}_2(\mathbf{^{6Me}py\text{-}pz\text{-}py})_2(NO_3)]\cdot H_2O$	–/–	[25]
$[Co^{II}_2(\mathbf{^{6Me}py\text{-}pz\text{-}py})Cl_2(OH)]$	–/–	[25]
$[Ni^{II}_2(\mathbf{^{6Me}py\text{-}pz\text{-}py})Cl_2(OH)]$	–/–	[25]
$[Cu^{II}_2(\mathbf{^{6Me}py\text{-}pz\text{-}py})Cl_3]$	−180.2	[41]
$[Cu^{II}_2(\mathbf{^{6Me}py\text{-}pz\text{-}py})Br_3]$	−174.7	[41]
$(NH_4)_2[Cu^{II}_2(\mathbf{(O_2C)_2\text{-}pz})_2]$ (**34**)	−100.1	[47]
$\textit{cis}\text{-}(Et_3NH)_2[Cu^{II}_2(\mathbf{(O_2C)_2\text{-}pz})_2(H_2O)_2]$ (**35**)	$J/k_b = -153$ K	[48]
$[Cu^{II}_2(H\mathbf{(O_2C)_2\text{-}pz})_2]\cdot 4,4'\text{-}dpdo$ (**39**)	−124	[53]
$[\{Na_2(\mu\text{-}H_2O)_2\}\{Cu^{II}_2(\mathbf{(O_2C)_2\text{-}pz})_2]_\infty$ (**40**)	$J/k_b = -154$ K	[48]
$Na[Cr^{III}_2\mathbf{(O_2C)_2\text{-}pz}(acac)_4]$	−0.42	[55]
$[Cu^{II}_3(\mathbf{(O_2C)_2\text{-}pz})_2(Me_2en)_2(H_2O)_2]\cdot 8H_2O$ (**51**)	−15	[62]
$[Cu^{II}_3(\mathbf{(O_2C)_2\text{-}pz})_2(MeOH)_6(H_2O)_4]$ (**52**)	−19	[62]
$[Cu^{II}_3(\mathbf{(O_2C)_2\text{-}pz})_2(H_2O)_4]_\infty$ (**53**)	$J/k_b = -32$ K	[63]
$[Cu^{II}_2(\mathbf{N_2\text{-}pz})_2Br_2]$ (**54**)	−192.0	[64]
$[Cu^{II}_2(\mathbf{N_2\text{-}pz})_2Cl_2]$	−200.8	[64]
$[Ag^{I}(\mathbf{INO_2\text{-}pz})]_\infty$ (**55**)	–/–	[66]
$\{[Ni^{II}_2(\mathbf{(Me_2PhN)_2\text{-}pz})_2Cl_2]$ (**63**)	−23.2	[72]
$[Ni^{II}_2(\mathbf{(Me_2PhN)_2\text{-}pz})_2]Cl_2$ (**64**)	–/–	[72]
$[Cu^{II}_2(\mathbf{(N^{OH}{=}C)_2\text{-}pz(Me)})_2Cl_2]\cdot 2H_2O$ (**97b**)	−159	[86]
$[Cu^{II}_2(\mathbf{(EtO_2C)_2\text{-}pz})_2(NO_3)(H_2O)](NO_3)$ (**98**)	−191	[87]
$[Cu^{II}_2(\mathbf{S_2\text{-}pz})_2(OCMe_2)(BF_4)(\mu\text{-}BF_4)]$ (**99**)	−206	[88]
$\textit{trans}\text{-}[Cu^{II}_2(\mathbf{MeS_2\text{-}pz})_2(ONO_2)_2]$ (**100**)	−243	[89]
$\textit{trans}\text{-}[Cu^{II}_2(\mathbf{MeS_2\text{-}pz})_2(ClO_4)_2(MeOH)_2]$ (**101**)	−231	[89]
$[Cu^{II}_4(H\mathbf{(pyN^{CO})_2\text{-}pz})_4]\cdot 8H_2O$ (**104**)	−8.2	[94]
$[Cu^{II}_2\mathbf{(pyN^{CO})_2\text{-}pz}(N_3)]$	−371	[93]
$[Cu^{II}_2\mathbf{(N^{Et}N^{CO})_2\text{-}pz}(N_3)]$	−335	[93]
$[Cu^{II}_2\mathbf{(N^{Me}C_3N^{CO})_2\text{-}pz}(N_3)]$	−297	[93]
$[Cu^{II}_2\mathbf{(pyN^{CO})_2\text{-}pz}(OAc)]$	+8.9	[93]
$[Cu^{II}_2(\mathbf{(N^{Et}N)_2\text{-}pz})_2](BPh_4)_2$ (**107**)	−214	[95]
$[Cu^{II}_2(\mathbf{(N^{Me}C_3N)_2\text{-}pz})_2](BPh_4)_2$	−181	[95]
$[Mn^{II}_2\mathbf{(pyN)_2\text{-}pz}](BPh_4)_2\cdot 2tol$ (**108**)	−0.40	[96]
$[Cu^{II}_2\mathbf{(N^{Me}C_3N^{Me})_2\text{-}pz}(\mu\text{-}Cl)Cl_2]$ (**116**)	−13.5	[99]
$[Cu^{II}_4(\mathbf{(N^{Me}N^{Me})_2\text{-}pz})_2(\mu\text{-}Cl)_4(Cl)_2]$ (**117**)	−11.1	[99]
$[Cu^{II}_2\mathbf{(N^{Me}N^{Me})_2\text{-}pz}(\mu\text{-}Cl)_3]$ (**118**)	−9.1 (μ-pz); −7.7	[99]
$[Ni^{II}_4(\mathbf{(N^{Me}N^{Me})_2\text{-}pz})_2(OC(NH_2)_2)_2(\mu_3\text{-}OC(NH_2)(NH))_2](ClO_4)_4$ (**121**)	+3.4	[100]
$[Ni^{II}_2\mathbf{(N^{Me}N^{Me})_2\text{-}pz}(\mu\text{-}OAc)(OC(NHMe)_2)_2(MeOH)_2](ClO_4)_2$ (**122**)	−1.2	[101]
$[Ni^{II}_2\mathbf{(N^{Me}N^{Me})_2\text{-}pz}(\mu\text{-}1,3\text{-}N_3)_3]_\infty$ (**130**)	–/–	[103]
$[Ni^{II}_4(\mathbf{(N^{Me}C_3N^{Me})_2\text{-}pz})_2(\mu\text{-}1,1\text{-}N_3)_2(\mu_3\text{-}1,1,3\text{-}N_3)_2(N_3)_2]$ (**131**)	−19.7; +6.0	[109]
$[Ni^{II}_2(\mathbf{(N^{Me}C_3N^{Me})_2\text{-}pz})(\mu\text{-}1,1\text{-}N_3)(O_2NO)_2]\cdot C_4H_{10}O$ (**132**)	+5.1	[110]
$[Ni^{II}_4(\mathbf{(N^{Me}C_3N^{Me})_2\text{-}pz})_2(\mu\text{-}1,1\text{-}N_3)_2(\mu\text{-}1,3\text{-}N_3)_2](ClO_4)_2\cdot 2CH_4O\cdot 0.5H_2O$ (**133**)	+1.8	[110]
$[Ni^{II}_4(\mathbf{(N^{Me}C_3N^{Me})_2\text{-}pz})_2(\mu\text{-}1,1\text{-}N_3)_2(\mu\text{-}1,3\text{-}N_3)_2](ClO_4)_2\cdot C_3H_6O\cdot C_5H_{12}$ (**134**)	+2.5	[110]
$[Ni^{II}_4(\mathbf{(N^{Me}C_3N^{Me})_2\text{-}pz})_2(\mu\text{-}1,1\text{-}N_3)_2(\mu\text{-}1,3\text{-}N_3)_2](BPh_4)_2\cdot C_3H_6O$ (**135**)	+3.4	[110]
$[Ni^{II}_2(\mathbf{(pyC_2N^{Me})_2\text{-}pz})(\mu\text{-}Cl)Cl_2(H_2O)_2]_2\cdot 2H_2O$ (**140**)	−3.9	[114]
$[Cu^{II}_2(H\mathbf{(py{=}NN^{CO})_2\text{-}pz})(\mu\text{-}OH)(NO_3)(H_2O)](NO_3)\cdot 2H_2O$ (**143**)	−443	[116]
$[Cu^{II}_2(H\mathbf{(py{=}NN^{CO})_2\text{-}pz})(\mu\text{-}OH)(H_2O)_2](ClO_4)\cdot H_2O$ (**144**)	−398	[116]
$[Cu^{II}_2(H\mathbf{(pim{=}NN^{CO})_2\text{-}pz})(\mu\text{-}OH)(H_2O)][Cu^{II}_2(H\mathbf{(pim{=}NN^{CO})_2\text{-}pz})(\mu\text{-}OH)(ClO_4)](ClO_4)_3\cdot 4H_2O$ (**145**)	−187	[116]
$[Mn^{III}_4(\mathbf{(Obz{=}N)_2\text{-}pz})_2(\mu\text{-}OMe)_4(MeOH)_4](ClO_4)_2$ (**146**)	–/–	[117]
$[Cu^{II}_2\mathbf{(pyS)_2\text{-}pz}(\mu\text{-}N_3)(N_3)_2]\cdot {}^{i}PrOH$ (**147**)	–/–	[121]
$[Cu^{II}_2\mathbf{(pyS)_2\text{-}pz}(\mu\text{-}Br)Br(H_2O)]Br\cdot 2H_2O$ (**148**)	−46.6	[121]
$[Ni^{II}_4(\mathbf{(SN)_2\text{-}pz})_2(\mu_4\text{-}1,1,3,3\text{-}N_3)(\mu\text{-}1,1\text{-}N_3)_2(\mu\text{-}OAc)_2](ClO_4)$ (**150**)	−110; +106	[122]
$[Ni^{II}_4(\mathbf{(SN)_2\text{-}pz})_2(\mu_4\text{-}1,1,3,3\text{-}N_3)(\mu\text{-}1,1\text{-}N_3)_2(\mu\text{-}O_2CPh)_2](ClO_4)$ (**151**)	−111; +51	[122]
$[Co^{II}_2\mathbf{(N^{Et}{}_2N)_2\text{-}pz}(OAc)](BPh_4)_2\cdot OCMe_2$	–/–	[123]

Table 2 (*Continued*)

Complex	Magnetic coupling constant J/cm^{-1} or observed SCO phenomenon	Refs.
$[\mathrm{Co^{II}}_2\mathbf{(N^{Et}{}_2N)_2\text{-}pz}(\mathrm{N_3})](\mathrm{BPh_4})_2\cdot 2\mathrm{OCMe_2}$[b]	–/–	[123]
$[\mathrm{Cu^{II}}_2\mathbf{(N^{Et}{}_2N)_2\text{-}pz}(\mathrm{OAc})](\mathrm{BPh_4})_2$	−7.02	[123]
$[\mathrm{Cu^{II}}_2\mathbf{(N^{Et}{}_2N)_2\text{-}pz}(\mathrm{N_3})](\mathrm{BPh_4})_2\cdot \mathrm{OCMe_2}$	–/–	[123]
$[\mathrm{Mn^{II}}_2\mathbf{(py_2N)_2\text{-}pz}(\mathrm{OBz})](\mathrm{BPh_4})_2\cdot \mathrm{DMF}$	−0.25	[96]
$[\mathrm{Mn^{II}}_2\mathbf{(N^{Et}{}_2N)_2\text{-}pz}(\mathrm{OAc})](\mathrm{BPh_4})_2\cdot \mathrm{MeOH}$	−0.37	[96]
$[\mathrm{Co^{II}}_2\mathbf{(N^{Et}{}_2N)_2\text{-}pz}(\mu\text{-Cl})](\mathrm{BPh_4})_2$ (**156**)	–/–	[97]
$[\mathrm{Co^{II}}_2\mathbf{(N^{Et}{}_2N)_2\text{-}pz}(\mu\text{-Br})](\mathrm{BPh_4})_2$ (**160**)	−1 – 0	[126]
$[\mathrm{Co^{II}}_2\mathbf{(N^{Et}{}_2N)_2\text{-}pz}(\mu\text{-1,3-N}_3)](\mathrm{BPh_4})_2$ (**161**)[b]	−12.0	[126]
$[\mathrm{Ni^{II}}_2\mathbf{(N^{Me}{}_2C_3N)_2\text{-}pz}(\mu\text{-OH})](\mathrm{BPh_4})_2$ (**169**)	−56.9	[127]
$[\mathrm{Ni^{II}}_2\mathbf{(N^{Me}{}_2C_3N)_2\text{-}pz}(\mu\text{-O}_2\mathrm{H}_3)](\mathrm{BPh_4})_2$ (**170**)	–/–	[127]
$[\mathrm{Ni^{II}}_2\mathbf{(N^{Et}{}_2N)_2\text{-}pz}(\mu\text{-cnge})](\mathrm{ClO_4})_2$ (**181**)	<1	[128]
$[\mathrm{Ni^{II}}_2\mathbf{(N^{Et}{}_2N)_2\text{-}pz}(\mu\text{-1,3-N}_3)](\mathrm{ClO_4})_2$ (**184**)	−25.7	[109]
$[\mathrm{Ni^{II}}_2\mathbf{(N^{Me}{}_2C_3N)_2\text{-}pz}(\mu\text{-1,1-N}_3)(\mathrm{NO_3})_2]$ (**185**)	+4.0	[109]
$[\mathrm{Ni^{II}}_4(\mathbf{(N^{Me}{}_2C_3N)_2\text{-}pz})_2(\mu\text{-1,1-N}_3)_2(\mu\text{-1,3-N}_3)_2](\mathrm{BPh_4})_2$ (**186**)	+2.0 (μ-1,1-N_3); −16.2 (μ-1,3-N_3)	[109]
$[\mathrm{Ni^{II}}_2\mathrm{H}\mathbf{(N^{Me}{}_2C_3N)_2\text{-}pz}(\mu\text{-OH})(\mathrm{MeCN})_2](\mathrm{ClO_4})_3$ (**187**)	−46.7	[98]
$[\mathrm{Ni^{II}}_2\mathrm{H}_4\mathbf{[(FN)_2C_3N]_2\text{-}pz}(\mu\text{-Cl})\mathrm{Cl}_2]$ (**197**)	–/–	[132]
$[\mathrm{Co^{II}}_2\mathrm{H}_4\mathbf{[(FN)_2C_3N]_2\text{-}pz}(\mu\text{-Cl})\mathrm{Cl}_2]$ (**198**)	–/–	[132]
$[\mathrm{Ni^{II}}_2\mathbf{[(pyC_2)_2N]_2\text{-}pz}(\mu\text{-Cl})\mathrm{Cl}_2]\cdot 2\mathrm{MeOH}$ (**211**)	−3.6	[114]
$[\mathrm{Ni^{II}}_2\mathbf{[(pyC_2)_2N]_2\text{-}pz}(\mu\text{-Cl})\mathrm{MeOH}](\mathrm{ClO_4})_2$ (**212**)	−3.4	[114]
$[\mathrm{Ni^{II}}_2\mathbf{(py_2N)_2\text{-}pz}(\mu\text{-Cl})\mathrm{Cl}(\mathrm{MeOH})_2]\mathrm{Cl}\cdot 2\mathrm{MeOH}$ (**213**)	−1.7	[114]
$[\mathrm{Cu^{II}}_2\mathbf{(Im_2N)_2\text{-}pz}(\mathrm{OMe})(\mathrm{MeOH})](\mathrm{ClO_4})_2\cdot \mathrm{MeCN}$ (**224**)	−35.3	[139]
$[\mathrm{Cu^{II}}_2\mathbf{(Im_2N)_2\text{-}pz}(\mathrm{NO_3})(\mathrm{H_2O})]_2(\mathrm{NO_3})_4\cdot 5\mathrm{H_2O}$ (**226**)	−100.6	[139]
$[\mathrm{Ni^{II}}_2\mathbf{(S_2N)_2\text{-}pz}(\mu\text{-Cl})\mathrm{Cl}_2](\mathrm{ClO_4})_2$ (**227**)	−12.0	[141]
$[\mathrm{Ni^{II}}_4(\mathbf{(S_2N)_2\text{-}pz})_2(\mu\text{-1,1,3-N}_3)_2(\mu\text{-1,3-N}_3)(\mu\text{-OAc})](\mathrm{ClO_4})_2$ (**230**)	−51 (μ-pz); +57 (μ-1,1,3-N_3); +6 (μ-1,3-N_3); −18 (μ-1,1,3-N_3)	[143]
$[\mathrm{Ni^{II}}_4(\mathbf{(S_2N)_2\text{-}pz})_2(\mu\text{-1,1,3,3-N}_3)(\mu\text{-1,1-N}_3)_2(\mu\text{-OAc})_2)](\mathrm{ClO_4})$ (**231**)	−110 (μ-pz); +106 (μ-1,1,3,3-pz); +2 (μ-1,1,3,3-pz)	[122]
$[\mathrm{Ni^{II}}_4(\mathbf{(S_2N)_2\text{-}pz})_2(\mu\text{-1,1,3,3-N}_3)(\mu\text{-O}_2\text{C-Ada})_4)](\mathrm{ClO_4})$ (**232**)	−50 (μ-pz); +66 (μ-1,1,3,3-pz); +7 (μ-1,1,3,3-pz)	[122]
$[\mathrm{Ni^{II}}_4(\mathbf{(S_2N)_2\text{-}pz})_2(\mu\text{-1,1,3,3-N}_3)(\mu\text{-1,1-N}_3)_2(\mu\text{-O}_2\text{CPh})_2)](\mathrm{ClO_4})$ (**233**)	−111 (μ-pz); +51 (μ-1,1,3,3-pz); +9 (μ-1,1,3,3-pz)	[122]
$[\mathrm{Ni^{II}}_4(\mathbf{(^{\mathit{i}}PrS_2N)_2\text{-}pz})_2(\mu\text{-1,1,3,3-N}_3)(\mu\text{-1,1-N}_3)_2(\mu\text{-OAc})_2)](\mathrm{ClO_4})$ (**234**)	−133 (μ-pz); +129 (μ-*1*,1,3,3-pz); +26 (μ-1,1,3,3-pz)	[122]
$[\mathrm{Ni^{II}}_4(\mathbf{(^{\mathit{i}}PrS_2N)_2\text{-}pz})_2(\mu\text{-1,1,3,3-N}_3)(\mu\text{-1,1-N}_3)_2(\mu\text{-O}_2\text{C-Ada})_2)](\mathrm{ClO_4})$ (**235**)	−111 (μ-pz); +86 (μ-1,1,3,3-pz); +5 (μ-1,1,3,3-pz)	[122]
$[\mathrm{Ni^{II}}_4(\mathbf{(MeS_2N)_2\text{-}pz})_2(\mu\text{-1,1,3,3-N}_3)(\mu\text{-1,1-N}_3)_2(\mu\text{-O}_2\text{C-Ada})_2)](\mathrm{ClO_4})$ (**236**)	−39 (μ-pz); +98 (μ-1,1,3,3-pz); −12 (μ-1,1,3,3-pz)	[122]
$[\mathrm{Ni^{II}}_4(\mathbf{(S_2N)_2\text{-}pz})_2(\mu\text{-1,1,3-N}_3)_2(\mu\text{-1,3-N}_3)(\mu\text{-O}_2\text{CPh})](\mathrm{ClO_4})_2$ (**237**)	−61 (μ-pz); +25 (μ-1,1,3-N_3); +5 (μ-1,3-N_3); −12 (μ-1,1,3-N_3)	[143]
$[\mathrm{Ni^{II}}_4(\mathbf{(^{\mathit{i}}PrS_2N)_2\text{-}pz})_2(\mu\text{-1,1,3-N}_3)_2(\mu\text{-1,3-N}_3)(\mu\text{-O}_2\text{CPh})](\mathrm{ClO_4})_2$ (**238**)	−53 (μ-pz); +27 (μ-1,1,3-N_3); +6 (μ-1,3-N_3); −3 (μ-1,1,3-N_3)	[143]
$[\mathrm{Ni^{II}}_2\mathbf{(S_2N)_2\text{-}pz}(\mu\text{-1,3-N}_3)(\mathrm{OCMe_2})](\mathrm{ClO_4})_2$ (**239**)	−82.0	[144]
$[\mathrm{Ni^{II}}_2\mathbf{(S_2N)_2\text{-}pz}(\mu\text{-1,3-N}_3)(\mathrm{OCMe_2})](\mathrm{BPh_4})_2$ (**240**)	−28.7	[144]
$[\mathrm{Ni^{II}}_4(\mathbf{(S_2N)_2\text{-}pz})_2(\mu\text{-1,1,3-N}_3)_2(\mathrm{MeOH})_2](\mathrm{ClO_4})_4$ (**241**)	−42.6	[144]
$[\mathrm{Ni^{II}}_2\mathbf{(S_2N)_2\text{-}pz}(\mu\text{-1,3-N}_3)_2]_n(\mathrm{ClO_4})_n\cdot 2n\mathrm{CH_2Cl_2}$ (**242**)	−29.5	[144]
$[\mathrm{Ni^{II}}_2\mathbf{(S_2N)_2\text{-}pz}(\mu\text{-1,3-N}_3)_2]_n(\mathrm{ClO_4})_n\cdot 2n\mathrm{CH_2Cl_2}$ (**243**)	−34.7	[144]
$[\mathrm{Ni^{II}}_2\mathbf{(S_2N)_2\text{-}pz}(\mu\text{-1,3-N}_3)_2]_n(\mathrm{BPh_4})_n\cdot 0.58n\mathrm{OCMe_2}$ (**244**)	−36.1	[144]
$[\mathrm{Ni^{II}}_2\mathbf{(S_2N)_2\text{-}pz}(\mu\text{-1,3-N}_3)(\mathrm{N_3})_2]$ (**245**)	−81 (low temp.); −24 (>230 K)	[145]
$[\mathrm{Ni^{II}}_2(\mathbf{S_2N\text{-}pz\text{-}N_3})(\mu\text{-Cl})\mathrm{Cl}_2]$ (**246**)	−13.1	[141]
$[\mathrm{Ni^{II}}_2(\mathbf{S_2N\text{-}pz\text{-}N_3})(\mu\text{-Cl})\mathrm{Cl}](\mathrm{BPh_4})$ (**247**)	−8.1	[141]
$[\mathrm{Cu^{II}}_2\mathbf{(\mathit{c}NS_2)_2\text{-}pz}(\mu\text{-Cl})](\mathrm{ClO_4})_2$ (**252**)	−136	[147]
$[\mathrm{Cu^{II}}_2\mathrm{H}_6\mathbf{[N(NC_3)_2\text{-}pz]_{2m}}](\mathrm{ClO_4})_2$ (**269**)	−299	[162]
$[\mathrm{Cu^{II}}_2\mathrm{H}_8\mathbf{[N(NC_3)_2\text{-}pz]_{2m}}](\mathrm{ClO_4})_4\cdot 2\mathrm{H_2O}$	−286	[162]
$[\mathrm{Cu^{II}}_2\mathbf{[(N{=}C)_2\text{-}pz]_{2m}}(\mathrm{OAc})_2]$ (**272**)	−169	[115]
$[\mathrm{Cu^{II}}_2\mathbf{[(N{=}C)_2\text{-}pz]_{2m}}(\mathrm{NCS})_2]$ (**273**)	−213	[115]
$[\mathrm{Ni^{II}}_4(\mathrm{H}_2\mathbf{(N^{CO}\text{-}pz\text{-}py)_2})_2(\mathrm{DMSO})_6(\mathrm{NO_3})(\mathrm{H_2O})](\mathrm{NO_3})_3\cdot \mathrm{H_2O}\cdot 3\mathrm{DMSO}\cdot \mathrm{OCMe_2}$ (**287**)	−15.8	[166]
$[\mathrm{Cu^{II}}_4(\mathrm{H}_2\mathbf{(N^{CO}\text{-}pz\text{-}py)_2})_2(\mathrm{H_2O})_4](\mathrm{NO_3})_4\cdot 5.5\mathrm{H_2O}$ (**289**)	−201	[166]

[a] See references for more details.

[b] Disagreeable reports of the plots of the variable-temperature molar susceptibility.

formulated as $[\mathrm{Ni^{II}}_2(\mathbf{py_2\text{-}pz})_2(\mathrm{H_2O})_2(\mathrm{NO_3})_2]$ and $[\mathrm{Ni^{II}}_2(\mathbf{py_2\text{-}pz})_2(\mathrm{H_2O})(\mathrm{MeOH})(\mathrm{NO_3})_2]$, respectively [23]. However it took some 20 years until, in 1989, Casabó et al. were able to structurally characterise the first 2:2-type complex of such kind, namely $[\mathrm{Ni^{II}}_2(\mathbf{py_2\text{-}pz})_2(\mathrm{MeOH})_4]\mathrm{Cl}_2\cdot 2\mathrm{H_2O}$ (**1**) (Table 1) [24]. The molecular structure of **1** consists of two anionic coplanar $\mathbf{py_2\text{-}pz}^-$ ligands, which coordinate in a bis-bidentate fashion to the two nickel(II) ions in the equatorial positions. Each distorted octahedral coordination environment about the nickel(II) ions is completed by two methanol co-ligands in the axial positions. The authors also reported the formation of analogous 2:2-type complexes of manganese(II), cobalt(II), copper(II), zinc(II) and cadmium(II) (Table 2) [24,25] and, in 1992, they published the first crystal structure of a 2:2-copper(II) complex of $\mathbf{py_2\text{-}pz}^-$, which forms a couple of dimers in the solid state $\{[\mathrm{Cu^{II}}_2(\mathbf{py_2\text{-}pz})_2(\mathrm{H_2O})_2](\mathrm{NO_3})_2\cdot 2\mathrm{H_2O}\}_2$ (**2**) (Tables 1 and 2) [26]. Similar to the dinickel(II) complex **1**, the dinuclear subunits of **2** are formed by two coplanar anionic $\mathbf{py_2\text{-}pz}^-$ ligands which coordinate to the two copper(II) ions in a double pyrazolato-bridging manner. The distorted square-pyramidal coordination environment about the copper(II) ions in **2** is completed by two water molecules which occupy the apical positions of the same side of the ligand meanplanes (*cis* conformation). In the solid state tetranuclear dimers are formed to give a pseudo-tetrahedral arrangement of the copper(II) ions.

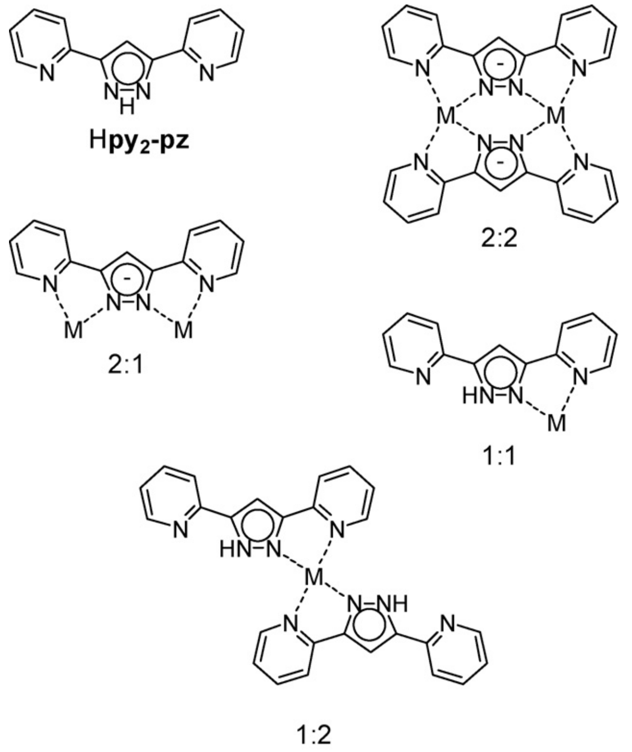

Scheme 2. The bis-bidentate ligand H**py₂-pz** and some coordination modes of H**py₂-pz** and **py₂-pz**⁻.

Magnetic measurements of **2** revealed a strong antiferromagnetic coupling ($J = -180\ \mathrm{cm}^{-1}$) between the copper(II) ions in the dimeric unit. A similar monomeric dinuclear complex with *cis*-co-ligand conformation ($[\mathrm{Cu^{II}}_2$(**py₂-pz**)$_2(\mathrm{H_2O})_2](\mathrm{ClO_4})_2$, **3**; Tables 1 and 2) was reported in 2005 by Du et al. [27]. Remarkably, the antiferromagnetic interaction of **3** ($J = -368.3\ \mathrm{cm}^{-1}$) is more than twice the value found for **2**. In 1995, another dimeric 2:2-type copper(II) complex, namely $\{[\mathrm{Cu_2}$(**py₂-pz**)$_2(\mathrm{ClO_4})_2]\cdot\mathrm{H_2O}\}_2$ (**4**; Tables 1 and 2), was reported by Munakata et al. [28]. The main difference between **4** and **2** is the nature (perchlorate rather than water) and conformation (*trans* rather than *cis*) of the co-ligands that occupy the apexes of the square pyramids, and thus the different stacking mode of the tetranuclear dimeric unit, which in **4** forms a rhombus-like arrangement of the copper(II) ions. Only in 2001 other 2:2-type complexes of **py₂-pz**⁻ and the first iron(II) compounds of that ligand were reported by Suemura et al. [29]. Although no molecular structures were reported, the complexes were described as *trans*-$[\mathrm{Fe^{II}}_2$(**py₂-pz**)$_2(\mathrm{NCS})_2(\mathrm{py})_2]$ and *trans*-$[\mathrm{Fe^{II}}_2$(**py₂-pz**)$_2(\mathrm{NCS})_2$(3-Brpy)$_2]$, featuring octahedrally coordinated iron(II) centres. The authors were able to observe light-induced spin transitions by measuring the variable temperature Raman spectra and magnetic susceptibilities of the compounds. In 2004 the first structure of an iron(II) complex of **py₂-pz**⁻, namely $[\mathrm{Fe^{II}}_2$(**py₂-pz**)$_2(\mathrm{NCBH_3})_2(\mathrm{py})_2]$ (**5**) (Fig. 1, Tables 1 and 2) was reported by Nakano et al. corroborated the assumed *trans*-structures of the earlier compounds [30].

Spin-crossover behaviour of **5** could be observed and both, the high-spin and the low-spin form of the compound, could be identified by X-ray crystallography. In the same year the authors also reported a very similar iron(II) complex (*trans*-$[\mathrm{Fe^{II}}_2$(**py₂-pz**)$_2(\mathrm{NCBH_3})_2$(4-Phpy)$_2]$, **6**; Tables 1 and 2), which showed a two-step spin crossover. With this complex, for the first time an intermediate spin state of [HS–HS]···[LS–LS] could be observed and characterised by IR, Raman and by X-ray crystallography [31]. Following those publications, a comprehensive study for the substituent effect of complexes of the type $[\mathrm{Fe^{II}}_2$(**py₂-pz**)$_2$(NCE)$_2$(X-py)$_2]$ (NCE = NCS or $\mathrm{NCBH_3}$; X-py = 3-Brpy, 3-Clpy, 3-Mepy, py, 4-$\mathrm{NMe_2}$py or 4-Mepy) on the spin-crossover behaviour was published in 2005 [32]. The authors concluded that the spin-crossover temperatures depend on the electronic effect of the substituents in the coordinated pyridine derivative. The spin-crossover phenomenon was also observed for a powdered sample of $[\mathrm{Fe^{II}}_2$(**py₂-pz**)$_2(\mathrm{NCS})_2(\mathrm{py})_2]$ (Table 2) but surprisingly, a crystalline sample of $[\mathrm{Fe^{II}}_2$(**py₂-pz**)$_2(\mathrm{NCS})_2(\mathrm{py})_2]$ (**7**; Tables 1 and 2) stayed in the [HS–HS] state at all temperatures [33]. Magnetic studies on *trans*-$[\mathrm{Co^{II}}_2$(**py₂-pz**)$_2(\mathrm{NCS})_2$(4-Phpy)$_2]$ (**8**; Tables 1 and 2), the isomorphous compound $[\mathrm{Fe^{II}}_2$(**py₂-pz**)$_2(\mathrm{NCS})_2$(4-Phpy)$_2]$ (Table 2) [34] and on the one-dimensional polymer (*trans*-$[\mathrm{Fe^{II}}_2$(**py₂-pz**)$_2(\mathrm{NCS})_2$(4,4′-bpy)$])_\infty$ (**9**; Tables 1 and 2) [35] showed high-spin cobalt(II) ions in the former and the spin-crossover phenomenon on the latter two iron(II) compounds.

2.1.2. 2:1-Type and other complexes of H**py₂-pz**

2:1-Type complexes of **py₂-pz**⁻ are accessible if additional chelating co-ligands are employed. Kaizaki and co-workers were the first to use this strategy, since they reported the synthesis of heterodinuclear 2:1-complexes of **py₂-pz**⁻ with chromium(III) and iron(II) [36,37] or lanthanide(III) salts [38]. As starting materials for the preparation of heterodinuclear 2:1-type complexes, 1:1-type chromium(III) complexes of **py₂-pz** with the general formulation of $[\mathrm{Cr^{III}}$(H**py₂-pz**)(nta)] [36,37] or $[\mathrm{Cr^{III}}$(**py₂-pz**)(acac)$_2]$ [38] (nta = nitrilotriacetate; acac = acetyl acetonate) were used. By simply reacting the precursor complex $[\mathrm{Cr^{III}}$(H**py₂-pz**)(nta)] with iron(II) tetrafluoroborate and the supplementary chelating co-ligand picen (picen = *N*,*N*′-bis-(2-pyridylmethyl)ethylenediamine) [36] or dpea (dpea = (2-aminoethyl)-bis-(2-pyridylmethyl)amine) [37], heterodinuclear compounds with the composition of $[(\mathrm{nta})\mathrm{Cr^{III}}$(**py₂-pz**)$\mathrm{Fe^{II}}(\mathrm{picen})](\mathrm{BF_4})$ (**10**) (Fig. 2, Table 1) [36] and $[(\mathrm{nta})\mathrm{Cr^{III}}$(**py₂-pz**)$\mathrm{Fe^{II}}(\mathrm{dpea})](\mathrm{BF_4})$ [37] were obtained (Table 2). A similar procedure using $[\mathrm{Cr^{III}}$(**py₂-pz**)(acac)$_2]$ and $[\mathrm{Ln^{III}}(\mathrm{hfac})_3(\mathrm{H_2O})_2]$ (hfac = hexafluoromethylacetylacetonate, Ln = Ce, Nd, Sm, Gd, Dy, Er and Yb) as components resulted in the formation of the heterodinuclear compounds $[(\mathrm{acac})_2\mathrm{Cr^{III}}$(**py₂-pz**)$\mathrm{Ln^{III}}(\mathrm{hfac})_3]$ (**11**: Ln = Ce; **12**: Ln = Nd; **13**: Ln = Sm; **14**: Ln = Gd; **15**: Ln = Dy; **16**: Ln = Er; **17**: Ln = Yb; Table 1) [38]. The homodinuclear 2:1-type ruthenium(II) complexes $[\mathrm{Ru^{II}}_2$(**py₂-pz**)(trpy)$_2(\mu$-Cl)$](\mathrm{PF_6})_2$ (**18**; Table 1) and $[\mathrm{Ru^{II}}_2$(**py₂-pz**)(trpy)$_2(\mu$-OAc)$](\mathrm{PF_6})_2$ (**19**; Table 1) (trpy = 2,2′:6′,2″-terpyridine) were reported in 2004 by Llobet and co-workers [39]. Complex **19** was the first example of a well-characterised dinuclear ruthenium complex capable of oxidising water to $\mathrm{O_2}$ without the Ru–O–Ru motif.

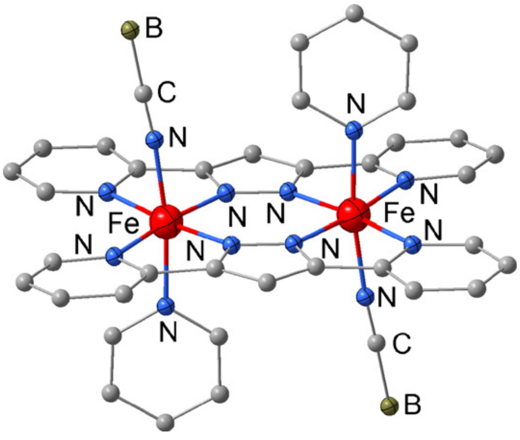

Fig. 1. Molecular structure of the 2:2-type complex $[\mathrm{Fe^{II}}_2$(**py₂-pz**)$_2(\mathrm{NCBH_3})_2(\mathrm{py})_2]$ (**5**) at 298 K.

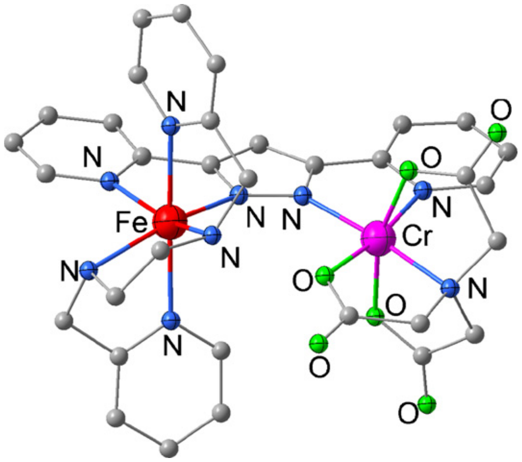

Fig. 2. Molecular structure of the 2:1-type complex cation of [(nta)Cr^{III}(**py$_2$-pz**)Fe^{II}(picen)](BF$_4$) (**10**).

The pentanuclear bis(triple-helical) complex with six ligand strands, namely [{Fe^{II}(**py$_2$-pz**)$_3$}$_2$Fe$^{II}_3$(μ_3-O)](NCS)$_2$·10H$_2$O (**20**; Tables 1 and 2), reported by Kawata, Kaizaki and co-workers is a 6:5-type of complex [40]. In principle two different types of iron(II) ions can be distinguished. The donor atoms of the two N$_6$-distorted octahedrally coordinated iron(II) ions belong to three ligand strands which each donate a pyridine and a pyrazole nitrogen atom forming a [Fe^{II}(**py$_2$-pz**)$_3$]$^-$-unit. A [Fe$^{II}_3$O]$^{4+}$-core with distorted N$_4$O trigonal bipyramidally coordinated iron(II) ions is then wrapped by two [Fe^{II}(**py$_2$-pz**)$_3$]$^-$-units forming the bis(triple-helical) complex **20** (Fig. 3).

2.1.3. *Complexes of **py$_2$-pz** derivatives*

Primarily 2:1-type complexes have been obtained using methyl substituted derivatives of H**py$_2$-pz**, even without the use of chelating co-ligands. The first 2:1-complexes of such type, namely [M$^{II}_2$(**^{6Me}py$_2$-pz**)$_2$(NO$_3$)$_2$(OH)]·H$_2$O (M = Ni, Co) [25] and [Cu$^{II}_2$(**^{6Me}py$_2$-pz**)X$_2$Y] (X = Br; Y = OH, pz) [41] were obtained with the ligand 3,5-bis(6-methyl-2-pyridyl)-3,5-pyrazole (**^{6Me}py$_2$-pz**, Scheme 3) and characterised by elemental and IR analyses (Table 2). The authors argued that, due to the steric demand of the methyl groups in the 6-position of the pyridine rings, coordination of two ligand molecules **^{6Me}py$_2$-pz**$^-$ to two metal ions is not favoured, and therefore only metal-to-ligand ratios of 2:1 can be realised. They corroborated their findings by the fact that, using the unsymmetrically monomethylated derivative **^{6Me}py-pz-py** (Scheme 3), 2:2-type complexes are formed with "weakly coordinating" anions like NO$_3$$^-$, and only with strong coordinating anions, like Cl$^-$, 2:1-type complexes are accessible (Table 2) [25,41].

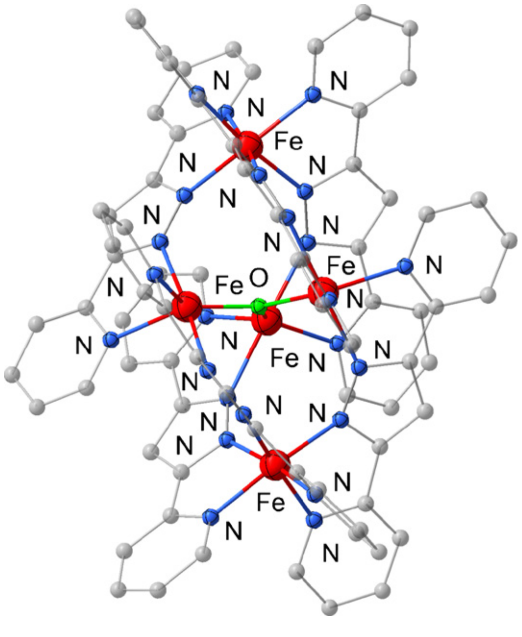

Fig. 3. Molecular structure of the 6:5-type complex cation of [{Fe^{II}(**py$_2$-pz**)$_3$}$_2$Fe$^{II}_3$(μ_3-O)](NCS)$_2$·10H$_2$O (**20**).

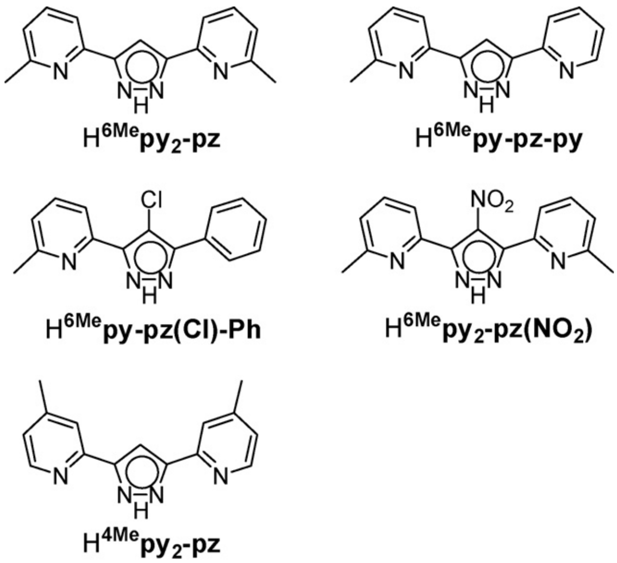

Scheme 3. Derivatives of H**py$_2$-pz**: H**^{6Me}py$_2$-pz**, H**^{6Me}py-pz-py**, H**^{6Me}py-pz(Cl)-Ph**, H**^{6Me}py$_2$-pz(NO$_2$)**, and H**^{4Me}py$_2$-pz**.

Along with that idea, an unusual 4:4-type complex [Cu$^{II}_4$(**^{6Me}py-pz-py**)$_4$(μ-NO$_3$)(NO$_3$)$_2$](NO$_3$) (**21**) was obtained in 2003 by Pons et al., employing the same ligand H**^{6Me}py-pz-py** (Fig. 4, Table 1) [42]. The structure of **21** consists of four copper(II) ions linked to four ligands **^{6Me}py-pz-py**$^-$ and three nitrato co-ligands, one of them coordinating in a bidentate bridging fashion, forming a cyclic system (Fig. 4). The copper(II) ions are in a N$_4$O-five-coordinate coordination sphere. The authors explain the formation of the unusual cyclic complex with the steric hindrance of the ligand methyl group, which inhibits the formation of a 2:2-dinuclear species. Therefore the cyclic system is favoured as the increase of

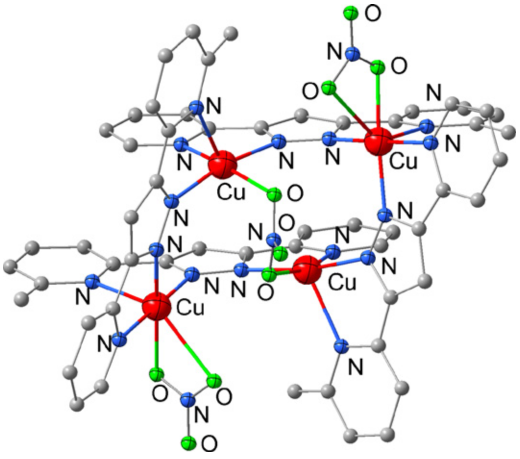

Fig. 4. Molecular structure of the 4:4-type complex cation of [Cu$^{II}_4$(**^{6Me}py-pz-py**)$_4$(μ-NO$_3$)(NO$_3$)$_2$](NO$_3$) (**21**).

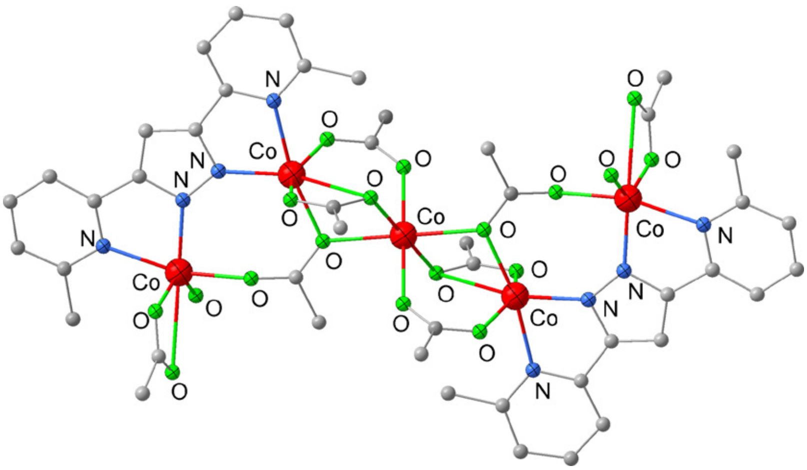

Fig. 5. Molecular structure of the 5:2-type complex $[\mathrm{Co^{II}_5}(\mathbf{^{6Me}py_2\text{-}pz})_2(\mathrm{OAc})_8(\mathrm{H_2O})_2]$ (**32**).

the number of copper(II) ions and the non-coplanar disposition of the ligands avoids a steric bulk [42].

A 2:2-type complex of the monomethylated ligand 4-chloro-3-phenyl-5-(6-methyl-2-pyridyl)pyrazole ($\mathrm{H}\mathbf{^{6Me}py\text{-}pz(Cl)\text{-}Ph}$, Scheme 2) could be isolated by Pons et al. [43] ($[\mathrm{Cu^{II}_2}(\mathbf{^{6Me}py\text{-}pz(Cl)\text{-}Ph})_2\mathrm{Cl_2}(\mathrm{DMF})_2]$, **22**; Table 1). The ligand features one bidentate and one monodentate ligand half, therefore in the complex the non-coordinating phenyl group of the monodentate ligand half is twisted by 44° with respect to the pyrazolate ring to account for the sterical hindrance of the methyl group of the opposed pyridyl ring.

A dinuclear 2:1-type ruthenium(II) cymene complexes of the dimethylated ligand $\mathbf{^{6Me}py_2\text{-}pz}^-$, $[\mathrm{Ru^{II}_2}(\mathbf{^{6Me}py_2\text{-}pz})(\eta^6\text{-}p\text{-cymene})_2\mathrm{Cl_2}](\mathrm{PF_6})$ (**23**; Table 1) was synthesised and characterised in 2000 by Catalano and Craig [44]. The reactivity of **23** was studied and during that course several similar 2:1-type complexes, namely $[\mathrm{Ru^{II}_2}(\mathbf{^{6Me}py_2\text{-}pz})(\eta^6\text{-}p\text{-cymene})_2\mathrm{X_2}](\mathrm{PF_6})$ (**24**: X = $\mathrm{NO_3}$; **25**: X = $\mathrm{NO_2}$), $[\mathrm{Ru^{II}_2}(\mathbf{^{6Me}py_2\text{-}pz})(\eta^6\text{-}p\text{-cymene})_2\mathrm{L_2}](\mathrm{BF_4})_3$ (**26**: L = $\mathrm{H_2O}$; **27**: L = MeCN) and $[\mathrm{Ru^{II}_2}(\mathbf{^{6Me}py_2\text{-}pz(NO_2)})(\eta^6\text{-}p\text{-cymene})_2\mathrm{Cl_2}](\mathrm{PF_6})$ (**28**) (for $\mathrm{H}\mathbf{^{6Me}py_2\text{-}pz(NO_2)}$ see Scheme 3), were isolated and characterised by X-ray analyses (Table 1) [44]. In 2003 the same authors studied the reactivity of another 2:1-type ruthenium(II) complex of $\mathbf{^{6Me}py_2\text{-}pz}^-$, synthesised with the help of the terdentate co-ligand trpy $[\mathrm{Ru^{II}_2}(\mathbf{^{6Me}py_2\text{-}pz})(\mathrm{trpy})_2\mathrm{OH}](\mathrm{PF_6})_2$. In several co-ligand exchange experiments complexes of the type $[\mathrm{Ru^{II}_2}(\mathbf{^{6Me}py_2\text{-}pz})(\mathrm{trpy})_2\mathrm{X}](\mathrm{PF_6})_2$ [X = Cl, Br, I, $\mathrm{N_3}$, OBz; **29**: X = $\mathrm{CH_2(O)CMe}$) could be isolated [45]. In addition, the X-ray analyses of **29**·$\mathrm{OCMe_2}$, $[\mathrm{Ru^{II}_2}(\mathbf{^{6Me}py_2\text{-}pz})(\mathrm{trpy})_2\mathrm{Cl}](\mathrm{BF_4})_2$ (**30**), and $[\mathrm{Ru^{II}_2}(\mathbf{^{4Me}py_2\text{-}pz})(\mathrm{trpy})_2\mathrm{Cl}](\mathrm{PF_6})_2\cdot0.5\mathrm{MeOH}$ (**31**) (for $\mathrm{H}\mathbf{^{4Me}py_2\text{-}pz}$ see Scheme 3) were presented (Table 1) [45].

An unusual 5:2-type complex of cobalt(II), $[\mathrm{Co^{II}_5}(\mathbf{^{6Me}py_2\text{-}pz})_2(\mathrm{OAc})_8(\mathrm{H_2O})_2]$ (**32**) (Fig. 5, Table 1) was reported in 2002, employing the dimethylated ligand $\mathrm{H}\mathbf{^{6Me}py_2\text{-}pz}$ [46].

Complex **32** consists of a centrosymmetrical pentanuclear cobalt(II) complex containing two anionic ligands $\mathbf{^{6Me}py_2\text{-}pz}^-$, eight acetate anions and two water molecules, all coordinating. A central cobalt(II) atom is linked to four neighbouring cobalt(II) atoms by four μ-acetato and two μ_3-acetato ligands. The terminal cobalt(II) atoms are bridged by the pyrazolate moiety of the $\mathbf{^{6Me}py_2\text{-}pz}^-$ ligand, supported by its chelate side arms, and a μ_3-acetato moiety.

2.2. *Pyrazole-3,5-dicarboxylic acid* ($\mathrm{H_3}\mathbf{(O_2C)_2\text{-}pz}$)

The ligand $\mathrm{H_3}\mathbf{(O_2C)_2\text{-}pz}$ is an extremely versatile ligand and offers multiple coordination sites in the form of the two pyrazole nitrogen atoms and the four carboxylic oxygen atoms. Therefore $\mathrm{H_3}\mathbf{(O_2C)_2\text{-}pz}$ and its anions $\mathrm{H_2}\mathbf{(O_2C)_2\text{-}pz}^-$, $\mathrm{H}\mathbf{(O_2C)_2\text{-}pz^{2-}}$ and $\mathbf{(O_2C)_2\text{-}pz^{3-}}$ can act as mono-, to sexidentate ligands and as metal···metal bridges to generate di-, oligo- or polynuclear complexes. In Scheme 4 some coordination modes of $\mathrm{H_3}\mathbf{(O_2C)_2\text{-}pz}$ and its anions are highlighted. This section will focus on complexes that contain pyrazolato-bridged metal centres.

2.2.1. *Discrete and extended structures based on 2:2-type coordination of* $\mathrm{H_3}\mathbf{(O_2C)_2\text{-}pz}$

The first pyrazolato metal···metal-bridged complexes of $\mathrm{H_3}\mathbf{(O_2C)_2\text{-}pz}$ or its anions were discrete dinuclear 2:2-type complexes of fully deprotonated ligands $\mathbf{(O_2C)_2\text{-}pz^{3-}}$ with platinum(II), palladium(II), nickel(II) and copper(II) [47]. The crystal structures of $(\mathrm{NBu_4})_2[\mathrm{M^{II}_2}(\mathbf{(O_2C)_2\text{-}pz})_2]$ (**33**: M = Pd; **34**: M = Cu) were reported (Tables 1 and 2) [47]. Similar to the 2:2-complexes (**1**–**6**) of the $\mathbf{py_2\text{-}pz}^-$ ligand, the deprotonated $\mathbf{(O_2C)_2\text{-}pz^{3-}}$ ligands of **33** and **34** coordinate to the metal ions in a doubly pyrazolato bridging manner, thus forming a square-planar coordination sphere around each metal ion. Additional co-ligands are not present, but weak interactions exist with pyrazolate nitrogen and carboxylate oxygen atoms of adjacent dinuclear units. The antiferromagnetic coupling in **34** ($J = -100.1\ \mathrm{cm^{-1}}$) is considerably smaller than that in similar copper(II) complexes of $\mathbf{py_2\text{-}pz}^-$ (**2**: $J = -180\ \mathrm{cm^{-1}}$; **3**: $J = -368.3\ \mathrm{cm^{-1}}$). In 2004 and 2005, similar discrete 2:2-type copper(II) complexes of $\mathbf{(O_2C)_2\text{-}pz^{3-}}$, *cis*-$(\mathrm{Et_3NH})_2[\mathrm{Cu^{II}_2}(\mathbf{(O_2C)_2\text{-}pz})_2(\mathrm{H_2O})_2]$ (**35**; Fig. 6) [48] and $(\mathrm{Me_2NH_2})_2[\mathrm{Cu^{II}_2}(\mathbf{(O_2C)_2\text{-}pz})_2(\mathrm{H_2O})_2]$ (**36**) [49] were reported (Tables 1 and 2). The distinct difference between compound **34** and the compounds **35** and **36** is the coordination environment about the copper(II) ions, which is square-pyramidal

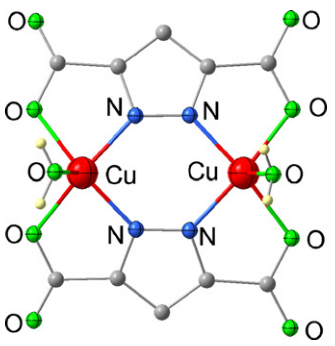

Fig. 6. Molecular structure of the 2:2-type complex anion of *cis*-$(\mathrm{Et_3NH})_2[\mathrm{Cu^{II}_2}(\mathbf{(O_2C)_2\text{-}pz})_2(\mathrm{H_2O})_2]$ (**35**).

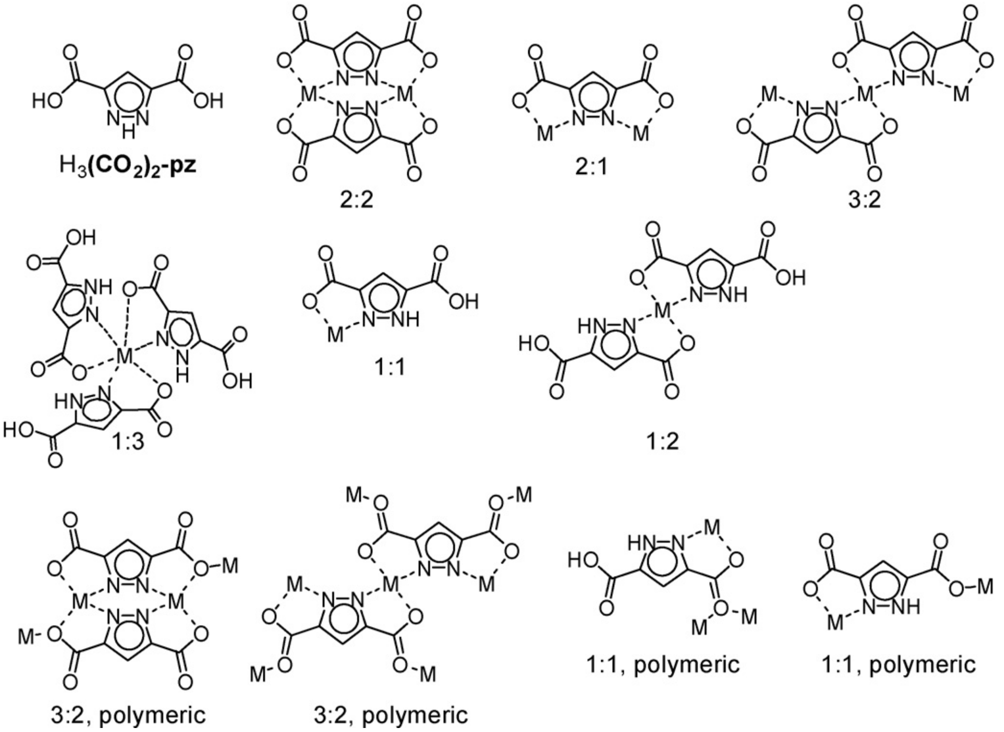

Scheme 4. The ligand $H_3\mathbf{(O_2C)_2\text{-}pz}$ and some coordination modes of $H_3\mathbf{(O_2C)_2\text{-}pz}$ and it anions.

(water co-ligands) for **35** and **36**. A similar zinc(II) complex, $[Zn^{II}_2(\mathbf{(O_2C)_2\text{-}pz})_2(H_2O)_4](Him)_2$ (**37**) (Him = imidazolium cation) (Table 1) with octahedrally coordinated metal(II) ions (water co-ligands) was also reported [50].

2:2-Type *cis*-oxovanadium(IV) complexes of $\mathbf{(O_2C)_2\text{-}pz^{3-}}$ were reported in 1992 $(Bu_4N)_2[(V^{IV}O)_2(\mathbf{(O_2C)_2\text{-}pz})_2]$, **38**; Table 1) [51] and 1998 [52]. Similarly to **32**–**37**, the deprotonated ligands $\mathbf{(O_2C)_2\text{-}pz^{3-}}$ in **38** form coordination squares around the vanadium(IV) ions. The coordination spheres around the vanadium(IV) ions are best described as N_2O_3 square-pyramidal, as *cis*-arranged vanadyl oxygen atoms occupy the apexes of the coordination pyramids, respectively.

An unusual neutral 2:2-type structure of copper(II) and the merely doubly deprotonated ligand $H\mathbf{(O_2C)_2\text{-}pz^{2-}}$, namely $[Cu^{II}_2(H\mathbf{(O_2C)_2\text{-}pz})_2]\cdot$4,4′-dpdo (**39**) (4,4′-dpdo = 4,4′-dipyridyl-*N*,*N*′-dioxide), was structurally characterised in 2003 by Tian et al. [53] (Tables 1 and 2). In the dinuclear unit, each copper(II) ion is coordinated by two doubly deprotonated ligands $H\mathbf{(O_2C)_2\text{-}pz^{2-}}$, forming the bases of distorted N_2O_3 square-pyramidal coordination spheres about the copper(II) ions. Remarkably, while the pyrazole nitrogen atom is deprotonated, one of the carboxylic groups remains protonated. The metal···metal distance (3.439 Å) of **39** is remarkably shorter than the shortest distance (3.96 Å for **35**) observed for copper(II) complexes of the fully deprotonated ligand $\mathbf{(O_2C)_2\text{-}pz^{3-}}$.

As a general trend for discrete 2:2-type complexes of the fully deprotonated ligand $\mathbf{(O_2C)_2\text{-}pz^{3-}}$ one can state that the difference in the intermetallic separation increases in the order Pd^{II} (**33**: 3.89 Å) < Cu^{II} (**34**: 3.99; **35**: 3.96 Å) < $V^{IV}O$ (**38**: 4.2 Å) and demonstrates a remarkable adaptability of this otherwise rigid ligand system.

Extended structures based on 2:2-type complexes of $\mathbf{(O_2C)_2\text{-}pz^{3-}}$ where reported in 2004 by King et al. [48]. In the complex $[\{Na_2(\mu\text{-}H_2O)_2\}\{Cu^{II}_2(\mathbf{(O_2C)_2\text{-}pz})\}_2]_\infty$ (**40**) dinuclear building blocks are stacked in such a way that the axial coordination sites of the copper(II) ions are *trans*-occupied by weakly coordinating pyrazolate nitrogen ($Cu^{II}\cdots N$ = 3.034 Å) and carboxylate oxygen atoms ($Cu^{II}\cdots O$ = 3.145 Å) of adjacent dinuclear complexes, respectively (Table 1). This motif has been observed earlier in the complexes **33** and **34** [47], but in complex **40**, the stacks of dinuclear units are further linked into a 3D array via chains of $[Na(\mu\text{-}H_2O)]_\infty$. The structure of $[\{Ni^{II}(H_2O)_4\}\{Ni^{II}_2(\mathbf{(O_2C)_2\text{-}pz})_2(H_2O)_4\}]_\infty$ (**41**) is made up of 1D chains of 2:2-type dinuclear subunits. The nickel(II) ions of the dinuclear subunits are in a distorted N_2O_4 octahedral environment, made up be the equatorially coordinating $\mathbf{(O_2C)_2\text{-}pz^{3-}}$ ligands and completed by two axially coordinating water molecules, respectively. The dinuclear building blocks are linked by $[Ni^{II}(H_2O)_4]^{2+}$ fragments, which bind to carboxylate oxygen atoms of adjacent subunits [48].

2.2.2. 2:1-Type complexes of $H_3\mathbf{(O_2C)_2\text{-}pz}$

By analogy to the formations of 2:1-type complexes of $\mathbf{py_2\text{-}pz^-}$, 2:1-type complexes of $\mathbf{(O_2C)_2\text{-}pz^{3-}}$ are accessible in the presence of chelating co-ligands. The first 2:1-type complexes of $H_3\mathbf{(O_2C)_2\text{-}pz}$ or any of its anions were reported in 1991 by Bayón, Rasmussen and co-workers. The complexes $(R_4N)[M^I_2\mathbf{(O_2C)_2\text{-}pz}(COD)_2]$ (COD = 1,5-cyclooctadiene) (R = Me, Pr, Bu; M = Rh, Ir) were synthesised by adding R_4NOH to a suspension of $[M^I(\mu\text{-}Cl)(COD)]_2$ and $H_3\mathbf{(O_2C)_2\text{-}pz}$ in acetonitrile [54]. Co-ligand exchange of COD by CO afforded the complexes $(R_4N)[M^I_2\mathbf{(O_2C)_2\text{-}pz}(CO)_4]$ of which the compound $(Bu_4N)[Rh^I_2\mathbf{(O_2C)_2\text{-}pz}(CO)_4]$ (**42**) was structurally characterised (Table 1). The most significant feature of the structure is the distortion from planar geometry, resulting from rotations of the carboxylate groups with respect to the pyrazolate ring to minimize the contact between the carbonyl co-ligands. The rhodium(I)···rhodium(I) distance (4.53 Å) is thus longer than the distances observed for the 2:2-type complexes **32**–**39**. Remarkably, the electrochemical or chemical oxidation of **42** in acetonitrile affords the neutral mixed-valence compound $[Rh^{II}Rh^I\mathbf{(O_2C)_2\text{-}pz}(CO)_4]$, while the same reaction conditions applied on the analogous iridium(I) complex

$(Bu_4N)[Ir^I{}_2$**(O$_2$C)$_2$-pz**$(CO)_4]$ afford the intermediate-state complex $(Bu_4N)_{0.5}[Ir^{1.25}{}_2(CO)_4$**(O$_2$C)$_2$-pz**$]$ as partially oxidized material [54].

In 1993, Nakahanada and Kaizaki reported the synthesis and characterisation of isomeric (*rac*- and *meso*-) 2:1-type chromium(III) complexes ($Na[Cr^{III}{}_2$**(O$_2$C)$_2$-pz**$(acac)_4]$; Table 2), using acac as bidentate chelating co-ligand [55]. In 1996, those studies where extended using the quadridentate O–N–N–O co-ligands $edda^{2-}$ and $trdda^{2-}$ ($edda^{2-}$ = ethylenediamine-*N*,*N*′-diacetate; $trdda^{2-}$ = trimethylethylenediamine-*N*,*N*′-diacetate), and in the course of those studies both the crystal structures and absolute configurations of $Na[Cr^{III}{}_2$**(O$_2$C)$_2$-pz**$(edda)_2]\cdot 5H_2O$ (**43**) and $Na[Cr^{III}{}_2$**(O$_2$C)$_2$-pz**$(trdda)_2]\cdot 3H_2O$ (**44**) have been determined (Table 1) [56]. The use of $eddp^{2-}$ and *R*,*R*-, *S*,*S*-, or *R*,*S*-$cdda^{2-}$ ($eddp^{2-}$ = ethylenediamine-*N*,*N*′-dipropionate; $cdda^{2-}$ = 1,2-cyclohexanediamine-*N*,*N*′-diacetate) as yet other type of O–N–N–O quadridentate co-ligands resulted, in 2000, in further configurational studies and the report of the crystal structure of $Na[Cr^{III}{}_2$**(O$_2$C)$_2$-pz**$(eddp)_2]\cdot 6H_2O$ (**45**) [57]. The structures of all reported dinuclear chromium(III) complexes (**43**–**45**) consist of discrete 2:1-type complex anions, featuring two chromium(III) ions in distorted octahedral N_3O_3 coordination spheres. The octahedral coordination spheres about the chromium(III) ions are completed by the quadridentate co-ligands that wrap around one metal ion. In that way 12 conformational isomers can be formed [56].

The crystal structures and absolute configurations of homo- and heterodinuclear 2:1-type complexes of ruthenium(II) and osmium(II) with **(O$_2$C)$_2$-pz^{3-}**, synthesised with the help of the neutral bidentate ligand bpy (bpy = 2,2′-bipyridine), were reported by Baitalik and Nag [58,59]. Isostructural complexes $[Ru^{II}{}_2$**(O$_2$C)$_2$-pz**$(bpy)_4](ClO_4)\cdot H_2O$ (**46**) [58], $[Ru^{II}Os^{II}$**(O$_2$C)$_2$-pz**$(bpy)_4](ClO_4)\cdot H_2O$ (**47**) [58] and $[Os^{II}{}_2$**(O$_2$C)$_2$-pz**$(bpy)_4](ClO_4)\cdot H_2O$ (**48**; Fig. 7) [59] were described as the *rac*($\Lambda\Lambda/\Delta\Delta$) isomers (Table 1).

In 2004 the authors were able to isolate the corresponding *meso*-isomers of **46** and **48**, but unfortunately no X-ray crystallographic characterisation could be carried out [59].

Using COD as chelating co-ligand, Grobbelaar, Purcell and Basson investigated the oxidative addition reactions with iodomethane of the dinuclear iridium(I) complex $Bu_4N[Ir^I{}_2$**(O$_2$C)$_2$-pz**$(COD)_2]$, to find out that the reaction occurs mainly *via* the direct pathway (and much slower on the solvent-assisted pathway), as the solvent effect is remarkably small [60].

Two organostannoxane 2D networks based on 2:1-type coordination of **(O$_2$C)$_2$-pz** were published in 2007 [61]. In $[(Bz_2Sn^{IV})_6($**(O$_2$C)$_2$-pz**$)_4(\mu\text{-}OH)_2(Bz_2Sn^{IV}Cl)_2]_\infty$ (**49**; Table 1) rectangular box-type hexatin(IV) units $[(Bz_2Sn^{IV})_6($**(O$_2$C)$_2$-pz**$)_4(\mu\text{-}OH)_2]$ are interconnected by two $Bz_2Sn^{IV}Cl$ bridging groups, resulting in a O_2ClC_2-fivefold coordination for the bridging tin(IV) ions. The hexatin units consist of two symmetry-related tritin subunits where each tin(IV) ion is coordinated by at least one bridging pyrazolate nitrogen and one carboxylate oxygen. Hexatin(IV) macrocycles as found in **49** and tetratin(IV) ladder motifs are bridged to build the polymeric tape-structure of $[\{(Bz_2Sn^{IV})_6($**(O$_2$C)$_2$-pz**$)_4(\mu\text{-}OH)_2(py)_2\}\{(Bz_2Sn^{IV})_2(\mu_3\text{-}O)(\mu\text{-}OH)\}_2]_\infty$ (**50**; Table 1).

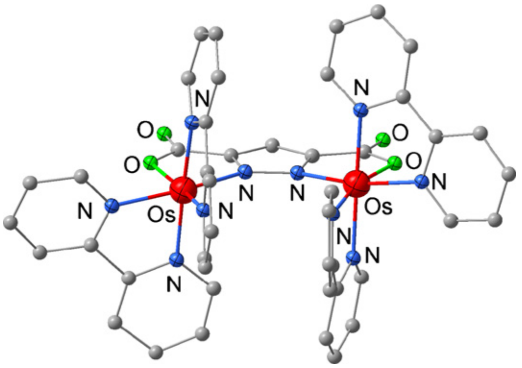

Fig. 7. Molecular structure of the cation of the 2:1-type complex $[Os^{II}{}_2$**(O$_2$C)$_2$-pz**$(bpy)_2](ClO_4)\cdot H_2O$ (**48**).

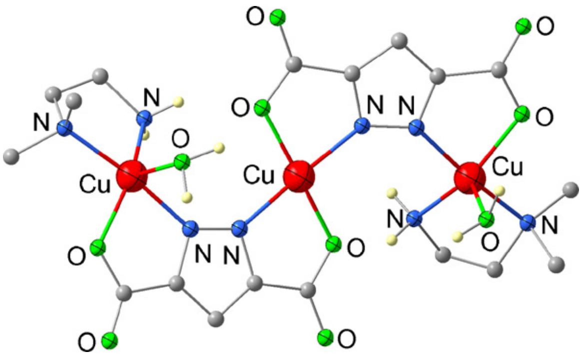

Fig. 8. Molecular structure of the 3:2-type complex of $[Cu^{II}{}_3($**(O$_2$C)$_2$-pz**$)_2(Me_2en)_2(H_2O)_2]\cdot 8H_2O$ (**51**).

2.2.3. Discrete and extended structures based on 3:2-type coordination of H_3**(O$_2$C)$_2$-pz**

The only 3:2-type complexes of H_3**(O$_2$C)$_2$-pz** or any of its anions, discrete as well as polymeric, that have been published so far are of copper(II). The complex $[Cu^{II}{}_3($**(O$_2$C)$_2$-pz**$)_2(Me_2en)_2(H_2O)_2]\cdot 8H_2O$ (**51**) (Fig. 8, Table 1) (Me_2en = *N*,*N*′-dimethylethylenediamine) and $[Cu^{II}{}_3($**(O$_2$C)$_2$-pz**$)_2(MeOH)_6(H_2O)_4]$ (**52**; Tables 1 and 2) derived from hydrolysis of the amide-based ligands *N*,*N*′-bis[2-(2-pyridyl)ethyl]pyrazole-3,5-dicarboxamide (H_3**(pyC$_2$N^{CO})$_2$-pz**) and *N*,*N*′-bis[2-(*N*,*N*-dimethylamino)ethyl]pyrazole-3,5-dicarboxamide (H_3**(N^{Me}N^{CO})$_2$-pz**) (compare Scheme 7) [62].

In **51** and **52** a linear arrangement of the copper(II) ions is achieved by two bridging **(O$_2$C)$_2$-pz^{3-}** anions, respectively. The central copper(II) ion of **51** is in a distorted N_2O_2 square-planar coordination sphere, built up by two bidentate coordination pockets of the bridging ligands. Two additional methanol co-ligands complete the distorted octahedral coordination sphere of the central copper(II) ion in **52**.

In $[Cu^{II}{}_3($**(O$_2$C)$_2$-pz**$)_2(H_2O)_4]_\infty$ (**53**) (Tables 1 and 2) a 3D network of 3:2-type building blocks is formed through additional bridging of ligand carboxyl oxygen atoms to terminal copper(II) ions of adjacent trinuclear units [48,63].

2.3. Other bis-bidentate pyrazolate ligands

2.3.1. N-pz-N-type ligands

The simplest and first reported N-pz-N-type ligand without a pyridine group is 3,5-bis(aminomethyl)pyrazole (H**N$_2$-pz**) (Scheme 5) [64].

In 1991, Kamiusuki, Ōkawa and co-workers reported its synthesis together with the synthesis and magnetic properties of the 2:2-type complexes $[Cu^{II}{}_2($**N$_2$-pz**$)_2X_2]$ (X = Cl, Br) and the X-ray crystal structure of *trans*-$[Cu^{II}{}_2($**N$_2$-pz**$)_2Br_2]$ (**54**) (Tables 1 and 2). In the same year the bis-bidentate ligand 3,5-bis(4-methylpyrazol-1-yl)-4-methylpyrazole (**pz$_2$-pz(Me)**) (Scheme 5) and its complexation behaviour towards rhodium(I) and the chelating co-ligands COD and TFB (TFB = tetrafluorobenzo[5,6]bicyclo[2.2.2]octa-2,5,7-triene) leading to 1:1- and 2:1-type complexes was reported [65].

The unusual N-pz-N-type ligand pyrazole-3,5-diyl bis(imino nitroxide) (H**INO$_2$-pz**) was reported by Yamada, Ishida and co-workers, together with the crystal structure and magnetic analyses of an unusual 1:1-type polymeric silver(I) complex ($[Ag^I($**INO$_2$-**

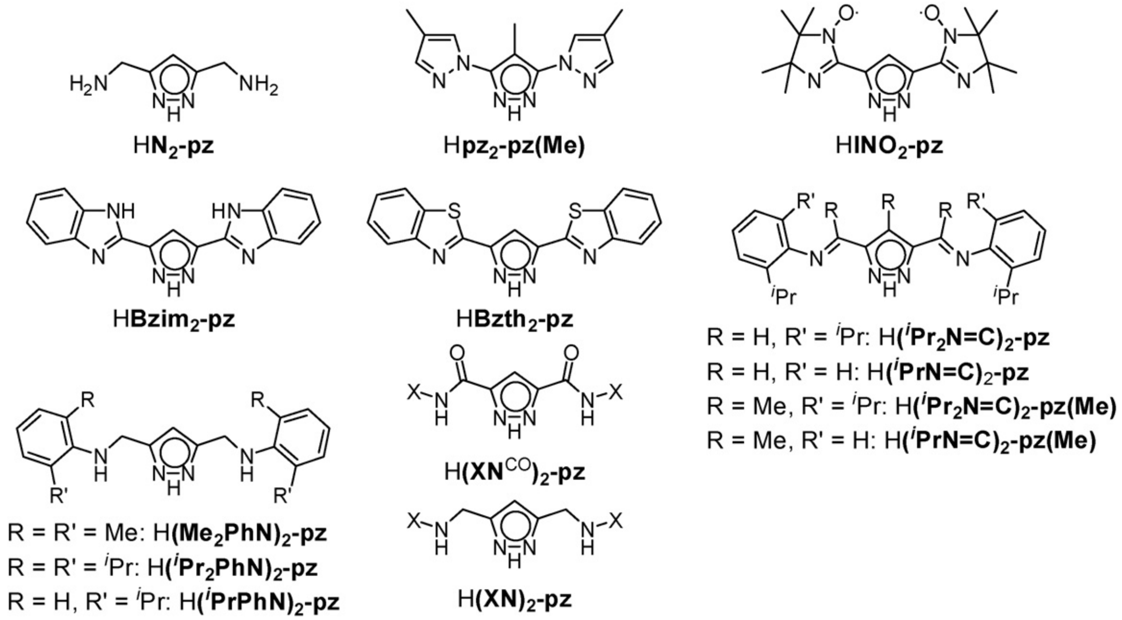

Scheme 5. N-pz-N-type ligands: H**N$_2$-pz**, H**pz$_2$-pz(Me)**, H**INO$_2$-pz**, H**Bzim$_2$-pz**, H**Bzth$_2$-pz**, H(**^{i}Pr$_2$N=C)$_2$-pz**, H(**^{i}PrN=C)$_2$-pz**, H(**^{i}Pr$_2$N=C)$_2$-pz(Me)**, H(**^{i}PrN=C)$_2$-pz(Me)**, H(**Me$_2$PhN)$_2$-pz**, H(**^{i}Pr$_2$PhN)$_2$-pz**, H(**^{i}PrPhN)$_2$-pz**, H(**XN^{CO})$_2$-pz** and H(**XN)$_2$-pz**.

pz)]$_\infty$, **55**), that features pyrazolato-bridged metal ions (Fig. 9, Table 1) [66].

The silver(I) ions in **55** are basically coordinated in a linear fashion by a pyrazolate nitrogen atom of one **INO$_2$-pz**$^-$ ligand and an imidazoline nitrogen atom of a neighbouring **INO$_2$-pz**$^-$ ligand. Per silver(I) ion two more distal donor atoms, an imidazoline nitrogen of the former and a pyrazolate nitrogen of the latter ligand, are present to result in an overall tetracoordinate geometry.

The ligands 3,5-bis(benzimidazol-2-yl)pyrazole (H**Bzim$_2$-pz**) and 3,5-bis(benzothiazol-2-yl)pyrazole (H**Bzth$_2$-pz**) (Scheme 5) in their deprotonated anionic form, give 1:1- and 2:1-type ruthenium(II) complexes in the presence of chelating co-ligands [67–69]. In 1999, Baitalik, Nag and co-workers reported the crystal structures of the 2:1-type complexes *meso*($\Lambda\Delta$)-[Ru$^{II}_2$**Bzim$_2$-pz**(bpy)$_4$](ClO$_4$)$_3$·5H$_2$O (**56**) [67] and [Ru$^{II}_2$**Bzth$_2$-pz**(bpy)$_4$](ClO$_4$)$_3$·H$_2$O (**57**) (Table 1) [68]. Spectroscopic analyses coupled with isomer studies of the ruthenium(II)–rhodium(III) heterodinuclear 2:1-type complex [(bpy)$_2$Ru^{II}(**Bzim$_2$-pz**)Rh^{III}(bpy)$_2$](ClO$_4$)$_4$ followed in 2004 [69].

The imine-based pyrazole derivatives H(**^{i}Pr$_2$N=C)$_2$-pz**, H(**^{i}PrN=C)$_2$-pz**, H(**^{i}Pr$_2$N=C)$_2$-pz(Me)**, and H(**^{i}PrN=C)$_2$-pz(Me)** (Scheme 5) can be described as binucleating versions of the well-known α-diimine type ligands [70,71]. They form a series of dinuclear palladium(II) complexes [Pd$^{II}_2$(**L**)Cl$_3$] (**58**: H**L** = H(**^{i}Pr$_2$N=C)$_2$-pz**; **59**: H**L** = H(**^{i}Pr$_2$N=C)$_2$-pz(Me)**; Table 1), where the palladium(II) is found in roughly square-planar environment (Fig. 10). The bulky aryl substituents shield the bimetallic entity from the outer sides, while the central part is accessible for further reactivity.

With nickel(II), the same ligands give oligonuclear aggregates [Ni$^{II}_2$(**L**)X$_3$]$_x$ (X = Cl, Br), where the metal ions are six-coordinate and in the high-spin state [70]. The hexanuclear complex [Ni$^{II}_6$((**^{i}Pr$_2$N=C)$_2$-pz**)$_3$(μ-Cl)$_8$(μ_6-Cl)] (**60**) is obtained from H(**^{i}Pr$_2$N=C)$_2$-pz**, two equivalents of [NiCl$_2$(dme)] (dme = 1,2-dimethoxyethane) and one equivalent of base (Fig. 11; Table 1) [70]. Single crystal analyses on compound **61** (H**L** = H(**^{i}Pr$_2$N=C)$_2$-pz**, $x = 3$; Table 1) showed it to be iso-structural to the chloro-bridged nickel(II) complex **60** [71].

The three dinuclear building blocks of **60** are connected through chlorido-bridges to constitute a hexanuclear array. The central Ni$_6$Cl$_9$ core consists of two roughly planar Ni$_3$Cl$_3$ ring systems that are capped by a μ_3-Cl atom and interconnect by a μ_6-Cl-bridge [70]. In the presence of chloroform, the hexanuclear entity of **60** is

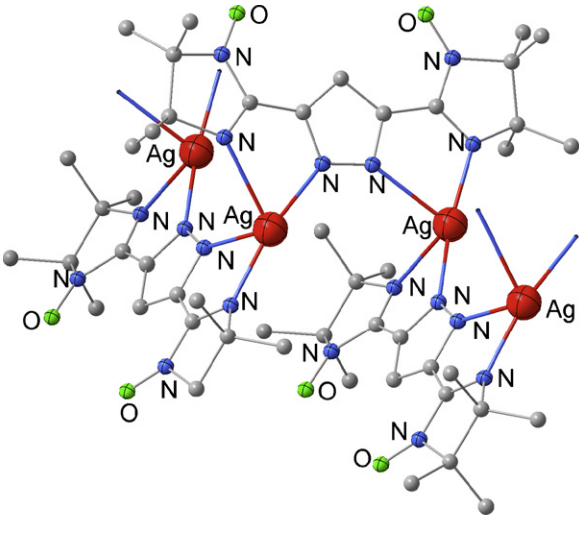

Fig. 9. Section of the molecular structure of the polymeric complex [Ag^I(**INO$_2$-pz**)]$_\infty$ (**55**).

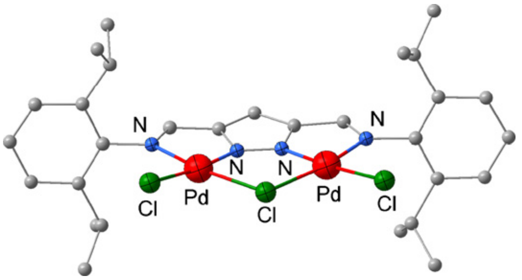

Fig. 10. Molecular structure of the 2:1-type complex [Pd$^{II}_2$((**^{i}Pr$_2$N=C)$_2$-pz**)Cl$_3$] (**58**).

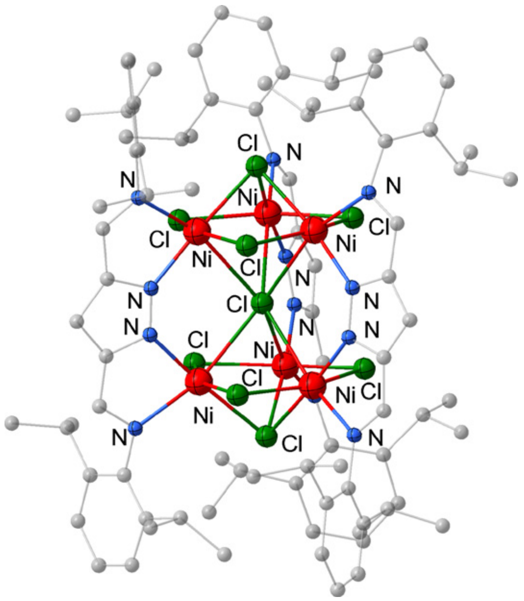

Fig. 11. Molecular structure of the extended 2:1-type structure $[\mathrm{Ni^{II}}_6(\mathbf{(^{i}Pr_2N{=}C)_2\text{-}pz})_3(\mu\text{-Cl})_8(\mu_6\text{-Cl})]$ (**60**).

degraded to form a tetranuclear complex $[\mathrm{Ni^{II}}_4(\mathbf{(^{i}Pr_2N{=}C)_2\text{-}pz})_2(\mu\text{-Cl})_2(\mu_3\text{-Cl})_2\mathrm{Cl_2(EtOH)_2}]$ (**62**) (Table 1). In **62** two dinuclear building blocks are linked through μ- and μ_3-Cl-bridges to form a stair like dimeric tetranuclear aggregate with N_2OCl_3 distorted octahedrally coordinated nickel(II) ions [70].

The complexes of the type $[\mathrm{Pd^{II}}_2(\mathbf{L})\mathrm{Cl_3}]$ and $[\mathrm{Ni^{II}}_2(\mathbf{L})\mathrm{Br_3}]_x$ were studied as catalyst precursors for ethylene polymerisation using MAO as cocatalyst, describing them as bimetallic version of Brookhart-type α-diimine complexes (MAO = metyl aluminoxane). As expected, the dinuclear nickel(II) complexes are significantly more active than the corresponding palladium(II) systems. For both series of complexes the reactivity increases in the order $\mathbf{(^{i}PrN{=}C)_2\text{-}pz} < \mathbf{(^{i}Pr_2N{=}C)_2\text{-}pz} < \mathbf{(^{i}PrN{=}C)_2\text{-}pz(Me)} < \mathbf{(^{i}Pr_2N{=}C)_2\text{-}pz(Me)}$ suggesting that sterically demanding substituents at the ligand backbone are advantageous [71].

Monomeric 2:2-type complexes of nickel(II) or palladium(II) are formed with the related ligands H$\mathbf{(Me_2PhN)_2\text{-}pz}$ {*trans*-$[\mathrm{Ni^{II}}_2(\mathbf{(Me_2PhN)_2\text{-}pz})_2\mathrm{Cl_2}]$ (**63**), $[\mathrm{Ni^{II}}_2(\mathbf{(Me_2PhN)_2\text{-}pz})_2]\mathrm{Cl_2}$ (**64**), $[\mathrm{Ni^{II}}_2(\mathbf{(Me_2PhN)_2\text{-}pz})_2](\mathrm{ClO_4})_2$ (**65**) and $[\mathrm{Pd^{II}}_2(\mathbf{(Me_2PhN)_2\text{-}pz})_2](\mathrm{BF_4})_2$ (**66**)}, H$\mathbf{(^{i}Pr_2PhN)_2\text{-}pz}$ {$[\mathrm{Ni^{II}}_2(\mathbf{(^{i}Pr_2PhN)_2\text{-}pz})_2](\mathrm{ClO_4})_2$ (**67**) and $[\mathrm{Pd^{II}}_2(\mathbf{(^{i}Pr_2PhN)_2\text{-}pz})_2](\mathrm{BF_4})_2$ (**68**)} and H$\mathbf{(^{i}PrPhN)_2\text{-}pz}$ {$[\mathrm{Ni^{II}}_2(\mathbf{(^{i}PrPhN)_2\text{-}pz})_2](\mathrm{ClO_4})_2$ (**69**)} (Scheme 5, Table 1) [72]. A mixed ligand species $[\mathrm{Ni^{II}}_2\mathbf{(Me_2PhN)_2\text{-}pz})(\mathbf{^{i}Pr_2PhN)_2\text{-}pz})](\mathrm{ClO_4})_2$ (**70**; Fig. 12) was also reported [72].

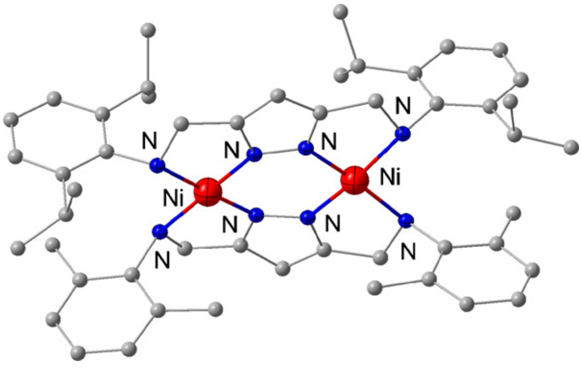

Fig. 12. Molecular structure of the 2:2-type complex cation of $[\mathrm{Ni^{II}}_2\mathbf{(Me_2PhN)_2\text{-}pz})(\mathbf{^{i}Pr_2PhN)_2\text{-}pz})](\mathrm{ClO_4})_2$ (**70**).

While with weakly coordinating anions the metal ions are found in roughly square-planar environments and are in the low-spin state (**65**–**70**), coordinating counter anions such as chloride can reversibly bind to axial sites of the dinickel(II) species in a solvent-dependent process, giving rise to five-coordinate high-spin nickel(II) (**63** versus **64**). Most interestingly, methyl or isopropyl substituents in the 2- and 6-positions are forced to come into close proximity to the metal sites from the axial directions, which gives rise to drastic low-field shifts in the ^{1}H NMR spectra, although attractive M···H interactions are not assumed to play any major role [72].

In 2007 Kaden and co-workers reported a series of amide and amine based ligands of the H$\mathbf{(XN^{CO})_2\text{-}pz}$ and H$\mathbf{(XN)_2\text{-}pz}$ type (Scheme 5) and studied their complexation potential for metal ions with square planar coordination geometry [X = CH_2-$(CH_2)_n$-NMe_2, CH_2-CH_2-NHY, CH_2-$(CH_2)_n$-OMe, CH_2-$(CH_2)_n$-OZ, CH_2-$CO_2{}^t$Bu, CH_2-$(CH_2)_n$-SMe, CH_2-CH_2-N(CH_2-CH_2-OZ)$_2$, CH_2-py-CH_2-OZ (only the amide-based ligand was isolated); n = 1, 2; Y = benzoylcarbonyl, tosyl; Z = *tert*-butyldimethylmethylsilyl] [73]. In the course of the studies the platinum(II) complexes $[\mathrm{Pt^{II}}_2\mathbf{(XN)_2\text{-}pz}\mathrm{I_3}]$ (X = CH_2-CH_2-OMe (**71**), CH_2-CH_2-CH_2-OMe, CH_2-CH_2-OH) were isolated (Table 1).

2.3.2. 3,5-Bis(diphenylphosphinomethyl)pyrazole (H*P₂-pz*)

The ligand 3,5-bis(diphenylphosphinomethyl)pyrazole (H$\mathbf{P_2\text{-}pz}$) (Scheme 6) was first synthesised by Schenck, Bosnich and co-workers as the 2:2-type nickel(II) complex $[\mathrm{Ni^{II}}_2(\mathbf{P_2\text{-}pz})_2](\mathrm{ClO_4})_2\cdot 2\mathrm{MeCN}$ [74]. As the free ligand is very air sensitive, the authors thought it convenient to store the ligand in form of its nickel(II) complex and to free it as required.

A variety of palladium(II), rhodium(I) and iridium(I) 2:1-type complexes with additional co-ligands have been synthesised either by metal transfer synthesis or by preceding liberation of the ligand [74]. In the same year (1985) Schenck, Bosnich and co-workers reported studies of stoichiometric and catalytic reactivities of the rhodium and iridium complexes [75]. In the course of those studies the crystal structure of the phosphido-bridged mixed-valent 2:1-type complex $[(\mathrm{CO})\mathrm{Rh^{III}}\mathbf{P_2\text{-}pz}(\mu\text{-}\mathrm{Ph_2P})\mathrm{Rh^{I}(CO)(CH_3)I}]\cdot\mathrm{Et_2O}$ (**72**) (Table 1) was reported. The two rhodium ions of **72** are bridged by the pyrazolate moiety and a phosphido co-ligand. The rhodium(I) ion is in a distorted square-planar coordination environment with the fourth position being occupied by a carbonyle molecule, whereas the rhodium(III) ion is in a distorted octahedral environment with the remaining positions being occupied by a carbonyl molecule, a methyl and an iodo co-ligand. In 2001, an unusual tetranuclear complex $[\mathrm{Rh^{I}}_4(\mathbf{P_2\text{-}pz})_2(\mathrm{CO})_4(\mu_4\text{-H})](\mathrm{BPh_4})$ (**73**) (Table 1) was reported by Akita and co-workers [76]. The dimeric complex **73** consists of two perpendicularly arranged 2:1-type $[\mathrm{Rh^{I}}\mathbf{P_2\text{-}pz}(\mathrm{CO})_2]$-fragments that are bridged by an unusual μ_4-hydrido ligand, forming a $\mathrm{Rh^{I}}_4$-tetrahedron.

Other 4:2-type rhodium(I) complexes incorporating bridging acetylide derivatives have been reported by Tanaka et al. [77]. The *p*-toluylethynyl complex $[\mathrm{Rh^{I}}_4(\mathbf{P_2\text{-}pz})_2(\mathrm{CO})_4(\mu_4\text{-}p\text{-tol-C}{\equiv}\mathrm{C})](\mathrm{BPh_4})$ (**74**) (Fig. 13, Table 1) exhibits a butterfly-like array of two dinuclear subunits. The C≡C moiety is coordinated in a μ_4-$\eta^1(C_\alpha)$:$\eta^2(C_\alpha{\equiv}C_\beta)$ fashion [77]. Deprotonation of the respective ethynyl complex $[\mathrm{Rh^{I}}_4(\mathbf{P_2\text{-}pz})_2(\mathrm{CO})_4(\mu_4\text{-C}{\equiv}\mathrm{CH})](\mathrm{BPh_4})$ with alumina or triethylamine resulted in the formation of the neutral species $[\mathrm{Rh^{I}}_4(\mathbf{P_2\text{-}pz})_2(\mathrm{CO})_4(\mu_4\text{-C}{\equiv}\mathrm{C})]$ (**75**) which was also characterised by X-ray crystallography (Table 1) [77]. The complex **75** has a tetrameric μ_4-dicarbide structure, in which the C≡C-bridge interacts with each dinuclear fragment in a μ-η^1:η^2 way, leading to a μ^4-η^1:η^1:η^2:η^2-C≡C bridging mode for the resulting (μ_4-C≡C)$\mathrm{Rh^{I}}_4$ moiety. The dinuclear fragments are further interconnected through a $\mathrm{Rh^{I}}$–$\mathrm{Rh^{I}}$-bond [77].

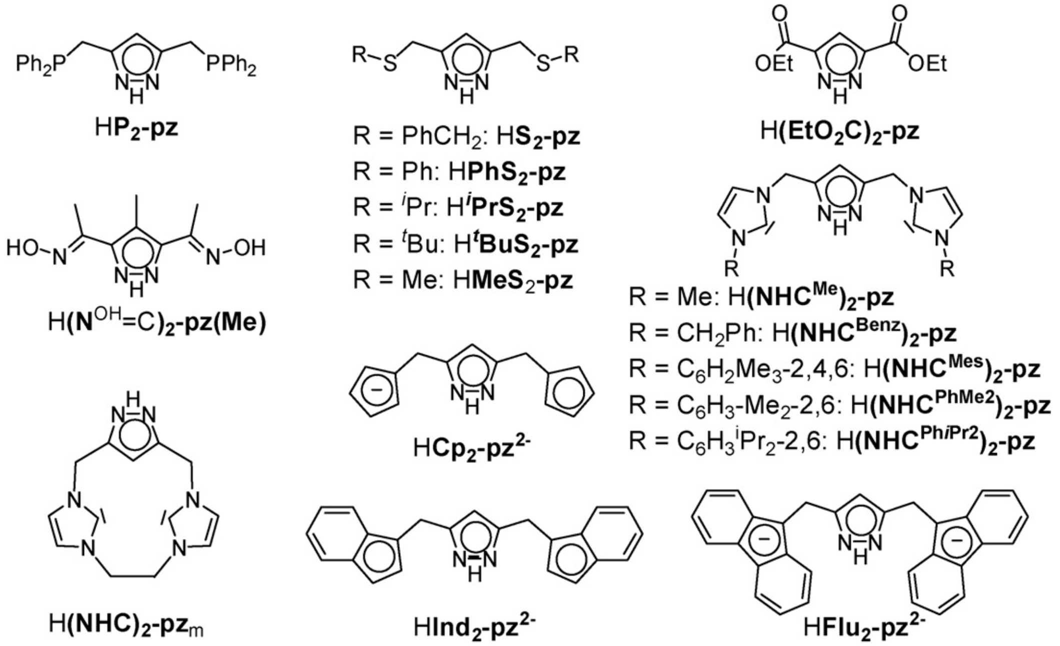

Scheme 6. D$_1$-pz-D$_1$-Type ligands: H**P$_2$-pz**, H**S$_2$-pz**, H**PhS$_2$-pz**, H^i**PrS$_2$-pz**, H^t**BuS$_2$-pz**, H**MeS$_2$-pz**, H**(EtO$_2$C)$_2$-pz**, H(**N^{OH}=C)$_2$-pz(Me)**, H(**NHC^{Me}**)$_2$**-pz**, H(**NHC^{Benz}**)$_2$**-pz**, H(**NHC^{Mes}**)$_2$**-pz**, H(**NHC^{PhMe2}**)$_2$**-pz**, H(**NHC^{PhiPr2}**)$_2$**-pz**, H(**NHC**)$_2$**-pz$_m$**, H**Cp$_2$-pz^{2-}**, H**Ind$_2$-pz^{2-}** and H**Flu$_2$-pz^{2-}**.

The reaction of the discrete 2:1-type complex [Rh$^{I}_{2}$**P$_2$-pz**(CO)$_4$](BF$_4$) with a variety of acetylides resulted in the formation of a variety of discrete dinuclear neutral 2:1-type ethynyl rhodium(I) complexes, namely [Rh$^{I}_{2}$(**P$_2$-pz**)(CO)$_2$(μ-C≡CR)] (**76**: R = H; **77**: R = SiMe$_3$; **78**: R = Bu; **79**: R = Ph; **80**: R = p-tol), which where characterised by X-ray crystallography [78]. The rhodium(I) coordination spheres are virtually planar with the acetylide ligands bridging the two metal ions in a μ-η^1:η^2 fashion. The μ-acetylide as well as the corresponding μ-vinyl complexes show dynamic behaviour *via* a windshield wiper motion of the unsaturated hydrocarbyl ligand. Systematic structural analysis of the series of μ-acetylide complexes **76**–**80** revealed three possible conformations of the Rh$^{I}_{2}$(**P$_2$-pz**)(CO)$_2$ backbone: C_s-, C_2- and C_{2v}-symetrical ones. The authors also described the reaction of the 2:1-type complex [Rh$^{I}_{2}$**P$_2$-pz**(CO)$_4$](BF$_4$) with PPN[M(CO)$_4$] (M = Co, Mn) (PPN$^+$ = bis(triphenylphosphoranylidene)ammonium) to form trinuclear Rh$_2$M complexes [Rh$_2$**P$_2$-pz**(CO)$_2$(μ-M(CO)$_n$)] (**81**: M = Co, n = 4; **82**: M = Mn, n = 5) (Table 1), with a 2:1-type substructure (Fig. 14) [78].

The trinuclear structures **81** and **82** are virtually isostructural, except for the number of μ-CO co-ligands forming the respective (μ-M(CO)$_n$)-fragment, and consist of an open Rh–M–Rh bent linkage with angles of around 90° [78].

Reactions of the 2:1-type precursor complex [Rh$^{I}_{2}$**P$_2$-pz**(CO)$_4$](BF$_4$) with vinyllithium or simple neutral molecules like cyclohexylisonitrile, dimethyl sufide or hexyne lead to the formation simple 2:1-type complexes bearing a μ-co-ligand or in the case of cyclohexylisonitrile non-bridging M–N≡C-cy-moieties [78]. The authors also describe the syntheses of the (except for R = Ph) previously reported [76,77] 4:2-type [Rh$^{I}_{4}$(**P$_2$-pz**)$_2$(CO)$_4$(μ_4-C≡C-R)](BPh$_4$) (R = SiMe$_3$, Bu, Ph, p-tol) complexes [78]. Additionally, the crystal structures of the previously reported complexes **73** [76], **74** [77], and **75** [77] are discussed, together with the crystal structure of the new μ_4-oxo-bridged complex [Rh$^{I}_{4}$(**P$_2$-pz**)$_2$(CO)$_4$(μ_4-O)] (**83**) [78]. The molecular structure of

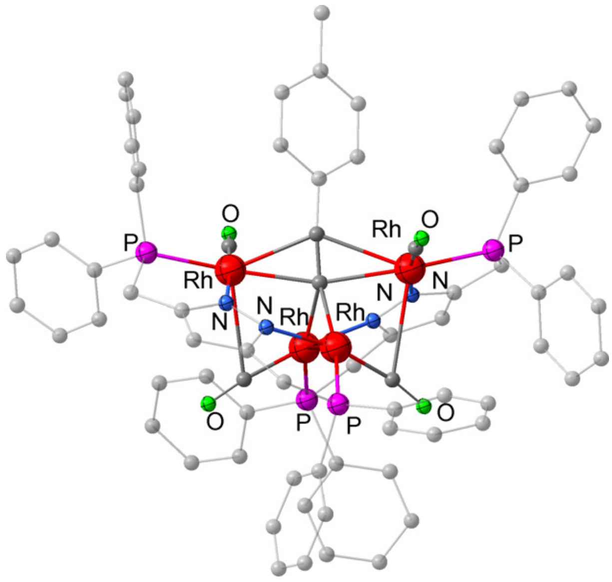

Fig. 13. Molecular structure of the complex cation of the tetranuclear complex [Rh$^{I}_{4}$(**P$_2$-pz**)$_2$(CO)$_4$(μ_4-p-tol-C≡C)](BPh$_4$) (**74**).

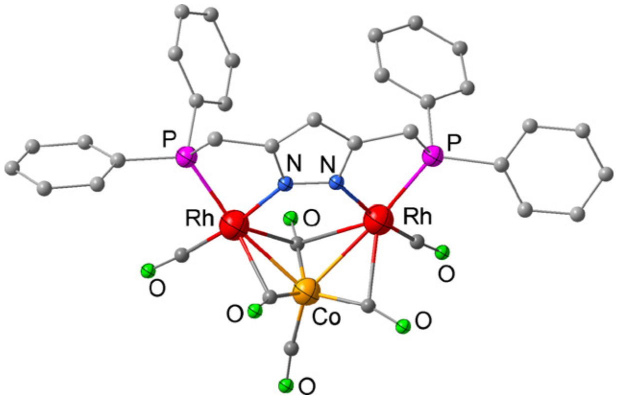

Fig. 14. Molecular structure of the trinuclear molecule [Rh$_2$**P$_2$-pz**(CO)$_2$(μ-Co(CO)$_4$)] (**81**).

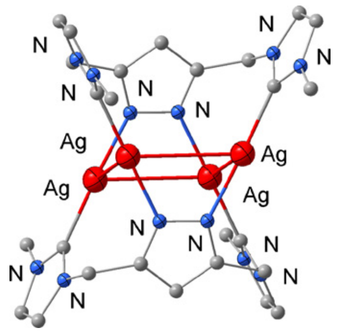

Fig. 15. Molecular structure of the 4:2-type complex cation of [Ag$^{I}_{4}$((**NHC^{Me})$_2$-pz**)$_2$](PF$_6$)$_2$·0.5Et$_2$O (**85**).

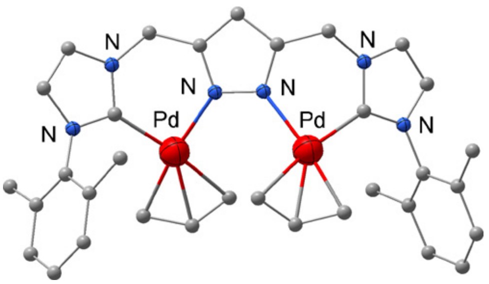

Fig. 16. Molecular structure of the 2:1-type complex cation of [Pd$^{II}_{2}$((**NHC^{PhMe2})$_2$-pz**)(allyl)$_2$](PF$_6$) (**92**).

the tetranuclear complex **83** is virtually isostructural with the complex cation of the μ_4-hydrido-bridged complex **73** (Table 1).

In 2006 Akita and co-workers showed synthetic methods for preparing heterodinuclear complexes of the ligand **P$_2$-pz** [79]. The 2:1-type complexes [(COD)Ir^{I}(**P$_2$-pz**)Rh^{I}(COD)](BF$_4$) and [(COD)Ir^{I}(**P$_2$-pz**)Pd^{II}(allyl)](BF$_4$) were characterised by spectroscopic data. By carbonylation of the COD complexes [(COD)Ir^{I}(**P$_2$-pz**)Rh^{I}(COD)](BF$_4$), [(COD)Ir^{I}(**P$_2$-pz**)Ir^{I}(COD)](BF$_4$), [(COD)Rh^{I}(**P$_2$-pz**)Rh^{I}(COD)](BF$_4$) and [(COD)Ir^{I}(**P$_2$-pz**)Pd^{II}(allyl)](BF$_4$) the COD co-ligand is readily substituted by two CO co-ligands [80]. The resulting tetracarbonyl complexes [Rh$^{I}_{2}$(**P$_2$-pz**)(CO)$_4$](BF$_4$), [Ir$^{I}_{2}$(**P$_2$-pz**)(CO)$_4$](BF$_4$) and [Rh^{I}Ir^{I}(**P$_2$-pz**)(CO)$_4$](BF$_4$) serve as catalysts for the alkyne hydrogenation, alkene hydroformylation and allylation with allylic alcohol. Also they react with lithium acetylide to form the corresponding μ-η^1:η^2-acetylide complexes [MM′(**P$_2$-pz**)(CO)$_2$(μ-C≡CR)] (M, M′ = Rh, Ir; R = *p*-tol, SiMe$_3$). X-ray crystallographic analyses on complex **84** (M = Rh, M′ = Ir, R = *p*-tol; Table 1) revealed that the *p*-tol-C≡C ligand is σ-bonded to iridium(I) and π-bonded to rhodium(I) [80].

2.3.3. *Bis-bidentate pyrazole ligands with NHC side arms*

Pyrazole-bridged organometallic complexes have been prepared with a new class of ligands that feature N-heterocyclic carbenes (NHC) tethered to the 3- and 5-positions of the central pyrazol core, H(**NHC^{Me})$_2$-pz**, H(**NHC^{Benz})$_2$-pz**, H(**NHC^{Mes})$_2$-pz**, H(**NHC^{PhMe2})$_2$-pz**, H(**NHC^{PhiPr2})$_2$-pz** and H(**NHC)$_2$-pz$_m$** (Scheme 6). Silver complexes [Ag$^{I}_{4}$((**NHC^{Me})$_2$-pz**)$_2$](PF$_6$)$_2$·0.5Et$_2$O (**85**) [81], [Ag$^{I}_{4}$((**NHC^{Benz})$_2$-pz**)$_2$](PF$_6$)$_2$·4MeCN (**86**) and [Ag$^{I}_{4}$((**NHC^{Mes})$_2$-pz**)$_2$](BF$_4$)$_2$·4MeCN (**87**) [82] of the respective bis-(NHC)-ligands are readily obtained from the bis(imidazolium) precursors and Ag$_2$O. They form oligonuclear aggregates both in solution and in the solid state, the most prominent being a planar tetrasilver core held together by two ligands (Fig. 15). Both ligands link all four different silver ions, and all silver ions are coordinated by a NHC and a pyrazolate-N in an almost linear fashion. The resulting silver ring that results from argentophilic interactions is rectangular, with relatively long Ag···Ag contacts.

A similar motif is observed for the gold(I) complex [Au$^{I}_{4}$((**NHC^{Me})$_2$-pz**)$_2$](PF$_6$)$_2$ (**88**) [81] as well as for the silver(I) complex [Ag$^{I}_{4}$((**NHC)$_2$-pz$_m$**)$_2$](BF$_4$)$_2$·4MeOH (**89**) [82] of the cyclic ligand H(**NHC)$_2$-pz$_m$**. Depending on the NHC substituent, equilibria between different oligomeric aggregates have recently been detected in solution by DOSY NMR spectroscopy, and the unusual double-crowned octasilver complex [Ag$^{I}_{8}$((**NHC^{PhiPr2})$_2$-pz**)$_4$](PF$_6$)$_4$ (**90**) could be characterised crystallographically [83]. It contains an inner ring of four silver ions and the four bridging pyrazolates, and in the periphery four silver(I) ions that are each ligated by two NHC-groups from different ligands. Such coinage metal complexes are of interest because of their luminescence properties.

The silver(I) complexes can also be used for transmetallation, and a series of pyrazolato-bridged bimetallic (allyl)palladium and (methallyl)palladium complexes have been prepared *via* this route, using [(allyl)Pd^{II}Cl]$_2$ or [(methallyl)Pd^{II}Cl]$_2$, respectively [84]. In [Pd$^{II}_{2}$((**NHC^{R})$_2$-pz**)(allyl)$_2$](PF$_6$) (R = Me: **91**; R = C$_6$H$_3$Me$_2$-2,6: **92**; R = C$_6$H$_3$*i*Pr$_3$-2,6: **93**; Fig. 16) and [Pd$^{II}_{2}$((**NHC^{PhMe2})$_2$-pz**)(methallyl)](PF$_6$) (**94**) the two (allyl)- and (methallyl)palladium fragments are positioned in close proximity within the bimetallic pocket, respectively, which might be a favourable situation for cooperative effects in metal-mediated reaction. C_s- and C_2-

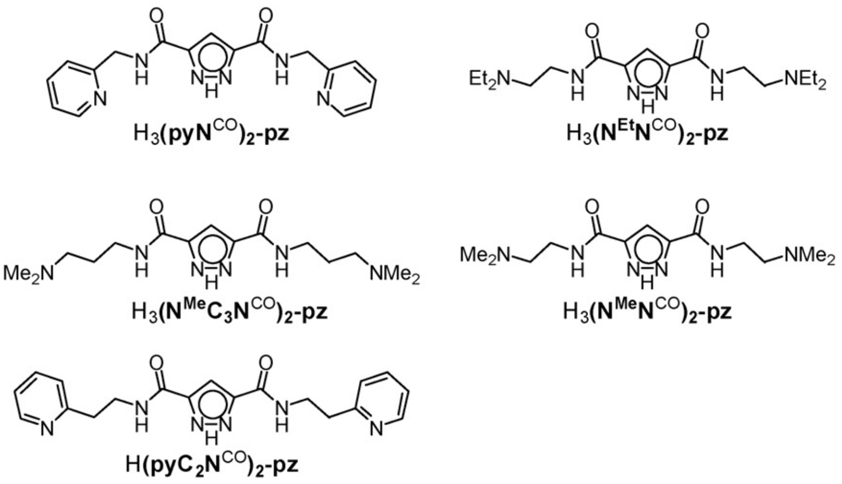

Scheme 7. N$_2$-pz-N$_2$-type amide based ligands: H$_3$(**pyN^{CO})$_2$-pz**, H$_3$(**N^{Et}N^{CO})$_2$-pz**, H$_3$(**N^{Me}C$_3$N^{CO})$_2$-pz**, H$_3$(**N^{Me}N^{CO})$_2$-pz** and H(**pyC$_2$N^{CO})$_2$-pz**.

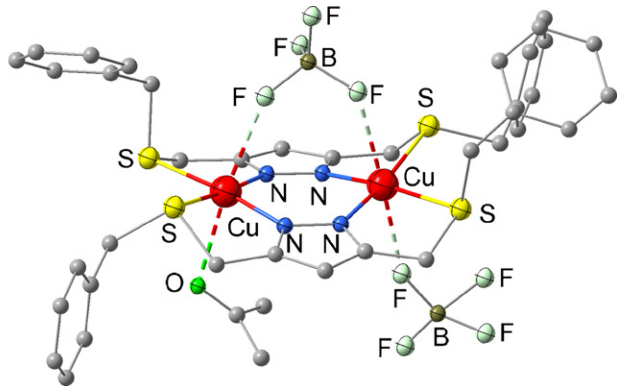

Fig. 17. Molecular structure of the 2:2-type complex [Cu$^{II}_2$(**S$_2$-pz**)$_2$(OCMe$_2$)(BF$_4$)(μ-BF$_4$)] (**99**).

symmetry is observed, which slowly interconvert in solution, according to NMR spectroscopy (k = 0.05–0.4 s^{-1}).

Jeon and Waymouth reported the structures of the related complexes [Rh$^I_2$((**NHC^{PhiPr2}**)$_2$**-pz**)(COD)$_2$](PF$_6$) (**95**) and [Ni$^{II}_2$((**NHC^{PhiPr2}**)$_2$**-pz**)$_2$](PF$_6$)$_2$ (**96**) [85]. The former shows a C_2-symmetrical bimetallic core, while the latter forms a highly sterically crowded bis(pyrazolato)-bridged structure.

2.3.4. *Other D$_1$-pz-D$_1$-type ligands*

Mernari, Abraham and co-workers published in 1993 a 2:2-type copper(II) complex of the oxime ligand 1,1′-(4-methylpyrazole-3,5-diyl)diacetaldehyde dioxime (H(**N^{OH}=C)$_2$-pz(Me)**) (Scheme 7) [86]. The centrosymmetric complex *trans*-[Cu$^{II}_2$((**N^{OH}=C)$_2$-pz(Me)**)$_2$Cl$_2$]·2H$_2$O exists in two isomeric forms, which are practically isostructural. The brown isomer **97a** crystallises from water at 15 °C whereas the dark green isomer **97b** forms at 25 °C (Table 1). The role of the two oxime groups of the ligand is quite different. One oxime function is present in the classical form R$_2$C = NOH and coordinates with the nitrogen atom, whereas the other function exists in the zwitterionic form R$_2$C=N$^+$H–O$^-$ and coordinates with the oxygen atom. Each copper(II) ion is additionally coordinated by a chloro-co-ligand and therefore exhibits a N$_3$OCl distorted square-pyramidal coordination sphere [86].

A dinuclear 2:2-type copper(II) complex (*trans*-[Cu$^{II}_2$((**EtO$_2$C)$_2$-pz**)$_2$(NO$_3$)(H$_2$O)](NO$_3$), **98**; Table 1) is formed with the **H(O$_2$C)$_2$-pz** derivative diethyl-3,5-pyrazole dicarboxylate **H(EtO$_2$C)$_2$-pz** (Scheme 7) [87].

The synthesis of a variety of 3,5-bis(RSCH$_2$)-pzH-type ligands (H**S$_2$-pz**: R = PhCH$_2$; H**PhS$_2$-pz**: R = Ph; H**^{i}PrS$_2$-pz**: R = ^{i}Pr; H**^{t}BuS$_2$-pz**: R = ^{t}Bu; H**MeS$_2$-pz**: R = Me, Scheme 7) bearing a thioether function was described in 1997 [88] and 2005 [89]. Complexation studies with silver(I), copper(I) and copper(II) have been carried out, during which course the copper(II) 2:2-type complexes [Cu$^{II}_2$(**S$_2$-pz**)$_2$(OCMe$_2$)(BF$_4$)(μ-BF$_4$)] (**99**) (Table 1; Fig. 17) [88], *trans*-[Cu$^{II}_2$(**MeS$_2$-pz**)$_2$(ONO$_2$)$_2$] (**100**) and *trans*-[Cu$^{II}_2$(**MeS$_2$-pz**)$_2$(ClO$_4$)$_2$(MeOH)$_2$] (**101**) (Tables 1 and 2) [89] were obtained and structurally characterised.

The cyclopentadienyl ligand H**Cp$_2$-pz^{2-}** could be isolated in form of its dinuclear manganese(I) complex [Mn$^I_2$(H**Cp$_2$-pz**)(CO)$_6$] [90,91]. After deprotonation of the ligand to achieve pyrazole bridging in the complex and light irradiation, the 2:1-type complex K[Mn$^I_2$(**Cp$_2$-pz**)(CO)$_4$] (**102**) could be isolated and structurally characterised (Table 1; Fig. 18) [90,91].

Stoichiometric oxidation of **102** with silver(I) tetrafluoroborate leads to the neutral complex [Mn^{I}Mn^{II}(**Cp$_2$-pz**)(CO)$_4$], a rare example of a neutral mixed-valent d^5/d^6 complex [90]. An in-depths analysis of the spectroscopic properties and electronic structures of **102**, [Mn^{I}Mn^{II}(**Cp$_2$-pz**)(CO)$_4$] and the higher oxidised species [Mn$^{II}_2$(**Cp$_2$-pz**)(CO)$_4$]$^+$ was reported in 2003 [91]. Strong electronic coupling in the mixed-valent complex was observed, but time- (and temperature-) dependent valence detrapping occurs, thus placing [Mn^{I}Mn^{II}(**Cp$_2$-pz**)(CO)$_4$] in class II according to the Robin and Day assignment, close to the class II/III transition. From variable temperature EPR spectroscopy a rough estimate of the activation energy and rate for thermal electron transfer could be deduced, with E_{th} = 13.6 kJ mol^{-1} and k_{th} = 2.6 × 10^{10} s^{-1} at 298 K.

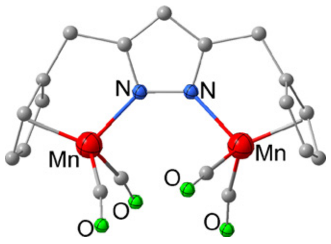

Fig. 18. Molecular structure of the 2:1-type complex anion of K[Mn$^I_2$(**Cp$_2$-pz**)(CO)$_4$] (**102**).

Binucleating ligands H(**Cp$_2$-pz**), H(**Ind$_2$-pz**), and H(**Flu$_2$-pz**) can be formally viewed as coupled versions of the widely used mononuclear amino-Cp or amido-Cp systems. Neutral ligands H$_3$(**Ind$_2$-pz**) and H$_3$(**Flu$_2$-pz**) have been isolated in free form and can be triply lithiated with n-BuLi. Single crystals of the solvent-separated ion pair [Li$_2$(**Flu$_2$-pz**)(thf)$_4$][Li(thf)$_4$] (**103**; Fig. 19) have been characterised crystallographically, as well as the partially lithiated compound [Li$_2$H(**Ind$_2$-pz**)(thf)$_5$] [92].

Each of the two lithium atoms of the anion of **103** is coordinated by one of the pyrazolate N atoms, one of the tethered sidearm fluorenyl moieties, and two thf molecules. The bonding mode between the lithium atoms and the fluorenyl can be described as η^2. In solution, ^{7}Li NMR spectroscopy indicates the predominant presence of contact ion pairs [92].

3. Symmetrical pyrazolate ligands with bidentate side arms: bis-terdentate pyrazolate ligands

In the former chapters we have seen the tendency of D$_1$-pz-D$_1$-type ligands to often form 2:2-type complexes, even with an excess of metal ions. 2:1-Type complexes of D$_1$-pz-D$_1$-type ligands have mainly been obtained in the presence of appropriate co-ligands. Extending the D$_1$-pz-D$_1$-systems to D$_2$-pz-D$_2$-systems, this trend could be shifted to the preferable formation of 2:1-type complexes, as the D$_2$-pz-D$_2$-type ligands with their increased number of donor atoms in the side arms could potentially stabilise 2:1-type complexes by themselves. In contrast to the 2:2-type systems or the 2:1-type complexes of D$_1$-pz-D$_1$-systems with additional chelating co-ligands, 2:1-type compounds of D$_2$-pz-D$_2$-systems would still bear enough free binding sites for substrate binding and/or conversion.

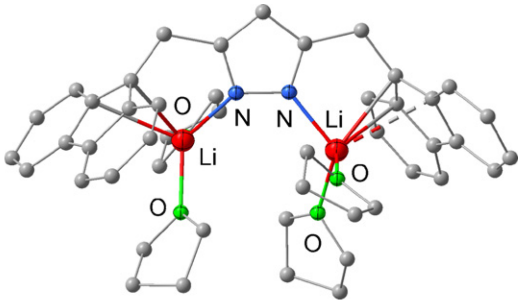

Fig. 19. Molecular structure of the anion of the solvent-separated ion pair [Li$_2$(**Flu$_2$-pz**)(thf)$_4$][Li(thf)$_4$] (**103**).

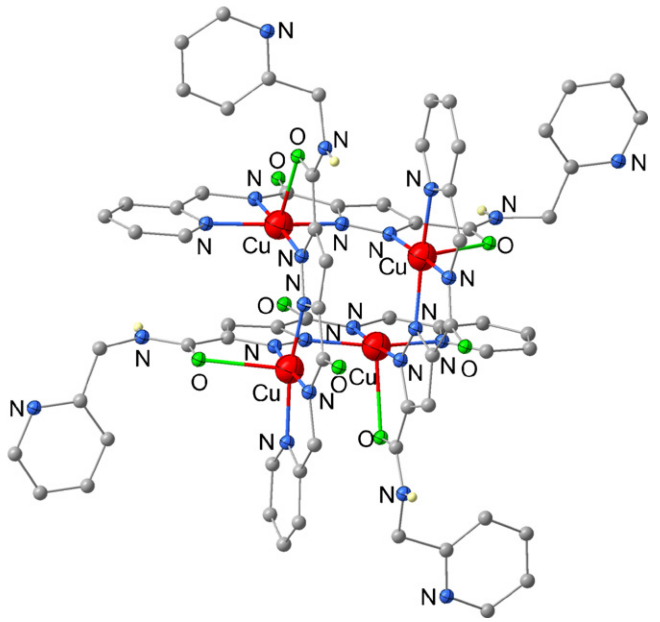

Fig. 20. Molecular structure of the complex molecule of $[\mathrm{Cu^{II}}_4(\mathrm{H}\mathbf{(pyN^{CO})_2\text{-}pz})_4]$ (**104**).

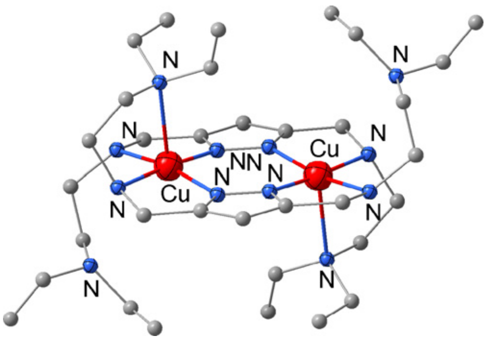

Fig. 21. Molecular structure of the 2:2-type complex cation of $[\mathrm{Cu^{II}}_2(\mathbf{(N^{Et}N)_2\text{-}pz})_2](\mathrm{BPh_4})_2$ (**107**).

3.1. N_2-pz-N_2-type ligands

The first potentially bis-terdentate N_2-pz-N_2-type ligands that where reported were the amide based ligands $\mathrm{H_3}\mathbf{(pyN^{CO})_2\text{-}pz}$, $\mathrm{H_3}\mathbf{(N^{Et}N^{CO})_2\text{-}pz}$ and $\mathrm{H_3}\mathbf{(N^{Me}C_3N^{CO})_2\text{-}pz}$ (Scheme 7) [93]. Their syntheses from 3,5-bis(chloromethyl)pyrazole and some complexation experiments were reported in 1989 by Kamiusuki, Ōkawa and co-workers. The authors describe the synthesis, IR-, and magnetic-characterisation of dinuclear copper(II) complexes (Table 2), and indeed those complexes were of the 2:1-type, bearing one triply deprotonated pyrazole-based ligand and additional azide or acetate anions as bridging co-ligands [93]. Similar experiments with the amide-based ligands $\mathrm{H_3}\mathbf{(N^{Me}N^{CO})_2\text{-}pz}$ or $\mathrm{H_3}\mathbf{(pyC_2N^{CO})_2\text{-}pz}$ (Scheme 7) merely resulted in the hydrolytic cleavage of the ligands and in complexes of $\mathbf{(O_2C)_2\text{-}pz^{3-}}$ [62].

In 2007 $\mathrm{H_3}\mathbf{(pyN^{CO})_2\text{-}pz}$ was employed to obtain [2 × 2] grid-type complexes. Compounds $[\mathrm{M^{II}}_4(\mathrm{H}\mathbf{(pyN^{CO})_2\text{-}pz})_4]\cdot 8\mathrm{H_2O}$ (**104**: M = Cu; **105**: M = Ni) (Tables 1 and 2) and the mixed-metal species $[\mathrm{Cu^{II}}_2\mathrm{Ni^{II}}_2(\mathrm{H}\mathbf{(pyN^{CO})_2\text{-}pz})_4]\cdot 8\mathrm{H_2O}$ (**106**; Table 1) with a statistical distribution of copper(II) and nickel(II) ions were structurally characterised [94]. The complexes were found to be isomorphous. Each ligand strand is acting as a hybrid N_3–NO chelator where only one ligand half acts as terdentate binding pocket whereas the other ligand half coordinates with the pyrazole-N and the amide-O atom, respectively (Fig. 20).

The potentially bis-terdentate pyrazolate ligands $\mathrm{H}\mathbf{(N^{Et}N)_2\text{-}pz}$ and $\mathrm{H}\mathbf{(N^{Me}C_3N)_2\text{-}pz}$ (Scheme 8) based on secondary amine linkers were first reported in 1990 by Kamiusuki et al. [95].

Surprisingly, with copper(II) 2:2-type complexes ($[\mathrm{Cu^{II}}_2(\mathbf{(N^{Et}N)_2\text{-}pz})_2](\mathrm{BPh_4})_2$ (**107**) and $[\mathrm{Cu^{II}}_2(\mathbf{(N^{Me}C_3N)_2\text{-}pz})_2](\mathrm{BPh_4})_2$) are formed, where only half of the terminal tertiary amine groups are coordinated, leaving one side arm per ligand strand dangling (Fig. 21, Table 1) [95].

In 1995, the same group described the preparation and crystal structure of a 2:2-type complex of octahedrally coordinated manganese(II) ions [96]. In the centrosymmetric complex $[\mathrm{Mn^{II}}_2(\mathbf{(pyN)_2\text{-}pz})_2](\mathrm{BPh_4})_2\cdot 2\mathrm{tol}$ (**108**) all amine donor atoms of the ligands are coordinating. The pyridyl groups of one ligand strand coordinate from the same side of the dinuclear core (Table 1).

The ligands $\mathrm{H}\mathbf{(N^{Me}N^{Me})_2\text{-}pz}$ and $\mathrm{H}\mathbf{(N^{Me}C_3N^{Me})_2\text{-}pz}$ (Scheme 8), based on tertiary amine linkers, have been intensively studied [97–107]. Several 2:1-type complexes as well as complexes based on extended 2:1-type structures of the deprotonated ligands $\mathbf{(N^{Me}N^{Me})_2\text{-}pz^-}$ and $\mathbf{(N^{Me}C_3N^{Me})_2\text{-}pz^-}$ have been reported. The ligands usually act as true bis-terdentate chelates, respectively, coordinating with all amine donor atoms of the side arms. This feature leaves two or three coordination sites on the metal ions unoccupied that can be used for further coordination of co-ligands, giving the potential to carry out subsequent stoichiometric or catalytic reactions on the resulting complexes. The 4:2-type complex $[\mathrm{Zn^{II}}_2\mathbf{(N^{Me}N^{Me})_2\text{-}pz}(\mathrm{H_2O})(\mathrm{oaa})]_2(\mathrm{ClO_4})$ (oaa = 2-oxazetidinylacetate) (**109**; Table 1, Fig. 22) was the first structurally characterised example of β-lactam amide-O atom coordination to zinc(II) which is relevant with respect to the mechanism of natural metallo-β-lactamase enzymes [108]. An overall tetranuclear array is formed as the carboxylate group of oaa coordinates in a bridging manner to the two zinc(II) ions of the second dinuclear subunit.

A 2:1-type cobalt(II) complex with distorted trigonal-bipyramidally coordinated metal ions was isolated using the ligand $\mathrm{H}\mathbf{(N^{Me}C_3N^{Me})_2\text{-}pz}$ [97]. In the complex $[\mathrm{Co^{II}}_2\mathbf{(N^{Me}C_3N^{Me})_2\text{-}pz}(\mu\text{-Cl})\mathrm{Cl_2}]$ (**110**) the nitrogen donor atoms of the deprotonated ligand occupy two equatorial coordination positions (pz-N, terminal N) and an apex (central N) per cobalt(II) ion (Table 1). The other apex and the third equatorial position is occupied by a chloro- and a μ-chloro-co-ligand, respectively. The similar 2:1-type nickel(II) complex $[\mathrm{Ni^{II}}_2\mathbf{(N^{Me}C_3N^{Me})_2\text{-}pz}(\mu\text{-OH})(\mathrm{MeCN})_2](\mathrm{ClO_4})_2$ (**111**) features five coordinate nickel(II) ions and a μ-OH-bridge between the metal ions (Table 1) [98]. The remaining coordination sites are occupied in a *cis*-manner by two acetonitrile co-ligands. The similar μ-OH-bridged 2:1 copper(II) complex $[\mathrm{Cu^{II}}_2\mathbf{(N^{Me}C_3N^{Me})_2\text{-}pz}(\mu\text{-OH})(\mathrm{EtOH})_2]$ (**112**) with *trans*-positioned ethanol co-ligands

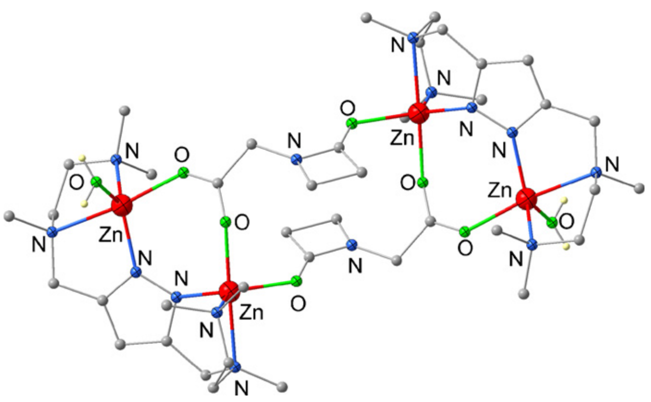

Fig. 22. Molecular structure of the 4:2-type complex cation $[\mathrm{Zn^{II}}_2\mathbf{(N^{Me}N^{Me})_2\text{-}pz}(\mathrm{H_2O})(\mathrm{oaa})]_2(\mathrm{ClO_4})$ (**109**).

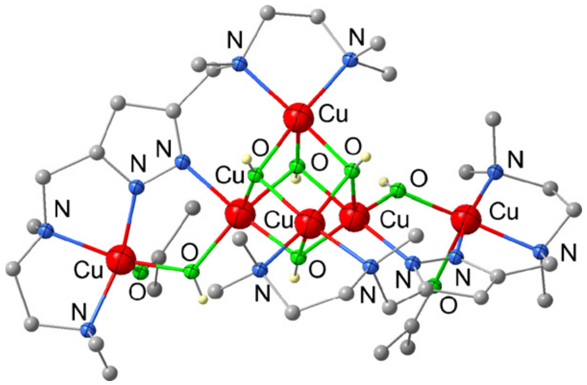

Fig. 23. Molecular structure of the complex cation of $[\mathrm{Cu^{II}}_6(\mathbf{(N^{Me}N^{Me})_2\text{-}pz})_2(\mu\text{-OH})_6](\mathrm{BF_4})_4$ (**115**).

was also reported (Table 1) [104]. The work also describes $\mathrm{CO_2}$-absorption from air by the coordination compound first formed in the reaction of the ligand $\mathrm{H}\mathbf{(N^{Me}N^{Me})_2\text{-}pz}$, that features the shorter side arms, with two equivalents of copper perchlorate and two equivalents of base in methanol [104]. The resulting complex $[\mathrm{Cu^{II}}_2\mathbf{(N^{Me}N^{Me})_2\text{-}pz}(\mu\text{-O_2COMe})(\mathrm{MeOH})_2](\mathrm{ClO_4})_2$ (**113**) was characterised by X-ray crystallography, and features a methyl carbonato-bridge with a drastically tilted carbonate plane with respect to the pyrazolate plane (Table 1) [104]. Two *trans*-positioned methanol co-ligands complete the distorted square-pyramidally coordination spheres of the copper(II) ions. The complex $[\mathrm{Cu^{II}}_4(\mathbf{(N^{Me}N^{Me})_2\text{-}pz})_2(\mu_3\text{-CO_3})(\mathrm{H_2O})_2(\mu\text{-ClO_4})](\mathrm{ClO_4})$ (**114**) (Table 1) on the other hand, is formed under the same reaction conditions but quickly removing the solvent under reduced pressure and recrystallising the residue from acetone/pentane instead of methanol/diethyl ether [107]. The unusual hexanuclear complex $[\mathrm{Cu^{II}}_6(\mathbf{(N^{Me}N^{Me})_2\text{-}pz})_2(\mu\text{-OH})_6](\mathrm{BF_4})_4$ (**115**) (Fig. 23, Table 1) has been isolated by using copper(II) tetrafluoroborate instead of the respective perchlorate salt [107]. The prominent feature in **115** is a cubane-type $\mathrm{Cu_4}(\mu\text{-OH})_4$ array that interconnects two 2:1-type subunits.

Using both the ligands $\mathrm{H}\mathbf{(N^{Me}C_3N^{Me})_2\text{-}pz}$ with the longer side arms and $\mathrm{H}\mathbf{(N^{Me}N^{Me})_2\text{-}pz}$ with the shorter side arms μ-chloro-bridged copper(II) complexes were isolated and characterised [99]. The monomeric 2:1-type complex $[\mathrm{Cu^{II}}_2\mathbf{(N^{Me}C_3N^{Me})_2\text{-}pz}(\mu\text{-Cl})\mathrm{Cl_2}]$ (**116**) was obtained using the ligand with the longer side arms while a dimeric tetranuclear 4:2-type complex ($[\mathrm{Cu^{II}}_4(\mathbf{(N^{Me}N^{Me})_2\text{-}pz})_2(\mu\text{-Cl})_4(\mathrm{Cl})_2]$, **117**) and a polymeric 2:1-type complex ($[\mathrm{Cu^{II}}_2\mathbf{(N^{Me}N^{Me})_2\text{-}pz}(\mu\text{-Cl})_3]$, **118**) were obtained using the ligand $\mathrm{H}\mathbf{(N^{Me}N^{Me})_2\text{-}pz}$ with the shorter side arms (Table 1) [99].

Recapitulating the results obtained by X-ray crystal structure analyses of several complexes obtained with the ligand $\mathrm{H}\mathbf{(N^{Me}C_3N^{Me})_2\text{-}pz}$ with the longer side arms and the ligand $\mathrm{H}\mathbf{(N^{Me}N^{Me})_2\text{-}pz}$ with the shorter side arms, it was concluded that generally shorter metal···metal distances will be accessible with the former ligand whereas larger metal···metal separations will be enforced by the latter one (Table 1). This finding can be explained, taken that longer side arms generally enable less strained embraces of the metal ions and push them closer to the pyrazolate moiety, hence shortening the metal···metal distance, whereas shorter side arms pull the metal ions back and further away from the pyrazolate moiety, to enable a less restrained coordination, therefore enlarging the metal···metal distance.

Following those results, catecholase activity studies with the complexes $[\mathrm{Cu^{II}}_2\mathbf{(N^{Me}C_3N^{Me})_2\text{-}pz}(\mu\text{-OH})(\mathrm{MeOH})_2]$, a methanol derivative of the ethanol containing complex **112** and **113**, have been carried out [104]. It was found that the conversion of 3,5-DTBC (3,5-DTBC = 3,5-di-*tert*-butylcatechol) to 3,5-DTBQ (3,5-DTBQ = 3,5-di-*tert*-butylquinone) with $[\mathrm{Cu^{II}}_2\mathbf{(N^{Me}C_3N^{Me})_2\text{-}pz}(\mu\text{-}$

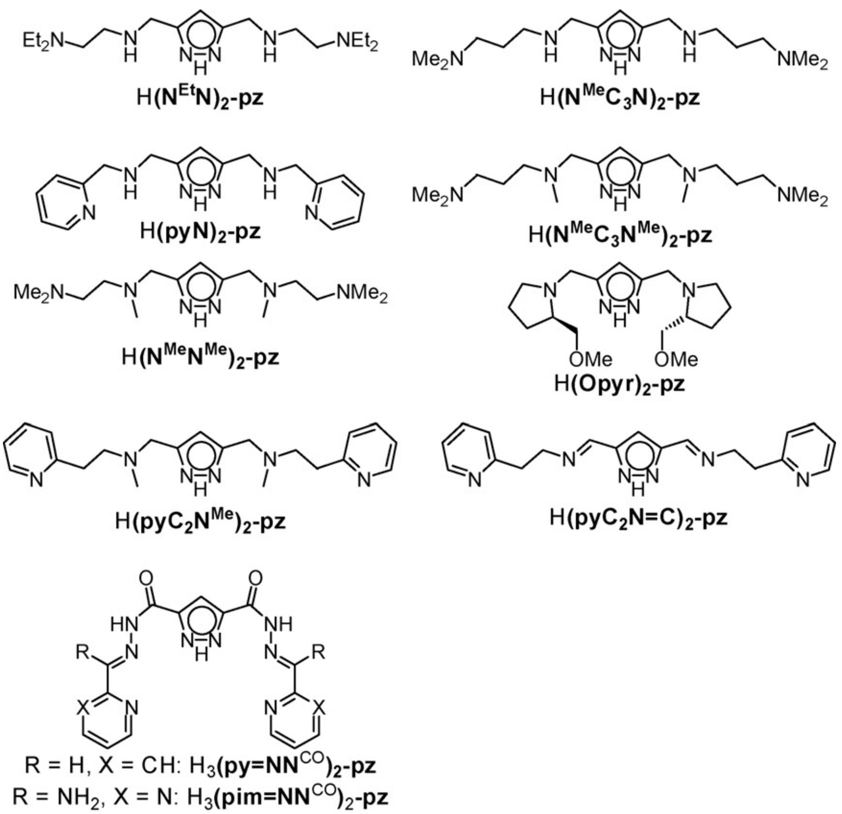

Scheme 8. $\mathrm{N_2}$-pz-$\mathrm{N_2}$-type amine based ligands: $\mathrm{H}\mathbf{(N^{Et}N)_2\text{-}pz}$, $\mathrm{H}\mathbf{(N^{Me}C_3N)_2\text{-}pz}$, $\mathrm{H}\mathbf{(pyN)_2\text{-}pz}$, $\mathrm{H}\mathbf{(N^{Me}C_3N^{Me})_2\text{-}pz}$, $\mathrm{H}\mathbf{(N^{Me}N^{Me})_2\text{-}pz}$, $\mathrm{H}\mathbf{(Opyr)_2\text{-}pz}$, $\mathrm{H}\mathbf{(pyC_2N^{Me})_2\text{-}pz}$, $\mathrm{H}\mathbf{(pyC_2N{=}C)_2\text{-}pz}$, $\mathrm{H_3}\mathbf{(py{=}NN^{CO})_2\text{-}pz}$ and $\mathrm{H_3}\mathbf{(pim{=}NN^{CO})_2\text{-}pz}$.

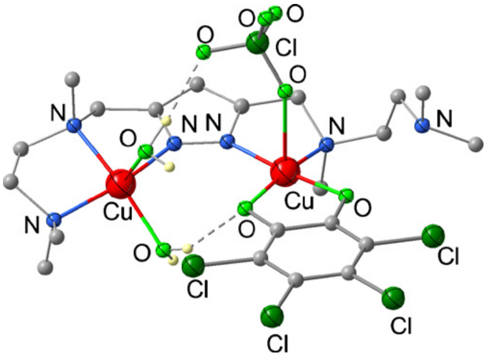

Fig. 24. Molecular structure of the 2:1-type complex cation of the TCC^{2-} containing [Cu$^{II}_2$(H**N^{Me}N^{Me})$_2$-pz**(TCC)(H$_2$O)$_2$(ClO$_4$)](ClO$_4$) (**119**).

OH)(MeOH)$_2$] is much higher than that of **113** ($k_{obs} = 1400 \pm 200$ and $514 \pm 70\,h^{-1}$, respectively). The authors explained this finding with a correlation of metal···metal distance and catecholase activity, stating that the shorter the distance, the greater the activity. Given that a shorter side arm in **113** enforces a longer metal···metal distance, this resulted in a diminished catecholase activity, with respect to [Cu$^{II}_2$(**N^{Me}C$_3$N^{Me})$_2$-pz**(μ-OH)(MeOH)$_2$] [104]. In the course of those studies a less reactive substrate TCCH$_2$ (TCCH$_2$ = tetrachloro-*o*-catechol) was employed in the hope of isolating a substrate complex, and indeed a TCC^{2-} containing complex [Cu$^{II}_2$(H**N^{Me}N^{Me})$_2$-pz**(TCC)(H$_2$O)$_2$(ClO$_4$)](ClO$_4$) (**119**) was isolated (Fig. 24, Table 1).

In **119** the pyrazolate ligand acts as a hybrid bidentate-terdentate chelate, resulting in very different coordination spheres for the two square-pyramidally coordinated pyrazolato-bridged copper(II) ions. The TCC^{2-} substrate coordinates as a bidentate chelate meridionally to one of the two copper(II) ions, displacing the now protonated terminal amine donor of the pyrazolate ligand. This ligand coordination pocket hence coordinates as a bidentate chelating site, leaving the ligand in a zwitterionic form. The remaining axial coordination position of the copper(II) ion is occupied by a perchlorate anion. The other copper(II) ion is meridionally coordinated by the terdentate ligand half, the remaining coordination sites being occupied by water molecules [104]. A similar complex ([Cu$^{II}_2$(**N^{Me}N^{Me})$_2$-pz**(TCC)(EtCN)(H$_2$O)](PF$_6$), **120**) of the deprotonated ligand (**N^{Me}N^{Me})$_2$-pz**$^-$ was obtained by the *in situ* reaction of H(**N^{Me}N^{Me})$_2$-pz**, copper(I), KO^{t}Bu as base and TCQ (TCQ = tetrachloro-*o*-quinone) as oxidant [104]. In **120** the ligand acts as regular bis-terdentate chelate, coordinating the meridionally sites, respectively. Again, the TCC^{2-} co-ligand coordinates solely to one of the two copper(II) ions and is stabilized by hydrogen bonding a water ligand at the adjacent copper(II) [104].

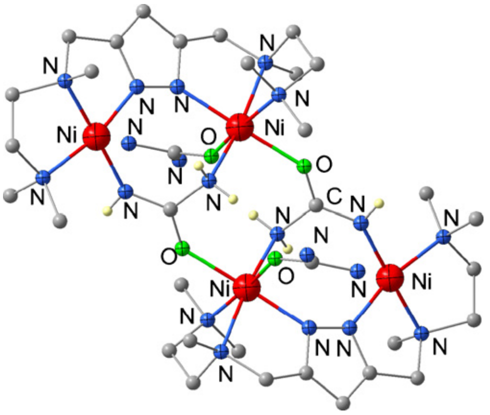

Fig. 25. Molecular structure of the 4:2-type complex cation of [Ni$^{II}_4$((**N^{Me}N^{Me})$_2$-pz**)$_2$(OC(NH$_2$)$_2$)$_2$(μ_3-OC(NH$_2$)(NH))$_2$](ClO$_4$)$_4$ (**121**).

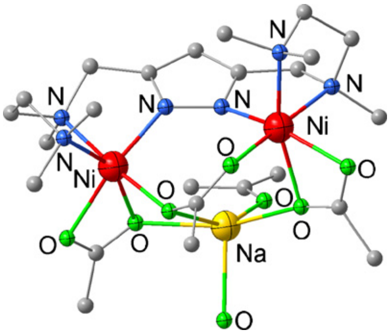

Fig. 26. Molecular structure of the complex cation of [Ni$^{II}_2$(**N^{Me}N^{Me})$_2$-pz**(μ-OAc)(OAc)$_2$Na(H$_2$O)(OCMe$_2$)](BPh$_4$) (**123**).

The treatment of H(**N^{Me}N^{Me})$_2$-pz** with nickel(II) perchlorate hexahydrate in the presence of an excess of urea affords the unique 4:2-type complex [Ni$^{II}_4$((**N^{Me}N^{Me})$_2$-pz**)$_2$(OC(NH$_2$)$_2$)$_2$(μ_3-OC(NH$_2$)(NH))$_2$](ClO$_4$)$_4$ (**121**) (Fig. 25, Table 1) [100].

Compound **121** consists of two dinuclear subunits, each containing a bis-terdentate deprotonated ligand (**N^{Me}N^{Me})$_2$-pz**$^-$, that are connected by two μ_3-κN:$\kappa N'$:κO-bridging deprotonated urea co-ligands, a very unusual binding mode of urea. A further urea molecule per dinuclear unit is *O*-bound to one of the two nickel(II) ions. The distorted octahedral coordination sphere of that nickel(II) ion is completed by the neutral NH$_2$- and the O-function of the anionic bridging urea co-ligand. The stronger anionic NH$^-$-function of the respective urea molecule is coordinated to the second nickel(II) ion of the other dinuclear subunit, respectively, hence completing its square-planar coordination environment [100]. This results in a mixed-spin situation.

The reaction of H(**N^{Me}N^{Me})$_2$-pz** with one equivalent of base and two equivalents of nickel(II) ions in the presence of 0.5 equiv. of acetate ions and an excess of *N*,*N'*-dimethylurea affords the 2:1-type μ-acetate complex [Ni$^{II}_2$(**N^{Me}N^{Me})$_2$-pz**(μ-OAc)(OC(NHMe)$_2$)$_2$(MeOH)$_2$](ClO$_4$)$_2$ (**122**) [101]. The sodium containing 2:1-type complex [Ni$^{II}_2$(**N^{Me}N^{Me})$_2$-pz**(μ-OAc)(OAc)$_2$Na(H$_2$O)(OCMe$_2$)](BPh$_4$) (**123**) was isolated in a reaction of H(**N^{Me}N^{Me})$_2$-pz** without the addition of *N*,*N'*-dimethylurea, in the presence of an excess of acetate and addition of NaBPh$_4$ (Fig. 26) [101]. Both nickel(II) ions of **123** are in a N$_3$O$_3$ distorted octahedral coordination geometry. The donor atoms derive from a ligand pocket (3 × N), a chelating acetato- (2 × O) and a μ-acetato (1 × O) co-ligand. The acetate ions are further connected to a sodium cation.

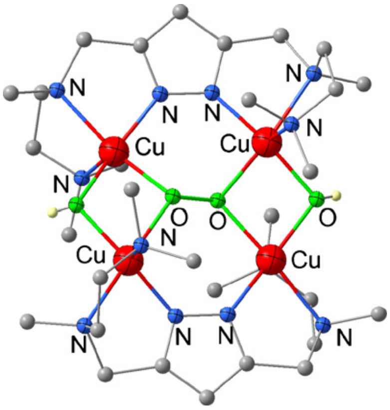

Fig. 27. Molecular structure of the complex cation of the peroxo complex [Cu$^{II}_4$((**N^{Me}N^{Me})$_2$-pz**)$_2$(μ_4-O$_2$)(μ-OH)$_2$](PF$_6$)$_2$ (**124**).

By diffusion of molecular oxygen into a solution of **(N^{Me}N^{Me})$_2$-pz**$^-$ and two equivalents of copper(I) hexafluorophosphate in propionitrile that has been layered with diethyl ether at −80 °C the unusual tetranuclear peroxo complex [Cu$^{II}_4$(**(N^{Me}N^{Me})$_2$-pz**)$_2$(μ_4-O$_2$)(μ-OH)$_2$](PF$_6$)$_2$ (**124**) has been obtained (Fig. 27, Table 1) [102].

The bis-terdentate pyrazolate ligands in **124** each coordinate facially to the copper(II) ions. The remaining two equatorial coordination sites of the square-pyramidally coordinated metal centres are occupied by a hydroxide and a μ_4-peroxo co-ligand, that also link the edges and the centre of the dinuclear subunits to form the tetranuclear complex **124**, respectively. On leaving the peroxo complex **124** for a few days at room temperature and on air the 4:2-type complex [Cu$^{II}_4$(**(N^{Me}N^{Me})$_2$-pz**)$_2$(μ-OH)$_4$](PF$_6$)$_2$ (**125**) is formed. In **125**, formally the O–O bond of the central peroxo unit of **124** has decomposed and instead a OH···OH linkage is now present (Table 1), while the overall tetranuclear array is retained [102].

Using zinc(II) salts and the ligand H**(N^{Me}N^{Me})$_2$-pz** the μ-nitrato *O*-bridged 2:1-type complex ([Zn$^{II}_2$**(N^{Me}N^{Me})$_2$-pz**(μ-ONO$_2$)(NO$_3$)$_2$], **126**; Table 1) has been obtained under nitrogen atmosphere, while the μ_4-carbonato-bridged tetranuclear complex [Zn$^{II}_4$(**(N^{Me}N^{Me})$_2$-pz**)$_2$(μ_4-CO$_3$)(μ-OH)$_2$](BPh$_4$)$_2$ (**127**) (Fig. 28, Table 1) has been obtained when leaving the reaction solution on air. In **127**, dinuclear subunits of the 2:1-type are interconnected, by a μ_4-η^2:η^1:η^1 carbonate in the centre and two μ-OH-bridges at the edges, in such a way that the tetranuclear **L**$_2$Zn$_4$(μ-OH)$_2$-core is capped by the carbonato-bridge on top of the Zn$_4$ rectangle [105].

Phosphatase model studies have been carried out on *in situ* prepared 2:1-type complexes of zinc(II) and H**(N^{Me}N^{Me})$_2$-pz**, and it was found that at pH > 8.5 the activity of cleaving NaBNPP (NaBNPP = sodium bis(4-nitrophenyl)phosphate) and liberating 4-nitrophenol drops rapidly due to the instability of the dinuclear complexes under basic conditions [106]. A product inhibited complex [Zn$^{II}_4$(**(N^{Me}N^{Me})$_2$-pz**)$_2$(μ_4-NPP)(μ-OH)$_2$](ClO$_4$)$_2$ (**128**) (NPP = 4-nitrophenyl phosphate) (Table 1) was isolated and characterised by X-ray crystallography [106]. The molecular structure of compound **128** features two 2:1-type subunits that are interconnected by a μ_4-η^2:η^1:η^1 bridging NPP co-ligand at the centre and two μ-hydroxo co-ligands at the edges, quite similar to the carbonato-bridged complex **127**. Additionally the binding of the less reactive DMP (DMP = dimethyl phosphate) has been investigated and the X-ray crystal structure of [Zn$^{II}_2$**(N^{Me}N^{Me})$_2$-pz**(μ-DMP)(NO$_3$)$_2$] (**129**), where the DMP coordinates in the bidentate fashion was reported (Table 1) [106].

Various nickel(II) azido complexes have been obtained with these types of ligands, namely [Ni$^{II}_2$**(N^{Me}N^{Me})$_2$-pz**(μ-1,3-N$_3$)$_3$]$_\infty$ of the ligand with the shorter side arms (**130**; Table 1) [103] and the complexes [Ni$^{II}_4$(**(N^{Me}C$_3$N^{Me})$_2$-pz**)$_2$(μ-1,1-N$_3$)$_2$(μ_3-1,1,3-N$_3$)$_2$(N$_3$)$_2$] (**131**; Table 1) [109], [Ni$^{II}_2$(**(N^{Me}C$_3$N^{Me})$_2$-pz**)(μ-1,1-N$_3$)(O$_2$NO)$_2$]·C$_4$H$_{10}$O (**132**), [Ni$^{II}_4$(**(N^{Me}C$_3$N^{Me})$_2$-pz**)$_2$(μ-1,1-N$_3$)$_2$(μ-1,3-N$_3$)$_2$]X$_2$·Y (**133**: X = ClO$_4$, Y = 2CH$_4$O·0.5H$_2$O; **134**: X = ClO$_4$, Y = C$_3$H$_6$O·C$_5$H$_{12}$; **135**: X = BPh$_4$, Y = C$_3$H$_6$O) (Tables 1 and 2) of the ligand with the longer side arms [110]. Compound **130** with the shorter side arms and hence the longer metal–pz–metal distance exhibits μ-1,3-N$_3$-bridged 2:1-type subunits [103]. On the other hand, **131–135** with the longer side arms and shorter metal–pz–metal distances exhibit μ-1,1-N$_3$-bridged 2:1-type subunits, again demonstrating the effect of side-arm chain length on metal···metal separation [109]. The 2:1-type subunits of compound **130** are interconnected by two μ-1,3-N$_3$-bridges and form a polymeric structure [103]. Compounds **131** and **133–135** exhibit a dimeric structure with μ-1,1,3-N$_3$ (**131**) or μ-1,3-N$_3$ (**133–135**) bridged 2:1-type subunits [109,110]. The μ-1,1,3-N$_3$-bridges consist of an inter-subunit μ-1,3- and an intra-subunit μ-1,1-motif [109].

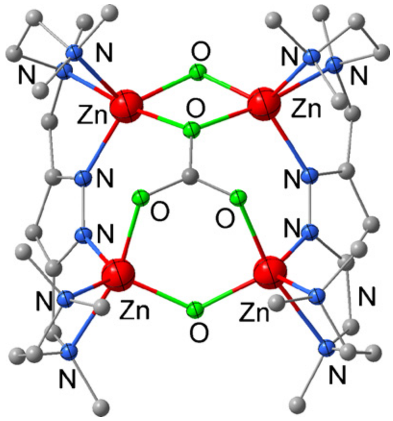

Fig. 28. Molecular structure of the complex cation of the carbonato-bridged complex [Zn$^{II}_4$(**(N^{Me}N^{Me})$_2$-pz**)$_2$(μ_4-CO$_3$)(μ-OH)$_2$](BPh$_4$)$_2$ (**127**).

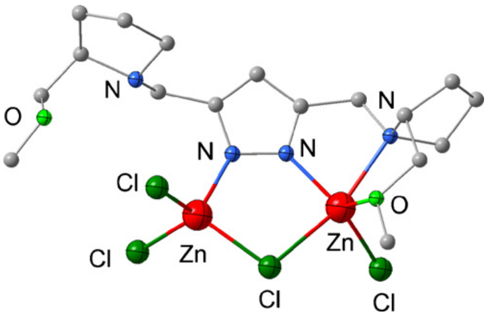

Fig. 29. Molecular structure of [Zn$^{II}_2$H(**Opyr**)$_2$**-pz**(μ-Cl)Cl$_3$] (**136**).

The pyrrolidine based ligand H**(Opyr)$_2$-pz** (pyr = pyrrolidine), bearing two (*R*)-2-(methoxymethyl)pyrrolidine side arms represents the first enantiomerically pure *C*$_2$-symmetric pyrazole based ligand (Scheme 8) [111]. The synthesis and structural characterisation of a dinuclear complex [Zn$^{II}_2$H**(Opyr)$_2$-pz**(μ-Cl)Cl$_3$]·0.5OCMe$_2$ (**136**) of **(Opyr)$_2$-pz**$^-$ was reported (Table 1, Fig. 29) [111], where unexpectedly only one side arm of the pyrazolate ligand is coordinating to a zinc(II) ion while the other side arm remains dangling. The dangling pyrrolidine side arm picks up the proton formerly bound to the pyrazole ring, leaving the ligand in a zwitterionic form [111].

The pyridine based ligand H**(pyC$_2$N^{Me})$_2$-pz** forms 2:1-type copper(II) complexes (Scheme 8) [112]. In all three complexes [Cu$^{II}_2$(**(pyC$_2$N^{Me})$_2$-pz**)F(MeOH)$_2$(BF$_4$)](BF$_4$) (**137**), [Cu$^{II}_2$(**(pyC$_2$N^{Me})$_2$-pz**)F(H$_2$O)$_2$(MeOH)](BF$_4$)$_2$ (**138**) [112] and [Cu$^{II}_2$(**(pyC$_2$N^{Me})$_2$-pz**)(MeOH)$_2$(NO$_3$)$_2$] (**139**) [113] the copper(II) ions exist in distorted square-pyramidal coordination geometries (Table 1). The base of the pyramid is formed by the terdentate binding pocket of the ligand, respectively, and a F···HOMe moiety in **137**, a F···HOH moiety in **138** and a nitrate-O moiety in **139**. Copper(II)-bound methanol molecules are involved in hydrogen bonding to the nitrate-O that coordinate to the adjacent copper(II) ion, resulting in double MeO-H···O-NO$_2$ linkages. Catecholase activities of compounds **137** and **139** were probed with 3,5-DTBC as test substrate [113].

The distorted octahedral N$_3$Cl$_2$O coordination sphere of the nickel(II) ions in [Ni$^{II}_2$(**(pyC$_2$N^{Me})$_2$-pz**)(μ-Cl)Cl$_2$(H$_2$O)$_2$]$_2$·2H$_2$O (**140**; Tables 1 and 2) is build up by three facially bound N-atoms of one ligand half, the pyridine N-atom being *trans* to a coordinated water molecule, a μ-Cl and a chloro-co-ligand. Each chloro-ligand of one dinuclear subunit is involved in two hydrogen-bonding contacts to a water co-ligand of the other subunit and *vice versa*, thus forming the tetranuclear entity. The dimerised arrangement is capped by hydrogen bonds to two additional water molecules included in the crystal lattice [114].

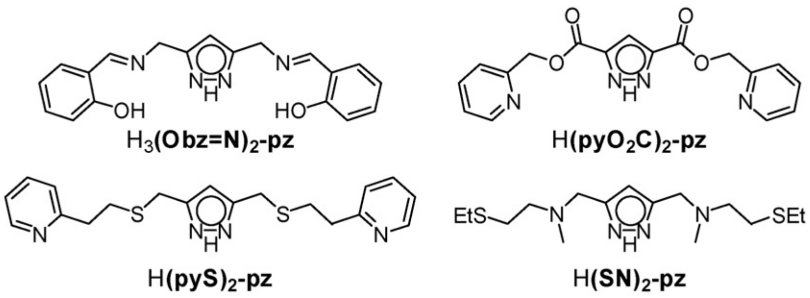

Scheme 9. D_2-pz-D_2-type ligands: H$_3$**(Obz=N)$_2$-pz**, H**(pyO$_2$C)$_2$-pz**, H**(pyS)$_2$-pz** and H**(SN)$_2$-pz**.

In 2007 Brooker and co-workers prepared 2:1-type copper(II) complexes involving the *in situ* prepared Schiff-base complex H**(pyC$_2$N=C)$_2$-pz** [115]. The ligand coordinates meridionally as bis-terdentate chelate to form the copper(II) complexes [Cu^{II}$_2$(**(pyC$_2$N=C)$_2$-pz**)(H$_2$O)$_2$(OAc)$_3$] (**141**) and [Cu^{II}$_2$(**(pyC$_2$N=C)$_2$-pz**)(NCS)$_2$(DMF)](BF$_4$) (**142**) (Table 1). Both complexes feature two distinct copper(II) centres. In **141** a distorted trigonal bipyramidal and a distorted octahedral coordination is distinguished whereas square-pyramidal and a square-planar coordination is distinguished in **142**.

2:1-Type copper(II) complexes are formed by the hydrazone-based ligands H$_3$**(py=NN^{CO})$_2$-pz** and H$_3$**(pim=NN^{CO})$_2$-pz** (**143**: [Cu^{II}$_2$(H**(py=NN^{CO})$_2$-pz**)(μ-OH)(NO$_3$)(H$_2$O)](NO$_3$)·2H$_2$O; **144**: [Cu^{II}$_2$(H**(py=NN^{CO})$_2$-pz**)(μ-OH)(H$_2$O)$_2$](ClO$_4$)·H$_2$O; **145**: [Cu^{II}$_2$(H**(pim=NN^{CO})$_2$-pz**)(μ-OH)(H$_2$O)][Cu^{II}$_2$(H**(pim=NN^{CO})$_2$-pz**)(μ-OH)(ClO$_4$)](ClO$_4$)$_3$·4H$_2$O; Tables 1 and 2) [116]. All three complexes feature hydroxo-bridged metal ions. The dimeric structure of **145** is build up by two dinuclear subunits, each with a square planar and a square pyramidal metal centre. The subunits are interconnected by a concerted hydrogen-bonding network involving the external O–N–N groups of the ligand [116].

3.2. *Other D_2-pz-D_2-type ligands*

The imine based ON-pz-NO-type ligand H$_3$**(Obz=N)$_2$-pz** was reported in 1992 by Ōkawa and co-workers (Scheme 9) [117].

With manganese(II) acetate a 4:2-type complex of manganese(III) [Mn^{III}$_4$(**(Obz=N)$_2$-pz**)$_2$(μ-OMe)$_4$(MeOH)$_4$](ClO$_4$)$_2$ (**146**) (Fig. 30, Table 1) is formed upon neutralisation of the methanolic solution with triethylamine.

The dimeric tetranuclear structure of **146** is build up by a linear array of four manganese(III) ions, two terminal and two central ones. The two terminal metal ions each are coordinated by the NNO-coordination pocket of one ligand half. The distorted octahedral coordination environment is completed by two axial methanol co-ligands and one anionic μ-OMe co-ligand, that bridges to a central manganese(III) ion. Additionally, the central manganese(III) ions each are bound to one μ-pyrazole nitrogen donor, bridged to the respective terminal metal ion and a NO-ligand arm of the second ligand.

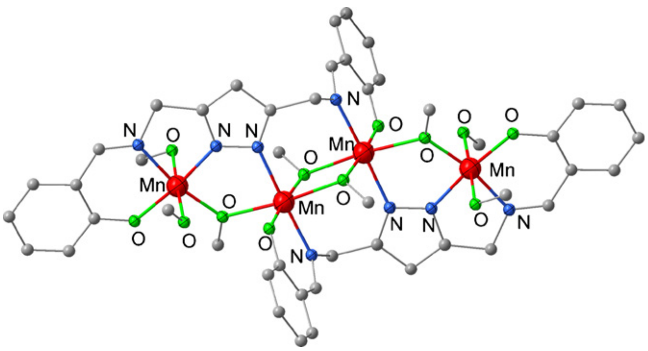

Fig. 30. Molecular structure of the 4:2-type complex cation of [Mn^{III}$_4$(**(Obz=N)$_2$-pz**)$_2$(μ-OMe)$_4$(MeOH)$_4$](ClO$_4$)$_2$ (**146**).

In 1995 Bueno, Varro and co-workers published the NO-pz-ON-type ester ligand H**(pyO$_2$C)$_2$-pz** and performed pK_A studies without and with the addition of zinc(II) ions [118]. In the course of those studies a 2:2- and a 2:1-type complex were isolated.

The bis-terdentate thioether based NS-pz-SN-type ligand H**(pyS)$_2$-pz** forms 2:1-type complexes with copper(II) ions [119–121]. A catalytic study of the oxidation of 3,5-DTBC with molecular oxygen was conducted by Urbach and co-worker on the complex [Cu^{II}$_2$**(pyS)$_2$-pz**(μ-OH)](ClO$_4$) [119]. Later the crystal structures of an azido- ([Cu^{II}$_2$**(pyS)$_2$-pz**(μ-N$_3$)(N$_3$)$_2$]·^{i}PrOH, **147**) [120,121], a bromo- ([Cu^{II}$_2$**(pyS)$_2$-pz**(μ-Br)Br(H$_2$O)]Br·2H$_2$O, **148**) [120,121] and a chloro-bridged complex ([Cu^{II}$_2$**(pyS)$_2$-pz**(μ-Cl)Cl(H$_2$O)]Cl·2H$_2$O, **149**) [121] were reported by the same group (Table 1). All those complexes **147**–**149** contain fivefold coordinated copper(II) ions with *cis*-arranged square-pyramids. The donor atoms of the **(pyS)$_2$-pz**$^-$ ligand coordinate in a meridional configuration, respectively.

Tetranuclear 4:2-type complexes of the SN-pz-NS type ligand **(SN)$_2$-pz**$^-$ were isolated [122], where in the nickel(II) complexes [Ni^{II}$_4$(**(SN)$_2$-pz**)$_2$(μ_4-1,1,3,3-N$_3$)(μ-1,1-N$_3$)$_2$(μ-O$_2$CR)$_2$](ClO$_4$) (**150**: R = Me; **151**: R = Ph) all nickel(II) ions are in distorted octahedral coordination environment, each facially encapsulated in a terdentate pocket of one ligand half. The two nickel(II) ions of the dinuclear subunits are μ-1,3-N$_3$-bridged, while the same N$_3$-ion also bridges to the second dinuclear subunit to eventually act as an unprecedented μ_4-1,1,3,3-N$_3$ unit capping the tetranuclear **L**$_2$Ni$_4$-core. Two further μ-1,1-intersubunit-N$_3$-bridges and two μ-intersubunit-carboxylate units are present in the tetranuclear cation.

4. Symmetrical pyrazolate ligands with terdentate side arms: bis-quadridentate pyrazolate ligands

Following the trend of stabilising 2:1-type complexes by means of increasing the number of donor atoms in the ligand side arms, the next logical step is the use of D_3-pz-D_3 type ligands. Each binding pocket of a D_3-pz-D_3-type ligand provides four donor functions for the coordination with metal ions. This geometrical demand should prevent dimerisation, hence the formation of 2:2-type complexes. On the other hand, coordination of metal ions preferring five- or sixfold coordination should still allow for one or two “free” binding sites, respectively, accessible for potential substrate binding and subsequent (catalytic) conversions.

4.1. *N_3-pz-N_3-type ligands with acyclic side arms*

The first D_3-pz-D_3-type ligand used in coordination chemistry, was the amine based ligand 3,5-bis{*N*,*N*-bis[2-(diethylamino)ethyl]

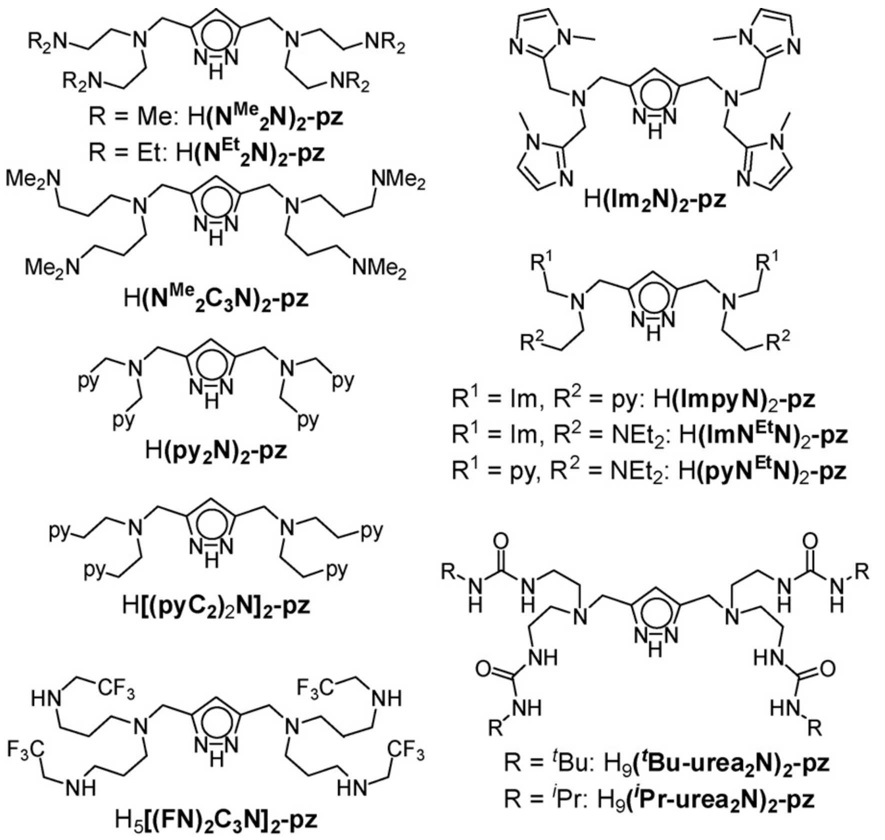

Scheme 10. N_3-pz-N_3-type ligands: H$\mathbf{(N^{Me}{}_2N)_2\text{-}pz}$, H$\mathbf{(N^{Et}{}_2N)_2\text{-}pz}$, H$\mathbf{(Im_2N)_2\text{-}pz}$, H$\mathbf{(N^{Me}{}_2C_3N)_2\text{-}pz}$, H$\mathbf{(ImpyN)_2\text{-}pz}$, H$\mathbf{(ImN^{Et}N)_2\text{-}pz}$, H$\mathbf{(pyN^{Et}N)_2\text{-}pz}$, H$\mathbf{(py_2N)_2\text{-}pz}$, H$\mathbf{[(pyC_2)_2N]_2\text{-}pz}$, $H_5$$\mathbf{[(FN)_2C_3N]_2\text{-}pz}$, $H_9$$\mathbf{(^tBu\text{-}urea_2N)_2\text{-}pz}$ and $H_9$$\mathbf{(^iPr\text{-}urea_2N)_2\text{-}pz}$.

aminomethyl}pyrazole (H$\mathbf{(N^{Et}{}_2N)_2\text{-}pz}$) that was published in 1991 by Ōkawa and co-workers (Scheme 10) [123].

The authors describe the syntheses, IR and magnetic characterisations of two cobalt(II) and two copper(II) complexes that feature azide or acetate ions as co-ligands, respectively (Table 2) [123]. All four complexes indeed were of the dinuclear 2:1-type, similar to the corresponding complexes of the amide based ligands $H_3$$\mathbf{(pyN^{CO})_2\text{-}pz}$, $H_3$$\mathbf{(N^{Et}N^{CO})_2\text{-}pz}$ and $H_3$$\mathbf{(N^{Me}C_3N^{CO})_2\text{-}pz}$ [93] and attempts to obtain dinuclear 2:2-type complexes of H$\mathbf{(N^{Et}{}_2N)_2\text{-}pz}$ were unsuccessful. Later, the authors published the syntheses and magnetic characterisations of 2:1-type complexes of manganese(II) (Table 2) with the amine based ligand H$\mathbf{(N^{Et}{}_2N)_2\text{-}pz}$ with aliphatic side arms and the pyridine-based ligand H$\mathbf{(py_2N)_2\text{-}pz}$ (Scheme 10) with a benzoato or an acetato co-ligand, respectively [96]. Together with the 2:2-type complex **108** of the similar bis-terdentate ligand H$\mathbf{(pyN)_2\text{-}pz}$, the catalase-like function of the complexes was tested. As it turned out, complex **108** of the ligand with the lower number of donor atoms showed the highest activity in decomposing H_2O_2 [96]. Following those publications the ligand H$\mathbf{(N^{Et}{}_2N)_2\text{-}pz}$ and the very similar ligand H$\mathbf{(N^{Me}{}_2C_3N)_2\text{-}pz}$ have found many applications (Scheme 10) [97,98,104,106,109,124–132]. The most significant difference between H$\mathbf{(N^{Et}{}_2N)_2\text{-}pz}$ and H$\mathbf{(N^{Me}{}_2C_3N)_2\text{-}pz}$ is the length of the ligand side arms; whereas H$\mathbf{(N^{Et}{}_2N)_2\text{-}pz}$ features ethylene linkers and the shorter side arms, H$\mathbf{(N^{Me}{}_2C_3N)_2\text{-}pz}$ has propylene linkers and hence the longer side arms. In 1997 the 2:1-type cobalt(II) complexes $[Co^{II}{}_2$$\mathbf{(N^{Et}{}_2N)_2\text{-}pz}$$(\mu\text{-Cl})Cl_2]$ (**152**) and $[Co^{II}{}_2$$\mathbf{(N^{Me}{}_2C_3N)_2\text{-}pz}$$(\mu\text{-Cl})Cl_2]$ (**153**) were synthesised and structurally characterised (Table 1) [97]. Surprisingly, in both complexes the cobalt(II) ions feature fivefold coordination, which leaves one side arm per ligand half dangling. Similar complexes of nickel(II) ions ($[Ni^{II}{}_2$$\mathbf{(N^{Et}{}_2N)_2\text{-}pz}$$(\mu\text{-Cl})Cl_2]$, **154** and $[Ni^{II}{}_2$$\mathbf{(N^{Me}{}_2C_3N)_2\text{-}pz}$$(\mu\text{-Cl})Cl_2]$, **155**), both with *trans*-positioned coordinated side arms, were also reported [132]. The treatment of **152** and **153** with two equivalents of sodium tetraphenylborate in ethanol results in the formation of the 2:1-type complexes $[Co^{II}{}_2$$\mathbf{(N^{Et}{}_2N)_2\text{-}pz}$$(\mu\text{-Cl})](BPh_4)_2$ (**156**) and $[Co^{II}{}_2$$\mathbf{(N^{Me}{}_2C_3N)_2\text{-}pz}$$(\mu\text{-Cl})](BPh_4)_2$ (**157**), respectively [97]. With respect to the complexes **152** and **153**, in **156** as well as in **157** the former dangling side arms are now coordinated, substituting the non-bridging chloro-co-ligands of the former complexes. Each cobalt(II) ion is therefore in a distorted trigonal-bipyramidal N_4Cl coordination sphere. Against the generally observed trend that longer side arms in the ligand system enforce shorter metal···metal distances and *vice versa*, the cobalt(II) complexes with the longer side arms (**153**, **157** and **110**), also feature the longer metal···metal distances (**153**: 3.942; **157**: 3.909; **110**: 3.913; **152**: 3.818; **156**: 3.833 Å). In contrast, two further cobalt(II) complexes of the deprotonated ligands $\mathbf{(N^{Me}{}_2C_3N)_2\text{-}pz^-}$ and $\mathbf{(N^{Et}{}_2N)_2\text{-}pz^-}$ could be isolated in 1998 [126]. Both the complexes $[Co^{II}{}_2$$\mathbf{(N^{Me}{}_2C_3N)_2\text{-}pz}$$(\mu\text{-F})](BPh_4)_2$ (**158**) and $[Co^{II}{}_2$$\mathbf{(N^{Et}{}_2N)_2\text{-}pz}$$(H_2O)F](BPh_4)_2$ (**159**) feature distorted trigonal-bipyramidal coordinated cobalt(II) ions. All the ligand arms are metal bound. Complex **158** with the longer ligand side arms and complex **159** with the shorter ligand side arms follow the general trend of the correlation between the lengths of the side arms and the metal···metal distances (**158**: 3.577; **159**: 4.282 Å). The shorter metal···metal distance in **158** imbeds a fluoro-bridge, whereas in complex **159**, which features the longer metal···metal distance a HOH···F-bridge is found between the metal centres. In both complexes the coordinated fluoride ions derive from hydrolysis of tetrafluoroborate counter ions. The HOH···F-bridge is readily exchanged by a bromo-bridge, by the simple addition of potassium bromide to the acetonitrile solution of **159**, leading to complex $[Co^{II}{}_2$$\mathbf{(N^{Et}{}_2N)_2\text{-}pz}$$(\mu\text{-Br})](BPh_4)_2$ (**160**; Table 1). The addition of sodium azide to an acetonitrile solution of the HOH···F-bridged

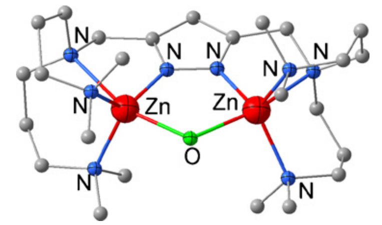

Fig. 31. Molecular structure of the 2:1-type complex cation of the hydroxo-bridged complex $[\mathrm{Zn^{II}}_2\mathbf{(N^{Me}{}_2C_3N)_2\text{-}pz}(\mu\text{-OH})](\mathrm{BPh_4})_2$ (**162**).

complex **159** results in the formation of the μ-1,3-N_3-bridged complex $[\mathrm{Co^{II}}_2\mathbf{(N^{Et}{}_2N)_2\text{-}pz}(\mu\text{-1,3-N_3})](\mathrm{BPh_4})_2$ (**161**). Compared to the HOH···F-bridged complex **159**, the metal···metal distance in **161** (4.415 Å) has increased by 0.133 Å. Other examples of fine tuning the metal···metal distances in 2:1-type complexes of N_3-pz-N_3-type ligands have been published using the metal ions zinc(II) [106,124], nickel(II) [127,130] and copper(II) [130]. The reaction of $\mathrm{H}\mathbf{(N^{Me}{}_2C_3N)_2\text{-}pz}$ having the longer side arms with two equivalents of zinc(II) ions and two equivalents of base resulted in the formation of the hydroxo-bridged complex $[\mathrm{Zn^{II}}_2\mathbf{(N^{Me}{}_2C_3N)_2\text{-}pz}(\mu\text{-OH})](\mathrm{BPh_4})_2$ (**162**; Fig. 31, Table 1) [106,124].

On the other hand the same synthetic procedure but replacing $\mathrm{H}\mathbf{(N^{Me}{}_2C_3N)_2\text{-}pz}$ with the ligand $\mathrm{H}\mathbf{(N^{Et}{}_2N)_2\text{-}pz}$ with the shorter side arms, the 2:1-type complex $[\mathrm{Zn^{II}}_2\mathbf{(N^{Et}{}_2N)_2\text{-}pz}(\mu\text{-O_2H_3})](\mathrm{BPh_4})_2$ (**163**) (Fig. 32, Table 1) was obtained [106,124]. The molecular structure of compound **163** strongly resembles that of **162** but features a wider HOHOH-bridge that formally replaces the narrow OH-bridge of **162**, since the small hydroxide cannot span the larger metal···metal separation enforced by the ligand with shorter side arms.

The higher reactivity of the complex **163** featuring the "hydrated hydroxide ion" relative to complex **162** with the hydroxo-bridge was demonstrated by bubbling CO_2 into solutions of the respective zinc(II) complexes. While no reaction was monitored using complex **162**, the bicarbonate complex $[\mathrm{Zn^{II}}_2\mathbf{(N^{Et}{}_2N)_2\text{-}pz}(\mu\text{-O_2COH})](\mathrm{BPh_4})_2$ (**164**) was isolated from the reaction mixture containing complex **163** [124]. On the other hand, complex **163** barely promotes the cleavage of penicillin G whereas compound **162** proved to do so quite efficiently [108]. Substituting the $O_2H_3^-$-bridging unit of **163**, an oxazetidinylacetate-bridged complex $[\mathrm{Zn^{II}}_2\mathbf{(N^{Et}{}_2N)_2\text{-}pz}(\mu\text{-oaa})](\mathrm{ClO_4})_2$ (**165**) could be isolated and structurally characterised (Table 1) [108]. The carboxylate group of oaa has completely displaced the $O_2H_3^-$-bridge while the β-lactam moiety remains uncoordinated. Formal displacement of the hydroxo-bridge in **162** results in compound $[\mathrm{Zn^{II}}_2\mathbf{(N^{Me}{}_2C_3N)_2\text{-}pz}(\mathrm{oaa})_2](\mathrm{H_3O})(\mathrm{ClO_4})_2$ (**166**) with semibidentate chelating acetate groups. In **166** the pyrazolate remains as the only bridge between the two metal ions. Coordination of oaa leads to de-coordination of one side arm per ligand half, which in **166** remains dangling [108]. Replacement of the $O_2H_3^-$-bridging unit of **163** with 2-azetidinone leads to compound $[\mathrm{Zn^{II}}_2\mathbf{(N^{Et}{}_2N)_2\text{-}pz}(\mu\text{-C_3H_4NO})](\mathrm{ClO_4})_2\cdot\mathrm{MeOH}$ (**167**) where the 2-azetidinone is incorporated in an N,O-fashion as bridging co-ligand in its *N*-deprotonated lactamide form within the dimetallic pocket (Table 1) [133]. The substitution of the H_3O_2-moiety in $[\mathrm{Zn^{II}}_2\mathbf{(N^{Me}{}_2N)_2\text{-}pz}(\mu\text{-O_2H_3})]^{2+}$ and $[\mathrm{Zn^{II}}_2\mathbf{(py_2N)_2\text{-}pz}(\mu\text{-O_2H_3})]^{2+}$ to form HO–H–OMe and MeO–H–OMe functionalities has been studied by Jaime and Weston, performing an extensive density functional investigation [134]. A carboxylato-bridged complex $[\mathrm{Zn^{II}}_2\mathbf{(N^{Et}{}_2N)_2\text{-}pz}(\mu\text{-OAc})](\mathrm{ClO_4})_2\cdot\mathrm{MeOH}$ (**168**) could be isolated treating the deprotonated ligand $\mathbf{(N^{Et}{}_2N)_2\text{-}pz}^-$ with zinc(II) and sodium acetate (Table 1) [135].

Using the same ligands, similar nickel(II) complexes with five coordinate metal centres could be isolated [127]. The hydroxo-bridged complex $[\mathrm{Ni^{II}}_2\mathbf{(N^{Me}{}_2C_3N)_2\text{-}pz}(\mu\text{-OH})](\mathrm{BPh_4})_2$ (**169**) (Tables 1 and 2) is obtained with the ligand featuring the longer side arms, whereas ligand $\mathrm{H}\mathbf{(N^{Et}{}_2N)_2\text{-}pz}$ with the shorter side arms affords the complexes $[\mathrm{Ni^{II}}_2\mathbf{(N^{Et}{}_2N)_2\text{-}pz}(\mu\text{-O_2H_3})](\mathrm{BPh_4})_2$ (**170**) [127] and $[\mathrm{Ni^{II}}_2\mathbf{(N^{Et}{}_2N)_2\text{-}pz}(\mu\text{-O_2H_3})](\mathrm{ClO_4})_2$ (**171**) [130] that each bear a (H)OH···O(H)-bridge (Tables 1 and 2). A similar dinuclear copper(II) complex $[\mathrm{Cu^{II}}_2\mathbf{(N^{Et}{}_2N)_2\text{-}pz}(\mu\text{-O_2H_3})](\mathrm{BPh_4})_2$ (**172**) could also be isolated (Table 1) [130]. With the nickel(II) complex **171**, the reactivity of the "hydrated hydroxide ion" could be demonstrated by substitution reactions [127]. The ability of **171** to act as base was shown by the reaction with urea, which results in coordination of a deprotonated urea as *N*,*O*-bridging ligand ($[\mathrm{Ni^{II}}_2\mathbf{(N^{Et}{}_2N)_2\text{-}pz}(\mu\text{-NHCONH_2})](\mathrm{ClO_4})_2$ (**173**; Table 1) [125]. However, no reaction occurred when replacing urea by the less acidic *N*,*N*-dimethylurea [127]. Compound **173** could also be obtained when using *N*,*N*-bis(trimethylsilyl)urea which resulted in the cleavage of the N–$SiMe_3$ bond during the reaction [125]. In order to definitely exclude the presence of an *O*,*O*-bridging carbamate, instead of the *N*,*O*-bridging urea in **173**, additionally the carbamate complex $[\mathrm{Ni^{II}}_2\mathbf{(N^{Et}{}_2N)_2\text{-}pz}(\mu\text{-O_2CNH_2})](\mathrm{BPh_4})_2$ (**174**; Table 1) was synthesised independently. Comparison of **173** and **174** corroborated the results described before [125]. Urea binding to dinickel cores is of particular interest since the enzyme urease contains two nickel ions within its active site. Hence a detailed study of the behaviour and equilibrium of urea binding of **171** in various solvents has been carried out [131]. In the course of those studies the MeOH···OMe-bridged complex $[\mathrm{Ni^{II}}_2\mathbf{(N^{Et}{}_2N)_2\text{-}pz}(\mathrm{MeOH\cdots OMe})](\mathrm{ClO_4})_2$ (**175**; Table 1) was obtained by very fast ligand exchange when dissolving the (H)OH···O(H)-bridged complex **171** in anhydrous methanol. The authors resumed that in the reactions of **171** or **175** with urea, initially, the substrate substitutes the solvent molecules to form steady-state intermediates $[\mathrm{Ni^{II}}_2\mathbf{(N^{Et}{}_2N)_2\text{-}pz}(\mathrm{OR})(\mathrm{urea})_n]$ ($R = Me, H; n = 1, 2$) in a fast pre-equilibrium. The rate limiting step comprises a bidentate *N*,*O*-coordination of an urea substrate and a deprotonation of an *O*-bound urea co-ligand [131]. Also the ability of **171** to hydrate nitriles to the corresponding amides was tested [127]. Upon heating of **171** in acetonitrile, acrylonitrile or benzonitrile, μ-(amidato-N,O) complexes of the type $[\mathrm{Ni^{II}}_2\mathbf{(N^{Et}{}_2N)_2\text{-}pz}(\mu\text{-NHOCR})](\mathrm{ClO_4})_2$ ($R = Me, CH{=}CH_2$; **176**: $R = Ph$) form, whereas no reaction occurs when treating the corresponding hydroxo-bridged complex **169** under the same reaction conditions. The authors assume that the first step in the formation of amidato compounds is the replacement of a water molecule of the HOHOH-moiety in **171** by an *N*-coordinated nitrile substrate. A nucleophilic attack of the nitrile carbon atom by the hydroxide group still coordinated to the second nickel(II) atom and a proton shift from the O- to the N-atom of the newly formed bridge, finally results in the formation of the stable μ-(amidato-N,O)-bridge. Additionally, the molecular structure of the benzamidato compound **176** was revealed by X-ray analysis (Fig. 33, Table 1) [127].

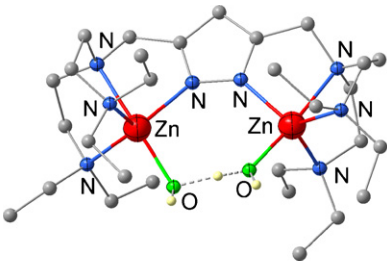

Fig. 32. Molecular structure of the 2:1-type complex cation of the hydroxo-bridged complex $[\mathrm{Zn^{II}}_2\mathbf{(N^{Et}{}_2N)_2\text{-}pz}(\mu\text{-O_2H_3})](\mathrm{BPh_4})_2$ (**163**).

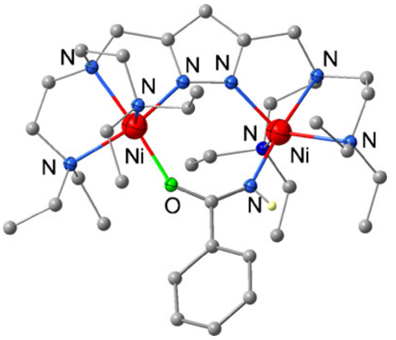

Fig. 33. Molecular structure of the complex cation of the benzamidato complex $[\mathrm{Ni^{II}}_2\mathbf{(N^{Et}_2N)_2\text{-}pz}(\mathrm{NHOCPh})](\mathrm{ClO_4})_2$ (**176**).

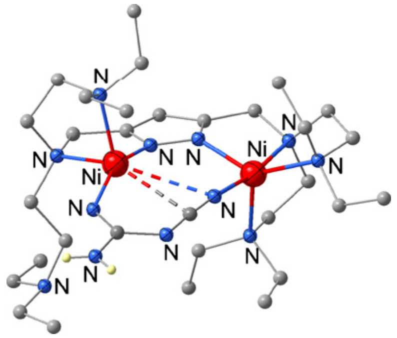

Fig. 34. Molecular structure of the complex cation of the cnge-bridged complex $[\mathrm{Ni^{II}}_2\mathbf{(N^{Et}_2N)_2\text{-}pz}(\mu\text{-}\mathrm{cnge})](\mathrm{ClO_4})_2$ (**181**).

Both nickel(II) ions in **176** adopt a five coordinate geometry, in between square-pyramidal and trigonal-bipyramidal. As expected, the nickel(II) centres are amidato-*N*,*O*-bridged. Employing the amino-substituted nitrile dimethylcyanamide and the active precursor complex **171**, the cyanato-bridged complex $[\mathrm{Ni^{II}}_2\mathbf{(N^{Et}_2N)_2\text{-}pz}(\mu\text{-}1,3\text{-}\mathrm{NCO})](\mathrm{BPh_4})_2$ (**177**; Table 1) could be isolated. Compound **177** was also formed by heating the deprotonated urea-bridged complex **174** for a prolonged period to >110 °C under reduced pressure [127]. Again, the substitution of a water molecule from the $\mathrm{H_3O_2}^-$-moiety by the nitrile substrate was assumed to be the first step in the formation of **177** from the precursor complex **171**. Similar to the formation of the benzamidato complex **176**, this substitution reaction is then followed by the hydration of the nitrile function of the cyanamide to generate a *N*,*O*-bridging deprotonated *N*,*N*-dimethylurea, which subsequently loses a dimethylamine molecule to yield compound **177**. In order to examine if this proposed mechanism for nitrile hydration also results in hydrolase activity, the precursor complex **171** was reacted with DMF, DMA (DMA = dimethyl acetamide) or carboxylic esters and indeed the corresponding carboxylato-bridged dinickel(II) complexes ($[\mathrm{Ni^{II}}_2\mathbf{(N^{Et}_2N)_2\text{-}pz}(\mu\text{-}\mathrm{O_2CR})](\mathrm{ClO_4})_2$, R = H, Me or Et), respectively were obtained. The hydrolytic cleavage of the cyclic ester γ-butyrolactone, upon treatment with **171** resulted in the formation of the complex $[\mathrm{Ni^{II}}_2\mathbf{(N^{Et}_2N)_2\text{-}pz}(\mu\text{-}\mathrm{O_2CC_3H_6OH})](\mathrm{ClO_4})_2$ (**178**) that was structurally characterised and features a 4-hydroxybutyrate co-ligand as carboxylic bridging ligand (Table 1) [127]. The reaction of **170** with a large excess of potassium acetate showed that the integrity of the bimetallic $[\mathrm{Ni^{II}}_2\mathbf{(N^{Et}_2N)_2\text{-}pz}]^{2+}$-framework would not necessarily persist in the presence of an excess of potentially coordinating chelating carboxylate ions. The complex $[\mathrm{Ni^{II}}_2\mathbf{(N^{Et}_2N)_2\text{-}pz}(\mu\text{-}\mathrm{OAc})(\mathrm{OAc})](\mathrm{BPh_4})$ (**179**), isolated from the reaction, features two different types of coordinating acetate ions. As usual a bridging acetato co-ligand is present, but also present is a chelating acetato ligand, that displaced one of the side arms from the respective nickel(II) ion. The respective nickel(II) ion therefore resides in a distorted octahedral geometry [127].

Reaction of the reactive $\mathrm{H_3O_2}$-bridged complex **171** with cyanamide resulted in the formation of a hydrogencyanamido-bridged complex $[\mathrm{Ni^{II}}_2\mathbf{(N^{Et}_2N)_2\text{-}pz}(\mu\text{-}\mathrm{NHC{\equiv}N})](\mathrm{ClO_4})_2$ (**180**; Table 1) [128]. Compound **180** was only the second example of a complex featuring a bridging HNCN^--group. Besides the main product **180** the dicyandiamido-bridged byproduct $[\mathrm{Ni^{II}}_2\mathbf{(N^{Et}_2N)_2\text{-}pz}(\mu\text{-}\mathrm{cnge})](\mathrm{ClO_4})_2$ (**181**) (Hcnge = 2-cyanoguanidine = dicyandiamide) (Fig. 34, Tables 1 and 2) was isolated [128].

The cnge-bridged compound **181** was obtained in higher yield by the direct treatment of **171** with 2-cyanoguanidine [128]. In **181** the deprotonated cnge^--co-ligand binds in an unprecedented fashion. The nitrile function is bound end-on to one nickel(II) atom that remains in a fivefold coordination environment, encapsulated by the donor atoms of the ligand. The other nickel(II) ion is coordinated by the deprotonated NH^--group of the cnge^--co-ligand. Of that ligand half, one side arm is dangling, which leaves the corresponding nickel(II) ion in an unexpected fourfold coordination (Fig. 34). Apparently an open coordination space is directed towards the inside of the bimetallic pocket, where the cnge^--moiety is suitably located between the two nickel(II) ions, to additionally interact with the four coordinate nickel(II) ion in a side-on fashion ($\mathrm{Ni^{II}}$–N: 2.963, $\mathrm{Ni^{II}}$–C: 2.864 Å) [128]. The unusual bonding interaction was confirmed by DFT calculations. The treatment of **171** with a large excess of Hcnge affords compound $[\mathrm{Ni^{II}}_2\mathbf{(N^{Et}_2N)_2\text{-}pz}(\mathrm{cnge})_2](\mathrm{ClO_4})_3$ (**182**), where two neutral Hcnge co-ligands are bound with the nitrile nitrogen atom to the nickel(II) ion in an end-on fashion (Table 1). Owing to a congestion caused by the Hcnge binding, the metal ions are forced to displace rather drastically out of the pyrazolate meanplane (+0.784 and −0.647 Å, respectively). Therefore the metal···metal separation of 4.586 Å is rather large in **182**. To further examine the unusual binding mode of the nitrile group in the bridging cnge^- molecule of compound **181**, the reactive precursor complex **171** was furthermore treated with 2-hydroxybenzonitrile, which in its phenolate form provides a bifunctional ligand of a geometry similar to deprotonated cnge^- [128]. From the reaction mixture compound $[\mathrm{Ni^{II}}_2\mathbf{(N^{Et}_2N)_2\text{-}pz}(\mu\text{-}o\text{-}\mathrm{O(N{\equiv}C)Ph})](\mathrm{ClO_4})_2$ (**183**) was isolated, and structurally characterised (Fig. 35, Table 1).

The structure of **183** differs fundamentally from that of the cnge-bridged complex **181**. As usual, each nickel(II) ion in **183** is embedded in one of the binding pockets of the $\mathbf{(N^{Et}_2N)_2\text{-}pz}^-$ ligand, which donates four nitrogen atoms. The bifunctional 2-oxybenzonitrile ligand occupies the remaining coordination sites with the nitrile nitrogen and the oxy oxygen atom, respectively, completing the fivefold coordination of each nickel(II) ion. In contrast to the binding mode of the cnge^--co-ligand in **181**, the nitrile unit of the co-ligand in **183** exhibits plain end-on coordination, and

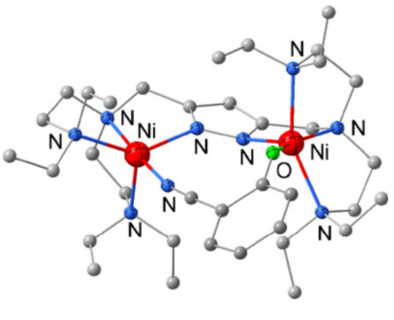

Fig. 35. Molecular structure of the complex cation of the 2-oxybenzonitrilo-bridged complex $[\mathrm{Ni^{II}}_2\mathbf{(N^{Et}_2N)_2\text{-}pz}(\mu\text{-}o\text{-}\mathrm{O(N{\equiv}C)Ph})](\mathrm{ClO_4})_2$ (**183**).

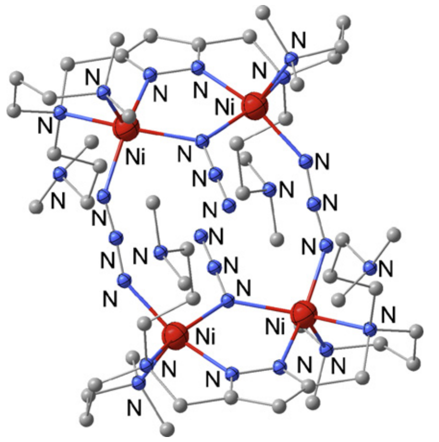

Fig. 36. Molecular structure of the 4:2-type complex cation of [Ni$^{II}_4$($\mathbf{(N^{Me}{}_2C_3N)_2}$**-pz**)$_2$($\mu$-1,1-N$_3$)$_2$($\mu$-1,3-N$_3$)$_2$](BPh$_4$)$_2$ (**186**).

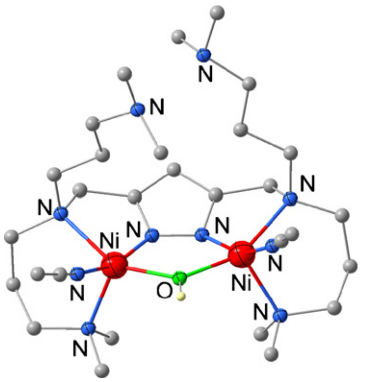

Fig. 37. Molecular structure of the 2:1-type complex cation of [Ni$^{II}_2$H$\mathbf{(N^{Me}{}_2C_3N)_2}$**-pz**($\mu$-OH)(MeCN)$_2$](ClO$_4$)$_3$ (**187**).

no interaction between the *O*-coordinated nickel(II) centre and the C≡N-moiety can be observed [128].

Comparing the metal···metal distances in the complexes **171** and **173**–**183** of the ligand H$\mathbf{(N^{Et}{}_2N)_2}$**-pz** with the shorter side arms, one observes a remarkable flexibility (3.985 Å for **181** with the cnge-bridge versus 4.587 Å for **183** with the *o*-O(N≡C)Ph-bridge), despite the relatively rigid ligand system (Table 1). In all cases, however, the metal···metal separation is >3.9 Å, which is too wide to allow bridging by small groups such as hydroxide within the bimetallic pocket.

Quite similarly to the ligands H$\mathbf{(N^{Me}N^{Me})_2}$**-pz** and H$\mathbf{(N^{Me}C_3N^{Me})_2}$**-pz** [109,110], the above-mentioned trend of obtaining longer metal···metal distances with shorter ligand side arms and *vice versa* is convincingly shown when treating solutions of both the ligands $\mathbf{(N^{Et}{}_2N)_2}$**-pz**$^-$ and $\mathbf{(N^{Me}{}_2C_3N)_2}$**-pz**$^-$ with two equivalents of nickel(II) salts and one equivalent of sodium azide, respectively [109]. The use of the ligand $\mathbf{(N^{Et}{}_2N)_2}$**-pz**$^-$ with the shorter side arms and nickel(II) perchlorate affords complex [Ni$^{II}_2$$\mathbf{(N^{Et}{}_2N)_2}$**-pz**($\mu$-1,3-N$_3$)](ClO$_4$)$_2$ (**184**) (Tables 1 and 2), that has a larger metal···metal distance (4.421 Å) and therefore contains an end-to-end coordinating azide ion. On the other hand, using the ligand $\mathbf{(N^{Me}{}_2C_3N)_2}$**-pz**$^-$ with the longer side arms the complex [Ni$^{II}_2$$\mathbf{(N^{Me}{}_2C_3N)_2}$**-pz**($\mu$-1,1-N$_3$)(NO$_3$)$_2$] (**185**) is formed (Tables 1 and 2). The metal···metal distance in **185** (3.660 Å) is around 0.76 Å shorter than that in **184**, and therefore the metal ions are μ-1,1-azido- instead of μ-1,3-azido-bridged. In **185**, one ligand side arm per ligand half remains dangling and the coordination sphere of the respective nickel(II) ion is instead completed by a semi-chelating nitrate ion, and the overall structure compares well to the structure of complex **132** of the N$_2$-pz-N$_2$-type ligand H$\mathbf{(N^{Me}C_3N^{Me})_2}$**-pz** [109]. The employment of two equivalents of sodium azide and nickel perchlorate results, with the ligand $\mathbf{(N^{Me}{}_2C_3N)_2}$**-pz**$^-$ with the longer side arms, in the formation of a tetranuclear species that was isolated as its tetraphenylborate salt ([Ni$^{II}_4$($\mathbf{(N^{Me}{}_2C_3N)_2}$**-pz**)$_2$($\mu$-1,1-N$_3$)$_2$($\mu$-1,3-N$_3$)$_2$](BPh$_4$)$_2$ (**186**; Tables 1 and 2, Fig. 36).

The nickel(II) coordination spheres in the centrosymmetric dimeric complex **186** are distorted N$_5$ square-pyramidal, respectively. The semi-chelating nitrate ions of **185** have formally exchanged in **186** with μ-1,3-azido-bridges that interconnect the two dimeric subunits. The nickel(II) ions within a subunit are pyrazolato- and additionally μ-1,1-azido-bridged. The dangling side arms of **185** formally remain uncoordinated in **186**, whose structure again resembles strongly the structures of the tetranuclear compounds **133–135** of the N$_2$-pz-N$_2$-type ligand H$\mathbf{(N^{Me}C_3N^{Me})_2}$**-pz** [109].

Another 2:1-nickel(II) complex of H$\mathbf{(N^{Me}{}_2C_3N)_2}$**-pz** with dangling side arms ([Ni$^{II}_2$H$\mathbf{(N^{Me}{}_2C_3N)_2}$**-pz**($\mu$-OH)(MeCN)$_2$](ClO$_4$)$_3$, **187**; Tables 1 and 2, Fig. 37) was isolated from acetonitrile solution. In contrast to the related hydroxo-bridged compound **169** of the same ligand, the coordination geometry of **187** resembles strongly that of the 2:1-type complex **111**, of the bis-terdentate ligand $\mathbf{(N^{Me}C_3N^{Me})_2}$**-pz**$^-$, given that both the complexes **187** and **111** feature hydroxo-bridged N$_4$O coordinated nickel(II) ions that coordinate an acetonitrile co-ligand each. In compound **187** the ligand is in a zwitterionic form and features a strong hydrogen bond between the terminal tertiary amine nitrogen atoms (N···N: 2.751 Å).

The main difference in the synthesis of **187** and **169**, respectively, is the ligand to base stoichiometry. Whereas the formation of the "protonated" hydroxo-bridged complex **187** occurs with the addition of one equivalent of base [98], the synthesis of the "deprotonated" hydroxo-bridged complex **169** affords the addition of two equivalents of base [127]. The additional amine side arms in **187** thus serve as an internal base to generate the Ni-bound hydroxide.

The ability of **187** to coordinate potential substrates was tested [98]. Dissolution of the parent complex **187** in DMF or reaction of the complex with thiocyanate affords the complexes [Ni$^{II}_2$H$\mathbf{(N^{Me}{}_2C_3N)_2}$**-pz**($\mu$-OH)(DMF)$_2$](ClO$_4$)$_3$ (**188**) and [Ni$^{II}_2$H$\mathbf{(N^{Me}{}_2C_3N)_2}$**-pz**($\mu$-OH)(NCS)$_2$](ClO$_4$) (**189**), respectively (Table 2). In contrast to the previously described facile substitutions of the HOHOH-bridge of complex **171**, a substitution reaction on the μ-OH-bridged complex **187** merely causes replacement of the weakly bound acetonitrile co-ligands. In both the complexes **188** and **189** the hydrogen bond between the terminal nitrogen atoms of the dangling side arms remains intact [98]. Attempts to coordinate urea to **187** have failed [98].

Unusual cyanido-bridged nickel(II) complexes of the ligand $\mathbf{(N^{Et}{}_2N)_2}$**-pz**$^-$ with the shorter side arms were also reported [129]. The reaction of the ligand H$\mathbf{(N^{Et}{}_2N)_2}$**-pz** with one equivalent of base, two equivalents of nickel(II) perchlorate and one or two equivalents of tetraethylammonium cyanide resulted in the formation of the complexes [Ni$^{II}_2$$\mathbf{(N^{Et}{}_2N)_2}$**-pz**($\mu$-CN)(MeCN)](ClO$_4$)$_2$ (**190**; Fig. 38) and {[Ni$^{II}_2$$\mathbf{(N^{Et}{}_2N)_2}$**-pz**($\mu$-CN)]$_4$[Ni^{II}($\mu$-CN)$_4$]}(ClO$_4$)$_6$ (**191**; Fig. 39), respectively (Table 2).

Both complexes **190** and **191** have in common a different coordination environment for the two nickel(II) ions in the dinuclear unit, resulting in a mixed-spin situation. Whereas one of the nickel(II) ions is in a distorted octahedral environment and therefore high spin, the other nickel(II) ion resides in a distorted square-planar environment and is therefore low spin. In both compounds the cyanide ligand is housed within the bimetallic pocket, thereby inducing the pronounced asymmetry of the dinuclear subunit. The square-planar nickel(II) ion is coordinated by the strong-field cyanide carbon atom, leaving one of the respective side arms dan-

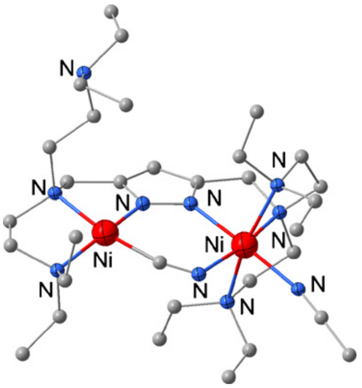

Fig. 38. Molecular structure of the 2:1-type complex cation of [Ni^{II}_2**($N^{Et}_2N)_2$-pz**(μ-CN)(MeCN)](ClO_4)$_2$ (**190**).

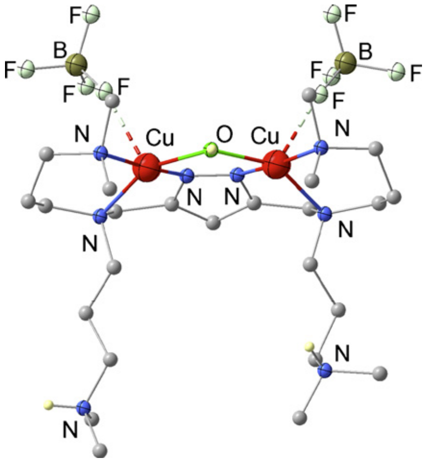

Fig. 40. Molecular structure of the 2:1-type complex *cis*-[$Cu^{II}_2H_2$**($N^{Me}_2C_3N)_2$-pz**(μ-OH)(BF_4)$_2$] (**192**).

gling. The other nickel(II) ion is coordinated by the lower-field cyanide nitrogen atom and both side arms of the respective ligand half. Due to the constraints of the binucleating scaffold, the intramolecular cyanide bridge is extremely bent with an acute angle C≡N–Ni of 111.2(2)°. In the nonanuclear complex **191** four dinuclear [Ni^{II}_2**($N^{Et}_2N)_2$-pz**(μ-CN)]$^{2+}$-entities are held together, *via* the sixth coordination site of the octahedral nickel(II) ion, by a central [$Ni^{II}(CN)_4$]$^{2-}$-unit that coordinates with a nitrogen atom of a cyanido-bridge, respectively. In **191** an unprecedented nonanuclear starlike topology with three different types of nickel(II) ions is achieved [129].

Analogous to the nickel(II) complexes, i.e. the hydroxo-bridged complex **187** and the MeOH···OMe-bridged complex **175** of the ligands with the longer and the shorter side arms, respectively, similar copper(II) complexes can be obtained [104]. The μ-OH-bridged complex [$Cu^{II}_2H_2$**($N^{Et}_2N)_2$-pz**(μ-OH)(BF_4)$_2$] (**192**) and the MeOH···OMe-bridged complex [Cu^{II}_2**($N^{Et}_2N)_2$-pz**(MeOH···OMe)](ClO_4)$_2$ (**193**) were obtained by the reaction of the respective ligand with two equivalents of copper(II) salt in methanol (Table 1). In the case of **193** two equivalents of base were added. In **192**, each copper(II) ion is in a roughly square-planar coordination environment build up by three donor atoms of the ligand, which leaves one side arm dangling, and a bridging hydroxide ion (Fig. 40). Anyhow, weak coordination of tetrafluoroborate ions to the copper(II) ions in a *cis*-arrangement leads to a distorted square-pyramidal geometry for each metal ion. Per complex molecule **192** two protons are retained at the terminal nitrogen atoms of the dangling side arms, which serve as internal base [104].

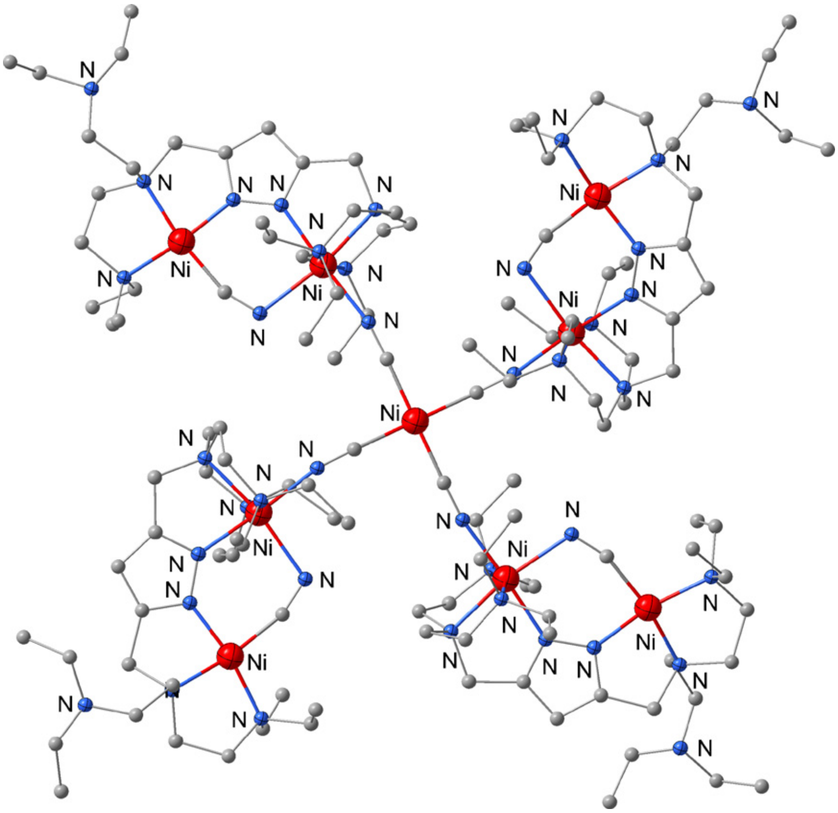

Fig. 39. Molecular structure of the 9:4-type complex cation of {[Ni^{II}_2**($N^{Et}_2N)_2$-pz**(μ-CN)]$_4$[$Ni^{II}(\mu\text{-CN})_4$]}(ClO_4)$_6$ (**191**).

The molecular structure of the C_2-symmetric complex **193** is very similar to that of **175**, but has two five coordinate metal centres that are connected by a MeOH···OMe-bridge [104].

Together with the previously described complexes **112** and **113** of the ligands H**$(N^{Me}C_3N^{Me})_2$-pz** and H**$(N^{Me}N^{Me})_2$-pz** that are of the D_2-pz-D_2 type, the catecholase activity of the complexes **192** and **193** was tested using 3,5-DTBC as the substrate [104]. Complexes **112** and **192** bearing the longer ligand side arms and a hydroxo-bridge show very high catecholase activity whereas the respective activity in **113** and **193** that bear the shorter ligand side arms is lower and significantly lower, respectively (k_{obs}: **192** = 2430; **112** = 1400; **113** = 514; **193** = 22.8 h^{-1}). In all cases the reaction rate is first order in catalyst concentration. It appears as if catecholase activity in such complexes is correlated to the metal···metal distance ($Cu^{II}\cdots Cu^{II}$: **192** = 3.447; **112** = 3.540; **113** = 4.088; **193** = 4.553 Å) in such a way that the shorter the distance the more reactive the complex. In the course of the studies with the less reactive catechole derivative H_2TCC, an adduct of **193** with TCC^{2-} [$Cu^{II}{}_2$H**$(N^{Et}{}_2N)_2$-pz**(TCC)(H_2O)]$(ClO_4)_2$, **194**) was isolated and structurally characterised (Table 1) [104]. The molecular structure of **194** resembles the structures of the previously described TCC^{2-} adducts **119** (Fig. 24) and **120** of the ligand H**$(N^{Me}N^{Me})_2$-pz** in a way that the TCC^{2-} molecule is bound in a bidentate chelating fashion to one of the two copper(II) ions only [104].

2:1-Type zinc(II) complexes with a hydroxo-bridge (**162**; Fig. 31) [106,124] or a HOHOR-bridge (**163**: R = H; Fig. 31 [106,124] and [$Zn^{II}{}_2$**$(N^{Et}{}_2N)_2$-pz**(HO···HOMe)]$(ClO_4)_2$, **195**; Table 1) [106], similar to the nickel(II) and copper(II) complexes **169**, **171** and **172**, **192** (R = H) and **193** (R = Me), respectively, were also obtained [106,124]. Together with the previously described zinc(II) complex **162**, the phosphate diester hydrolysis using NaBNPP as substrate and the stability constants of the HO···HOMe-bridged complex **195** were studied [106]. Binding of $BNPP^-$ to the complex in methanol solution occurs *via* complete substitution of the HOHOR-bridge in the case of **195**. The bidentate bridging coordination of the resulting DMP in the thus formed complex [$Zn^{II}{}_2$**$(N^{Et}{}_2N)_2$-pz**(μ-DMP)]$(ClO_4)_2$ (**196**; Table 1) was verified by X-ray crystallography (Fig. 41) [106].

In order to use bimetallic complexes of the type [$M^{II}{}_2$**$(N^{Et}{}_2N)_2$-pz**(HO···HOR)]$^{2+}$ as they were described for M = Co, Ni, Cu and Zn in this chapter, for mimicking functional principles of biological metallohydrolases, and to finally understand their observed reactivity, some information about the behaviour in aqueous solution is necessary. Therefore the complexation equilibria and the stability of nickel(II), copper(II) and zinc(II) complexes of the ligand H**$(N^{Et}{}_2N)_2$-pz** in water was studied by potentiometry and other methods [130].

Using the acyclic bis-quadridentate ligand H_5**$[(FN)_2C_3N]_2$-pz** (Scheme 10) which features secondary terminal amine donors, 2:1-type nickel(II) and cobalt(II) complexes were obtained [132]. With the addition of external base the complexes [$Ni^{II}{}_2H_4$**$[(FN)_2C_3N]_2$-pz**(μ-Cl)Cl_2] (**197**) and [$Co^{II}{}_2H_4$**$[(FN)_2C_3N]_2$-pz**(μ-Cl)Cl_2] (**198**) are formed, whereas complexes with the composition [$Ni^{II}{}_2H_5$**$[(FN)_2C_3N]_2$-pz**Cl_4] and [$Co^{II}{}_2H_5$**$[(FN)_2C_3N]_2$-pz**Cl_4] (**199**) are obtained without the addition of an external base, respectively. Unexpectedly, all complexes **197**–**199** and [$Ni^{II}{}_2H_5$**$[(FN)_2C_3N]_2$-pz**Cl_4] feature asymmetric dinuclear cores with two distinct different coordination geometries within the dinuclear units. In **197**, as well as in **198** (Fig. 42) one metal centre is in a distorted square-pyramidal geometry, coordinated by three nitrogen donors of the respective ligand half, leaving one side arm dangling. The fivefold geometry is completed by the coordination of two chloro-co-ligands, one of them bridging to the second metal ion. This second metal ion is in a distorted octahedral coordination environment, consistent of the four nitrogen donor atoms of the respective ligand half and two chloro-co-ligands. This geometric asymmetry is surprising, as there is no obvious geometric or electronic distinction between the binding pockets [132]. While UV–vis spectra of the nickel(II) complex **197** are quite similar in ethanol and in the solid state, the spectra of the cobalt(II) complex **198** undergo considerable changes upon dissolution of the complex in ethanol, suggesting detachment of a further ligand side arm.

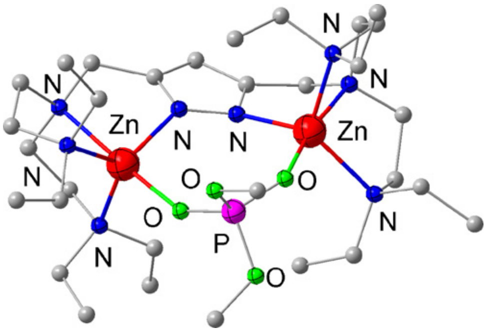

Fig. 41. Molecular structure of the 2:1-type complex cation of [$Zn^{II}{}_2$**$(N^{Et}{}_2N)_2$-pz**(μ-DMP)]$(ClO_4)_2$ (**196**).

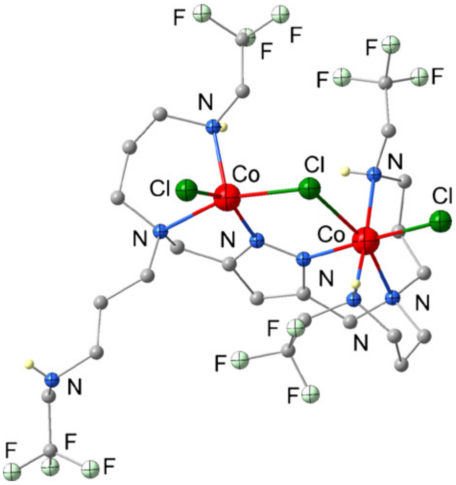

Fig. 42. Molecular structure of the 2:1-type complex [$Co^{II}{}_2H_4$**$[(FN)_2C_3N]_2$-pz**(μ-Cl)Cl_2] (**198**).

The complexes [$Ni^{II}{}_2H_5$**$[(FN)_2C_3N]_2$-pz**Cl_4] and **199**, obtained without the addition of external base, differ quite distinctively from each other. Single crystals of [$Ni^{II}{}_2H_5$**$[(FN)_2C_3N]_2$-pz**Cl_4] were obtained but were of poor quality such that only the overall molecular structure was clarified but no detailed discussion was possible [132]. The pyrazolate core has lost its bridging coordination mode and is detached from one of the nickel(II) ions. The pyrazole detached nickel(II) ion is found in a fivefold geometry, coordinated by the three donor atoms of the respective ligand side arm and two additional chloro-co-ligands. The pyrazole coordinated nickel(II) ion resides in a N_4Cl_2 distorted octahedral coordination sphere, similar to the environment of **197**. The geometric situation in the cobalt(II) complex **199** is quite different. One of the cobalt(II) ions resides in a distorted octahedral coordination environment similar to the octahedral nickel(II) ion in [$Ni^{II}{}_2H_5$**$[(FN)_2C_3N]_2$-pz**Cl_4], but is connected with the second cobalt(II) ion *via* the pyrazolate nitrogen atoms and a μ-chloro-co-ligand. This second cobalt(II) ion is distorted tetrahedrally coordinated, the remaining sites being occupied by two chloro-co-ligands. The ligand side arms of the respective ligand half therefore are completely detached and dangling. The tertiary amine atom of that side arm is protonated, which leaves the ligand H_5**$[(FN)_2C_3N]_2$-pz** in a zwitterionic form. A hydro-

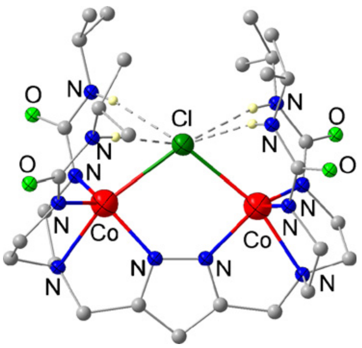

Fig. 43. Molecular structure of the complex anion of the 2:1-type complex $[nPr_4N]_2[Co^{II}_2H_4\mathbf{(^tBu\text{-}urea_2N)_2\text{-}pz}(\mu\text{-}Cl)]\cdot DMA$ (**200**).

gen bond is formed to one of the chloro-co-ligands of the respective cobalt(II) ion [132].

In 2006 Borovik, Sorrell and co-workers described the urea-derived bis-quadridentate ligands $H_9\mathbf{(^tBu\text{-}urea_2N)_2\text{-}pz}$ and $H_9\mathbf{(^iPr\text{-}urea_2N)_2\text{-}pz}$ (Scheme 10), which feature four NH-groups within the ligand cavities that are potentially able to serve as H-bond donors [136]. This structural motif is nicely shown on the dinuclear chloro-bridged cobal(II) complexes $[nPr_4N]_2[Co^{II}_2H_4\mathbf{(^tBu\text{-}urea_2N)_2\text{-}pz}(\mu\text{-}Cl)]\cdot DMA$ (**200**; Table 1, Fig. 43) and $[nPr_4N]_2[Co^{II}_2H_4\mathbf{(^iPr\text{-}urea_2N)_2\text{-}pz}(\mu\text{-}Cl)]\cdot 0.5DMA$ (**201**; Table 1). Both complexes feature N_4Cl coordinate cobalt(II) centres with distorted trigonal-bipyramidal geometries. The ligand coordinates as quadridentate chelate, coordinating with the pyrazole-N atoms, the tertiary amine functions and the α-N-atoms of the urea function, respectively. The chloro-bridge is involved in a H-bond network, ligated to all four urea α'-N-H groups. A symmetrical H-bond network is achieved in **201** (N···Cl distance: 3.366(1) Å) whereas two "diagonal" pairs of H-bonds are formed in **200** [136]. Later the authors described the μ-OH-bridged cobalt(II) complexes $[nPr_4N]_2[Co^{II}_2H_4\mathbf{(^tBu\text{-}urea_2N)_2\text{-}pz}(\mu\text{-}OH)]$ and $[nPr_4N]_2[Co^{II}_2H_4\mathbf{(^iPr\text{-}urea_2N)_2\text{-}pz}(\mu\text{-}OH)]$ (**202**; Table 1) that co-crystallised with 18.2% with the isodimensional anion of **201** [137]. In **202** no intramolecular H-bonds are observed. The complexes have been found to hydrate unactivated nitriles and hydrolyse unactivated esters, similar to the related system, that lack the urea groups [119]. The acetamidato-bridged complexes $[nPr_4N]_2[Co^{II}_2H_4\mathbf{(^iPr\text{-}urea_2N)_2\text{-}pz}(\mu\text{-}1,3\text{-}OC(NH)Me)]\cdot DMA$ (**203**) and $[nPr_4N]_2[Co^{II}_2H_4\mathbf{(^tBu\text{-}urea_2N)_2\text{-}pz}(\mu\text{-}1,3\text{-}OC(NH)Me)]\cdot DMA$ (**204**; Table 1) and the acetato-bridged complexes $[nPr_4N]_2[Co^{II}_2H_4\mathbf{(^iPr\text{-}urea_2N)_2\text{-}pz}(\mu\text{-}1,3\text{-}OAc)]\cdot DMA$ (**205**; Table 1) and $[nPr_4N]_2[Co^{II}_2H_4\mathbf{(^tBu\text{-}urea_2N)_2\text{-}pz}(\mu\text{-}1,3\text{-}OAc)]\cdot DMA$ (**206**; Table 1) could be isolated by reacting the corresponding hydroxo-bridged complexes with acetonitrile and ethyl acetate, respectively [137]. In all those complexes **203–206** the ligand is involved in hydrogen bonds to the heteroatoms of the bridging co-ligand. The authors suggest, that the ability of the ligands to form hydrogen bonds within the binding pockets may facilitate hydration/hydrolysis by stabilising hydroxo intermediates [137].

The ligands $H\mathbf{(py_2N)_2\text{-}pz}$ and $H\mathbf{[(pyC_2)_2N]_2\text{-}pz}$ feature aromatic side arms, respectively, and are therefore different from the ligands $H\mathbf{(N^{Et}{}_2N)_2\text{-}pz}$, $H\mathbf{(N^{Me}{}_2C_3N)_2\text{-}pz}$ and $H_5\mathbf{[(FN)_2C_3N]_2\text{-}pz}$ described before, that all feature aliphatic side arms (Scheme 10). Dinuclear 2:1-type copper(II) complexes with MeOH···F-bridges ($[Cu^{II}_2\mathbf{(py_2N)_2\text{-}pz}(MeOH)F](BF_4)_2$, **207** and $[Cu^{II}_2\mathbf{[(pyC_2)_2N]_2\text{-}pz}(MeOH)F](BF_4)_2$, **208**; Table 1) were obtained by reacting the respective ligand with two equivalents of copper tetrafluoroborate and two equivalents of base [112]. Despite the obvious similarities of the two complexes, close inspection of **207** and **208** reveals crucial differences between them, due to the different chain lengths of the ligand side arms [112]. While trigonal-bipyramidal in **207** with the shorter side arms, the coordination environment for both copper(II) centres in **208** is distorted square-pyramidal with a *cis*-arrangement of the apical positions. Unexpectedly the metal···metal separation of 4.430(1) Å in **208** is larger than that in **207** (4.291(1) Å), despite the shorter side arms of the ligand in the latter complex. This is in contrast to the fact that longer side arms usually inflict shorter metal···metal separations, as was observed for the related aliphatic ligands $H\mathbf{(N^{Et}{}_2N)_2\text{-}pz}$ and $H\mathbf{(N^{Me}{}_2C_3N)_2\text{-}pz}$, that differ by the lengths of their side arms, just as $H\mathbf{(py_2N)_2\text{-}pz}$ differs from $H\mathbf{[(pyC_2)_2N]_2\text{-}pz}$. Comparison of **207** and **208** leads to the conclusion that the metal···metal distances of around 4.25–4.45 Å in those complexes is mainly determined by the requirement of the MeOH···F-bridge, rather than by the lengths of the side arms [112]. The use of copper perchlorate or copper triflate and $H\mathbf{[(pyC_2)_2N]_2\text{-}pz}$ on the other hand results in the formation of the hydroxo-bridged 2:1-species $[Cu^{II}_2\mathbf{[(pyC_2)_2N]_2\text{-}pz}(OH)](ClO_4)_2$ (**209**; Table 1) and $[Cu^{II}_2\mathbf{[(pyC_2)_2N]_2\text{-}pz}(OH)](CF_3SO_3)_2$ (**210**; Table 1), respectively, with considerably shorter metal···metal separations (3.44–3.52 Å) compared to the compounds **207** and **208** [113].

Chloro-bridged dinickel(II) complexes are formed with $H\mathbf{[(pyC_2)_2N]_2\text{-}pz}$ with the longer side arms [114]. In $[Ni^{II}_2\mathbf{[(pyC_2)_2N]_2\text{-}pz}(\mu\text{-}Cl)Cl_2]\cdot 2MeOH$ (**211**; Tables 1 and 2, Fig. 44) both nickel(II) ions are N_4Cl_2 six coordinate, the terminal chloro-co-ligands coordinating once in a *trans* and once in a *cis* position relative to the pyrazolate nitrogen atom of the respective binding pocket.

A single bridging chloro-ligand is present in $[Ni^{II}_2\mathbf{[(pyC_2)_2N]_2\text{-}pz}(\mu\text{-}Cl)MeOH](ClO_4)_2$ (**212**; Tables 1 and 2) [114]. As the metal···metal separation increases using $H\mathbf{(py_2N)_2\text{-}pz}$ with the shorter side arms an unusual Ni–Cl···H–O(Me)–Ni-bridge is found in $[Ni^{II}_2\mathbf{(py_2N)_2\text{-}pz}(\mu\text{-}Cl)Cl(MeOH)_2]Cl\cdot 2MeOH$ (**213**; Tables 1 and 2) [114].

Since 2005 several 2:1 type dizinc(II) complexes of $H\mathbf{(py_2N)_2\text{-}pz}$ and $H\mathbf{[(pyC_2)_2N]_2\text{-}pz}$ [108,133,135,138] have been reported and their catalytic potential studied as model phosphodiesterase [138], or metallo-ß-lactamase [108,133]. Using the ligand with the shorter side arms, the acetato-bridged dizinc(II) complex $[Zn^{II}_2\mathbf{(py_2N)_2\text{-}pz}(\mu\text{-}OAc)](ClO_4)_2\cdot OCMe_2$ (**214**; Table 1) was isolated and structurally characterised. As expected, the ligand coordinates as a bis-quadridentate chelate. A fifth binding site is occupied by a bridging acetato co-ligand, leaving the zinc(II) ions in a fivefold coordination sphere [135]. The hydroxo-bridged compound $[Zn^{II}_2\mathbf{[(pyC_2)_2N]_2\text{-}pz}(\mu\text{-}OH)](ClO_4)_2$ (**215**; Table 1) of the ligand with the longer side-arms and the H–O···H–OMe-bridged compound $[Zn^{II}_2\mathbf{(py_2N)_2\text{-}pz}(OH)(MeOH)](ClO_4)_2$ (**216**; Table 1) of the ligand with the shorter side arms have been used for reactivity studies on the cleavage of BNPP [138]. The studies

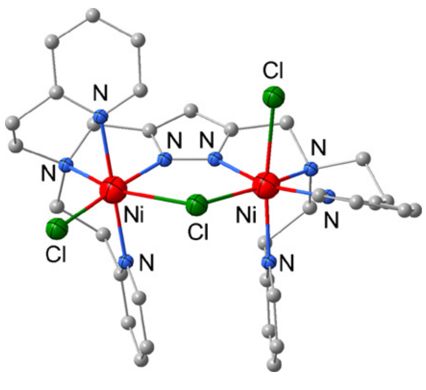

Fig. 44. Molecular structure of the 2:1-type complex $[Ni^{II}_2\mathbf{[(pyC_2)_2N]_2\text{-}pz}(\mu\text{-}Cl)Cl_2]\cdot 2MeOH$ (**211**).

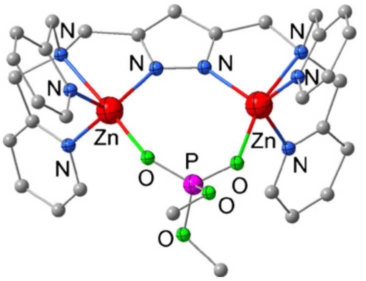

Fig. 45. Molecular structure of the 2:1-type complex cation of $[Zn^{II}_2\mathbf{(py_2N)_2\text{-}pz}(O_2P(OMe)_2)](ClO_4)_2$ (**218**).

revealed that **215** with the larger metal···metal separation is hydrolytically more potent in the hydrolysis as well as in the transesterification of BNPP. Complexes of the hydrolytically inert DMP $[Zn^{II}_2\mathbf{[(pyC_2)_2N]_2\text{-}pz}(O_2P(OMe)_2)](ClO_4)_2$ (**217**) and $[Zn^{II}_2\mathbf{(py_2N)_2\text{-}pz}(O_2P(OMe)_2)](ClO_4)_2$ (**218**; Fig. 45) (Table 1) were prepared in order to elucidate the binding mode of the phosphate unit in the product-inhibited form. In both cases the $(MeO)_2PO_2^-$ co-ligand coordinates in a bidentate bridging mode within the dinuclear scaffold.

In **217**, where a μ-OH-bridge has formally been replaced by a much larger μ-$O_2P(OMe)_2$-bridge, this results in severe distortion of the bimetallic framework and displacement of the zinc(II) ions out of the plane of the pyrazolate heterocycle [138]. Studies on the hydrolytic cleavage of penicillin G were performed on the hydroxo-bridged complex **215** and the H–O···H–OH-bridged compound $[Zn^{II}_2\mathbf{(py_2N)_2\text{-}pz}(OH)(H_2O)](ClO_4)_2$ together with the similar complexes **162** and **163** of the ligands $\mathbf{(N^{Me}{}_2C_3N)_2\text{-}pz}$ and $\mathbf{(N^{Et}{}_2N)_2\text{-}pz}$ with aliphatic side arms [108,133]. Drastic differences in the activity are ascribed to the lower stability of the six-membered chelate rings in $[Zn^{II}_2\mathbf{[(pyC_2)_2N]_2\text{-}pz}]^{3+}$ and $[Zn^{II}_2\mathbf{(N^{Me}{}_2C_3N)_2\text{-}pz}]^{3+}$, compared to the five-membered rings in $[Zn^{II}_2\mathbf{(py_2N)_2\text{-}pz}]^{3+}$ and $[Zn^{II}_2\mathbf{(N^{Et}{}_2N)_2\text{-}pz}]^{3+}$, that allow for partial detachment of ligand side arms and hence for open sites to be available for activation and/or binding of substrates [108]. Also, the 2-azetidinone-bridged compound $[Zn^{II}_2\mathbf{(py_2N)_2\text{-}pz}(\mu\text{-}C_3H_4NO)](ClO_4)_2\cdot OCMe_2$ (**219**; Table 1) was structurally characterised (Fig. 46). As in **167** of the similar aliphatic ligand $H\mathbf{(N^{Et}{}_2N)_2\text{-}pz}$ the 2-azetidinone in **219** is incorporated in an N,O-fashion as bridging co-ligand in its *N*-deprotonated lactamide form [133].

Using dizinc(II) complexes of the aliphatic ligand $H\mathbf{(N^{Et}{}_2N)_2\text{-}pz}$ (**168**), the pyridine-based ligand $H\mathbf{(py_2N)_2\text{-}pz}$ (**214**) as well as the aromatic new ligands $H\mathbf{(Im_2N)_2\text{-}pz}$, $H\mathbf{(ImpyN)_2\text{-}pz}$ and $H\mathbf{(ImN^{Et}N)_2\text{-}pz}$ (Scheme 10) a series of acetato-bridged complexes could be crystallised (**220**: $[Zn^{II}_2\mathbf{(Im_2N)_2\text{-}pz}(\mu\text{-}OAc)](ClO_4)_2\cdot 2OCMe_2$, **221**: $[Zn^{II}_2\mathbf{(Im_2N)_2\text{-}pz}(\mu\text{-}OAc)](ClO_4)_2\cdot 2MeCN$, **222**: $[Zn^{II}_2\mathbf{(ImpyN)_2\text{-}pz}(\mu\text{-}OAc)](ClO_4)_2\cdot 0.5OCMe_2$, **223**: $[Zn^{II}_2\mathbf{(ImN^{Et}N)_2\text{-}pz}(\mu\text{-}OAc)](ClO_4)_2\cdot OCMe_2$; Table 1), which nicely shows the great flexibility of the acetato-bridge. Additionally the ligand $H\mathbf{(pyN^{Et}N)_2\text{-}pz}$ is introduced in that work [135].

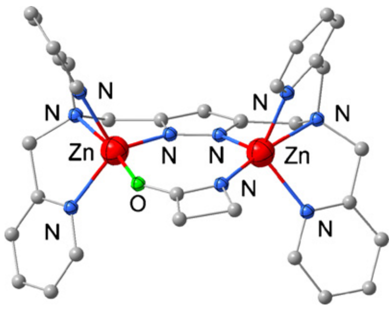

Fig. 46. Molecular structure of the 2:1-type complex cation of $[Zn^{II}_2\mathbf{(py_2N)_2\text{-}pz}(\mu\text{-}C_3H_4NO)](ClO_4)_2\cdot OCMe_2$ (**219**).

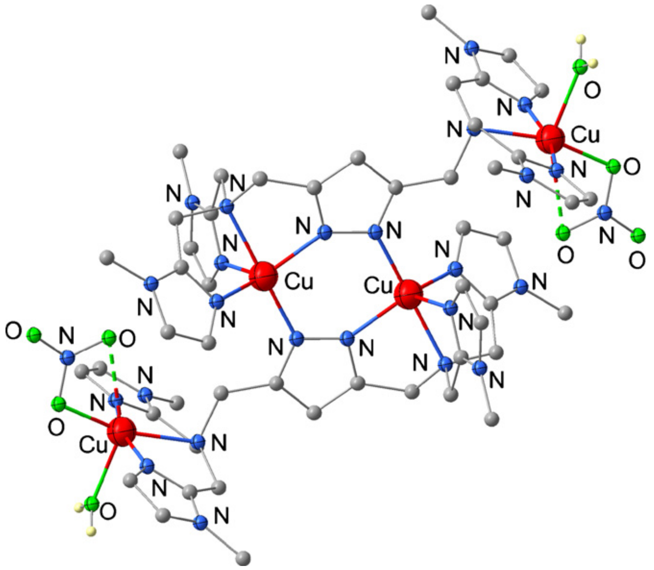

Fig. 47. Molecular structure of the 4:2-type complex cation of $[Cu^{II}_2\mathbf{(Im_2N)_2\text{-}pz}(NO_3)(H_2O)]_2(NO_3)_4\cdot 5H_2O$ (**226**).

By carefully varying the reaction conditions and pH, different copper(II) complexes of $\mathbf{(Im_2N)_2\text{-}pz}^-$ were isolated [139]. The MeO–H···OMe-bridged 2:1-type complexes $[Cu^{II}_2\mathbf{(Im_2N)_2\text{-}pz}(OMe)(MeOH)](ClO_4)_2\cdot MeCN$ (**224**) and $[Cu^{II}_2\mathbf{(Im_2N)_2\text{-}pz}(OMe)(MeOH)](NO_3)_2\cdot 5H_2O$ (**225**) and the tetranuclear compound $[Cu^{II}_2\mathbf{(Im_2N)_2\text{-}pz}(NO_3)(H_2O)]_2(NO_3)_4\cdot 5H_2O$ (**226**) were structurally characterised (Tables 1 and 2, Fig. 47). In **226** a 2:2-moiety is formed, where one side-arm of each ligand is not coordinating to the pyrazolato-bound copper(II) ion. Instead, a third and fourth copper(II) ion are coordinated by the terdentate binding pocket of the ligand side arm, respectively. The fivefold coordination sphere of those copper(II) ions is completed by a water and a nitrato co-ligand. The central pyrazolato-bridged copper(II) ions reside in a N_5-trigonal-bipyramidal coordination sphere, build up by the donors of a quadridentate coordination pocket of one ligand and a pyrazolate nitrogen atom of a second ligand, respectively [139].

224 is an active catalyst for the oxidative C–C coupling of 2,4,6-trimethylphenol to give the corresponding stilbenequinone, using aerial dioxygen [140].

4.2. Other D_3-pz-D_3-type ligands with acyclic side arms

The ligand $H\mathbf{(S_2N)_2\text{-}pz}$ (Scheme 11) is an acyclic aliphatic ligand of the S_2N-pz-NS_2-type and has been intensely studied in nickel-azido chemistry [101,122,141–143].

The ligand, together with a 2:1-type chloro-bridged complex $[Ni^{II}_2\mathbf{(S_2N)_2\text{-}pz}(\mu\text{-}Cl)Cl_2]$ (**227**; Tables 1 and 2), was first isolated and characterised in 1998 [141]. Both potentially quadridentate binding pockets of the ligand in **227** function as N_2S_2-chelate, each imbedding one distorted octahedrally coordinated nickel(II) ion. The sulfur atoms of the ligand halfs are situated *trans* to each other. In 1999 a 2:1-type acetato-bridged dinuclear nickel(II) complex $[Ni^{II}_2\mathbf{(S_2N)_2\text{-}pz}(\mu\text{-}OAc)(OCMe_2)_2](ClO_4)_2$ (**228**; Table 1) was structurally characterised [101]. The overall geometry of **228** strongly resembles that of **227**, having substituted the chloro-bridge of the latter with an acetato-bridge in the former, and the non-bridging chloro-co-ligands

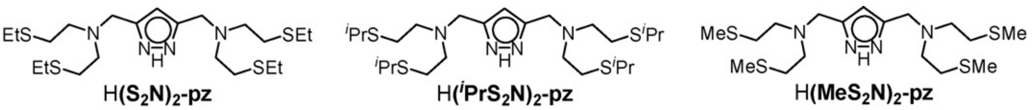

Scheme 11. S$_2$N-pz-NS$_2$-Type and S$_2$N-pz-N$_3$-type ligands: H**(S$_2$N)$_2$-pz**, H**(^{i}PrS$_2$N)$_2$-pz**, and H**(MeS$_2$N)$_2$-pz**.

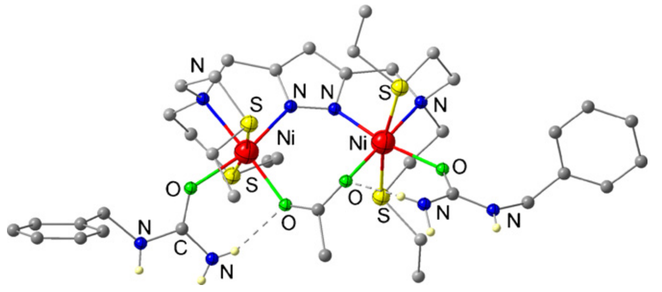

Fig. 48. Molecular structure of the 2:1-type complex cation of [Ni$^{\mathrm{II}}_2$**(S$_2$N)$_2$-pz**(μ-OAc)(benzylurea)$_2$](ClO$_4$)$_2$ (**229**).

of the latter with acetone co-ligands in the former complex [101]. Substitution reactions on **228** with urea, *N*,*N*-dimethylurea and benzylurea were carried out and resulted in the formation of the complexes [Ni$^{\mathrm{II}}_2$**(S$_2$N)$_2$-pz**(μ-OAc)(OC(NH$_2$)(NR$_2$))$_2$](ClO$_4$)$_2$ (NR$_2$ = NH$_2$, NMe$_2$; **229**: NR$_2$ = NH(CH$_2$Ph)) (Fig. 48, Table 1) of which **229** was structurally characterised [101]. The basic 2:1-type framework of **228** has been preserved in **229**, while the formerly bound acetone co-ligands have been replaced by *O*-coordinated benzylurea molecules.

Substitution reaction of **228** with azide ions resulted not only in the replacement of the labile acetone co-ligands but led to a complete reshuffling of the framework and formation of the unexpected 4:2-type complex [Ni$^{\mathrm{II}}_4$(**(S$_2$N)$_2$-pz**)$_2$(μ-1,1,3-N$_3$)$_2$(μ-1,3-N$_3$)(μ-OAc)](ClO$_4$)$_2$ (**230**; Fig. 49, Tables 1 and 2) [142].

The tetranuclear unit in **230** consists of two 2:1-type fragments that are connected by three azido-bridges in an unusual fashion and are additionally held together by a single acetato-bridge. The nickel(II) centres of the 2:1-subunit are μ-1,3-N$_3$-bridged, while those actual μ-1,1,3-azido ligands also function as μ-1,1-bridge to the other subunit, respectively. This feature results in a double μ-1,1-N$_3$-bridge between the two subunits. The coordination sphere of the respective nickel(II) ions is N$_4$SO distorted octahedral, as one of the sulfur sidearms of the respective ligand half has been replaced by an acetato co-ligand that also functions as a bridge between the two subunits. The two 2:1-type subunits are further connected by a μ-1,3-N$_3$-bridge between the two nickel(II) centres of the second ligand half, respectively. Those nickel(II) ions hence are coordinated in a distorted N$_4$S$_2$ octahedral way [142].

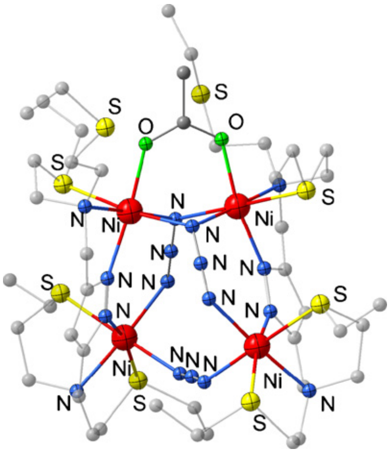

Fig. 49. Molecular structure of the 4:2-type complex cations of [Ni$^{\mathrm{II}}_4$(**(S$_2$N)$_2$-pz**)$_2$(μ-1,1,3-N$_3$)$_2$(μ-1,3-N$_3$)(μ-OAc)](ClO$_4$)$_2$ (**230**).

Upon treatment with additional acetate ions, two more thioether donors dissociate and the cage structure of **230** is opened to give the 4:2-type compound [Ni$^{\mathrm{II}}_4$(**(S$_2$N)$_2$-pz**)$_2$(μ-1,1,3,3-N$_3$)(μ-1,1-N$_3$)$_2$(μ-OAc)$_2$)](ClO$_4$) (**231**; Table 1). In **231** the nickel(II) centres of the tetranuclear unit form a rectangle where the long edges are spanned by the pyrazolate moieties and each short edge is spanned by an acetate and a μ-1,1-azide. The remaining azido co-ligand caps the rectangle as a μ-1,1,3,3-N$_3$-bridge, quite similar to the previously described complex **151** of the ligand **(SN)$_2$-pz**.

Using adamantyl carboxylate instead of acetate, the related 4:2-type complex [Ni$^{\mathrm{II}}_4$(**(S$_2$N)$_2$-pz**)$_2$(μ-1,1,3,3-N$_3$)(μ-O$_2$C-Ada)$_4$)](ClO$_4$) (**232**; Fig. 50) was isolated and the magnetic properties were investigated (Tables 1 and 2) [142]. In contrast to **231**, compound **232** contains double carboxylato-bridges at the short edges of the Ni$_4$-arrangement, but also features a μ-1,1,3,3-N$_3$-bridge. However, the binding situation of this bridge is completely different to that in **231**, as in the latter complex the Ni–N$_3$–Ni entities are almost planar with respect to the *end-to-end* linkages, whereas in the former complex they are in plane with the *end-on* linkages (Fig. 50) [142]. Similar complexes to **231** and **232**, namely [Ni$^{\mathrm{II}}_4$(**(S$_2$N)$_2$-pz**)$_2$(μ-1,1,3,3-N$_3$)(μ-1,1-N$_3$)$_2$(μ-O$_2$CPh)$_2$)](ClO$_4$) (**233**), [Ni$^{\mathrm{II}}_4$(**(^{i}PrS$_2$N)$_2$-pz**)$_2$(μ-1,1,3,3-N$_3$)(μ-1,1-N$_3$)$_2$(μ-OAc)$_2$)](ClO$_4$) (**234**), [Ni$^{\mathrm{II}}_4$(**(^{i}PrS$_2$N)$_2$-pz**)$_2$(μ-1,1,3,3-N$_3$)(μ-1,1-N$_3$)$_2$(μ-O$_2$C-Ada)$_2$)]-(ClO$_4$) (**235**) and [Ni$^{\mathrm{II}}_4$(**(MeS$_2$N)$_2$-pz**)$_2$(μ-1,1,3,3-N$_3$)(μ-O$_2$C-Ada)$_4$)](ClO$_4$) (**236**), could be isolated by a straight forward procedure from appropriate stoichiometric amounts of the respective ligand (Scheme 11), base, nickel perchlorate and azide ions (Tables 1 and 2) [122].

As it was shown in 2005, 4:2-type complexes similar to **230** can also be obtained directly from the respective components [143]. Using this strategy the complexes [Ni$^{\mathrm{II}}_4$(**(S$_2$N)$_2$-pz**)$_2$(μ-1,1,3-N$_3$)$_2$(μ-1,3-N$_3$)(μ-O$_2$CPh)](ClO$_4$)$_2$ (**237**) and [Ni$^{\mathrm{II}}_4$(**(^{i}PrS$_2$N)$_2$-pz**)$_2$(μ-1,1,3-N$_3$)$_2$(μ-1,3-N$_3$)(μ-O$_2$CPh)](ClO$_4$)$_2$ (**238**) were synthesised and structurally characterised (Table 1), revealing that the overall structure of the cation and the central Ni$_4$-core of all three complexes **230**, **233** and **238** is basically identical (Fig. 49) [143]. In 2007 the dinickel(II) complexes [Ni$^{\mathrm{II}}_2$**(S$_2$N)$_2$-pz**(μ-1,3-N$_3$)(OCMe$_2$)]X$_2$ (**239**: X = ClO$_4$; **240**: X = BPh$_4$) and the tetranickel (II) complex [Ni$^{\mathrm{II}}_4$(**(S$_2$N)$_2$-pz**)$_2$(μ-1,1,3-N$_3$)$_2$(MeOH)$_2$](ClO$_4$)$_4$ (**241**) were prepared (Tables 1 and 2) [144]. In **239** and **240** the sixfold coordination geometry of the nickel(II) ions is completed by an intramolecular μ-1,3-N$_3$-bridge and acetone co-ligands, respectively. Compound **241** has only one solvent molecule per dinuclear entity, therefore completion of the sixfold coordination geometry around the nickel(II) ions is achieved by dimerisation through two azide groups to give a tetranuclear species with two μ-1,1,3-N$_3$-bridging units. Complexes **239** and **240** were used for the synthesis of alternating 1D polymeric structures [Ni$^{\mathrm{II}}_2$**(S$_2$N)$_2$-pz**(μ-1,3-N$_3$)$_2$]$_n$(ClO$_4$)$_n$·2nCH$_2$Cl$_2$ (**242**) (space group P2$_1$/*c*; Fig. 51), [Ni$^{\mathrm{II}}_2$**(S$_2$N)$_2$-pz**(μ-1,3-N$_3$)$_2$]$_n$(ClO$_4$)$_n$·2nCH$_2$Cl$_2$ (**243**) (space group *P*2$_1$/*n*) and [Ni$^{\mathrm{II}}_2$**(S$_2$N)$_2$-pz**(μ-1,3-N$_3$)$_2$]$_n$(BPh$_4$)$_n$·0.58nOCMe$_2$ (**244**) (Tables 1 and 2), which can be described as Heisenberg antiferromagnetic systems with inherent bond alternation (HABA). In those chains the μ-1,3-N$_3$-bridged dinuclear subunits are linked *via* additional μ-1,3-N$_3$-bridges to give extended 1D structures

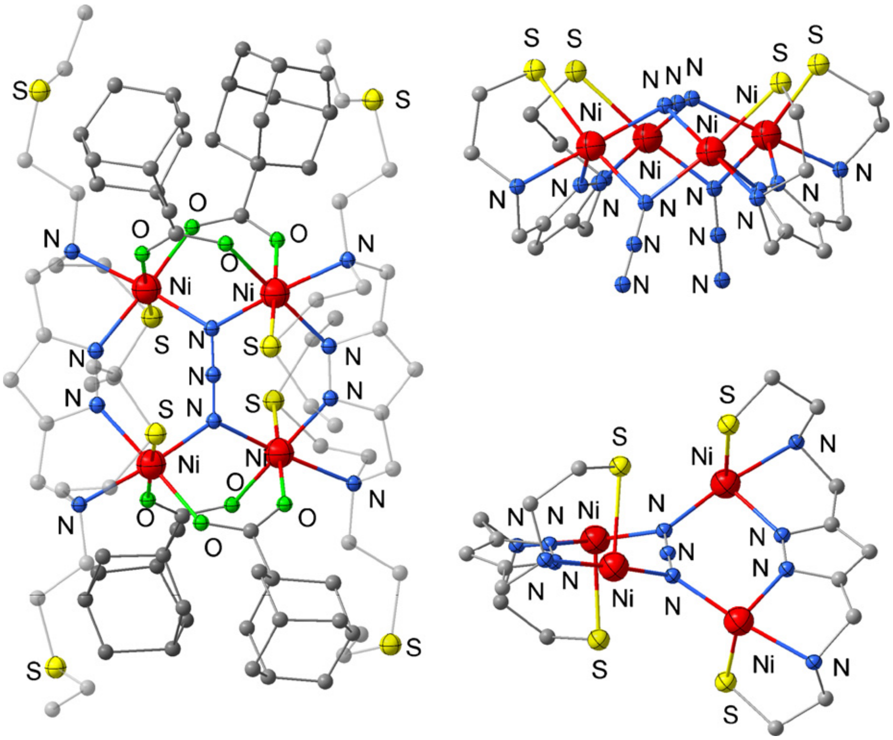

Fig. 50. Molecular structure of the 4:2-type complex cation of [Ni^{II}_4(**(S_2N)$_2$-pz**)$_2$(μ-1,1,3,3-N_3)(μ-O_2C-Ada)$_4$)](ClO_4) (**232**; left) and central Ni_4 cores of **231** (top right) and **232** (bottom right).

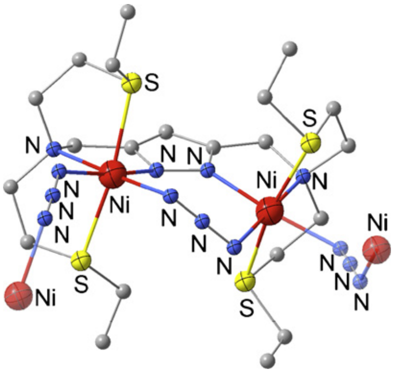

Fig. 51. Section of the molecular structure of the 2:1-type complex cation of [Ni^{II}_2(**(S_2N)$_2$-pz**)(μ-1,3-N_3)$_2$]$_n$(ClO_4)$_n$·2nCH_2Cl_2 (**242**).

[144]. Magnetic properties of those 1D systems were simulated by Quantum Monte Carlo methods. The μ-1,3-N_3-bridged metal ions of the dinickel(II) compound [Ni^{II}_2(**(S_2N)$_2$-pz**)(μ-1,3-N_3)(N_3)$_2$] (**245**; Fig. 52, Tables 1 and 2) complete their distorted octahedral coordination sphere with a terminal azido-co-ligand, respectively [145].

Compound **245** exhibits a thermal hysteresis when measuring $\chi_M T$ as a function of temperature ($\Delta T \approx 13$ K, $T_{\uparrow} = 223$ K). Inspection of the crystal structures above and below the hysteresis temperature reveals significant differences of the Ni–NNN–Ni torsion angle. Since this torsion has a strong effect on the antiferromagnetic coupling, the unusual behaviour can be rationalised on the basis of the crystallographic findings. Complex **245** was thus described as a molecular azide toggle switch, with the azide switch reversibly turning on or off the antiferromagnetic coupling [145].

The unsymmetrically substituted S_2N-pz-N_3-type ligand H**S_2N-pz-N_3** (Scheme 11), which is a close relative of the symmetrical ligands H**(S_2N)$_2$-pz** and H**(N^{Et}_2N)$_2$-pz** was synthesised and 2:1-type nickel(II) complexes of the ligand were isolated and

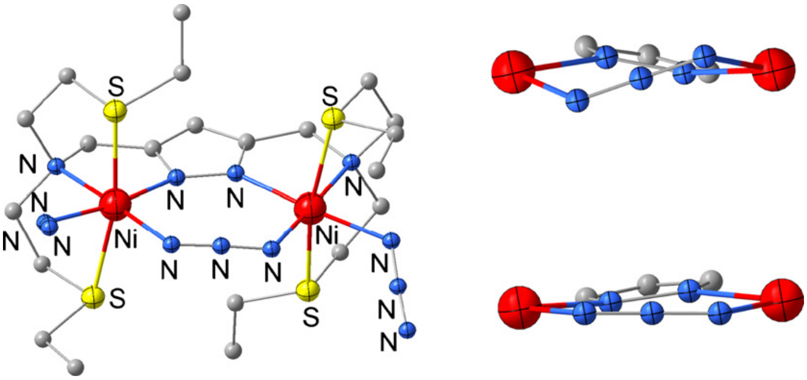

Fig. 52. Molecular structure of the 2:1-type complex [Ni^{II}_2(**(S_2N)$_2$-pz**)(μ-1,3-N_3)(N_3)$_2$] at 133 K (**245**; left) and central core at 253 K (top right) and 133 K (bottom right).

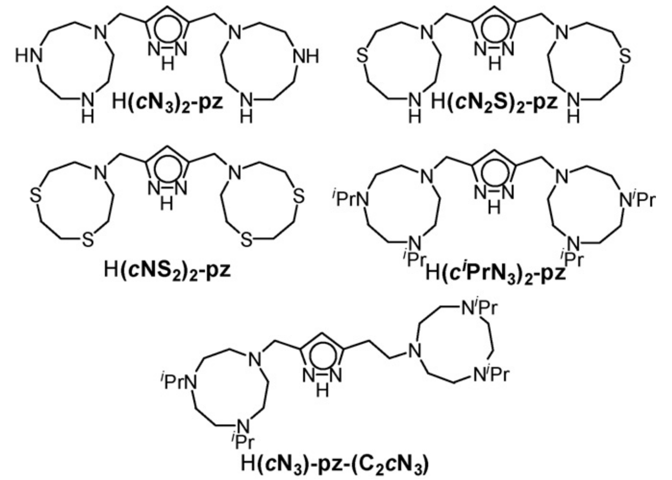

Scheme 12. cD_3-pz-cD_3-type ligands: H(***c*N$_3$**)$_2$**-pz**, H(***c*N$_2$S**)$_2$**-pz**, H(***c*NS$_2$**)$_2$**-pz**, H(***c*^{i}PrN$_3$**)$_2$**-pz** and H(***c*N$_3$**)**-pz-(C$_2$*c*N$_3$)**.

structurally characterised [101,141]. Following the synthesis of the chloro-bridged complexes **154** [132] and **227** [141] of the symmetrically substituted ligands H**(N^{Et}$_2$N)$_2$-pz** and H**(S$_2$N)$_2$-pz**, respectively, the unsymmetrical ligand H**S$_2$N-pz-N$_3$** was reacted with nickel chloride in the presence of base to yield the 2:1-type compound [Ni$^{II}_2$(**S$_2$N-pz-N$_3$**)(μ-Cl)Cl$_2$] (**246**; Table 1). The nickel(II) centres in **246** are located in a distorted $N_2S_2Cl_2$ octahedral geometry with both thioether side arms being coordinated and a distorted N_3Cl_2 square-pyramidal coordination sphere with one amine side arm dangling, respectively. Complex **246** therefore could be described as a mixture of the **(S$_2$N)$_2$-pz**-complex **227**, where all side arms are coordinated to the octahedral nickel(II) centres, and the **(N^{Et}$_2$N)$_2$-pz**-complex **154**, where per ligand half one side arm is dangling and not coordinating to the square-pyramidal nickel(II) centres. Reaction of the unsymmetrical complex **246** with one equivalent of sodium tetraphenylborate induces coordination of the formerly dangling side arm due to displacement of the terminal chloro-ligand and results in the formation of complex [Ni$^{II}_2$(**S$_2$N-pz-N$_3$**)(μ-Cl)Cl](BPh$_4$) (**247**; Table 1) [141]. Also, acetato-bridged complexes having urea or *N*,*N*-dimethyl urea as co-ligands ([Ni$^{II}_2$(**S$_2$N-pz-N$_3$**)(μ-OAc)(OC(NH$_2$)(NR$_2$))](ClO$_4$)$_2$ (R = Me; **248**: R = H), respectively, were isolated (Table 1) [101].

4.3. cD_3-pz-cD_3-type ligands with macrocyclic side arms

Complexes of cD_3-pz-cD_3-type (*c* = cyclic) ligands that bear triazacyclononane [106,146–152] diazathiocyclononane [147,153] or azadithiocyclononane [147] side arms (Scheme 12) have been studied by several groups [146–151,153].

Formally the cD_3-pz-cD_3-type ligands strongly resemble the previously discussed D_3-pz-D_3-type ligands as they too bear three donor atoms in each side arm and hence are potential bis-quadridentate chelating ligands. The major difference between the two types of ligands is the stronger chelating effect of the macrocyclic units that refrain from letting one part of the side arm dangling. The three donor atoms of a cD_3-pz-cD_3-type ligand side arm generally coordinate in a facial geometry.

The first studies of a cD_3-pz-cD_3-type ligand were reported by Kaden and co-workers in 1995, who carried out potentiometric and spectroscopic titration studies of the free ligand H(***c*N$_3$**)$_2$**-pz** and of solutions containing one or two equivalents of copper(II) ions, respectively (Scheme 12) [146]. Later, formation and dissociation kinetic studies of the ligand with copper(II) followed [150]. Potentiometric, spectroscopic and ESI-mass spectrometric studies of the ligand H(***c*N$_2$S**)$_2$**-pz** with copper(II) ions were also carried out (Scheme 12) [153]. The first structure of a cD_3-pz-cD_3-type ligand was the azido-bridged 2:1-type complex [Cu$^{II}_2$(***c*N$_3$**)$_2$**-pz**(μ-1,3-N$_3$)](PF$_6$)$_2$ (**249**; Fig. 53, Table 1) of the triazacyclononane ligand (***c*N$_3$**)$_2$**-pz**$^-$ and was reported in 1995 by Kaden and co-workers [146].

In 1997 the molecular structure of the related μ-1,3-azido-bridged dinickel(II) complex [Ni$^{II}_2$(***c*N$_3$**)$_2$**-pz**(μ-1,3-N$_3$)(H$_2$O)$_2$](ClO$_4$)$_2$ (**250**; Table 1) followed [147].

With the ligands H(***c*N$_2$S**)$_2$**-pz** and H(***c*NS$_2$**)$_2$**-pz** the sulfato-bridged 2:1-type complex [Cu$^{II}_2$(***c*N$_2$S**)$_2$**-pz**(μ-O$_2$SO$_2$)(H$_2$O)](PF$_6$) (**251**) and the chloro- and bromo-bridged dinuclear 2:1-type copper(II) complexes [Cu$^{II}_2$(***c*NS$_2$**)$_2$**-pz**(μ-Cl)](ClO$_4$)$_2$ (**252**) and [Cu$^{II}_2$(***c*NS$_2$**)$_2$**-pz**(μ-Br)](ClO$_4$)$_2$ (**253**) were isolated, respectively (Tables 1 and 2) [147]. Remarkably, the sulfato-bridged complex **251** has two different coordination geometries with different coordination numbers at the copper(II) sites. The coordination geometry of one copper(II) atom is distorted trigonal-bipyramidal with the oxygen atom of the sulfato-bridge at the axial position, whereas the coordination geometry of the other copper(II) atom is distorted octahedral with an additional water co-ligand in the sixth position. In contrast, both the halogeno-bridged complexes **252** and **253** show exclusively distorted trigonal-bipyramidal coordination geometries with the halogeno-bridge occupying an axial site [147].

Given that in such dinuclear complexes the metal centres can coordinate, e.g. azide or sulfate, Kaden and co-workers studied the ability of dinuclear nickel(II) and zinc(II) complexes of (***c*N$_3$**)$_2$**-pz**$^-$ to bind and activate possible substrates, and indeed they found that those complexes are active catalysts for the hydrolysis of phosphate diesters and phosphonate monoesters but do not catalyse the cleavage of phosphate monoester [148]. The mechanism of the hydrolysis of BNPP and (4-nitrophenyl)phenylphosphonate (NPPP) by the dinuclear complexes shows that a dinuclear monohydroxo complex is the active species. It binds the substrate in a pre-equilibrium to form an intermediate in which an intramolecular attack of the coordinated hydroxide ion leads to hydrolysis of the substrate [148]. Thereupon the activity of dinuclear complexes of (***c*N$_3$**)$_2$**-pz**$^-$ against some more biological relevant substrates such as TMPNP (thymidine 5′-monophosphate 4-nitrophenylester) was tested [151]. Furthermore a diphenyl phosphinato-bridged dinuclear copper(II) complex ([Cu$^{II}_2$(***c*N$_3$**)$_2$**-pz**(μ-O$_2$PPh$_2$)](ClO$_4$)$_2$, **254**; Table 1) and a tetranuclear 4:2-type μ_4-phosphato-bridged complex ([Cu$^{II}_4$((***c*N$_3$**)$_2$**-pz**)$_2$(μ_4-O$_4$P)](ClO$_4$)$_3$, **255**; Table 1) was isolated and structurally characterised [149]. A review of the reactivities of some complexes of H(***c*N$_3$**)$_2$**-pz**, H(***c*N$_2$S**)$_2$**-pz** and H(***c*NS$_2$**)$_2$**-pz** was revisualised by Kaden in 1999 [154].

Using the related ligand H(***c*^{i}PrN$_3$**)$_2$**-pz** (Scheme 12) the dinuclear 2:1-type zinc(II) complex [Zn$^{II}_2$(***c*^{i}PrN$_3$**)$_2$**-pz**(μ-OH)](ClO$_4$)$_2$ (**256**; Table 1) [106] was synthesised and studied. The ligand H(***c*^{i}PrN$_3$**)$_2$**-pz** formally evolves by connecting the two terminal nitrogen donors of the N$_3$-pz-N$_3$-type ligand H**(N^{Et}$_2$N)$_2$-pz** with an ethylene linkage. Although the latter ligand readily forms a O$_2$H$_3$-bridged dinuclear zinc(II) complex (**163**), complex **256** of the former ligand features merely a hydroxo-bridge. In contrast, using the same ligand H(***c*^{i}PrN$_3$**)$_2$**-pz** and nickel(II) or copper(II) salts

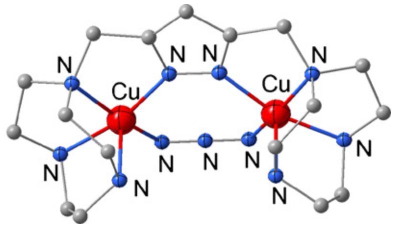

Fig. 53. Molecular structure of the complex cation of the μ-1,3-azido-bridged complex [Cu$^{II}_2$(***c*N$_3$**)$_2$**-pz**(μ-1,3-N$_3$)](PF$_6$)$_2$ (**249**).

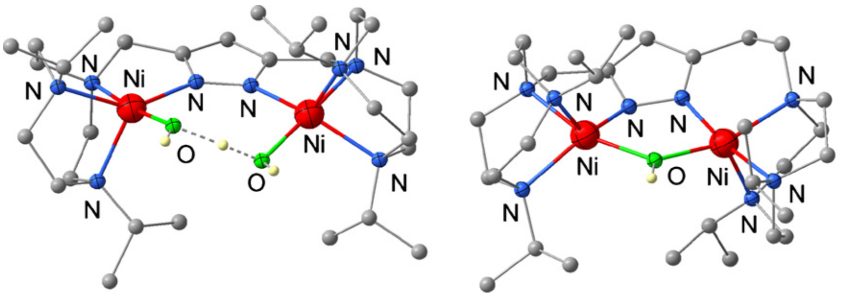

Fig. 54. Molecular structure of the 2:1-type complex cation of [Ni$^{II}_2$**(*c*$^{\boldsymbol{i}}$PrN$_3$)$_2$-pz**(μ-O$_2$H$_3$)](ClO$_4$)$_2$ (**257**; left) and [Ni$^{II}_2$**(*c*N$_3$)-pz-(C$_2$*c*N$_3$)**(μ-OH)](BPh$_4$)$_2$ (**259**; right).

the 2:1-type complexes [Ni$^{II}_2$**(*c*$^{\boldsymbol{i}}$PrN$_3$)$_2$-pz**(μ-O$_2$H$_3$)](ClO$_4$)$_2$ (**257**) [152] and [Cu$^{II}_2$**(*c*$^{\boldsymbol{i}}$PrN$_3$)$_2$-pz**(μ-O$_2$H$_3$)](ClO$_4$)$_2$ (**258**) [113] that feature the longer HOHOH-bridge were isolated (Fig. 54). As a fine tuning of the metal···metal distance by elongation of the ligand side arms is not easily achieved with this type of macrocyclic side arm, it was switched to another strategy to achieve an adjusting of the metal···metal separation. For that matter the new ligand H**(*c*N$_3$)-pz-(C$_2$*c*N$_3$)** that features a longer ligand shoulder was prepared (Scheme 12). Indeed, the hydroxo-bridged 2:1-type complexes [Ni$^{II}_2$**(*c*N$_3$)-pz-(C$_2$*c*N$_3$)**(μ-OH)](BPh$_4$)$_2$ (**259**; Table 1, Fig. 54) [152] and [Cu$^{II}_2$**(*c*N$_3$)-pz-(C$_2$*c*N$_3$)**(μ-OH)](ClO$_4$)$_2$ [113] could be isolated using this strategy.

It has been shown before on the similar complexes **171** and **169** of the related ligands H**(N$^{\mathbf{Et}}$$_2$N)$_2$-pz** and H**(N$^{\mathbf{Me}}$$_2C_3$N)$_2$-pz** with acyclic side arms, respectively, that the O$_2$H$_3$-bridge can readily be exchanged by various substrates, whereas the hydroxo-bridge is quite resistant to substitution. The same trend can be observed comparing the complexes **257** and **259**. For example the reaction of **257** with acetic acid leads to the formation of the acetato-bridged complex [Ni$^{II}_2$**(*c*$^{\boldsymbol{i}}$PrN$_3$)$_2$-pz**(μ-OAc)](BPh$_4$)$_2$ (**260**; Table 1). And whereas no substitution of urea occurs with the hydroxo-bridged complex **259**, the O$_2$H$_3$-bridge of **257** is readily exchanged by urea. Consequently the urea-bridged complex [Ni$^{II}_2$**(*c*$^{\boldsymbol{i}}$PrN$_3$)$_2$-pz**(μ-NHCONH$_2$)](ClO$_4$)$_2$ (**261**) and its derivatives [Ni$^{II}_2$**(*c*$^{\boldsymbol{i}}$PrN$_3$)$_2$-pz**(μ-NHCONHR)](ClO$_4$)$_2$ (**262**: R = Ph; **263**: R = CH$_2$Ph) could be isolated (Table 1) [152]. All three complexes feature deprotonated *N*,*O*-bridging urea derivatives. Under standard conditions no hydrolytic degradation of the urea in **261** could be achieved. However, since carbamate bound to the nickel ions is assumed as an intermediate in the urease mechanism, the *in situ* preparation of a carbamate complex was persecuted and the complex [Ni$^{II}_2$**(*c*$^{\boldsymbol{i}}$PrN$_3$)$_2$-pz**(μ-O$_2$CNH$_2$)](ClO$_4$)$_2$ (**264**) could be isolated (Table 1, Fig. 55) [152].

When samples of the urea-bridged complexes **261**, **262** or **263** were heated to high temperatures a complex could be isolated that, by comparison with *in situ* prepared samples, was identified as the cyanato-bridged complex [Ni$^{II}_2$**(*c*$^{\boldsymbol{i}}$PrN$_3$)$_2$-pz**(μ-OCN)](ClO$_4$)$_2$ [152]. A different cyanate-species, namely [Ni$^{II}_2$**(*c*$^{\boldsymbol{i}}$PrN$_3$)$_2$-pz**(μ-OCN)(NCO)](ClO$_4$) (**265**), could also be isolated using potassium cyanate, instead of the sodium salt used for the former complex (Table 1) [152]. In **265** a cyanato-bridge spans the two nickel(II) ions in the expected fashion, but a second cyanate ion is coordinated with the nitrogen donor to the nickel(II) atom that binds the oxygen atom of the bridge to yield an octahedral environment for the respective nickel(II) ion. Since intermediate formation and subsequent hydrolysis of cyanate has been proposed as an alternative model for the mechanism of urease, the solvolytic reactivity of the cyanate complexes was investigated and a 2:1-type dinickel(II) carbamate complex ([Ni$^{II}_2$**(*c*$^{\boldsymbol{i}}$PrN$_3$)$_2$-pz**(μ-NHCOOMe)](ClO$_4$)$_2$, **266**; Table 1) independently synthesised as a putative initial product resulting from nucleophilic attack of methanol on the cyanato-bridge (Table 1) [152].

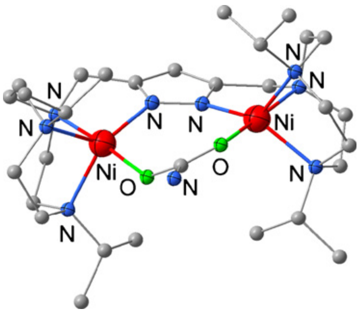

Fig. 55. Molecular structure of the 2:1-type complex cation of [Ni$^{II}_2$**(*c*$^{\boldsymbol{i}}$PrN$_3$)$_2$-pz**(μ-O$_2$CNH$_2$)](ClO$_4$)$_2$ (**264**).

Testing for catecholase activity, compounds **258** and [Cu$^{II}_2$**(*c*N$_3$)-pz-(C$_2$*c*N$_3$)**(μ-OH)](ClO$_4$)$_2$ were reacted with DTBC and the activities were compared with results obtained by using the related 2:1-type copper(II) complexes **113**, [Cu$^{II}_2$**(N$^{\mathbf{Me}}$C$_3$N$^{\mathbf{Me}}$)$_2$-pz**(μ-OH)(MeOH)$_2$](ClO$_4$)$_2$, **192** and **193** [113]. Summary of those results confirmed previous observations that shorter copper···copper distances are advantageous for high catecholase activity [104]. Additionally it was found that the redox potential of the respective compound plays an important role, as the activity is greatly diminished when the complex has a potential below a certain threshold value ($E_\mathrm{p}{}^\mathrm{Red}$ = −0.8 V versus Cp$_2$Fe$^+$/Cp$_2$Fe) [113].

5. Macrocyclic pyrazolate-based ligands

Macrocyclic pyrazolate-based ligands have mainly been studied by Navarro and co-workers. In principle they can be divided into two groups, according to their head unit-to-pyrazole unit ratio. A ratio of 2:2 is given in the ligands H$_4$**[N(N=C)$_2$-pz]$_{\mathbf{2m}}$**, H$_2$**[O(N=C)$_2$-pz]$_{\mathbf{2m}}$**, H$_8$**(NN$_2$-pz)$_{\mathbf{2m}}$**, H$_6$**(ON$_2$-pz)$_{\mathbf{2m}}$**, H$_8$**[N(NC$_3$)$_2$-pz]$_{\mathbf{2m}}$**, H$_2$**(OO$_2$-pz)$_{\mathbf{2m}}$**, H$_6$**(N$_2$-pz)$_{\mathbf{2m}}$** and H$_2$**[(N=C)$_2$-pz]$_{\mathbf{2m}}$** [155–158] whereas a 2:3-ratio is given in the cryptand ligands H$_3$**N$_2$[(N=C)$_2$-pz]$_{\mathbf{3m}}$** and H$_9$**N$_2$(N$_2$-pz)$_{\mathbf{3m}}$** (Scheme 13) [159–161].

As early as 1993, the synthesis of the Schiff-Base macrocyclic pyrazolate based ligands H$_4$**[N(N=C)$_2$-pz]$_{\mathbf{2m}}$** and H$_2$**[O(N=C)$_2$-pz]$_{\mathbf{2m}}$** along with the respective reduced species H$_8$**(NN$_2$-pz)$_{\mathbf{2m}}$** and H$_6$***m*(N$_2$O)$_2$-pz** (Scheme 13) was reported [155]. Using the latter two amine based ligand species, the formation of symmetrical dinuclear zinc(II) complexes of the doubly deprotonated pyrazolate ligands was detected by NMR spectroscopy [155]. Following those reports the authors described the isolation of dinuclear copper(II) complexes of the ligands H$_2$**[O(N=C)$_2$-pz]$_{\mathbf{2m}}$** and H$_8$**(NN$_2$-pz)$_{\mathbf{2m}}$** and reported the first molecular structure of a transition metal complex of such a macrocyclic ligand [156]. The dinuclear compound [Cu$^{II}_2$H$_6$**(NN$_2$-pz)$_{\mathbf{2m}}$**](ClO$_4$)$_2$ (**267**; Table 1, Fig. 56), features a pseudo 2:2-type arrangement with doubly pyrazolato-bridged distorted square-pyramidally coordinated copper(II) ions. The nitrogen atoms located in the middle of the flexible

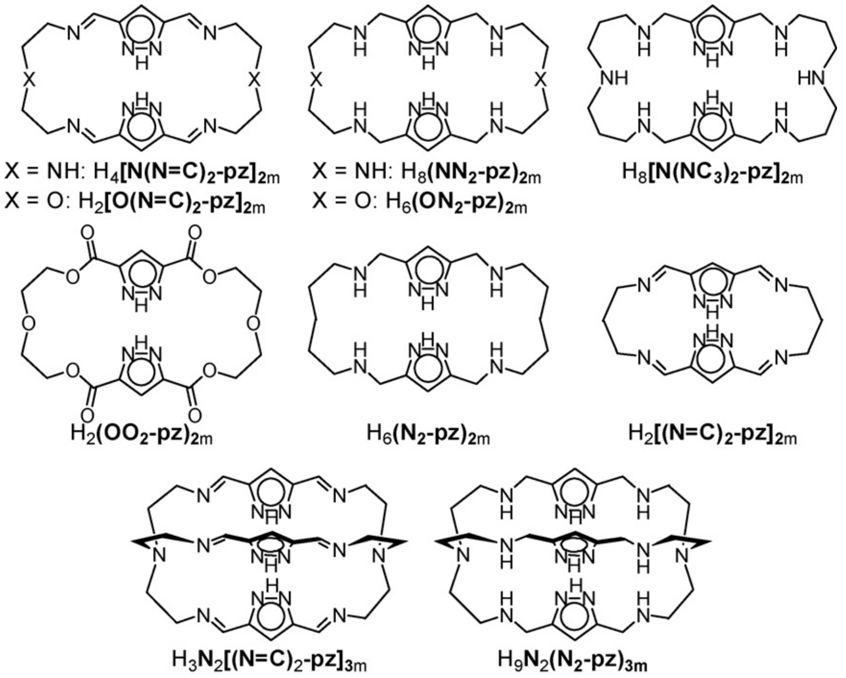

Scheme 13. Macrocyclic pyrazolate based ligands: $H_4\mathbf{[N(N{=}C)_2\text{-}pz]_{2m}}$, $H_2\mathbf{[O(N{=}C)_2\text{-}pz]_{2m}}$, $H_8\mathbf{(NN_2\text{-}pz)_{2m}}$, $H_6\mathbf{(ON_2\text{-}pz)_{2m}}$, $H_8\mathbf{[N(NC_3)_2\text{-}pz]_{2m}}$, $H_2\mathbf{(OO_2\text{-}pz)_{2m}}$, $H_6\mathbf{(N_2\text{-}pz)_{2m}}$, $H_2\mathbf{[(N{=}C)_2\text{-}pz]_{2m}}$, $H_3\mathbf{N_2[(N{=}C)_2\text{-}pz]_{3m}}$ and $H_9\mathbf{N_2(N_2\text{-}pz)_{3m}}$.

chains occupy the apexes of the copper(II) ions in a *cis*-manner [156].

Later, the molecular structures of the dinuclear complexes $[Zn^{II}_2H_6\mathbf{(NN_2\text{-}pz)_{2m}}](ClO_4)_2$ (**268**), $[Cu^{II}_2H_6\mathbf{[N(NC_3)_2\text{-}pz]_{2m}}](ClO_4)_2$ (**269**; Tables 1 and 2) and $[Zn^{II}_2H_6\mathbf{[N(NC_3)_2\text{-}pz]_{2m}}](ClO_4)_2$ (**270**; Table 1) were reported [162]. Square planar copper(II) ions are present in compound $[Cu^{II}_2H_8\mathbf{[N(NC_3)_2\text{-}pz]_{2m}}](ClO_4)_4{\cdot}2H_2O$ where the central nitrogen atoms of the bridging chains are protonated and therefore uncoordinated (Table 2) [162].

The synthesis of the tetraester crown compound $H_2\mathbf{(OO_2\text{-}pz)_{2m}}$ (Scheme 13) and NMR complexation studies with zinc(II) salts were performed in 1994 [157].

Another type of 2:2-macrocyclic ligand, without donor atoms in the middle of the flexible chain, namely $H_6\mathbf{(N_2\text{-}pz)_{2m}}$ that contains 1,5-diaminopentane spacers, was only reported in 2004 [158]. A tetranuclear pseudo 4:4-type dimeric copper(II) complex $[Cu^{II}_4(H_4\mathbf{(N_2\text{-}pz)_{2m}})_2(H_2O)_2(ClO_4)_2](ClO_4)_2$ (**271**) was isolated and structurally characterised (Fig. 57, Table 1) [158].

The centrosymmetric complex cation of **271** consists of a tetranuclear copper(II) complex and comprises two macrocyclic ligands $H_4\mathbf{(N_2\text{-}pz)_{2m}}^{2-}$. Each pyrazole end of a ligand coordinates to two copper(II) ions, which are additionally pyrazolato-bridged by a pyrazole end of a second macrocyclic ligand. In this way a cage-like structure is formed. Construction of a polyhedron by linking the secondary nitrogen atoms of the ligands leads to dimensions of $7.555 \times 6.583 \times 3.214$ Å^3 for the cage [158]. The macrocyclic Schiff-base ligand $H_2\mathbf{[(N{=}C)_2\text{-}pz]_{2m}}$ was prepared *in situ* by Brooker and co-workers and was isolated in form of its dinuclear copper(II) complexes $[Cu^{II}_2\mathbf{[(N{=}C)_2\text{-}pz]_{2m}}(OAc)_2]$ (**272**) and $[Cu^{II}_2\mathbf{[(N{=}C)_2\text{-}pz]_{2m}}(NCS)_2]$ (**273**) (Tables 1 and 2) [115].

The synthesis of the first pyrazolate based cryptand-type ligands $H_3\mathbf{N_2[(N{=}C)_2\text{-}pz]_{3m}}$ and $H_9\mathbf{N_2(N_2\text{-}pz)_{3m}}$ along with the preparation of some di- and tetranuclear complexes of silver(I), copper(II) and zinc(II) were reported in 1995 [159], but the first structure of a transition metal complex of a pyrazolate cryptand ligand was only reported in 2000 and 2001 [160,161]. Compound $[Cu^{II}_2H_8\mathbf{N_2(N_2\text{-}pz)_{3m}}](ClO_4)_3{\cdot}2H_2O$ (**274**) is a dinuclear pseudo 2:2-type complex with doubly pyrazolato-bridged metal ions (Fig. 58, Table 1) [160,161].

The non-coordinating pyrazole unit is protonated, as is one of the non-coordinating aliphatic nitrogen donor atoms. A water molecule is placed in the cavity formed between the non-coordinating pyrazole unit and the pseudo 2:2-type complex base, hydrogen bonded to the protonated aliphatic nitrogen and the non-protonated pyrazole nitrogen of the non-coordinating bridge [160,161]. As the cavity

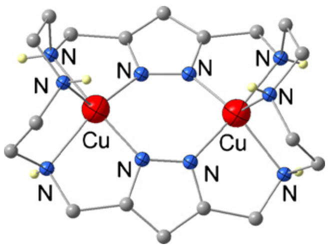

Fig. 56. Molecular structure of the 2:2-type complex cation of $[Cu^{II}_2H_6\mathbf{(NN_2\text{-}pz)_{2m}}](ClO_4)_2$ (**267**).

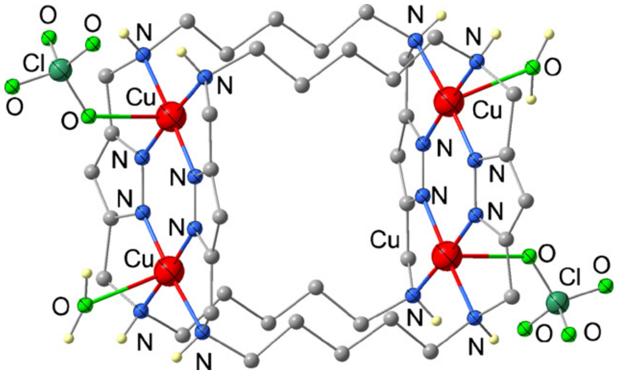

Fig. 57. Molecular structure of the complex cation of $[Cu^{II}_4(H_4\mathbf{(N_2\text{-}pz)_{2m}})_2(H_2O)_2(ClO_4)_2](ClO_4)_2$ (**271**).

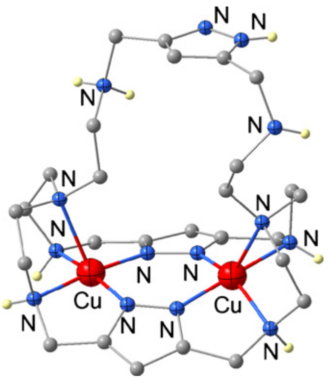

Fig. 58. Molecular structure of the complex cation of the pseudo 2:2-type cryptate $[\mathrm{Cu^{II}}_2\mathrm{H_8}\mathbf{N_2(N_2\text{-}pz)_{3m}}](\mathrm{ClO_4})_3\cdot 2\mathrm{H_2O}$ (**274**).

is obviously large enough to accommodate substrate molecules, the interaction of the free ligand $\mathrm{H_9}\mathbf{N_2(N_2\text{-}pz)_{3m}}$ and the pseudo 2:2-type complex **274** with the substrate dopamine has been analysed, and it has been found that in both cases stable complexes with the receptor are formed [160]. Furthermore the stability constants for the interactions of the free ligand $\mathrm{H_9}\mathbf{N_2(N_2\text{-}pz)_{3m}}$ with copper(II) [161] and the voltammetric behaviour of copper(II) complexes of $\mathrm{H_9}\mathbf{N_2(N_2\text{-}pz)_{3m}}$ and $\mathrm{H_6}\mathbf{(NN_2\text{-}pz)_{2m}}$ in aqueous solutions have been studied [163].

6. Unsymmetrical pyrazolate ligands

In dinuclear catalysis, in nature and in synthetic systems, the individual metal ions are often assumed to play distinct roles. The use of unsymmetrical instead of symmetrical bis-polydentate ligands, in principle, opens a way to unsymmetrical homo- or heterodinuclear systems, which as a consequence are highly desirable.

Pyrazolate based unsymmetrical ligands of the type P-pz-$\mathrm{N_2}$ and P-pz$\mathrm{NS_2}$ were used to synthesise dinuclear nickel(II)- and nickel(II)/palladium(II) complexes (Scheme 14) [164].

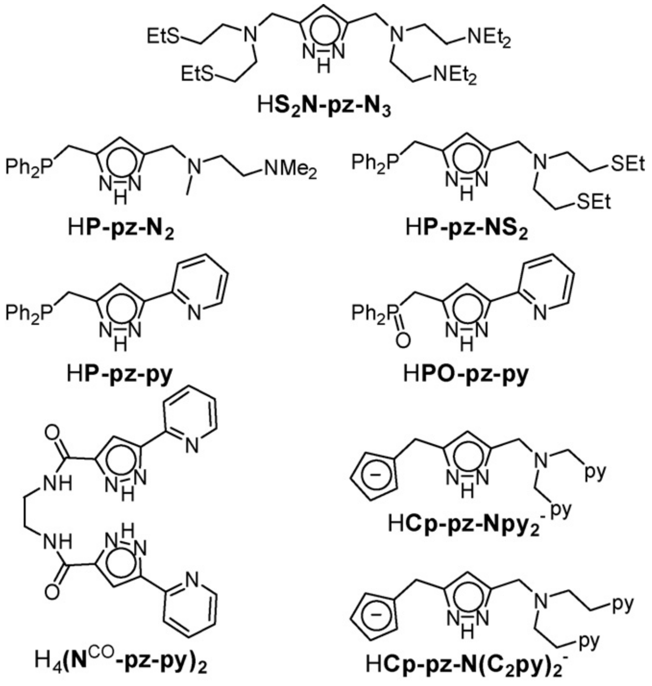

Scheme 14. Unsymmetrical $\mathrm{D^1}$-pz-$\mathrm{D^2}$-type pyrazolate ligands: H$\mathbf{S_2N\text{-}pz\text{-}N_3}$, H**P-pz-**$\mathbf{N_2}$, H**P-pz-**$\mathbf{NS_2}$, H**P-pz-py**, H**PO-pz-py**, $\mathrm{H_4}\mathbf{(N^{CO}\text{-}pz\text{-}py)_2}$, H**Cp-pz-**$\mathbf{Npy_2}^-$ and H**Cp-pz-**$\mathbf{N(C_2py)_2}^-$.

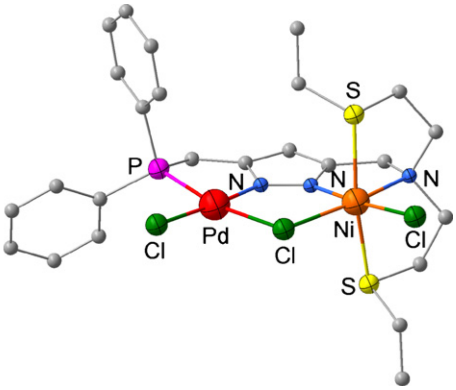

Fig. 59. Molecular structure of the 2:1-type complex $[\mathrm{Pd^{II}Ni^{II}}\mathbf{P\text{-}pz\text{-}NS_2}(\mu\text{-Cl})\mathrm{Cl_2}]$ (**277a**).

The dinuclear unsymmetrical complexes $[\mathrm{Ni^{II}}_4(\mathbf{P\text{-}pz\text{-}N_2})_2(\mu\text{-Cl})_4\mathrm{Cl_2}]$ (**275**) and $[\mathrm{Ni^{II}}_2\mathbf{P\text{-}pz\text{-}NS_2}(\mu\text{-Cl})\mathrm{Cl_2}]$ (**276**) form in a 1:2:1 mixture of the respective ligand to nickel(II) salt to base (Table 1). When first treating deprotonated ligand $\mathbf{P\text{-}pz\text{-}NS_2}^-$ with palladium(II) and only afterwards with nickel(II), complex $[\mathrm{Pd^{II}Ni^{II}}\mathbf{P\text{-}pz\text{-}NS_2}(\mu\text{-Cl})\mathrm{Cl_2}]$ (**277a**, **277b**) forms (Table 1, Fig. 59), the heterodinuclear analogous of **276** [164].

All complexes **275**–**277** have metal centres in different coordination environments. In each compound the bidentate P-pz-half of the unsymmetrical ligand coordinates in an equatorial fashion to the distorted square-planar coordinated metal ion (nickel(II) for **275** and **276**, palladium(II) for **277**). The remaining positions are occupied by a terminal and a metal···metal-bridging chloro-co-ligand, respectively. The other metal ion, nickel(II) in all three complexes, resides in a distorted octahedral geometry. In **275** the terdentate $\mathrm{N_2}$-pz half of the ligand binds facially to the metal centre. The two remaining coordination sites are occupied by two chloro-bridges that coordinate to a second dinuclear $[\mathrm{Ni^{II}}_2(\mathbf{P\text{-}pz\text{-}N_2})(\mu\text{-Cl})\mathrm{Cl}]^+$-unit, thus forming a tetranuclear dimeric compound. The terdentate $\mathrm{S_2N}$-side arm of both the compounds **276** and **277** coordinates meridionally to the nickel(II) ion, leaving an equatorial position for a chloro-co-ligand, respectively [164].

A similar P-pz-N-type ligand, namely H**P-pz-py**, was used by Dubs et al. [79,165], who also isolated its homodinuclear palladium(II) complex $[\mathrm{Pd^{II}}_2(\mathbf{P\text{-}pz\text{-}py})(\eta^3\text{-allyl})_2](\mathrm{BF_4})$ (**278**; Table 1, Fig. 60) [79].

Also, with this ligand mononuclear iridium(I) complexes can be obtained in which depending on the degree of protonation either the P-pz- or the py-pz-half of the ligand is occupied. In compound $[\mathrm{Ir^I}\mathrm{H}\mathbf{P\text{-}pz\text{-}py}(\mathrm{COD})](\mathrm{BF_4})$, which was later shown to be a dimeric species [79], the ligand coordinates with the py-pz ligand half, whereas in complex $[\mathrm{Ir^I}\mathbf{P\text{-}pz\text{-}py}(\mathrm{COD})]$ (**279**) the iridium(I) ion is imbedded in the P-pz-half of the ligand (Table 1, Fig. 61) [79,165].

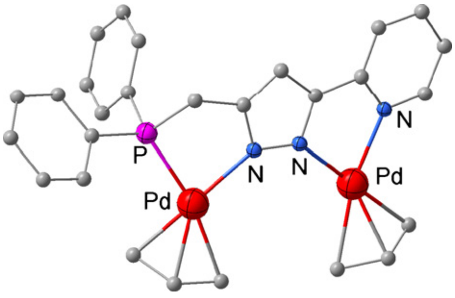

Fig. 60. Molecular structure of the 2:1-type complex cation of $[\mathrm{Pd^{II}}_2(\mathbf{P\text{-}pz\text{-}py})(\eta^3\text{-allyl})_2](\mathrm{BF_4})$ (**278**).

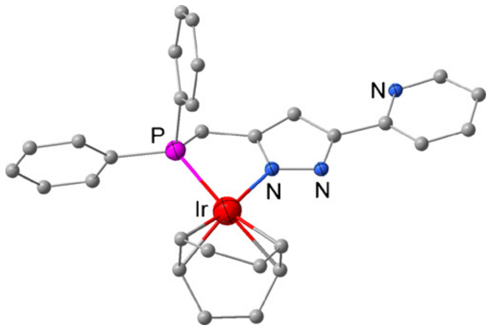

Fig. 61. Molecular structure of the 1:1-type complex [Ir^{I}**P-pz-py**(COD)] (**279**).

Therefore, by first adding another labile metal component [M(L)(COD)]BF$_4$ (M(L) = Pd(η^3-allyl), Rh(η^4-COD) before adding a base, the compounds [Pd^{II}(η^3-allyl)**P-pz-py**Ir^{I}(COD)](BF$_4$) (**280**) [79,165] and [Rh^{I}(η^4-COD)**P-pz-py**Ir^{I}(COD)](BF$_4$) are formed, where the iridium(I) ion is coordinated by the py-pz-half of the ligand, respectively. Instead, by simply reversing the order of addition of base and second metal ion, compounds [Ir^{I}(COD)**P-pz-py**Pd^{II}(η^3-allyl)](BF$_4$) (**281**) [79,165] and [Ir^{I}(COD)**P-pz-py**Rh^{I}(COD)](BF$_4$) (**282**) [79] are formed, where the iridium(I) ion is coordinated by the P-pz-half of the ligand, respectively (Table 1). Of those complexes **280**, **281** and **282** have been structurally characterised [79,165]. Conversion of the labile COD-complexes into the respective carbonyl complexes has also been carried out [80]. In the course of those studies the homodinuclear compounds [Rh$^{I}_2$**P-pz-py**(CO)$_4$](BF$_4$) (**283**; Table 1) and [Ir$^{I}_2$**P-pz-py**(CO)$_4$](BF$_4$), as well as the heterodinuclear compounds [Rh^{I}(CO)$_2$**P-pz-py**Ir^{I}(CO)$_2$](BF$_4$) and [Ir^{I}(CO)$_2$**P-pz-py**Rh^{I}(CO)$_2$](BF$_4$), where the rhodium (iridium) metal ion is once coordinated by the P-pz-half (py-pz-half) of the ligand and once by the py-pz-half (P-pz-half) of the ligand, were isolated. The dinuclear rhodium(I) compound **283** could be structurally characterised and it has been found that it cocrystallises with the P-oxidised species [Rh$^{I}_2$**PO-pz-py**(CO)$_4$](BF$_4$) (**284**) (for H**PO-pz-py** see Scheme 14). Also the palladium(II) isomers [Ir^{I}(CO)$_2$**P-pz-py**Pd^{II}(η^3-allyl)](BF$_4$) and [Pd^{II}(η^3-allyl)**P-pz-py**Ir^{I}(CO)$_2$](BF$_4$) (**285**; Table 1) were isolated. The latter complex **285**, were the palladium is imbedded in the P-pz-half of the ligand, was structurally characterised [80]. Conversions of the labile COD-complexes, with acetylides lead to the isolation of the Me$_3$Si-C≡C-bridged complex [Rh^{I}(CO)**P-pz-py**Rh^{I}(μ-Me$_3$Si-C≡C)(CO)] (**286**; Table 1) and the *p*-tol-C≡C-bridged compounds [Rh^{I}(CO)**P-pz-py**Rh^{I}(μ-*p*-tol-C≡C)(CO)] and [Rh^{I}(CO)**P-pz-py**Ir^{I}(μ-*p*-tol-C≡C)(CO)], whereas a corresponding homonuclear iridium(I) compound and a heterodinuclear iridium(I)–rhodium(I) compound with a P-bound iridium(I) metal ion could not be isolated [80].

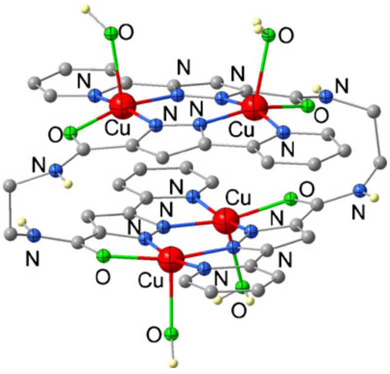

Fig. 63. Molecular structure of the tetranuclear complex cation of the copper(II) complex [Cu$^{II}_4$(H$_2$(**N^{CO}-pz-py)$_2$**)$_2$(H$_2$O)$_4$](NO$_3$)$_4$·5.5H$_2$O (**289**).

Another type of unsymmetrical ligand containing two pyrazole units was used by Krämer et al. [166]. The amide-based ligand H$_4$(**N^{CO}-pz-py)$_2$** forms mononuclear compounds [M^{II}(**N^{CO}-pz-py)$_2$**]$^{2-}$ (M = Cu [166], Ni [166], Pd [167], Pt [167]) after deprotonation with four equivalents of base and subsequent addition of one equivalent of metal salt. Both amide functions of the ligand are deprotonated and *N*-coordinating, respectively, leading to an in-plane metal coordination of the N-pz ligand halfs and leaving both the pz-py coordination pockets vacant. Dimeric tetranuclear copper(II) and nickel(II) complexes are obtained by adding a second equivalent of the respective metal salt to solutions of the mononuclear compounds [M^{II}(**N^{CO}-pz-py)$_2$**]$^{2-}$ (M = Cu, Ni) [166]. The molecular structures of the compounds [Ni$^{II}_4$(H$_2$(**N^{CO}-pz-py)$_2$**)$_2$(DMSO)$_6$(NO$_3$)(H$_2$O)](NO$_3$)$_3$·H$_2$O·3DMSO·OCMe$_2$ (**287**) (Fig. 62), [Cu$^{II}_4$(H$_2$(**N^{CO}-pz-py)$_2$**)$_2$(DMSO)$_2$(EtOH)$_2$](picrate)$_4$ (**288**) and [Cu$^{II}_4$(H$_2$(**N^{CO}-pz-py)$_2$**)$_2$(H$_2$O)$_4$](NO$_3$)$_4$·5.5H$_2$O (**289**) (Fig. 63) have been determined (Table 1) [166].

Although each complex **287**–**289** comprises two ligand threads, which provide the pyrazole and the pyridine nitrogen atoms as well as the amide oxygen donor atoms for in-plane coordination of four metal ions, the molecular structures of the tetranuclear compounds are fundamentally different. In the nickel(II) compound **287** two ligands are sprawled and arranged in a side-by-side manner, so that the four nickel(II) centres are arranged linearly in two decks which are linked in a stair-like fashion by the NH–(CH$_2$)$_2$–NH groups of the two ligands. The equatorial environment for the nickel(II) ions therefore is N$_4$ for the terminal and N$_2$O$_2$ for the central metal centres (Fig. 62). In contrast, in **288** and **289** the ligand threads find themselves in a wrapped double helicated conformation, which is stabilised by loose interligand py···pz and py···py off-set stacking interactions. As a consequence all metal ions are in the same equatorial N$_3$O environment [166].

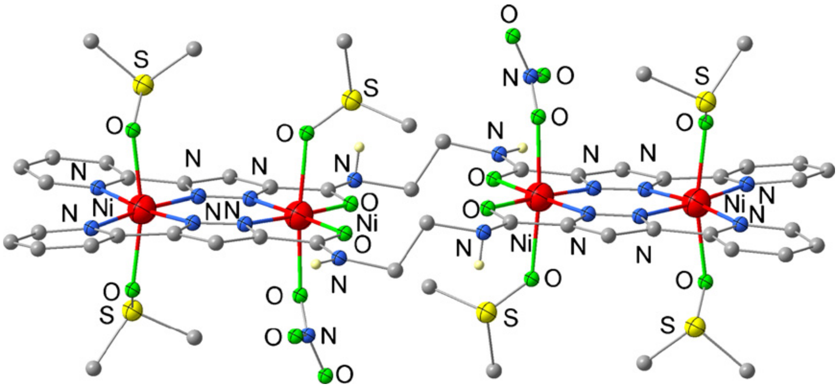

Fig. 62. Molecular structure of the tetranuclear complex cation of the nickel(II) complex [Ni$^{II}_4$(H$_2$(**N^{CO}-pz-py)$_2$**)$_2$(DMSO)$_6$(NO$_3$)(H$_2$O)](NO$_3$)$_3$·H$_2$O·3DMSO·OCMe$_2$ (**287**).

Addition of copper(II) salts to solutions of the mononuclear complexes [M^{II}**(N^{CO}-pz-py)$_2$**]$^{2-}$ (M = Pt, Pd) result in the formation of di- and trinuclear complexes, respectively, of which the trinuclear complex [Cu^{II}$_2$Pd**(N^{CO}-pz-py)$_2$**(μ-OH)(μ-OAc)] (**290**) was structurally characterised (Table 1) [167]. In complex **290** the formerly vacant py-pz coordination pockets of the mononuclear precursor compound are occupied by a square-planar coordinated copper(II) ion, respectively [167]. Additionally *in situ* prepared copper(II) complexes of the precursor compounds [M^{II}**(N^{CO}-pz-py)$_2$**]$^{2-}$ (M = Pt, Pd) have been studied as catalysts for the cleavage of HPNP (2-hydroxypropyl-*p*-nitrophenyl phosphate). The cleavage rates at 0–1 added equivalents of copper(II) are very low in both cases. Further additions of copper(II) salts do not increase the activity of the platinum(II) complex, but that of the palladium complex [167].

The mixed ligand systems H**Cp-pz-Npy$_2$**$^-$ and H**Cp-pz-N(C$_2$py)$_2$**$^-$ were synthesised to provide an organometallic and a Werner-type subunit [168–171]. The ligands were isolated as their manganese(I) complexes [Mn^I(CO)$_3$H**Cp-pz-Npy$_2$**] [168] and [Mn^I(CO)$_3$H**Cp-pz-N(C$_2$py)$_2$**] [169]. Several hetero- and homodinuclear complexes of **Cp-pz-Npy$_2$$^{2-}$** with zinc(II) [168], cobalt(II) [171], nickel(II) [172] and manganese(II) [170] and heterodinuclear complexes of H**Cp-pz-N(C$_2$py)$_2$$^{2-}$** with zinc(II) [169], cobalt(II) [171] and nickel(II) [172] have been isolated and structurally characterised. Syntheses of the dinuclear compounds start with irradiation of the precursor complexes [Mn^I(CO)$_3$H**Cp-pz-Npy$_2$**] and [Mn^I(CO)$_3$H**Cp-pz-N(C$_2$py)$_2$**], respectively, which leads to the loss of a CO-co-ligand and coordination of the manganese ion to the pyrazole moiety. Addition of one equivalent of base to the *in situ* prepared compound [Mn^I(CO)$_2$H**Cp-pz-Npy$_2$**], followed by zinc chloride or acetate or cobalt or nickel nitrate results in the formation of the heterodinuclear complexes [Mn^I(CO)$_2$**Cp-pz-Npy$_2$**Zn^{II}(Cl)] (**291**) [168], [Mn^I(CO)$_2$**Cp-pz-Npy$_2$**Zn^{II}(OAc)]·DMF·H$_2$O (**292**) [169], [Mn^I(CO)$_2$**Cp-pz-Npy$_2$**Ni^{II}(NO$_3$)]·DMF (**293**) [172] and [Mn^I(CO)$_2$**Cp-pz-Npy$_2$**Co^{II}(NO$_3$)]·Et$_2$O (**294**), respectively [171]. Similarly the use of manganese(II) chloride, bromide, acetate and perchlorate results in the formation of the dinuclear compounds [Mn^I(CO)$_2$**Cp-pz-Npy$_2$**Mn^{II}(Cl)] (**295**), [Mn^I(CO)$_2$**Cp-pz-Npy$_2$**Mn^{II}(Br)(DMF)] (**296**), [Mn^I(CO)$_2$**Cp-pz-Npy$_2$**Mn^{II}(OAc)] (**297**) and [Mn^I(CO)$_2$**Cp-pz-Npy$_2$**Mn^{II}(DMF)$_2$](ClO$_4$) (**298**), respectively [170]. The bivalent metal ions of **291**–**298** each are nested within the quadridentate coordination pocket of the pz-py$_2$-half of the ligand. With the exception of **294** where the binding situation of the cobalt(II) centre is best described as {5 + 1} coordination, the metal(II) centres are either distorted trigonal-bipyramidally coordinated (**291**, **292**, **295**) or reside in a distorted octahedral geometry (**296**–**298**). Using the *in situ* prepared precursor complex [Mn^I(CO)$_2$H**Cp-pz-N(C$_2$py)$_2$**] of the ligand with the longer py$_2$ side arm, and zinc perchlorate or acetate, or cobalt nitrate or acetate, or nickel nitrate or acetate, the heterodinuclear compounds [Mn^I(CO)$_2$**Cp-pz-N(C$_2$py)$_2$**Zn^{II}(OAc)] (**299**), [Mn^{II}(CO)$_2$**Cp-pz-N(C$_2$py)$_2$**Zn^{II}](ClO$_4$) (**300**) [169], [Mn^I(CO)$_2$**Cp-pz-N(C$_2$py)$_2$**Co^{II}(NO$_3$)]·0.5Et$_2$O (**301**) and [Mn^I(CO)$_2$**Cp-pz-N(C$_2$py)$_2$**Co^{II}(OAc)]·0.5Et$_2$O (**302**) [171], [Mn^I(CO)$_2$**Cp-pz-N(C$_2$py)$_2$**Ni^{II}(NO$_3$)] (**303**) and [Mn^I(CO)$_2$**Cp-pz-N(C$_2$py)$_2$**Ni^{II}(OAc)] (**304**) [172] are obtained, respectively (Table 1). The acetate compound **299** differs from its lower homologue **292**, as the coordination mode of the acetato co-ligand is unidentate in the latter compound, whereas it is chelating bidentate in the former compound, which therefore features an octahedrally coordinated zinc(II) ion. A similar coordination sphere with bidentate coordinating co-ligands is found for the cobalt(II) ions in the nitrato compound **301** and the acetato complex **302** (Figs. 64 and 65), as well as in the corresponding nickel complexes **303** and **304**. The perchlorate compound **300** on the other hand features distorted tetrahedral coordinated zinc(II) ions without coordination of further co-ligands [169]. IR and UV–vis spectroelectrochemistry on the manganese(I)–cobalt(II) compounds **294**, **301** and **302** as well as the manganese(I)–nickel(II) compounds **293**, **303** and **304** reveals that oxidation of the heterobimetallic system is highly localised at the organometallic manganese site, while electrochemical reduction occurs at cobalt or nickel [171,172].

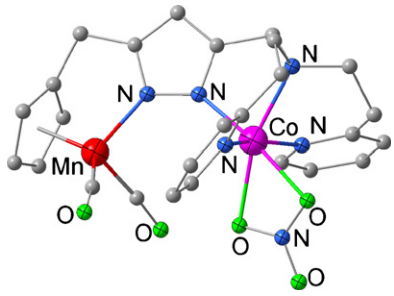

Fig. 64. Molecular structure of the 2:1-type complex molecule of [Mn^I(CO)$_2$**Cp-pz-N(C$_2$py)$_2$**Co^{II}(NO$_3$)]·0.5Et$_2$O (**301**).

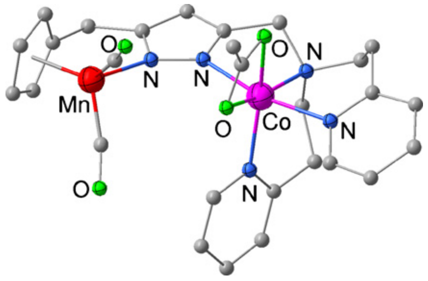

Fig. 65. Molecular structure of the 2:1-type complex molecule of [Mn^I(CO)$_2$**Cp-pz-N(C$_2$py)$_2$**Co^{II}(OAc)]·0.5Et$_2$O (**302**).

Acknowledgements

Work from the group of F.M. mentioned in this review has been generously supported by the DFG and the Fonds der Chemischen Industrie. Financial support to J.K. by the Schlieben-Lange program (Ministry of Science, Research and the Arts Baden-Württemberg and European Social Fund) is gratefully acknowledged. F.M. thanks all his co-workers involved in pyrazolate chemistry for their dedication. J.K. thanks Prof. Dr. Ingo Krossing and Prof. Dr. Harald Hillebrecht for their generous and continuous support.

References

[1] B. Bosnich, Inorg. Chem. 38 (1999) 2554.
[2] A.L. Gavrilova, B. Bosnich, Chem. Rev. 104 (2004) 349.
[3] P.J. Steel, Coord. Chem. Rev. 106 (1990) 227.
[4] S. Brooker, Eur. J. Inorg. Chem. (2002) 2535.
[5] S. Brooker, T.C. Davidson, S.J. Hay, R.J. Kelly, D.K. Kennepohl, P.G. Plieger, B. Moubaraki, K.S. Murray, E. Bill, E. Bothe, Coord. Chem. Rev. 216–217 (2001) 3.
[6] W. Kaim, Coord. Chem. Rev. 230 (2002) 127.
[7] J.G. Haasnoot, Coord. Chem. Rev. 200 (2000) 131.
[8] M.H. Klingele, S. Brooker, Coord. Chem. Rev. 241 (2003) 119.
[9] U. Beckmann, S. Brooker, Coord. Chem. Rev. 245 (2003) 17.
[10] E.S. Raper, Coord. Chem. Rev. 129 (1994) 91.
[11] S. Trofimenko, J. Am. Chem. Soc. (1970) 5118.
[12] S. Trofimenko, Chem. Rev. 72 (1972) 497.
[13] S. Trofimenko, Prog. Inorg. Chem. 34 (1986) 115.
[14] A.P. Sadimenko, S.S. Basson, Coord. Chem. Rev. 147 (1996) 247.
[15] G. La Monica, G.A. Ardizzoia, Prog. Inorg. Chem. 46 (1997) 151.
[16] R. Mukherjee, Coord. Chem. Rev. 203 (2000) 151.
[17] S. Trofimenko, J. Am. Chem. Soc. (1967) 3170.
[18] S. Trofimenko, Chem. Rev. 93 (1993) 943.
[19] C. Pettinari, R. Pettinari, Coord. Chem. Rev. 249 (2005) 525.
[20] F. Meyer, Eur. J. Inorg. Chem. (2006) 3789.
[21] J.A. Perez, J. Pons, X. Solans, M. Font-Bardia, J. Ros, Inorg. Chim. Acta 358 (2005) 617.
[22] C. Sens, M. Rodriguez, I. Romero, A. Llobet, Inorg. Chem. 42 (2003) 2040.
[23] P.W. Ball, A.B. Blake, J. Chem. Soc. A (1969) 1415.

[24] J. Casabó, J. Pons, K.S. Siddiqi, J. Chem. Soc. Dalton Trans. (1989) 1401.
[25] J. Pons, X. López, E. Benet, J. Casabó, Polyhedron 9 (1990) 2839.
[26] J. Pons, X. López, J. Casabó, F. Teixidor, A. Caubet, J. Rius, C. Miravittles, Inorg. Chim. Acta 195 (1992) 61.
[27] M. Du, S.-T. Chen, Y.-M. Guo, X.-H. Bu, J. Ribas, J. Mol. Struct. 737 (2005) 17.
[28] M. Munakata, L.P. Wu, M. Yamamoto, T. Kuroda-Sowa, M. Maekawa, S. Kawata, S. Kitagawa, J. Chem. Soc. Dalton Trans. (1995) 4099.
[29] N. Suemura, M. Ohama, S. Kaizaki, Chem. Commun. (2001) 1538.
[30] K. Nakano, N. Suemura, S. Kawata, A. Fuyuhiro, T. Yagi, S. Nasu, S. Morimoto, S. Kaizaki, J. Chem. Soc. Dalton Trans. (2004) 982.
[31] K. Nakano, S. Kawata, K. Yoneda, A. Fuyuhiro, T. Yagi, S. Nasu, S. Morimoto, S. Kaizaki, Chem. Commun. (2004) 2892.
[32] K. Nakano, N. Suemura, K. Yoneda, S. Kawata, S. Kaizaki, Dalton Trans. (2005) 740.
[33] C.J. Schneider, J.D. Cashion, B. Moubaraki, S.M. Neville, S.R. Batten, D.R. Turner, K.S. Murray, Polyhedron 26 (2007) 1764.
[34] K. Yoneda, K. Nakano, J. Fujioka, K. Yamada, T. Suzuki, A. Fuyuhiro, S. Kawata, S. Kaizaki, Polyhedron (2005) 2437.
[35] K. Yoneda, K. Adachi, S. Hayami, Y. Maeda, M. Katada, A. Fuyuhiro, S. Kawata, S. Kaizaki, Chem. Commun. (2006) 45.
[36] K. Ni-iya, A. Fuyuhiro, T. Yagi, S. Nasu, K. Kuzushita, S. Morimoto, S. Kaizaki, Bull. Chem. Soc. Jpn. 74 (2001) 1891.
[37] Y. Kawamura, Y. Tsukahara, S. Nasu, S. Morimoto, A. Fuyuhiro, S. Kaizaki, Inorg. Chim. Acta 357 (2004) 2437.
[38] R. Kawahata, T. Tsukuda, T. Yagi, M.A. Subhan, H. Nakata, A. Fuyuhiro, S. Kaizaki, Chem. Lett. 32 (2003) 1084.
[39] C. Sens, I. Romero, M. Rodríguez, A. Llobet, T. Parella, J. Benet-Buchholz, J. Am. Chem. Soc. 126 (2004) 7798.
[40] K. Yoneda, K. Adachi, K. Nishio, M. Yamasaki, A. Fuyuhiro, M. Katada, S. Kaizaki, S. Kawata, Angew. Chem. 118 (2006) 5585;
K. Yoneda, K. Adachi, K. Nishio, M. Yamasaki, A. Fuyuhiro, M. Katada, S. Kaizaki, S. Kawata, Angew. Chem. Int. Ed. 45 (2006) 5459.
[41] J. Pons, F.J. Sánchez, A. Labarta, J. Casabó, Inorg. Chim. Acta 208 (1993) 167.
[42] J. Pons, F.J. Sanchez, J. Casabó, A. Alvarez-Larena, J.F. Piniella, J. Ros, Inorg. Chem. Commun. 6 (2003) 833.
[43] J. Pons, A. Chadghan, A. Alvarez-Larena, J.F. Piniella, J. Ros, Inorg. Chem. Commun. 4 (2001) 610.
[44] V.J. Catalano, T.J. Craig, Polyhedron 19 (2000) 475.
[45] V.J. Catalano, T.J. Craig, Inorg. Chem. 42 (2003) 321.
[46] J.P. Picart, F.J. Sanchez, J. Casabó, J. Rius, A. Alvarez-Larena, J. Ros, Inorg. Chem. Commun. 5 (2002) 130.
[47] J.C. Bayón, P. Esteban, G. Net, P.G. Rasmussen, K.N. Baker, C.W. Hahn, M.M. Gumz, Inorg. Chem. 30 (1991) 2572.
[48] P. King, R. Clérac, C.E. Anson, A.K. Powell, Dalton Trans. (2004) 852.
[49] X.-H. Li, Acta Crystallogr. E 61 (2005) m2405.
[50] J.-F. Zhang, X.-H. Li, Acta Crystallogr. E 62 (2006) m125.
[51] C.W. Hahn, P.G. Rasmussen, C. Bayón, Inorg. Chem. 31 (1992) 1963.
[52] D. Sanna, G. Micera, P. Buglyó, T. Kiss, T. Gajda, P. Surdy, Inorg. Chim. Acta 268 (1998) 297.
[53] J.-L. Tian, S.-P. Yan, D.-Z. Liao, Z.-H. Jiang, P. Cheng, Inorg. Chem. Commun. 6 (2003) 1025.
[54] J.C. Bayón, G. Net, P. Esteban, P.G. Rasmussen, D.F. Bergstrom, Inorg. Chem. 30 (1991) 4771.
[55] M. Nakahanada, K. Ino, S. Kaizaki, J. Chem. Soc. Dalton Trans. (1993) 3681.
[56] N. Sakagami, M. Nakahanada, K. Ino, A. Hioki, S. Kaizaki, Inorg. Chem. 35 (1996) 683.
[57] N. Sakagami-Yoshida, M. Teramoto, A. Hioki, A. Fuyuhiro, S. Kaizaki, Inorg. Chem. 39 (2000) 5717.
[58] S. Baitalik, U. Flörke, K. Nag, Inorg. Chim. Acta 337 (2002) 439.
[59] S. Baitalik, P. Bag, U. Flörke, K. Nag, Inorg. Chim. Acta 357 (2004) 699.
[60] E. Grobbelaar, W. Purcell, S.S. Basson, Inorg. Chim. Acta 359 (2006) 3800.
[61] V. Chandrasekhar, R. Thirumoorthi, R. Azhakar, Organometallics 26 (2007) 26.
[62] W.L. Driessen, L. Chang, C. Finazzo, S. Gorter, D. Rehorst, J. Reedijk, M. Lutz, A.L. Spek, Inorg. Chim. Acta 350 (2003) 25.
[63] P. King, R. Clérac, C.E. Anson, C. Coulon, A.K. Powell, Inorg. Chem. 42 (2003) 3492.
[64] T. Kamiusuki, H. Ōkawa, K. Inoue, N. Matsumoto, M. Kodera, S. Kida, J. Coord. Chem. 23 (1991) 201.
[65] R.M. Claramunt, C. Lopez, D. Sanz, J. Elguero, J. Organomet. Chem. 412 (1991) 259.
[66] S. Yamada, T. Ishida, T. Nogami, J. Chem. Soc. Dalton Trans. (2004) 898.
[67] S. Baitalik, U. Flörke, K. Nag, Inorg. Chem. 38 (1999) 3296.
[68] S. Baitalik, U. Flörke, K. Nag, J. Chem. Soc. Dalton Trans. (1999) 719.
[69] S. Baitalik, B. Dutta, K. Nag, Polyhedron 23 (2004) 913.
[70] J.C. Röder, F. Meyer, H. Pritzkow, Chem. Commun. (2001) 2176.
[71] G. Noël, J.C. Röder, S. Dechert, H. Pritzkow, L. Bolk, S. Mecking, F. Meyer, Adv. Synth. Catal. 348 (2006) 887.
[72] J.C. Röder, F. Meyer, E. Kaifer, H. Pritzkow, Eur. J. Inorg. Chem. (2004) 1646.
[73] A. Eisenwiener, M. Neuburger, T.A. Kaden, Dalton Trans. (2007) 218.
[74] T.G. Schenck, J.M. Downes, C.R.C. Milne, P.B. Mackenzie, H. Boucher, J. Whelan, B. Bosnich, Inorg. Chem. 24 (1985) 2334.
[75] T.G. Schenck, C.R.C. Milne, J.F. Sawyer, B. Bosnich, Inorg. Chem. 24 (1985) 2338.
[76] S. Tanaka, M. Akita, Angew. Chem. 113 (2001) 2951;
S. Tanaka, M. Akita, Angew. Chem. Int. Ed. 40 (2001) 2865.
[77] S. Tanaka, C. Dubs, A. Inagaki, M. Akita, Organometallics 23 (2004) 317.
[78] S. Tanaka, C. Dubs, A. Inagaki, M. Akita, Organometallics 24 (2005) 163.
[79] C. Dubs, T. Yamamoto, A. Inagaki, M. Akita, Organometallics 25 (2006) 1344.
[80] C. Dubs, T. Yamamoto, A. Inagaki, M. Akita, Organometallics 25 (2006) 1359.
[81] Y. Zhou, W. Chen, Organometallics 26 (2007) 2742.
[82] Y. Zhou, X. Zhang, W. Chen, H. Qiu, J. Organomet. Chem. 693 (2008) 205.
[83] U.J. Scheele, M. Georgiou, M. John, S. Dechert, F. Meyer, Organometallics 27 (2008) 5146.
[84] U.J. Scheele, M. John, S. Dechert, F. Meyer, Eur. J. Inorg. Chem. (2008) 373.
[85] S.-J. Jeon, R.M. Waymouth, Dalton Trans. (2008) 437.
[86] B. Mernari, F. Abraham, M. Lagrenee, M. Drillon, P. Legoll, J. Chem. Soc. Dalton Trans. (1993) 1707.
[87] F. Degang, W. Guoxiong, Z. Zongyuan, Z. Xiangge, Trans. Met. Chem. 19 (1994) 592.
[88] F. Meyer, A. Jacobi, L. Zsolnai, Chem. Ber./Recl. 130 (1997) 1441.
[89] J. Teichgräber, G. Leibeling, S. Dechert, F. Meyer, Z. Anorg. Allg. Chem. 631 (2005) 2613.
[90] J.C. Röder, F. Meyer, E. Kaifer, Angew. Chem. 114 (2002) 2414;
J.C. Röder, F. Meyer, E. Kaifer, Angew. Chem. Int. Ed. 41 (2002) 2304.
[91] J.C. Röder, F. Meyer, I. Hyla-Kryspin, R.F. Winter, E. Kaifer, Chem. Eur. J. 9 (2003) 2636.
[92] J.C. Röder, F. Meyer, H. Pritzkow, Organometallics 20 (2001) 811.
[93] T. Kamiusuki, H. Ōkawa, E. Kitaura, M. Koikawa, N. Matsumoto, S. Kida, J. Chem. Soc. Dalton Trans. (1989) 2077.
[94] J. Klingele, A.I. Prikhod'ko, G. Leibeling, S. Demeshko, S. Dechert, F. Meyer, Dalton Trans. (2007) 2003.
[95] T. Kamiusuki, H. Ōkawa, N. Matsumoto, S. Kida, J. Chem. Soc. Dalton Trans. (1990) 195.
[96] M. Itoh, K.-I. Motoda, K. Shindo, T. Kamiusuki, H. Sakiyama, N. Matsumoto, H. Ōkawa, J. Chem. Soc. Dalton Trans. (1995) 3635.
[97] F. Meyer, S. Beyreuther, K. Heinze, L. Zsolnai, Chem. Ber./Recl. 130 (1997) 605.
[98] F. Meyer, A. Jacobi, B. Nuber, P. Rutsch, L. Zsolnai, Inorg. Chem. 37 (1998) 1213.
[99] F. Meyer, U. Ruschewitz, P. Schober, B. Antelmann, L. Zsolnai, J. Chem. Soc. Dalton Trans. (1998) 1181.
[100] F. Meyer, M. Konrad, E. Kaifer, Eur. J. Inorg. Chem. (1999) 1851.
[101] M. Konrad, F. Meyer, A. Jacobi, P. Kircher, P. Rutsch, L. Zsolnai, Inorg. Chem. 38 (1999) 4559.
[102] F. Meyer, H. Pritzkow, Angew. Chem. 112 (2000) 2199;
F. Meyer, H. Pritzkow, Angew. Chem. Int. Ed. 39 (2000) 2112.
[103] F. Meyer, H. Pritzkow, Inorg. Chem. Commun. 4 (2001) 305.
[104] J. Ackermann, F. Meyer, E. Kaifer, H. Pritzkow, Chem. Eur. J. 8 (2002) 247.
[105] B. Bauer-Siebenlist, F. Meyer, D. Vidovic, H. Pritzkow, Z. Anorg. Allg. Chem. 629 (2003) 2152.
[106] B. Bauer-Siebenlist, F. Meyer, E. Farkas, D. Vidovic, J.A. Cuesta-Seijo, R. Herbst-Irmer, H. Pritzkow, Inorg. Chem. 43 (2004) 4189.
[107] J. Ackermann, F. Meyer, H. Pritzkow, Z. Anorg. Allg. Chem. 630 (2004) 2627.
[108] B. Bauer-Siebenlist, S. Dechert, F. Meyer, Chem. Eur. J. 11 (2005) 5343.
[109] G. Leibeling, S. Demeshko, B. Bauer-Siebenlist, F. Meyer, H. Pritzkow, Eur. J. Inorg. Chem. (2004) 2413.
[110] S. Demeshko, G. Leibeling, S. Dechert, F. Meyer, Dalton Trans. (2006) 3458.
[111] J.C. Röder, F. Meyer, M. Konrad, S. Sandhöfner, E. Kaifer, H. Pritzkow, Eur. J. Org. Chem. (2001) 4479.
[112] J. Ackermann, F. Meyer, H. Pritzkow, Inorg. Chim. Acta 357 (2004) 3703.
[113] J. Ackermann, S. Buchler, F. Meyer, C. R. Chim. 10 (2007) 421.
[114] F.-M. Nie, G. Leibeling, S. Demeshko, S. Dechert, F. Meyer, Eur. J. Inorg. Chem. (2007) 1233.
[115] D.J. de Geest, A. Noble, B. Moubaraki, K.S. Murray, D.S. Larsen, S. Brooker, Dalton Trans. (2007) 467.
[116] S.K. Dey, T.S.M. Abedin, L.N. Dawe, S.S. Tandon, J.L. Collins, L.K. Thompson, A.V. Postnikov, M.S. Alam, P. Müller, Inorg. Chem. 46 (2007) 7767.
[117] K. Shindo, Y. Mori, K.-I. Motoda, H. Sakiyama, N. Matsumoto, H. Ōkawa, Inorg. Chem. 31 (1992) 4987.
[118] J.M. Bueno, L. Campayo, P. Navarro, C. Acerete, Anal. Quim. 91 (1995) 430.
[119] J.-P. Chyn, F.L. Urbach, Inorg. Chim. Acta 189 (1991) 157.
[120] J.-L. Chou, D.-N. Horng, J.-P. Chyn, K.-M. Lee, F.L. Urbach, G.-H. Lee, H.-L. Tsai, Inorg. Chem. Commun. 2 (1999) 392.
[121] J.-L. Chou, J.-P. Chyn, F.L. Urbach, D.F. Gervasio, Polyhedron 19 (2000) 2215.
[122] S. Demeshko, G. Leibeling, W. Maringgele, F. Meyer, C. Mennerich, H.-H. Klauss, H. Pritzkow, Inorg. Chem. 44 (2005) 519.
[123] T. Kamiusuki, H. Ōkawa, E. Kitaura, K. Inoue, S. Kida, Inorg. Chim. Acta 179 (1991) 139.
[124] F. Meyer, P. Rutsch, Chem. Commun. (1998) 1037.
[125] F. Meyer, H. Pritzkow, Chem. Commun. (1998) 1555.
[126] F. Meyer, K. Heinze, B. Nuber, L. Zsolnai, J. Chem. Soc. Dalton Trans. (1998) 207.
[127] F. Meyer, E. Kaifer, P. Kircher, K. Heinze, H. Pritzkow, Chem. Eur. J. 5 (1999) 1617.
[128] F. Meyer, I. Hyla-Kryspin, E. Kaifer, P. Kircher, Eur. J. Inorg. Chem. (2000) 771.
[129] F. Meyer, R.F. Winter, E. Kaifer, Inorg. Chem. 40 (2001) 4597.
[130] L. Siegfried, T.A. Kaden, F. Meyer, P. Kircher, H. Pritzkow, J. Chem. Soc. Dalton Trans. (2001) 2310.
[131] S.V. Kryatov, E.V. Rybak-Akimova, F. Meyer, H. Pritzkow, Eur. J. Inorg. Chem. (2003) 1581.
[132] S. Buchler, F. Meyer, A. Jacobi, P. Kircher, L. Zsolnai, Z. Naturforsch. B 54 (1999) 1295.
[133] F. Meyer, H. Pritzkow, Eur. J. Inorg. Chem. (2005) 2346.
[134] E. Jaime, J. Weston, Eur. J. Inorg. Chem. (2006) 793.
[135] M. Alvariño Gil, W. Maringgele, S. Dechert, F. Meyer, Z. Anorg. Allg. Chem. 633 (2007) 2178.

[136] P.J. Zinn, D.R. Powell, V.W. Day, M.P. Hendrich, T.N. Sorrell, A.S. Borovik, Inorg. Chem. 45 (2006) 3484.
[137] P.J. Zinn, T.N. Sorrell, D.R. Powell, V.W. Day, A.S. Borovik, Inorg. Chem. 46 (2007) 10120.
[138] B. Bauer-Siebenlist, F. Meyer, E. Farkas, D. Vidovic, S. Dechert, Chem. Eur. J. 11 (2005) 4349.
[139] A. Prokofieva, A.I. Prikhod'ko, E.A. Enyedy, E. Farkas, W. Maringgele, S. Demeshko, S. Dechert, F. Meyer, Inorg. Chem. 46 (2007) 4298.
[140] A. Prokofieva, A.I. Prikhod'ko, S. Dechert, F. Meyer, Chem. Commun. (2008) 1005.
[141] M. Konrad, F. Meyer, K. Heinze, L. Zsolnai, J. Chem. Soc. Dalton Trans. (1998) 199.
[142] F. Meyer, P. Kircher, H. Pritzkow, Chem. Commun. (2003) 774.
[143] F. Meyer, S. Demeshko, G. Leibeling, B. Kersting, E. Kaifer, H. Pritzkow, Chem. Eur. J. 11 (2005) 1518.
[144] S. Demeshko, G. Leibeling, S. Dechert, S. Fuchs, T. Pruschke, F. Meyer, Chem. Phys. Chem. 8 (2007) 405.
[145] G. Leibeling, S. Demeshko, S. Dechert, F. Meyer, Angew. Chem. 117 (2005) 7273; G. Leibeling, S. Demeshko, S. Dechert, F. Meyer, Angew. Chem. Int. Ed. 44 (2005) 7111.
[146] L. Behle, M. Neuburger, M. Zehnder, T.A. Kaden, Helv. Chim. Acta 78 (1995) 693.
[147] H. Weller, L. Siegfried, M. Neuburger, M. Zehnder, T.A. Kaden, Helv. Chim. Acta 80 (1997) 2315.
[148] C. Vichard, T.A. Kaden, Inorg. Chim. Acta 337 (2002) 173.
[149] M. Raidt, M. Neuburger, T.A. Kaden, J. Chem. Soc. Dalton Trans. (2003) 1292.
[150] M. Raidt, L. Siegfried, T.A. Kaden, J. Chem. Soc. Dalton Trans. (2003) 4493.
[151] C. Vichard, T.A. Kaden, Inorg. Chim. Acta 357 (2004) 2285.
[152] S. Buchler, F. Meyer, E. Kaifer, H. Pritzkow, Inorg. Chim. Acta 337 (2002) 371.
[153] H. Weller, T.A. Kaden, G. Hopfgartner, Polyhedron 17 (1998) 4543.
[154] T.A. Kaden, Coord. Chem. Rev. 190–192 (1999) 371.
[155] M. Kumar, V.J. Arán, P. Navarro, Tetrahedron Lett. 34 (1993) 3159.
[156] M. Kumar, V.J. Arán, P. Navarro, A. Ramos-Gallardo, A. Vegas, Tetrahedron Lett. 35 (1994) 5723.
[157] C. Acerete, J.B. Bueno, L. Campayo, P. Navarro, M.I. Rodriguez-Franco, Tetrahedron 50 (1994) 4765.
[158] F. Escartí, C. Miranda, L. Lamarque, J. Latorre, E. García-España, M. Kumar, V.J. Arán, P. Navarro, Chem. Commun. (2002) 936.
[159] M. Kumar, V.J. Arán, P. Navarro, Tetrahedron Lett. 36 (1995) 2161.
[160] L. Lamarque, C. Miranda, P. Navarro, F. Escartí, E. García-España, J. Latorre, J.A. Ramírez, Chem. Commun. (2000) 1337.
[161] L. Lamarque, P. Navarro, C. Miranda, V.J. Arán, C. Ochoa, F. Escartí, E. García-España, J. Latorre, S.V. Luis, J.F. Miravet, J. Am. Chem. Soc. 123 (2001) 10560.
[162] C. Miranda, F. Escartí, L. Lamarque, E. García-España, P. Navarro, J. Latorre, F. Lloret, H.R. Jiménez, M.J.R. Yunta, Eur. J. Inorg. Chem. (2005) 189.
[163] A. Doménech, E. García-España, P. Navarro, C. Miranda, Dalton Trans. (2006) 4926.
[164] M. Konrad, S. Wuthe, F. Meyer, E. Kaifer, Eur. J. Inorg. Chem. (2001) 2233.
[165] C. Dubs, A. Inagaki, M. Akita, Chem. Commun. (2004) 2760.
[166] R. Krämer, I.O. Fritsky, H. Pritzkow, L.A. Kovbasyuk, J. Chem. Soc. Dalton Trans. (2002) 1307.
[167] L. Kovbasyuk, H. Pritzkow, R. Krämer, I.O. Fritsky, Chem. Commun. (2004) 880.
[168] J.C. Röder, F. Meyer, R.F. Winter, E. Kaifer, J. Organomet. Chem. 641 (2002) 113.
[169] T. Sheng, S. Dechert, A.C. Stückl, F. Meyer, Eur. J. Inorg. Chem. (2005) 1293.
[170] T. Sheng, S. Dechert, I. Hyla-Kryspin, R.F. Winter, F. Meyer, Inorg. Chem. 44 (2005) 3863.
[171] H. Zhang, S. Dechert, J. Maurer, M. Linseis, R.F. Winter, F. Meyer, J. Organomet. Chem. 692 (2007) 2956.
[172] H. Zhang, S. Dechert, M. Linseis, R.F. Winter, F. Meyer, Eur. J. Inorg. Chem. (2007) 4679.
[173] R. Kawahata, T. Tsukuda, T. Yagi, A. Fuyuhiro, S. Kaizaki, J. Alloys Compd. 408–412 (2006) 976.